Characterisation of Pathophysiological function of NEDD4-2 in Kidney

A thesis submitted in total fulfilment of the requirements of the degree of Doctor of Philosophy

By
Pranay Goel
Masters of Biotechnology and Bioinformatics

School of Medicine, Discipline of Medicine
Faculty of Health Sciences, University of Adelaide
Adelaide, South Australia

April 2016

Table of Contents

ABSTRACT

Nedd4-2 (NEDD4L, neural precursor cell expressed, developmentally down regulated 4-like) belongs to the Nedd4 family of ubiquitin ligases. These ligases aid in maintaining cellular homeostasis by binding to, and ubiquitinating a number of membrane proteins to initiate their internalization and turnover. Previous work from our laboratory has suggested that Nedd4-2 plays an essential role in regulating ion channels, especially the epithelial sodium channel and voltage gated sodium channels. The misregulation of these channels has been implicated in multiple channelopathies, including hypertension and cystic fibrosis like disease. This study characterises a previously unknown function of Nedd4-2 in the kidney.

In order to understand this significance of Nedd4-2 in renal homeostasis, the previously generated *Nedd4-2*$^{-/-}$ (Nedd4-2 knockout) mice (Boase *et al.*, 2011) were characterised. The initial histological examination of postnatal kidneys suggested renal cyst formation in *Nedd4-2*$^{-/-}$ animals. Further analysis revealed that Nedd4-2 loss results in renal dysplasia. *Nedd4-2*$^{-/-}$ mice showed variable renal cystic index, onset of cyst formation starting from postnatal day 2 and progressing until the *Nedd4-2*$^{-/-}$ animals die due to respiratory distress around day 19-21. To investigate the prevalence of the cystic phenotype in other tissues histological analysis was performed in pancreas, liver, spleen, colon, stomach and thymus with no significant pathological differences observed in the knockout mice.

The *Nedd4-2*$^{-/-}$ kidneys showed increased cell proliferation, with no apoptotic differences in the cells lining the cystic epithelia suggesting an imbalance between cell proliferation and apoptosis in cyst formation. The cyst formation and kidney development disorders are associated with malformation in the kidney tissue leading to extracellular matrix modification with enhanced accumulation of collagens causing increased interstitial fibrosis. The *Nedd4-2*$^{-}$

$^{-/-}$ kidneys showed increased interstitial fibrosis, collagen-1 accumulation and expression during progression of the disease. The renal tissue membrane is made up of polysaccharides, glycogen and mucin, the *Nedd4-2*$^{-/-}$ kidneys were found to have decreased accumulation of polysaccharides. The cysts in the *Nedd4-2*$^{-/-}$ kidneys originated from different parts within the nephron. The larger cysts originated from loop of Henle and with the smaller cysts from collecting ducts and distal convoluted tubules. The cystic progression is dependent on cAMP flux initiated by fluid secretion within the cyst. The postnatal day 19 cystic kidneys in *Nedd4-2*$^{-/-}$ animals showed increased cAMP levels suggesting cystic disease progression. As renal cystic disorders may arise from abnormal cilia, ciliary anomalies were found in the *Nedd4-2*$^{-/-}$ around the cysts suggesting importance of cilia in kidney cyst formation.

Polycystins are known to be involved in renal cyst development with polycystin-1 and polycystin-2 together known to form calcium ion channel. To investigate the role of Nedd4-2 in the regulation of these polycystins, *in vitro* and *in vivo* studies were conducted. *In vitro* studies suggested that depletion of Nedd4-2 results in increased expression of polycystin-1 on the cell membrane with a decrease in polycystin-2 levels. Further, polycystin-1 was found to be ubiquitinated by Nedd4-2 *in vitro* providing the first evidence of Nedd4-2-mediated regulation of polycystins. *In vivo* Polycystin-1 was up-regulated in the *Nedd4-2*$^{-/-}$ kidneys suggesting an important role of Nedd4-2 in regulation of polycystins in cyst formation.

To analyse the transcriptional signature of the phenotype seen in the knockout kidneys, postnatal day 19 kidneys from wild-type and *Nedd4-2*$^{-/-}$ mice were subjected to RNA sequencing highlighting 537 genes that were differentially expressed between wild-type and knockout kidneys, with 167 genes down-regulated and 370 genes significantly up-regulated in the absence of Nedd4-2. DAVID and Ingenuity pathway analyses was used to highlight the

importance of genes involved in extracellular matrix modification, cell junction formation and cell-cell communication. The work presented in this thesis thus provides new information on the pathophysiological role of Nedd4-2 in kidney and identifies polycystin-1 as a Nedd4-2 target, along with transcriptional changes which may partially explain the cystic phenotype associated with renal dysplasia.

Declaration

I certify that this work contains no material which has been accepted for the award of any other degree or diploma in my name, in any university or other tertiary institution and, to the best of my knowledge and belief, contains no material previously published or written by another person, except where due reference has been made in the text. In addition, I certify that no part of this work will, in the future, be used in a submission in my name, for any other degree or diploma in any university or other tertiary institution without the prior approval of the university of Adelaide and where applicable, any partner institution responsible for the joint- award of this degree.

I give consent to this copy of my thesis when deposited in the University Library, being made available for loan and photocopying, subject to the provisions of the Copyright Act 1968.

The author acknowledges that copyright of published works contained within this thesis resides with the copyright holder(s) of those works.

I also give permission for the digital version of my thesis to be made available on the web, via the university digital research repository, the library search and also through web search engines, unless permission has been granted by the university to restrict access for a period of time.

Pranay Goel

April 2016

Publication, Awards and Conference Attendance: By Year

2012:

IPRS (International postgraduate student research scholarship 2012) from University of Adelaide / Adelaide Postgraduate Award for living allowance.

Poster presentation at Adelaide protein group meeting (2012).

Poster presentation in 2nd Adelaide ANZSCDB Cell and Developmental Biology meeting (Nov 23, 2012).

2013:

Poster presentation at Florey International Postgraduate Research Conference by University of Adelaide (September 2013).

Best student poster in 3rd Adelaide ANZSCDB Cell and Developmental Biology meeting on (November 19, 2013)**.**

2014:

Poster presentation at the Lorne protein conference, 39th Lorne Conference on Protein Structure & Function (February 2014).

3MT thesis competition University of Adelaide (October 2014).

Howard Florey Adelaide student post graduate student conference, Adelaide (October 2014).

EMBL student symposium October 2014 abstract selected for poster presentation.

Attended 4th Adelaide ANZSCDB Cell and Developmental Biology meeting (Nov 19, 2014).

SPMSSF funding for International Lorne protein conference, Melbourne from SA pathology (1000$).

EMBL AUSTRALIA student travel grant for EMBL student symposium Heidelberg (3000$)

Publications: During PhD Candidature

1. GENE: Invited Review

GOEL, P., MANNING, J. A. & KUMAR, S. 2015. NEDD4-2 (NEDD4L): The ubiquitin ligase for multiple membrane proteins. *Gene,* 557**,** 1-10.

Acknowledgements

Research is an endeavour, a sojourn with an opportunity for me to realise the realms of the unknown in science. My Principal Supervisor, Prof Sharad Kumar provided me this opportunity which is a life time experience enabling me to realise my untapped potential. I express my heartfelt sincere thanks to Prof Kumar for all his efforts, guidance, his unstinted commitment to my work and the help extended to me from time to time during the entire period without which this work would not have been in the current stage.

I also thank my co-supervisor, Dr. Loretta Dorstyn for her timely feedbacks & insights during the course of this research work and for patiently going through my draft manuscripts from time to time which were followed by useful inputs. I also thank Dr Natasha Boase for her help during the entire tenure of this work. She has been helpful in completion work, critically evaluating the manuscript and enlightening me on occasions when I was stuck up and in generation of Nedd4-2 mouse colony. Dr. Kimberly Mackenzie for the ubiquitination assay blot and reading the manuscript critically. Dr Jantina Manning for the cAMP assay and Nephronal marker staining. Dr Tanya Henshall for aiding in the renal dysplasia annotation along with John Finnie.

I thankfully acknowledge to the fellow past students in the molecular regulation laboratory (Dr. Andrew Fotia, Prof. Natasha Harvey and Prof. Kieran Harvey) who had been a kind of benchmark I always aspired to be as a research student, thanks for inspiring me through your body of work.

I also thankfully acknowledge Dr. Joseph Puccini (Graduate 2014), Swati Dawar, Shannon Nicolson and Cindy Xu current students for making me believe I was part of them. A special thanks to Dr. May Aung-Htut, Dr. Natalie Foot and Dr. Claire Wilson for all the help

rendered by them for final thesis preparation. I also thank the other members of the molecular regulation laboratory Dr. Ian Nicholson, Dr. Donna Denton, Alyshea Collaco, Andrej Nikolic, Dr. Sonia Shalini, and Omri Alfassy along with the other staff members for all the help rendered by them in the laboratory.

Special thanks are due to people at SA pathology anatomical services especially to Mrs Mandy for tissue histology work. A special word of thanks for all the people in Prof. Natasha Harvey's laboratory especially Dr. Drew Sutton for the antibodies and Dr. Kelly Betterman for help with confocal microscopy. A special thanks to all the Research groups and the facilities at Centre for Cancer Biology for helping me with antibodies and reagents during the work.

I also thank Adelaide microscopy especially Ruth Williams for the help in transmission electron microscopy. My special thanks to Mr. Jim Manavis for all his help. I also thank CCB ACRF facility for the help rendered by David Lawrence, bioinformatics expert for RNA sequencing work. I thank the confocal facility for providing me opportunity to utilise their facility. I thank IMVS animal care facility for taking care of the mice. I would also thank University of Adelaide for the IPRS/APA scholarship for aiding in me undertaking my PhD in a place with a history of its own.

I sincerely thank Prof. David Callen who helped me immensely at University through various support systems from time to time during the crisis has helped in concluding this work. Special thanks to my parents Mr. S.M.J.R Goel and Mrs. Poonam Goel for providing me unconditional support and instilling my faith in myself. I express my sincere thanks to my sister Pragya Goel for aiding me in understanding the life beyond science. I thank all my friends and well-wishers who stood by me and reminded that science and life go hand in hand not mutually exclusively, thus making life a bit easier during my tough times.

Last but not the least, I sincerely thank all those who directly or indirectly contributed to this research work in any capacity and their names are missed inadvertently, without your unsung contributions this work would not have taken shape.

Abbreviations

HCN1	Hyperpolarization activated cyclic nucleotide gated
P19	Post natal day 19
%	Percentage
µg	Microgram
ADAM23	ADAM metallopeptidase domain 23
ADPKD	Autosomal dominant polycystic kidney disease
AFF3	AF4/FMR2 family member 3
AGTR2	Angiotensin receptor 2
Akt	PKB- protein kinase B
AP	Alkaline phosphatase
APC	Anaphase-promoting complex
AQP2	Aquaporin 2
ARID5B	AT rich interactive domain 5B
ARPKD	Autosomal recessive polycystic kidney disease
Arrdcs	Arrestin domain containing proteins
ATA-2	Amino acid transporter
ATP	Adenosine tri phosphate
BCA	Bicinchoninic acid
BGN	Biglycan
BMP-4 ,7	Bone morphogenetic protein 4, 7
bp	Base pair
BW	Body weight
C	Centigrade
C termini	Carboxyl termini
C2	Ca^{2+} phospholipid binding domain
C3AR1	Complement component 3a receptor 1
Ca^{2+}	Calcium
CAKUT	Congential anomalies of the kidney and urinary tract
cAMP	Cyclic adenosine monophosphate

CAT	Catalase
CC	coiled–coil
CD	Collecting ducts
cDNA	complementary Deoxyribonucleic acid
CFTR	Cystic fibrosis transmembrane conductance regulator
Cl^-	Chloride
CLC-5	$H(^+)/Cl(^-)$ exchange transporter 5
ClCka/Barttin	chloride channel
cm	Centimeters
CO_2	Carbon dioxide
Col1a1	Collagen I alpha 1
CSF1	Colony stimulating factor 1
DAB	3, 3` diaminobenzidine
DAT	Dopamine transporter
DAVID	Database for Annotation, Visualization and Integrated Discovery
DBA	Dolichos Biflorus Agglutinin
DCN	Decorin
DCT	Distal convoluted tubule
DCTN-5	Dynactin-5
DEPC	Diethylpyrocarbonate
Dlg3	Drosophila disc large scaffolding protein
DMEM	Dulbeccos modified eagle medium
DMT1	Divalent metal ion transporter
DNA	Deoxy ribonucleic acid
DRG	Dorsal root ganglion
DTT	Dithiothreitol
DTX4	Deltex4 E3 ubiquitin ligase
DUBs	Deubiquitinating enzymes
Dvl2	Dishevelled-2
E. coli	Escherichia coli
E1	Ubiquitin activating enzyme
E18.5	Embryonic day 18.5 post coitum

E2	Ubiquitin-conjugating enzyme
E3	Ubiquitin protein ligases
EAAT1/2	The glial excitatory amino acid transporters
ECF	Enhanced chemifluoroescence
ECM	Extracellular matrix
EDTA	Ethylenediaminetetraacetic acid
EF2	EF-hand calcium binding motif
EGF	Epidermal growth factor
EGF	Epidermal growth factor
EMT	Epithelial to mesenchymal transition
ENaC	Epithelial sodium channel
ESCRT	Endosomal sorting complex
FBLN1	Fibrillin
FBS	Foetal Bovine Serum
FGA	Fibrinogen alpha chain
fr	Firststrand
FREM1	FRAS1 related extracellular matrix 1
G	Glomeruli
GAIN	G protein coupled receptor auto proteolysis inducing regulatory domain
gDNA	Genomic DNA
GFP	Green fluoroscent protein
GO	Gene Ontology
GP78	Glycoprotein 78
GPC-3	Glypican-3
GPCR	G protein coupled receptor
GPS	G-protein coupled receptor motif
H and E	Haematoxylin and Eosin
HB-EGF	Heparin binding-EGF
HCO_3^-	Bicarbonate

HECT	Homologous to the E6-AP C terminus
HEK	Human epithelial kidney
HepG2	Liver hepatocellular carcinoma cell line
HIF3A	Hypoxia inducible factor 3 alpha
HRP	Horse radish peroxidase
Hrs	Hours
IB	Immunoblot
ICAM1	Intercellular adhesion molecule 1
ICC	Immunocytochemistry
IF	Immunofluoroscence
IMCD	Inner medullary cortical collecting duct cells
IPA	Ingenuity pathway analysis
ITGAM	Integrin alpha M
iTRAQ	Isobaric tags for relative and absolute quantitiation
ITS	Insulin/ transferrin/selenium
K	Lysine
K^+	Potassium
KCNQs	Potassium voltage-gated channel subfamily
kDa	Kilodalton
KEGG	Kyoto Encyclopaedia for Genes and Genomes
KIF3A	Kinesin subunit 3A
KL	Klotho
KO	Knock out
KW	Kidney weight
L	Litre
LB	Luria- Bertani media
LPxY	Leucine-Proline-x-Tyrosine
LTL	Lotus Tetragonolobus Lectin
M	Molar
mA	Milliamperes

mDCT	mouse Distal collecting tubule
MEF	Mouse embryonic fibroblast
MEKK1	Mitogen associated protein kinase pathway
mg/mL	Milligram/Millilitre
Min	Minutes
mL	Millilitres
mm	Millimeters
mM	Millimolar
MMP	Matrix metallo protease
mpkCCD	Mouse pyruvate kinase cortical collecting duct
n.s	Not significant
Na^+	Sodium
Nav	Voltage-gated sodium channels
NCC	Na^+-Cl^- cotransporter
NCOR2	Nuclear receptor co repressor 2
NDFIP1/2	Nedd4 family interacting protein 1/2
NDRG1	N-myc downstream regulated gene-1
Nedd	Neuronally expressed, developmentally down-regulated gene
NEM	N-ethylmaleimide
ng	Nanogram
NKCC2	Na+-K+-2Cl- cotransporter
nm	Nanometers
NOX4	NADPH oxidase 4
^{o}	Degree
OD	Optical denstity
Orai1	Calcium channel
PAGE	Polyacrylamide gel electrophoresis
PARP3	Polymerase family member 3
PAS	Periodic acid schiff

PAX-2 Paired box gene-2

PBS Phosphate buffered saline

PC-1 Polcystin-1

pCNA Proliferation cell nuclear antigen

PCR Polymerase chain reaction

PDAC Pancreatic ductal adenocarcinoma

PHD Plant Homeo Domain

PIK3CD Bisphosphate 3- kinase catalytic subunit Δ

PIK3R5 Phosphoinositide-3-kinase regulatory subunit 5

PKD Polycystic kidney disease

PKHD1 Fibrocystin

PLAT Polycystin-1 lipoxygenase alpha-toxin

PLCB2 Phospholipase C β2

PP/LPXY Proline rich motifs

PVDF Polyvinylidene fluoride

RD Renal Dysplasia

RING Really interesting new gene

RIPA Radioimmunoprecipitation lysis buffer

RMA/RNF5 RING finger protein 5

RNA Ribonucleic acid

ROMK Renal outer medullary potassium channel

RPMI Roswell Park Memorial Institute media

RT^2 Real time / Reverse Transcriptase

RTKs Receptor protein tyrosine kinases

RUNX1 Runt-related transcription factor 1

SALL1 SAL-like 1

SCF Skp1- Cullin- F-box complex

SDS Sodium dodecyl sulphate

SEM Scanning Electron Microscope

SEM Standard error mean

Sgk1	Serum glucocorticoid-inducible kinase
SGLT1	Na^+ glucose transporter 1
SILAC	Stable isotope labelling of amino acid in cell culture
siRNA	small interfering Ribonucleicacid
Six1	Sineoculis homeobox 1
SLC	Solute carrier family
SLIT3	Slit homolog 3
SMA	Smooth Muscle Actin
SMAD2/3/7	Mothers against decapentaplegic
SMOC2	SPARC related modular calcium binding 2
SNPs	Single nucleotide polymorphisms
SMOC2	SPARC related modular calcium binding 2
SNPs	Single nucleotide polymorphisms
SP-C	Surfactant protein C
Src	Non- receptor protein tyrosine kinase
STAT3	Signal transducer and activator of transcription 3
SULF1	Sulfatase 1
SUMO	Small Ubiquitin-like Modifier
SVD	Singular value decomposition
TAE	Tris acetate EDTA
TBST	Tris-buffered saline/Tween 20
TCA	Trichloro acetic acid
TCF-2	Transcription factor-2
TEM	Transmission Electron Microscope
TGFβ	Transforming growth factor β
TGFβR1	Transforming growth factor beta receptor 1
THP	Tamm horsfall glycoprotein
TINAG	Tubulointerstitial nephritis antigen
TrkA	Neurotrophin receptor
TRPC6	Transient receptor potential Canonical 6

TRPM6	Transient receptor potential melastatin 6
TRPP2/PC-2	Transient receptor potential/ polycystin -2
TSHZ3	Teashirt zinc finger homeobox 3
TTYH	Tweety chloride channel
UB	Ubiquitin
UBC	Ubiquitin-conjugating domain
UBPs	Ubiquitin specific processing enzymes
UCHs	Ubiquitin carboxyl terminal hydrolases
UV	Ultra violet
V	Volts
V2R	Vasopressin receptor
VCB	Von Hippel Lindau-elongin C - elongin B- Cul2- Rbx1 complex
W	Watts
WNT4	Wingless gene 4
WT	Wild type
WT1	Wilms tumor 1
WW	Protein-Protein interaction tryptophan domains
Yeast	Saccharomyces cerevisiae
µg/ml	Microgram per millitre
µl	Micro litre
µm	Micrometer

List of Figures and Tables

Chapter 3: Figures and Tables

Chapter 4: Figures and Tables

Thesis Structure

This thesis contains already published work and unpublished work in the structure described below:

Chapter-1: Section 1.3.2, 1.3.3 (part), 1.3.4- 1.3.5, 7 and 8 are unpublished and provide the initial review of the literature and the context of the study related to the topic of the thesis. Sections 1 (1-1.1, 1.2-1.3, 1.3.3-1.3.4, 2-7 are part of the published review providing insights on the study on Nedd4-2.

GOEL, P., MANNING, J. A. & KUMAR, S. 2015. NEDD4-2 (NEDD4L): The ubiquitin ligase for multiple membrane proteins. *Gene,* 557**,** 1-10.

Chapter-2: This chapter consists of the characterisation of the Nedd4-2 knock out kidney phenotype, with introduction consisting of relevant literature on the renal disorder, materials and methods described in detail the methodology of the chapter results, the results on the kidney phenotype characterisation and discussion summarising the major findings with their relevance and limitations

Chapter-3: This chapter consists of the role of polycystins and their potential regulation by Nedd4-2 and its physiological relevance in context to Nedd4-2 knock out kidneys , with introduction consisting of relevant literature on the polycystin structure and function, materials and methods described in detail the methodology of the chapter results, the results describing the potential role of polycystin in context to Nedd4-2 mediated regulation and discussion summarising the major findings and limitations with their relevance to the given study.

Chapter-4: This chapter consists of differential gene expression analysis of Nedd4-2 knock out kidneys and their relevance in context to renal dysplasia (Nedd4-2 kidney phenotype), with introduction consisting of relevant literature on the next generation sequencing used prior to understand the disease as a model system, materials and methods described in detail the methodology of the chapter results through bioinformatics approaches, the results describing the potential role of genes and the pathways in context to Nedd4-2 mediated regulation and discussion summarising the major findings and limitations with their relevance to the given study.

Chapter-5: This chapter comprises of the overall summary of the major findings of the thesis and the linkage between the chapter 2, 3 and 4. This further discusses the limitations of the study and the future perspective in relevance to the given study undertaken.

Chapter 1: Introduction

Chapter 1: Introduction

Statement of Authorship

Title of Paper	NEDD4-2 (NEDD4L): The ubiquitin ligase for multiple membrane proteins.
Publication Status	☑ Published ☐ Accepted for Publication ☐ Submitted for Publication ☐ Unpublished and Unsubmitted w ork w ritten in manuscript style
Publication Details	**GOEL, P.**, MANNING, J. A. & KUMAR, S. 2015. NEDD4-2 (NEDD4L): The ubiquitin ligase for multiple membrane proteins. *Gene,* 557**,** 1-10.

Principal Author

Name of Principal Author (Candidate)	Pranay Goel
Contribution to the Paper	Wrote the manuscript, edited the manuscript., made the figures
Overall percentage (%)	80%
Certification:	This paper reports on original research I conducted during the period of my Higher Degree by Research candidature and is not subject to any obligations or contractual agreements with a third party that would constrain its inclusion in this thesis. I am the primary author of this paper.
Signature	Date 2/12/15

Co-Author Contributions

By signing the Statement of Authorship, each author certifies that:

i. the candidate's stated contribution to the publication is accurate (as detailed above);

ii. permission is granted for the candidate in include the publication in the thesis; and

iii. the sum of all co-author contributions is equal to 100% less the candidate's stated contribution.

Name of Co-Author	Dr. Jantina Manning
Contribution to the Paper	Edited the manuscript
Signature	Date 2-12-2015

Name of Co-Author	Prof.Sharad Kumar
Contribution to the Paper	Co-wrote the manuscript and edited the manuscript
Signature	Date 02.12.15

Please cut and paste additional co-author panels here as required.

Chapter 1: Introduction

1. Ubiquitination

Ubiquitination is a well-characterized protein modification system that leads to substrate degradation, stabilization or relocalization (Bonifacino and Weissman, 1998). A wide range of proteins are degraded by the proteasome or the lysosome following ubiquitination. These proteins include many membrane proteins, cell cycle regulators, transcription factors, tumor suppressors and oncogenes (Hershko and Ciechanover, 1998, Hicke, 2001a, Glickman and Ciechanover, 2002). Defects in the ubiquitination machinery have been implicated in cancer and other human pathologies (Ciechanover *et al*., 1998) .

Ubiquitination is a stepwise process involving three classes of enzymes. An ubiquitin activating enzyme (E1) activates the ubiquitin molecule in an ATP dependent manner resulting in a thioester bond formation between the carboxyl terminus of ubiquitin and the internal catalytic cysteine residue (Haas *et al*., 1983). The ubiquitin is then transferred to the catalytic cysteine residue of a ubiquitin-conjugating enzyme (E2) with an active cysteine (Jentsch, 1992, Hershko and Ciechanover, 1998) (**Fig 1.1A**). Following this, ubiquitin is transferred to the substrate via the ubiquitin protein ligases (E3). The human genome encodes only one E1 protein, 36 E2 proteins and several hundred E3s (Hershko and Ciechanover, 1998). Poly-ubiquitination is the sequential attachment of a multiple ubiquitin molecule chain to the lysine residues of the ubiquitin attached to the substrate (Jentsch, 1992) **(Fig 1.1A)**. There are seven lysine residues in the ubiquitin amongst which K11 and K48 linkages are associated with protein degradation signal by the proteasome whereas K63 linkage is associated with protein trafficking (Pickart, 2001b, 2001a, Weissman, 2001). Endocytosis and lysosomal degradation are further shown to occur via mono-ubiquitination and multiple mono-ubiquitination events. Mono-ubiquitination is also associated with DNA repair, histone modification and protein trafficking (Hicke, 2001b, Haglund *et al*., 2003) **(Fig 1.1A).**

Chapter 1: Introduction

1.1 Ubiquitin activating enzymes (E1)

There are single E1 enzymes that can regulate and initiate the entire ubiquitin pathway downstream in most organisms (Pickart, 2001a). The first discovered human E1 cloned was found to be expressed in all tissues (Handley *et al*., 1991). Mouse cells expressing mammalian temperature sensitive E1 was among the first studied, establishing the importance of E1 enzymes in ubiquitination (Finley and Varshavsky, 1985, Finley *et al*., 1984). They showed that inactivation of E1 proteins in these cells led to cell cycle defects associated with reduced degradation of proteins (Ciechanover *et al*., 1984, Finley *et al*., 1984).

1.2 Ubiquitin-conjugating enzymes (E2)

Studies in *Saccharomyces cerevisiae* (yeast) were the first to establish the ubiquitin pathway signaling mechanisms, with a total of 13 designated E2 proteins (UBC-1 to UBC-13), 11 of which are genuine ubiquitin-conjugating enzymes (Hochstrasser, 2000). In humans there are 36 known E2 enzymes (von Arnim, 2001). The structure of E2s include a 150-200 amino acid conserved ubiquitin-conjugating domain (UBC) which comprises a catalytic cysteine residue responsible for binding ATP-activated ubiquitin or a ubiquitin-like protein (Jentsch, 1992). The composition of the UBC domain can vary and comprise an amino, carboxy or intra UBC extension domain, which determines the E1 and E3 binding specificity. Furthermore, studies in yeast have shown that these enzymes are essential for multiple functions including transcription, DNA repair and cell cycle progression (Jentsch, 1992).

1.3. Ubiquitin protein ligases (E3)

E3 enzymes provide substrate specificity to the ubiquitin system and recognize multiple substrates through different protein-protein interactions. They are the largest family of enzymes which recognize multiple substrates There are two types of E3 ligases, HECT (homologous to the E6-AP C terminus) and RING (really interesting new gene) **(Fig 1.1B)**. E3s can target their substrates via two mechanisms: **(i)** HECT domain E3s accept ubiquitin

molecules from E2s and then transfer the conjugated ubiquitin to the substrate and **(ii)** RING E3s act as adaptors to bring the substrate and E2 enzyme in close proximity for direct transfer of ubiquitin to the substrates lysine residues (Hershko and Ciechanover, 1998, Fang and Weissman, 2004) **(Fig 1.1B)**. There are over 600 mammalian E3 family members, most belonging to the RING family, with 29 human members of the HECT family (Huibregtse *et al*., 1995, Scheffner and Kumar, 2014).

1.3.1 HECT E3s

The E3 ligases containing a HECT domain form a thioester bond with ubiquitin before transferring the ubiquitin to the substrate (Pickart, 2001a, Weissman, 2001) **(Fig 1.1B)**. The HECT E3s interact with E2 enzymes through their carboxy terminal HECT domain which accepts and binds ubiquitin, whereas the amino terminus is essential for substrate interaction (Pickart, 2001a). The HECT members E6-AP and NEDD4 were the first E3s discovered (Huibregtse *et al*., 1995, Scheffner *et al*., 1993, Kumar *et al*., 1997).The largest group of HECT E3s is the NEDD4 family, with 9 members. This thesis focuses on NEDD4-2, also known as KIAA0439 and NEDD4L (NEDD4L mostly used for human gene/protein) (Yang and Kumar, 2010) **(see introduction section 2)**.

1.3.2 RING and RING like E3s

In humans there are over 200 different RING finger containing proteins (von Arnim, 2001). RING family ligases consist of a core motif, with eight cysteine and histidine residues that bind Zn^{2+} (Borden and Freemont, 1996). These ligases act as adaptors to bring the substrate together with an E2 (Pickart, 2001a, Weissman, 2001). There are two types of RING E3s, single and multi-subunit ligases. The Ring E3's belonging to the single subunit family have a RING motif and distinct E2 and substrate binding sites (Pickart, 2001a). For example, c-Cbl promotes down regulation of receptor protein tyrosine kinases (RTKs) in an ubiquitin dependent manner (Pickart, 2001a). The binding of c-Cbl to its substrates is dependent on the

RING finger motif, and this interaction occurs between c-Cbl and the SH2 domain of RTK (Joazeiro *et al*., 1999, Waterman *et al*., 1999) **(Fig 1.1 B)**.

RING E3's that form multi-subunits are essential for active E3 complex formation via RING-domain interactions with substrates (Pickart, 2001a). Multi-subunit RING E3's are further divided into different families, including SCF (Skp1- Cullin- F-box complex), VCB (von Hippel Lindau-elongin C - elongin B- Cul2- Rbx1 complex) and the APC (anaphase-promoting complex) families (Tyers and Willems, 1999, Fang and Weissman, 2004). There are structural similarities among all families, including a backbone comprising a cullin family protein attached to RING finger subunit that facilitates E2 recruitment and binding of adaptor proteins, which in turn leads to attachment with a substrate recognition subunit (Pickart, 2001a, Weissman, 2001). The SCF E3 ubiquitin ligase complex is the largest family of E3 ligases, which associate through Skp1 adaptor proteins and utilize different substrate recognition subunits (F-Box proteins) (Deshaies, 1999). There are 46 reported F-box proteins in human, which confer substrate specificity to the SCF complex and thereby promote multiple substrate ubiquitination and exert a variety of physiological responses (Deshaies, 1999, von Arnim, 2001). SCF E3s are known to be associated with cell cycle regulation and transcriptional regulation (Deshaies, 1999). APC functions are best characterized in cell cycle regulation during mitosis (Harper *et al*., 2002, Peters, 2002). Other reported E3s include the Plant Homeo Domain (PHD) finger containing E3s and distant relatives U-Box containing E3s (Fang and Weissman, 2004). The PHD finger proteins are known to function in the mitogen associated protein kinase kinase associated pathway (MEKK1) (Lu *et al*., 2002). Some human malignancies are reported to be associated with mutations in VCB E3 RING ligase family members (Stebbins *et al*., 1999).

1.3.3 Ubiquitination control by DUBs and other mechanisms

Ubiquitination of proteins can also be regulated by proteins other than E1, E2 and E3's enzymes. One such family of proteins is the deubiquitinating enzymes (DUBs). They are further divided into two classes consisting of ubiquitin specific processing enzymes (UBPs) and ubiquitin carboxyl terminal hydrolases (UCHs) (Wilkinson, 2000). UCHs aid in ubiquitin precursor protein synthesis and UBPs help in disassembling polyubiquitin chain formation (Wilkinson, 2000). The DUB Usp2-45 is known to decrease ubiquitination of epithelial sodium channel (ENaC) and to increase its cell surface expression in *Xenopus* oocytes (Krzystanek *et al*., 2012, Oberfeld *et al*., 2011, Pouly *et al*., 2013). Both the catalytic domain and the N-terminal tail of Usp2-45 physically interact with the HECT domain of NEDD4-2 (Krzystanek *et al*., 2012). This interaction with NEDD4-2 is thought to favourably position Usp2-45 for ENaC deubiquitination (Krzystanek *et al*., 2012, Oberfeld *et al*., 2011). Thus it seems that this DUB regulates NEDD4-2 mediated ENaC control through binding the E3 and deubiquitinating the substrate in the complex.

E3s can also ubiquitinate themselves leading to their own degradation, known as auto-ubiquitination. NEDD4-2 weakly binds to the Leucine-Proline-x-Tyrosine ((LPxY), x is any amino acid) a motif in its HECT domain via its WW domain suggesting this intramolecular interaction could inhibit its auto-ubiquitination, thereby stabilizing NEDD4-2 (Bruce *et al*., 2008). Mutations in the LPxY motif decrease NEDD4-2 binding to ENaC subunits and its ability to inhibit ENaC activity (Bruce *et al*., 2008). Kinase activity can also have an inhibitory or a stimulatory effect on the process of ubiquitination. Phosphorylation can aid in the creation of binding sites for E3 ligases, or in some cases it can lead to the inactivation of E3's (Fang and Weissman, 2004). Acetylation or sumoylation (conjugation of Small Ubiquitin-like Modifier (SUMO)) of substrate ubiquitination site aids in the detachment of ubiquitin by blocking substrate sites for ubiquitin conjugation (Fang and Weissman, 2004).

1.3.4 Degradation by the proteasome

The proteasome is a large multi subunit complex composed of three subunits - a 20S catalytic subunit and two 19S regulatory subunits attached to each end (Hochstrasser, 1996). It is primarily responsible for degrading cellular proteins which are linked through K48 polyubiquitin chains into smaller peptides (Hershko and Ciechanover, 1998). Non-ubiquitinated proteins can also undergo degradation through the proteasome but is context dependent (Hoyt and Coffino, 2004). The 20S complex is formed by the stacking of two α and two β subunits, each composed of seven subunits, with two alpha rings attached at each end of adjacent beta subunits in a αββα arrangement (Hershko and Ciechanover, 1998). The α subunit forming rings provide a structural role whereas the β subunits have different enzymatic specificities with chymotrypsin-like, trypsin like or peptidyl-glutamyl peptide hydrolysing -like activity (Hershko and Ciechanover, 1998). Substrate recognition within the proteasome is carried out by the 19S regulatory complex through formation of high affinity attachments with polyubiquitin chains during proteasomal degradation (DeMartino and Slaughter, 1999). This complex also unfolds the proteins and disassociates polyubiquitin chains through its ATPase and UBP activity respectively (DeMartino and Slaughter, 1999).

1.3.5 Degradation by lysosomes

Intracellular organelles containing acidic proteases are called lysosomes (Pillay *et al*., 2002). Proteins are delivered in late endocytosis to the lysosomes for degradation (Pillay *et al*., 2002). The change in cellular environment can lead to proteins (including receptors, ion transporters and channels of the plasma membrane) to be degraded by lysosomes. Upon ubiquitination of a protein on the plasma membrane, the protein is endocytosed through invagination of the membrane leading to formation of intracellular membrane vesicles (Hicke, 2001a). The proteins which are endocytosed are either recycled back to the plasma membrane or degraded via lysosomes (Hicke, 1999). The signal for degradation of membrane

proteins through lysosomes is via monoubiquitination of the intracellular region of the protein, or an attachment of a K63 ubiquitin chain (Hicke, 2001b). Ubiquitination can also promote trafficking of newly synthesized proteins from golgi to lysosome for degradation (Hicke and Dunn, 2003, Di Fiore *et al*., 2003).

2. The NEDD4 family of Ubiquitin ligases

NEDD4-2 belongs to the NEDD4 family of ubiquitin ligases and is the closest homologue of NEDD4, the prototypic member of the family (Harvey and Kumar, 1999, Yang and Kumar, 2010). NEDD4 and NEDD4-2 share similar E2 specificities (Fotia *et al*., 2006). NEDD4 is an evolutionary conserved E3, with homologues in yeast, *Drosophila* and *C. elegans* (Kumar *et al*., 1992, Kumar *et al*., 1997, Harvey and Kumar, 1999). It was originally identified in the early embryonic central nervous system (CNS) as a neuronally expressed, developmentally down-regulated gene (Kumar *et al*., 1992). The NEDD4 family members are characterized by a unique modular domain architecture comprising the amino terminal Ca^{2+} phospholipid binding (C2) domain, between 2-4 WW domains (protein-protein interaction domains) and the HECT domain at the carboxyl terminus (Harvey and Kumar, 1999). WW domains consist of 35-40 amino acids and have two conserved tryptophan residues (Andre and Springael, 1994, Hofmann and Bucher, 1995). These domains generally bind PY (PPxY) motifs and to a lesser degree LPSY motifs in substrates and regulatory proteins. The multiple WW domains in NEDD4 members suggest that they can potentially interact with several proteins at once. The C2 domain binds lipid membranes, but has also been shown to bind proteins (Scheffner and Kumar, 2014). The HECT domain is the catalytic domain in NEDD4 ligases. Structural studies suggest that HECT is a bilobular domain with the C lobe containing the ubiquitin acceptor cysteine and N lobe interacting with the ubiquitin-charged E2 (Maspero *et al*., 2013, Rotin and Kumar, 2009). In addition to NEDD4 and NEDD4-2, other family members include itchy E3 protein ubiquitin ligase (ITCH), SMAD specific E3 protein ubiquitin ligase

1(SMURF1), SMURF2, WWP1, WWP2, NEDL1 and NEDL2 (Rotin and Kumar, 2009). The difference in the number of WW domains characterizes the variability among the family members along with substrate specificity and involvement in distinct biological processes. This could also be dependent upon the C2 domain, which may be absent in some alternately spliced isoforms of NEDD4 family members (Plant *et al*., 2000, Scheffner and Kumar, 2014).

3. NEDD4-2 structure and expression

While NEDD4 homologues are found in all eukaryotes, NEDD4-2 is likely to have evolved by gene duplication much later in evolution as NEDD4-2 orthologues are only found in vertebrates (Yang and Kumar, 2010). All NEDD4-2 proteins share a similar modular structure containing 4 WW domains, in addition to the C2 and HECT domains **(Fig 1.2A)**. Phylogenetic analysis shows that NEDD4-2 is highly conserved in vertebrates **(Fig 1.2B)**. NEDD4-2 transcripts are present in many tissues, with particularly high expression in the liver, kidney, heart and lung (Harvey *et al*., 2001, Araki *et al*., 2008). The human NEDD4-2 gene is located on chromosome 18q21.31. It contains 38 exons, which give rise to multiple spliced mRNA (Chen *et al*., 2001, Dunn *et al*., 2002, Araki *et al*., 2008). In the NCBI database there are at least 17 predicted isoforms of human NEDD4-2. However, in most tissues NEDD4-2 (both mouse and human) appears as two protein bands (130 and 110 kDa), one of which may vary slightly in a tissue specific manner. The most commonly expressed protein contains a C2 domain, 4 WW domains, and the HECT domain (Harvey *et al*., 2001, Fotia *et al*., 2003).

Fig 1.1 Overview of the ubiquitin system. A) Ubiquitin is activated in an ATP dependent manner by E1 enzymes, which in turn transfer the ubiquitin to the E2 enzyme. Transfer of ubiquitin occurs between E2s and E3 ligases resulting in ubiquitin conjugation to the substrate. The position of attachment within the substrate can be through a single ubiquitin (mono-ubiquitination), a chain of ubiquitin molecules which sequentially attach to the substrate (poly-ubiquitination), or a combination of both. **B)** HECT-E3's form a direct bond between ubiquitin through its active cysteine and then transfer it to the substrate whereas RING-E3's act as adaptors by bringing substrate and E2 in close proximity to facilitate direct transfer of ubiquitin to the substrate.

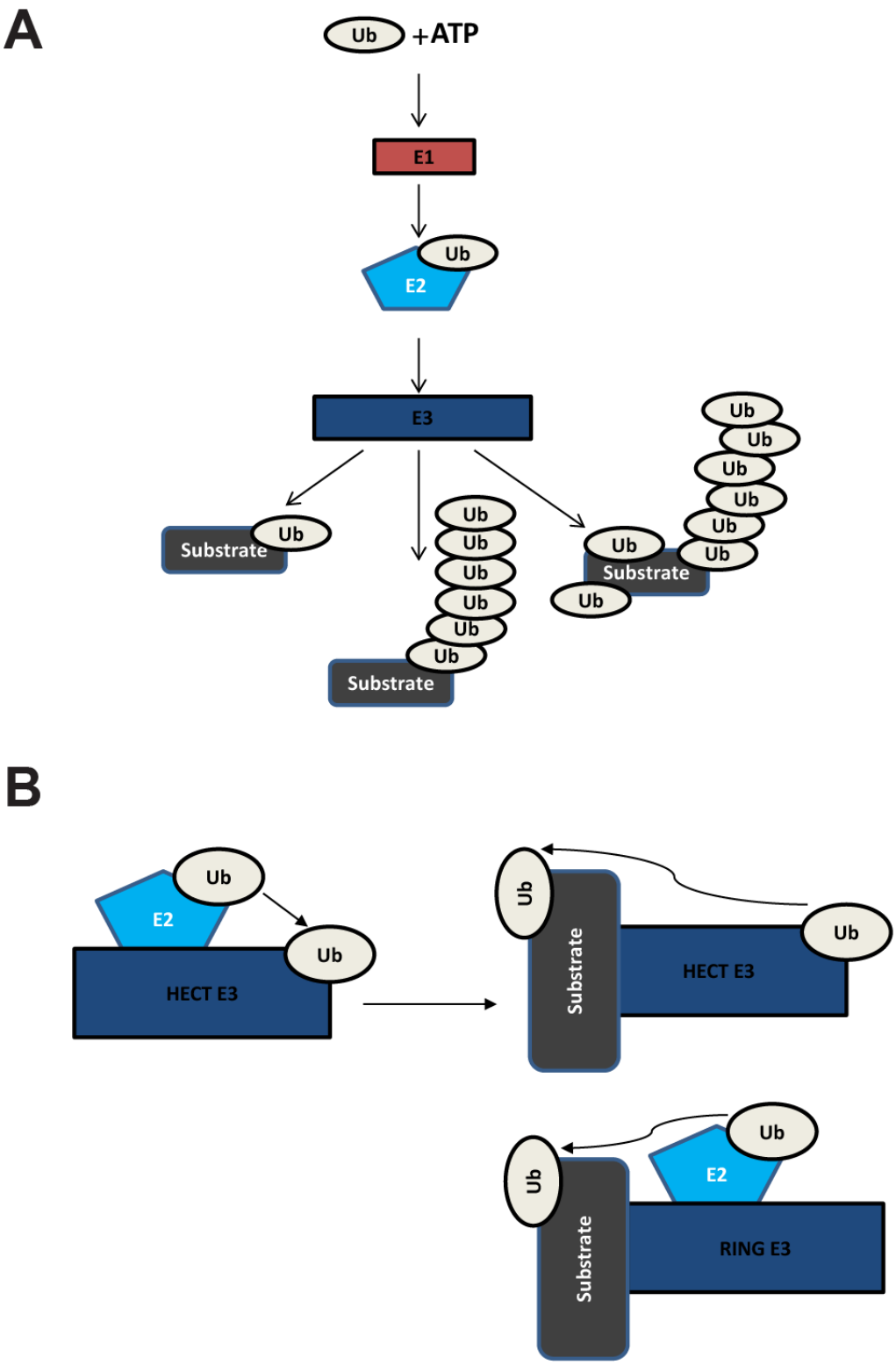
A
Ub
+ATP
E1
Ub
E2
E3
Ub
Substrate
Ub
Ub
Ub
Ub
Ub
Ub
Substrate
Ub
Ub
Ub
Ub
Ub
Ub
Ub
Substrate
B
Ub
E2
Ub
HECT E3
Ub
Substrate
Ub
HECT E3
Ub
Ub
E2
Substrate
RING E3

Fig 1.2 (A) The primary structure of NEDD4-2 protein. NEDD4-2 protein comprises an amino-terminal C2 domain, 4 WW domains and a carboxy-terminal HECT domain. C2 mediates lipid membrane binding, as well as acting as a protein-protein interaction motif. The WW domains are the main mediators of NEDD4-2 interaction with its substrates and adaptors. The HECT is the catalytic domain responsible for binding E2 and for transferring the ubiquitin to the substrate. **(B) The phylogenetic relationship between NEDD4-2 proteins from various species.** The neighbour joining phylogenetic tree construction was carried out using NCBI phylogenetic tree view (http://www.ncbi.nlm.nih.gov/blast/treeview/treeView.cgi). b: Bovine *(BosTaurus*); d: Dog *(Canis lupus familaris);* ma: Monkey *(Macaca mulatta);* p: Chimpanzee *(Pan troglodytes);* g: Chicken *(Gallus gallus);* z: Zebrafish *(Danio rerio);* h: Human *(Homo sapiens);* m: Mouse *(Mus musculus);* r: Rat *(Rattus novergicus); and* x: Frog *(Xenopus tropicalis)*.

A


C2
WW1
WW2
WW3
WW4
HECT E3

B

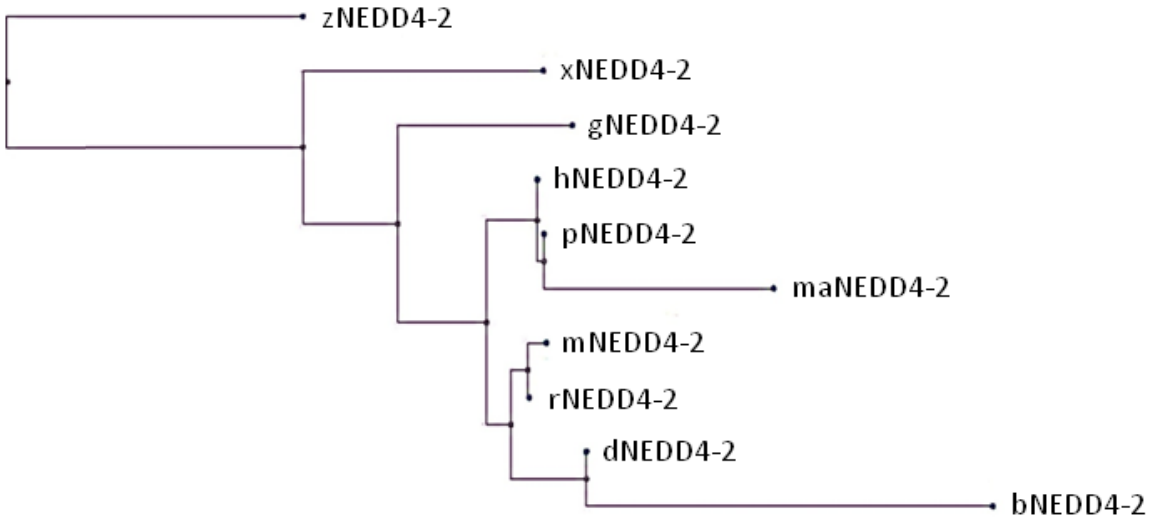
zNEDD4-2
xNEDD4-2
gNEDD4-2
hNEDD4-2
pNEDD4-2
maNEDD4-2
mNEDD4-2
rNEDD4-2
dNEDD4-2
bNEDD4-2

4. NEDD4-2 targets and function

The best known and most studied target of NEDD4-2 is the epithelial sodium channel (ENaC) (Harvey *et al*., 2001, Kamynina *et al*., 2001). In addition to ENaC, multiple proteins have been shown to bind NEDD4-2 and some shown to be ubiquitinated (**Table 1**) (Persaud *et al*., 2009). Fewer have been validated to be genuine NEDD4-2 targets *in vivo*. Below is a summary of the main regulatory functions and relevant targets of NEDD4-2.

Table 1 Potential substrates and/or binding partners of NEDD4-2

Interacting Protein	Functional Groups	References
14-3-3	Inhibitor of NEDD4-2	(Bhalla *et al*., 2005)
ACK-1	Activated Cdc42 associated kinase	(Chan *et al*., 2009)
ATA2	Amino acid transporter	(Hatanaka *et al*., 2006)
AQP2	Aquaporin channel	(de Groot *et al*., 2014)
CLC-5	Chloride channel	(Simon *et al*., 1997, Rickheit *et al*., 2010)
CLC-Ka/Barttin	Chloride channel	(Embark *et al*., 2004)
CFTR	Chloride channel	(Caohuy *et al*., 2009, Koeppen *et al*., 2012)
DAT	Dopamine transporter	(Sorkina *et al*., 2006, Vina-Vilaseca and Sorkin, 2010)
EAAT1/2	Glutamate transporter	(Boehmer *et al*., 2003, 2006)
ENaC	Epithelial sodium channel	(Harvey *et al*., 2001, Kamynina *et al*., 2001)
Dvl2	Dishevelled homolog	(Ding *et al*., 2013, Zhang *et al*.,

		2014)
Dlg3	Disks large homolog 3	(Van Campenhout *et al*., 2011)
KCNQ1	Voltage gated potassium	(Ekberg *et al*., 2007, Jespersen *et*
KCNQ2/3 and	channels	*al*., 2007, Schuetz *et al*., 2008)
KCNQ3/5		
Na_vs (many)	Voltage gated sodium channels	(Fotia *et al*., 2004, van Bemmelen
		et al., 2004, Rougier *et al*., 2005)
Sgk1	Serum glucocorticoid kinase	(Bhalla *et al*., 2005)
SGLT1	Glutamate transporter	(Dieter *et al*., 2004)
SP-C	Surfactant protein C	(Conkright *et al*., 2010)
Smad 2,3,4,7	TGFβ signaling	(Kuratomi *et al*., 2005, Gao *et al*.,
		2009, Moren *et al*., 2005)
TGFβR1	TGFβ signaling	(Kuratomi *et al*., 2005)
Trk	Neutrophin receptor	(Georgieva *et al*., 2011, Yu *et al*.,
		2014)
Tweety	Chloride channels	(He *et al*., 2008)
NCC	Sodium chloride co- transporter	(Arroyo *et al*., 2011)
Ndfip1/2	Adaptors	(Harvey *et al*., 2002, Shearwin-
		Whyatt *et al*., 2004, de Groot *et*
		al., 2014)
Occludin	Tight junction protein	(Raikwar *et al*., 2010)
NEDD4-2	HECT ubiquitin ligase	(Bruce *et al*., 2008)
USP2-45	Deubiquitiylating enzyme	(Oberfeld *et al*., 2011, Krzystanek
		et al., 2012)

4.1 ENaC regulation by NEDD4-2

ENaC is a heterotrimeric channel composed of three subunits (α, β and γ) with each subunit having a conserved protein structure consisting of two transmembrane regions, an extracellular loop and cytoplasmic N and C termini (Canessa *et al*., 1994, Mano and Driscoll, 1999, Staruschenko *et al*., 2005). It is a member of the DEG/ENaC family of ion channels shown to be widely expressed in epithelial tissues such as the kidney, distal colon, lung, skin and trachea (Kashlan and Kleyman, 2012). Normal ENaC function in renal sodium transport is critical as it is necessary for body sodium balance and maintenance of blood pressure (Garty and Benos, 1988). In the lung ENaC is responsible for normal fluid clearance from alveolar spaces and subsequently normal exchange of gases (Collawn *et al*., 2012).

ENaC is down-regulated by both NEDD4 and NEDD4-2 *in vitro*, and NEDD4-2 *in vivo* mediated by direct binding of the WW domains to PY motifs of ENaC (Staub *et al*., 1996, Dinudom *et al*., 1998, Harvey *et al*., 1999, Harvey *et al*., 2001, Kamynina *et al*., 2001, Fotia *et al*., 2003, Snyder *et al*., 2004b). This leads to ENaC ubiquitination and removal from the membrane **(Fig 1.3)**. Abnormal NEDD4-2 mediated ENaC regulation is seen in Liddle's syndrome where ENaC hyperactivity along with increased blood pressure with aberrant Na^+ reabsorption in the kidney is observed (Bhalla and Hallows, 2008). This is due to abrogation in the interaction of NEDD4-2 with ENaC due to mutations or deletions that affect the PY motifs of the αENaC or βENaC subunits. Potential inhibitors of sodium transport in the cellular pathways that affect ENaC via NEDD4-2 include phosphorylation, feedback inhibition by intracellular sodium and dietary sodium intake through aldosterone (Bhalla and Hallows, 2008) **(Fig 1.3)**.

Fig 1.3 NEDD4-2 is a critical regulator of ENaC. NEDD4-2 directly interacts with the PY motifs found in the carboxyl termini of the three ENaC subunits via WW domains 3 and 4 (red). Under conditions where ENaC mediated Na^+ uptake is not required (such as when intracellular Na^+ concentration is high), the ubiquitination of ENaC by NEDD4-2 leads to channel endocytosis and degradation. A disruption of this control mechanism results in increased cell surface ENaC and high ENaC activity, as seen in Liddle's syndrome and the NEDD4-2 KO mice. Under conditions where Na^+ intake through ENaC is active NEDD4-2 acts (at least in part) as a converging point for hormones, such as aldosterone and insulin, which stimulate ENaC activity (directly or indirectly through inactivating NEDD4-2 function). Under this scenario, signaling kinases Sgk1 (serum glucocorticoid-inducible kinase) and Akt (PKB- protein kinase B) phosphorylate NEDD4-2. This promotes binding of NEDD4-2 to 14-3-3, thus inhibiting the ability of NEDD4-2 to bind ENaC subunits.

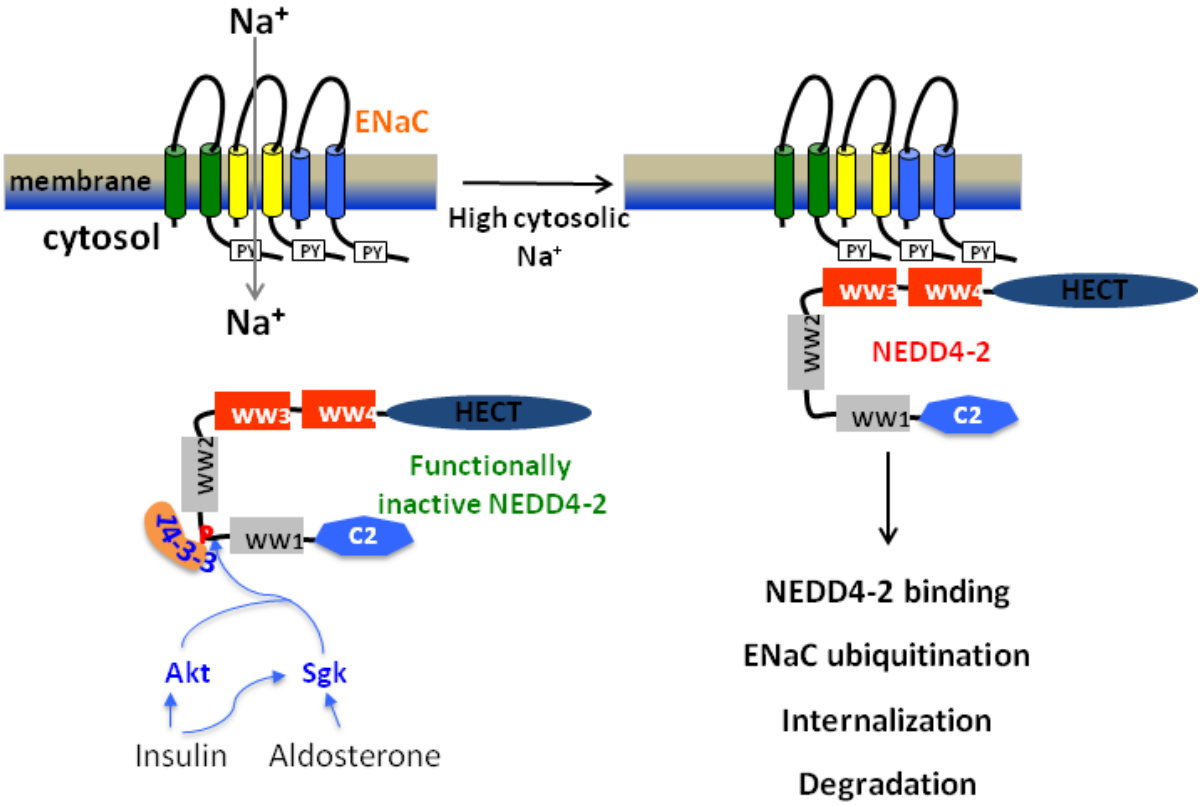
Na+
ENaC
membrane
cytosol
PY
PY
PY
Na+
High cytosolic
Na+
WW3
WW4
HECT
WW2
NEDD4-2
WW1
C2
Functionally
inactive NEDD4-2
14-3-3
P
Akt
Sgk
Insulin
Aldosterone
NEDD4-2 binding
ENaC ubiquitination
Internalization
Degradation

4.2. NEDD4-2 mediated regulation of renal Na^+-Cl^- cotransporter (NCC)

The Na^+-Cl^- cotransporter (NCC), critical for sodium absorption in the distal convoluted tubule (DCT) of the kidney, is also regulated by NEDD4-2. NEDD4-2 interacts with and ubiquitinates NCC at the surface of transfected cells and in Xenopus oocytes. Co-expression of NEDD4-2 with NCC reduces NCC activity and surface expression (Arroyo *et al*., 2011). As NCC does not have a classical PY motif and a PY-like motif in NCC is unable to bind NEDD4-2, it remains unclear how the two proteins interact. NCC has been shown to be regulated via serum glucocorticoid kinase (SGK1)-mediated inhibitory phosphorylation of Nedd4-2 and mutation of NEDD4-2 at both serine 328 and 222 (sites phosphorylated by Sgk1) significantly affected by Sgk1 function (Arroyo *et al*., 2011). Importantly, a deficiency of NEDD4-2 in mouse renal tubules and in cultured mouse distal collecting tubule (mDCT) cells increases NCC activity, suggesting that NEDD4-2 is an *in vivo* regulator of NCC. Furthermore, as discussed in introduction sections **6** and **7**, the regulation of NCC by NEDD4-2 in kidney is critical for Na^+ absorption and NEDD4-2 deficiency specifically in kidney leads to increased blood pressure (Ronzaud *et al*., 2013, Lagnaz *et al*., 2014). These results indicate that NEDD4-2 is an important regulator of NCC.

4.3. NEDD4-2 as a regulator of voltage-gated sodium channels (Na_vs)

Voltage-gated sodium channels (Na_vs) are essential for the generation of action potentials in electrically excitable cells via mediating the influx of Na^+ in response to local depolarizing stimuli. These channels are expressed in many cell types especially in the nervous system as they play a critical role in development, plasticity and tissue integrity (Goldin *et al*., 2000). There are 9 members of the Na_v family and seven of these contain carboxyl terminal PY motifs, which can interact with the WW3 and WW4 domains of both NEDD4 and NEDD4-2 (Fotia *et al*., 2004). Several of these NEDD4-2 interacting Na_v channels are also ubiquitinated by NEDD4-2 and in Xenopus oocytes, and Na_v currents are strongly inhibited by the co-

expression of NEDD4-2 and to a lesser extent by Nedd4 (Fotia *et al*., 2004, van Bemmelen *et al*., 2004). The cardiac Na_v ($Na_v1.5$) expressed in human epithelial kidney (HEK) cells is also strongly inhibited by NEDD4-2 co-expression, accompanied by reduced cell surface expression of $Na_v1.5$ (van Bemmelen *et al*., 2004). Furthermore Na_vs were reported to be down regulated by NEDD4-2 at the cell surface in adult rat dorsal root ganglion (DRG) neurons (Cachemaille *et al*., 2012). In animal models of neuropathic pain where Na_vs play an important role in neuronal excitability, NEDD4-2 was shown to be down regulated, and NEDD4-2-deficiency resulted in hyper excitability in DRG neurons, which contributed to pathological pain (Cachemaille *et al*., 2012, Laedermann *et al*., 2013). These studies collectively suggest a critical role for NEDD4-2 in post-translational regulation of Na_vs.

4.4. Chloride channels as NEDD4-2 targets

CFTR (Cystic fibrosis transmembrane conductance regulator) is a cAMP stimulated Cl^- channel that transports chloride ions across epithelial cell membranes (Pilewski and Frizzell, 1999). Ubiquitination is important for CFTR regulation and it has been reported that various ubiquitin ligases such as c-cbl, Ring finger protein 5 (RMA1/RNF5) and Glycoprotein 78 (GP78) are responsible for wild-type (WT) and mutant CFTR degradation (Morito *et al*., 2008, Ye *et al*., 2010). NEDD4-2 was also reported to be a ubiquitin ligase for CFTR *in vitro (Caohuy et al., 2009)*. NEDD4-2 co-immunoprecipitates with both WT and mutant ΔF508 CFTR which leads to predisposition to loss of protein at the membrane of airway cells. It was shown that NEDD4-2 interaction with both WT and ΔF508 CFTR leads to increased CFTR activity (Caohuy *et al*., 2009). However, a recent study in Xenopus oocytes showed that NEDD4-2 had no effect on CFTR chloride channel current (Koeppen *et al*., 2012). These studies need to be further validated *in vivo* to confirm whether NEDD4-2 interacts with CFTR in a physiological setting. Since CFTR does not have a PY motif, the mechanism by which it interacts with NEDD4-2 also requires further investigation.

Another chloride channel, CLC-5, is expressed in renal and epithelial tissues. Defects in this Cl^-/H^+ exchanger leads to impairment of endocytosis in renal proximal tubules causing kidney stones and Dent's disease (Rickheit *et al*., 2010). Although *in vitro* studies suggest a role for NEDD4-2 in regulating CLC-5, *in vivo* data in mice are inconsistent (Hryciw *et al*., 2004, Rickheit *et al*., 2010). Mice and humans lacking CLC-5 are reported to have hypercalciuria and hyperphosphaturia. Unlike CLC-5 knockout mice, CLC-5 PY knock-in mice display no abnormal proteinuria or hyperphosphorylation with endocytosis being normal (Rickheit *et al*., 2010). Thus, the physiological function of NEDD4-2 in regulating CLC-5 remains to be validated.

CLC-Ka/Barttin, a chloride channel involved in renal tubular transport is also a potential NEDD4-2 target (Embark *et al*., 2004). CLCka and CLCkb chloride channels require co-expression of an essential beta subunit of these channels called Barttin (Embark *et al*., 2004). Mutations in these genes have been shown to cause Barters syndrome variant BSND, with congenital deafness and renal salt wasting (Simon *et al*., 1997). NEDD4-2 binds to the PPxY motif of Barttin leading to its degradation (Embark *et al*., 2004). The Tweety family of chloride channels consists of 3 members identified in humans (TTYH1-3). NEDD4-2 binds to the TTYH2 and 3 family members containing the PPxY motif but not to TTYH1 as it lacks this motif. Also NEDD4-2 is reported to ubiquitinate TTYH2 and 3 (He *et al*., 2008). Neither Barttin nor Tweety channels have been validated as *in vivo* targets of NEDD4-2 as physiological data on the levels or regulation of these channels in NEDD4-2 knockout mice is currently not available.

4.5 Potassium channels as putative NEDD4-2 targets

KCNQs are a family of potassium channels. In the heart, KCNQ1 alpha subunit binds to the KCNE beta subunit to form a channel complex. KCNQ1/KCNE levels have been shown to be reduced upon expression with NEDD4-2 (Jespersen *et al*., 2007). Further *in vivo* evidence indicates that expression of the catalytically inactive form of NEDD4-2 in guinea pig cardiomyocytes leads to increased KCNQ1 current (Jespersen *et al*., 2007). NEDD4-2 co-expression decreases total levels of KCNQ1 in HEK293 cells due to ubiquitination (Jespersen *et al*., 2007). This was corroborated by a study in *Xenopus* oocytes and in collecting duct epithelial cells (Alzamora *et al*., 2010).

The activities of voltage gated KCNQ2/3 and KCNQ3/5 channels, which play pivotal roles in regulating neuronal excitability, are also shown to be affected by NEDD4-2 co-expression in *Xenopus* oocytes (Schuetz *et al*., 2008). NEDD4-2 has also been implicated in ubiquitinating and regulating the potassium channel encoded by the human Ether-a-go-go-related gene (hERG), which is important for cardiac repolarisation (Albesa *et al*., 2011, Guo *et al*., 2012, Cui and Zhang, 2013). NEDD4-2 mediated degradation of hERG channels was found upon disrupting the NEDD4-2 binding domain in hERG channels which completely ablated the effect of muscarinic receptor on hERG channel expression (Wang *et al*., 2014). These studies suggest that NEDD4-2 can potentially regulate a number of potassium channels. However, these conclusions are derived largely from *in vitro* studies and have not yet been validated in genetically modified animal models.

4.6. Surfactant protein C (SP-C) as a NEDD4-2 substrate

NEDD4-2 has been shown to bind to the surfactant protein C (SP-C), an interaction involving NEDD4-2 WW domains and a PPxY motif in SP-C (Kotorashvili *et al*., 2009, Conkright *et al*., 2010). SP-C is released as a phospholipid rich film synthesized by alveolar type 2 epithelial cells and is involved in reducing surface tension. As such, a lack of this surfactant

causes respiratory distress in premature infants and mutations in the SP-C gene have been shown to cause interstitial lung disease (Nogee *et al*., 2002). Mutation of the SP-C PY motif abrogated binding to NEDD4-2 and reduced secretion of SP-C. However, a physiological role of NEDD4-2 in SP-C regulation is not fully established as NEDD4-2-deficient mice fail to show any defects in the levels of surfactant protein C in the lungs (Boase *et al*., 2011).

4.7. Other channels and transporters

Other potential membrane protein substrates/targets of NEDD4-2 include EAAT1/2, the glial excitatory amino acid transporters that are responsible for glutamate and aspartate uptake (Boehmer *et al*., 2003, Boehmer *et al*., 2006). In separate studies these transporters were inhibited by co-expressed NEDD4-2 in *Xenopus* oocytes (Boehmer *et al*., 2003, Boehmer *et al*., 2006). This inhibitory effect of NEDD4-2 could be reversed upon additional expression with SGK1, SGK3 and PKB but not by an inactive mutant of SGK1, suggesting that phosphorylation inhibits NEDD4-2 function (**Fig.2**) (Lang *et al*., 2006). The amino acid transporter ATA-2, Na^+ glucose transporter 1 (SGLT1), divalent metal ion transporter DMT1, calcium channels Orai1/STIM1, neurotrophin receptor TrkA and hyperpolarization activated cyclic nucleotide gated HCN1 channel have also been shown to be inhibited *in vitro* by NEDD4-2 (Dieter *et al*., 2004, Hatanaka *et al*., 2006, Howitt *et al*., 2009, Eylenstein *et al*., 2011, Georgieva *et al*., 2011, Lang *et al*., 2012, Wilkars *et al*., 2014).

Another potential substrate of NEDD4-2 is the dopamine transporter (DAT), which is necessary to terminate dopamine neurotransmission (Sorkina *et al*., 2006). A model for NEDD4-2 mediated DAT endocytosis has been proposed where the PKC-induced ubiquitination of DAT is mediated by NEDD4–2. This leads to interaction of DAT with adaptor proteins in the coated pits, such as epsin and Eps15, promoting DAT endocytosis (Georgieva *et al*., 2011, Vina-Vilaseca *et al*., 2011). *In vivo* physiological significance of these studies awaits experiments in animal models.

4.8. Regulation of TGFβ signalling by NEDD4-2

Several studies propose a role for NEDD4-2 mediated ubiquitination in the control of TGFβ signalling, however *in vivo* validation of these studies requires further work. NEDD4-2 has been shown to down regulate TGFβR1 through Smad7, which acts as PY motif containing adaptor and induces the ubiquitin-mediated degradation of TGFβR1 (Kuratomi *et al*., 2005). Following receptor activation, NEDD4-2 was also shown to bind to regulatory Smad2 but not Smad3, leading to its degradation (Gao *et al*., 2009). Over expression of NEDD4-2 in the liver hepatocellular carcinoma cell line (HepG2) decreases TGFβ signaling whereas silencing NEDD4-2 increases it (Kuratomi *et al*., 2005). Thus NEDD4-2 can potentially regulate TGFβ signaling by targeting more than one component of the signaling cascade.

4.9. NEDD4-2 in virus budding

Nedd4-2 has been implicated in budding of enveloped RNA viruses, such as the human immunodeficiency virus-1 (HIV-1) (Martin-Serrano *et al*., 2005). These viruses interact with NEDD4-2 through its WW domains leading to ubiquitination of the viral matrix proteins, and in turn recognition by the ESCRT (endosomal sorting complex required for transport) machinery that the viruses recruit for budding. The late domains within the HIV-1 $p6^{Gag}$ recruits two ESCRT proteins, tumor susceptibility gene 101 (TSG101) and Apoptosis linked gene-2 interacting protein X (ALIX), to facilitate virus budding (Segura-Morales *et al*., 2005, Putz *et al*., 2008, Dussupt *et al*., 2009, Usami *et al*., 2009, Sette *et al*., 2010). Over expression of NEDD4-2 promotes release of the variant HIV-1 that is deficient in TSG101 and ALIX-binding late domains, whereas the knockdown of endogenous NEDD4-2 inhibited virus release (Chung *et al*., 2008). These results suggest a direct and critical role for NEDD4-2 in budding through interaction with the viral proteins and components of the ESCRT machinery.

4.10. Other substrates of NEDD4-2

Dishevelled-2 (Dvl2) is a critical player in the Wnt signalling and is important for embryogenesis and tissue homeostasis (Ding *et al*., 2013, Zhang *et al*., 2014). NEDD4-2 has been proposed to play a role in Wnt signalling by mediating Dvl2 degradation. In Xenopus embryos NEDD4-2 inhibits Dvl2 induced dorsal axis duplication upon activation of Wnt signalling pathway (Ding *et al*., 2013, Zhang *et al*., 2014). Another novel NEDD4-2 interacting protein is *Drosophila* disc large scaffolding protein (Dlg3), which is a tumour suppressor (Lickert and Van Campenhout, 2012). Dlg3 binds NEDD4-2 through its PPxY motif, resulting in Dlg3 monoubiquitination, regulating apical membrane recruitment and tight junction consolidation (Van Campenhout *et al*., 2011).

Occludin is an integral membrane protein in tight junctions responsible for tight junction integrity and paracellular barrier (Feldman *et al*., 2005). NEDD4-2 has been shown to interact with occludin through a PY motif, reduce occludin levels and inhibit tight junction formation (Raikwar *et al*., 2010). In cortical collecting duct (mpkCCD) cells NEDD4-2 over expression leads to reduced levels of occludin in tight junctions and increased levels of transient paracellular conductance with delay in tight junction formation. On the other hand, NEDD4-2 depletion results in increased levels of occludin and paracellular conductance (Raikwar *et al*., 2010). Thus NEDD4-2 may play a role in the controlling tight junctions in epithelia.

4.11 NEDD4-2 substrate interaction through adaptors

While most proteins interact with the NEDD4 family of ubiquitin ligases directly through PY motif-WW domain mediated binding, other targets use adaptors that bind the WW domains of the NEDD4 E3s. Two types of such adaptors have been described, the NDFIPs (NDFIP1 and NDFIP2) and Arrestin domain containing proteins (Arrdcs) (Lin *et al*., 2008, Nikko *et al*., 2008, Mund and Pelham, 2009). NDFIP1 (N4WBP5) was discovered in a screen to identify proteins that bind NEDD4 WW domains (Harvey *et al*., 2002). NDFIP2

(N4WBP5A) was identified as a protein closely related to NDFIP1 (Konstas *et al*., 2002, Shearwin-Whyatt *et al*., 2004, Shearwin-Whyatt *et al*., 2006). These proteins contain 3 transmembrane domains and localize to intracellular membranes in the Golgi, endosomes and the multivesicular bodies. Both proteins also contain 3 PY motifs which interact with NEDD4 family members via their WW domains. Through NDFIP1, NEDD4-2 and WWP2 ligases regulate the divalent metal ion transporter DMT1 (the primary non-heme iron transporter) (Foot *et al*., 2008). In addition, over expression of NDFIP1 in neurons recruits NEDD4, NEDD4-2 and ITCH proteins into exosomes (Howitt *et al*., 2009). More recently both NDFIP1 and NDFIP2 were shown to be adaptors for the water channel aquaporin 2 (AQP2) (Velic *et al*., 2005, de Groot *et al*., 2014). In transfected HEK293 cells NDFIP1 and NDFIP2 bound AQP2 and were essential for NEDD4/NEDD4-2-mediated ubiquitination and degradation of AQP2. In mpkCCD cells, down regulation of NDFIP1, but not NDFIP2, increased AQP2 levels and in mouse kidney, NDFIP1, but not NDFIP2, co localized and coimmunoprecipated with AQP2. These results indicate that NDFIP1 is more likely an adaptor for the AQP2-NEDD4/NEDD4-2 interaction (de Groot *et al*., 2014).

While a role for NDFIP2 as an adaptor or regulator of NEDD4-2 is less well established, it is suggested to be both a recruiter and an activator of several NEDD4 family members (Mund and Pelham, 2009). In *Xenopus* oocytes NDFIP2 increases surface expression and activity of ENaC possibly by interfering with Nedd4-2-mediated regulation of ENaC. NDFIP2 is highly expressed in renal collecting ducts along with ENaC, and thus may modulate NEDD4-2-mediated ENaC regulation *in vivo* (Konstas *et al*., 2002).

14-3-3 are a family of ubiquitously expressed adaptor proteins that bind to phosphoserine and phosphothreonine motifs (Bhalla *et al*., 2005, Bridges and Moorhead, 2005, Ichimura *et al*., 2005). They regulate signalling by preventing interaction of target proteins with their downstream interacting proteins. 14-3-3 proteins have been shown to bind to one of the

phosphoserine motifs in NEDD4-2. Several kinases like Sgk1 and Akt phosphorylate NEDD4-2 on specific serine residues, which promote recruitment and binding of 14-3-3 proteins (Snyder *et al*., 2002, Snyder *et al*., 2004a, Bhalla *et al*., 2005, Nagaki *et al*., 2006, Lee *et al*., 2007, 2009). The binding of 14-3-3 inhibits NEDD4-2 function by preventing it from interacting with its substrates, such as the ENaC (Nagaki *et al*., 2006). The kinase Sgk1 is itself shown to be a target of NEDD4-2, in addition to mediating NEDD4-2 phosphorylation (Bhalla *et al*., 2005).

5. NEDD4-2/NEDD4L in human disease

5.1. Hypertension

Consistent with *in vitro* and mouse studies, in humans NEDD4-2 is important in maintaining blood pressure and single nucleotide polymorphisms (SNPs) in NEDD4L (the human NEDD4-2) gene on chromosome 18q21 are linked to familial hypertension (Dunn *et al*., 2002, Russo *et al*., 2005, Svensson-Farbom *et al*., 2011). There are three main isoforms of NEDD4L: those containing a novel C2 domain (isoform I), an intact conserved C2 domain (isoform II), or an alternate start codon that lacks a C2 domain (isoform III) (Itani *et al*., 2005). Isoform 1 is abundant in kidney and adrenal gland and isoform 2 abundant in the lungs. Differences in isoform expression in multiple tissues could potentially alter NEDD4-2 function in regulating membrane proteins (Araki *et al*., 2008, Raikwar and Thomas, 2008).

There are numerous NEDD4L SNPs of which rs4149601 is the most common, carrying a G/A variation in exon 1 of isoform I (Dunn *et al*., 2002, Ishigami *et al*., 2010). Depending on ethnicity this variation is found in 16-41% individuals and leads to expression of a novel C2 domain (Luo *et al*., 2009). The G allele of this isoform is involved in hypertension and enhanced salt sensitivity, whereas the A allele is linked to hypertension due to increased Na^+ absorption (Fava *et al*., 2006). Carriers of rs4149601GG genotype along with rs2288774 CC genotype have increased salt sensitivity and increased blood pressure. In *Xenopus* oocytes,

isoform I (G allele) is shown to down regulate other NEDD4L isoforms and prevent ENaC down regulation (Araki *et al*., 2008, Svensson-Farbom *et al*., 2011).

Recently Dahlberg *et al*. (2014) reported genetic variations in NEDD4L associated G allele of SNP rs4149601with increased blood pressure leading to cardiovascular death (Dahlberg *et al*., 2014). In another study on the Chinese Han population, genetic variation of NEDD4L was found to be associated with essential hypertension and related phenotypes with three representative polymorphisms in NEDD4L (rs228874, rs3865418 and rs149601), which was attributed to sex dependent effect in hypertension development (Wen *et al*., 2008). The NEDD4L allelic variants rs12606138 and rs8094327 have also been implicated as risk factors in dyslexia, a disease characterized by impaired reading and writing (Mueller *et al*., 2014). However the mechanisms of how these variants affect functions that lead to the risk remain unclear.

5.2. Cancer

Through its potential functions in regulating key signalling pathways such as EGFR, TGFβ and Wnt, NEDD4L has been suggested to act as tumour suppressor, however direct experimental evidence for such a function is still lacking. Both increased and reduced expression of NEDD4L transcripts in human prostate cancer has been reported (Qi *et al*., 2003, Hu *et al*., 2009, Hellwinkel *et al*., 2010). Lower levels of NEDD4L have been seen in non-small cell lung cancer, gastric cancer, gliomas with poor prognosis, colorectal cancer where NEDD4L has been reported to inhibit Wnt signalling, and gall bladder cancer where NEDD4L has been reported to modulate the transcription of MMP-1 and MMP-13 involved in gall bladder cancer invasion (Takeuchi *et al*., 2011, Gao *et al*., 2012, He *et al*., 2012, Sakashita *et al*., 2013). Patients with Sezary syndrome, a cutaneous T cell lymphoma, show an increase in the transcripts of NEDD4L (Booken *et al*., 2008).

Recent reports indicated the possible involvement of NEDD4L in melanoma. The knockdown of NEDD4L in cultured melanoma cells reduces growth, whereas NEDD4L over expression in xenograft models promotes melanoma tumour growth (Kito *et al*., 2014). In pancreatic ductal adenocarcinoma (PDAC) NEDD4L was amongst the genes targeted by microRNAs (miR) miR21, miR23a and miR27a, which aid in reduction of cell proliferation in PDAC cells (Frampton *et al*., 2014). The N-myc downstream regulated gene-1 (NDRG1), a negative regulator of tumour progression in multiple neoplasms and pancreatic cancer, up regulates NEDD4L (Kovacevic *et al*., 2013). Hepatocellular carcinoma caused by altered Wnt/β-catenin signalling in human hepatoma cells shows an apparent increase in levels of NEDD4L (Kovacevic *et al*., 2013). Thus altered levels of NEDD4L are often associated with multiple tumour types. That said, there is no data directly showing that NEDD4-2 (NEDD4L) loss *in vivo* is responsible for tumour growth or suppression and much mechanistic and *in vivo* animal work is required before the function of NEDD4-2 in cancer can be fully established.

6. Studies with *NEDD4-2* knockout (KO) mice

At least three independent *NEDD4-2* KO mice lines have been generated to study the *in vivo* function of NEDD4-2. *NEDD4-2* KO mice reported by Shi *et al*. (2008) are developmentally normal, viable and live a normal life span. However they show a slight increase in ENaC expression and mild salt sensitive hypertension, suggesting that ENaC regulation by NEDD4-2 is critical, confirming *in vitro* data (Shi *et al*., 2008).

In contrast to the mice generated in a mixed genetic background by Shi *et al*., (2008), a *NEDD4-2* KO mouse model in a C57B16 pure genetic background showed foetal or perinatal lethality (Boase *et al*., 2011). These mice appear to be null as both *NEDD4-2* mRNA and protein were found to be absent (Boase *et al*., 2011). Most of the KO mice died just prior to birth due to collapsed alveolar spaces resulting in respiratory failure, and show elevated ENaC expression in the lung and kidney. Consistent with the higher expression, ENaC

currents in alveolar type II lung cells from embryonic day 18.5 KO mice were found to be greatly elevated and this presumably is the cause of premature lung fluid clearance and failure to inflate lungs (Boase *et al*., 2011). A small percentage of *NEDD4-2* KO animals that survive birth live for up to 22 days. They also show increased α and β ENaC expression in the kidneys and the lung and die due to severe lung inflammation. The phenotypic differences between the two strains of *NEDD4-2* KO mice may be due to the presence of a small amount of functional NEDD4-2 protein present in the Shi *et al*. (2008) KO strain.

Many of the observations from the Boase *et al*. (2011) studies were recapitulated in an independently generated *NEDD4-2* KO line by Kimura *et al.* (2011), which reported that NEDD4-2 deletion specifically in lung epithelia results in a cystic fibrosis-like disease, characterized by airway mucus obstruction in the airways and severe inflammation (Kimura *et al*., 2011). Like the Boase *et al*. (2011) mouse strain, the Kimura *et al.* (2011) mice showed elevated ENaC levels and activity in primary alveolar type II cells, and animals died within three weeks of birth due to severe lung inflammation (Kimura *et al*., 2011). Importantly, the lung phenotype could be rescued by the administration of amiloride (an inhibitor of ENaC) into the lungs of neonates, suggesting that the defect is directly due to increased ENaC function in the *NEDD4-2* KO mice (Kimura *et al*., 2011). The two studies combined confirm that NEDD4-2 is a critical regulator of ENaC in the lung and its absence results in lethality in mice.

In another study, Ronzaud *et al*. (2013) generated an inducible renal tubule-specific *NEDD4-2* deletion. When fed a high Na^+ diet these mice show hypercalciuria and hypertension. Interestingly these defects could be reversed by thiazide (an inhibitor of NCC) treatment. Consistent with this, NCC protein levels were increased in KO kidneys, along with increased βENaC and γENaC, as well as the renal outer medullary K^+ channel (ROMK). These observations confirm previous *in vitro* studies that NEDD4-2 is a regulator of NCC and

indicate that NEDD4-2 deficiency in adult renal tubules is sufficient to cause mild, salt-sensitive hypertension without hyperkalemia (Arroyo *et al*., 2011). They also suggest that NEDD4-2 is a key regulator of renal Na^+ homeostasis through a number of ion channels.

Using neuron-specific gene KO in mice and gene ablation experiments in *Xenopus*, NEDD4, the prototypic member of the family, has been shown to be essential for dendrite growth and arborization (Kawabe *et al*., 2010, Drinjakovic *et al*., 2010). A recent study using post mitotic neuron-specific *NEDD4-2* conditional KO mice shows that NEDD4-2 is also required for neurite growth, as NEDD4-2 deletion resulted in a reduction of neurite complexity (Hsia *et al*., 2014). While NEDD4 targets Rap2 for ubiquitination to modulate dendrite growth, the precise substrate(s) of NEDD4-2 that may explain the neurite complexity phenotype in the KO mice is not known (Kawabe *et al*., 2010, Hsia *et al*., 2014).

Finally, a recent study tested if the neurons derived from *NEDD4-2* KO mice show any aberrations in the control of Na_v (Ekberg *et al*., 2014). Using patch-clamping of neurons from *NEDD4-2* KO mice, surprisingly it was noted that at steady-state, the expression of Na_v channels on the plasma membrane of DRG and cortical neurons is not regulated by NEDD4-2. However, it was demonstrated that NEDD4-2 is involved in activation-induced down-regulation of Na_vs in cortical neurons isolated from the *NEDD4-2* KO embryos but not in embryonic DRG neurons (Ekberg *et al*., 2014). The activation-induced down-regulation involving NEDD4-2 occurs in response to increased intracellular Na^+, which suggests that like ENaC, Na_vs are regulated by a feedback inhibitory mechanism dependent on NEDD4-2 mediated ubiquitination, endocytosis and subsequent degradation (Ekberg *et al*., 2014). The pathophysiological consequences of such a mechanism of Na_v regulation require further study, perhaps using a conditional tissue specific *NEDD4-2* KO model.

7. Kidney structure, function and disease

The kidneys are a pair of bean-shape organs found in the abdominal region positioned to the left and right of the body that filter waste products from the blood, form and excrete urine, and regulate body fluid and electrolyte balance (Chmielewski, 2003). The kidney consists of renal parenchyma divided into two main portions, the cortex and the medulla. The cortex consists of glomeruli, required for blood filtration (Chmielewski, 2003). The medulla is further subdivided into renal pyramids which are required for the urine flow into the major and minor renal calyxes (Chmielewski, 2003). The renal pelvis is connected to the ureter from here and the urine flows into the ureter and into the bladder (Chmielewski, 2003, Kuo and Ehrlich, 2012) **(Fig 1.4).**

The kidney aids in regulating important functions within the body by maintaining urine production, elimination, electrolyte balance, nitrogenous waste dissemination, water level and pH regulation (Amirlak and Dawson, 2000). Urine is generated within the kidney in exchange to blood circulation. Nephrons are the basic building blocks of the kidney; they are responsible for the maintenance of excretory and reabsorbed electrolytes in the body (Amirlak and Dawson, 2000). During reabsorption, the level of pH, electrolytes and water are maintained by the kidney for proper function. The excretion of unwanted materials occurs after reabsorption where unwanted material like urea, creatinine, and uric acid are excreted out with urine (Amirlak and Dawson, 2000).

Nephrons can be divided into the renal corpuscle, needed for initial filtration, and renal tubules, where ion secretion and reabsorption takes place (Amirlak and Dawson, 2000). The renal corpuscle consists of the glomerulus and Bowman's capsule, and blood is filtered from the glomerulus through gaps between the Bowman's capsule, which is comprised of podocytes and epithelial cells (Amirlak and Dawson, 2000). The filtered fluid is then transferred to the renal tubules. The majority of ion homeostasis is undertaken here to

maintain sodium (Na^+), potassium (K^+), chloride (Cl^-), carbonate (HCO_3^-) and calcium (Ca^{2+}) concentration in the blood (Amirlak and Dawson, 2000, Kuo and Ehrlich, 2012) **(Fig 1.4).**

The fluid enters the loop of Henle, composed of descending and ascending parts. The ascending loop is responsible for maintaining Na^+, K^+ and Cl^- balance (Kuo and Ehrlich, 2012). The distal portion of the loop of Henle, called the thick ascending loop, is responsible for NaCl reabsorption via the Na^+-K^+-$2Cl^-$ (NKCC2) cotransporter, whereas K^+ is secreted through the K^+ channel ROMK, required for NKCC2 activity (Kuo and Ehrlich, 2012). In the loop of Henle around 90% of Ca^{2+} is reabsorbed into the bloodstream. In the distal convoluted tubule the Na^+-Cl^- cotransporter (NCC) is essential for NaCl reabsorption and fluid is reabsorbed via the chloride channel ClC-Kb (Kuo and Ehrlich, 2012). The modified filtrate then enters collecting duct system before entering the urinary bladder (Kuo and Ehrlich, 2012). This duct system consists of connecting tubules, cortical collecting ducts and medullary collecting ducts. Sodium in the filtrate is reabsorbed through ENaC on the luminal side of the duct epithelial cell membrane and exits into the bloodstream through the Na^+-K^+-ATPase pump (Kuo and Ehrlich, 2012).

Apart from the plasma membrane ion channels in the kidney, intracellular ion channels also play a role in kidney function. For example, polycystin-2 also known as TRPP2 (Transient receptor potential polycystin 2) belongs to family channel resides and is responsible for Ca^{2+} release at the endoplasmic reticulum within the renal epithelial cells with polycystin-2 expression widespread throughout the nephron, is expressed in the distal convoluted tubules predominantly (Kuo and Ehrlich, 2012). Alterations in polycystin-2 lead to the development of cysts throughout the nephronal segments (Mochizuki *et al*., 1996). Polycystin-2 (TRPP2) is known to interact with polycystin-1(Trans membrane protein) on the plasma membrane leading to the formation of an effective calcium permeable channel (Qian *et al*., 1997). Mice models suggest that polycystin-2 is one of the leading causes of cyst formation in the kidneys

apart from vascular defects, aneurysms and hypertension (Pennekamp *et al*., 2002). Other studies have suggested mutations in polycystin-1 and polycystin-2 increase fluid filled cysts causing end stage renal failure (Pennekamp *et al*., 2002). However, the role of polycystins in renal cyst development is still not very well characterised. There are 8 families of non-selective transient receptor potential channels with 8 members within these highly expressed within the kidney (Kuo and Ehrlich, 2012). Other than polycystin-2, two more channels TRPC6 (C stands canonical) and TRPM6 (M stands for melastatin) are associated with renal channelopathies (Kuo and Ehrlich, 2012). TRPC6 is responsible for intracellular Ca^{2+}, predominantly expressed in the glomerulus and collecting duct, with gain of function mutation in this channel leading to focal segmental glomerulosclerosis (Nilius, 2007, Heeringa *et al*., 2009, Dietrich *et al*., 2005). TRPM6 on the other hand preferentially conducts Mg^{2+} apart from Ca^{2+} conductance. Loss in function of TRPM6 due to mutations have been reported to cause loss in Mg^{2+} absorption leading to hypomagnesmia with loss of Ca^{2+} being a secondary effect in the renal epithelial cells (Voets *et al*., 2004, Voets *et al*., 2003). As described earlier, renal channelopathies could be due to genetic mutations and post translational defects causing alteration in the function of ion channels like ENaC, ROMK, CLC-5 and transient receptor potential family of ion channels responsible for renal homeostasis (Kuo and Ehrlich, 2012). To understand the novel role Nedd4-2 plays in renal homeostasis by regulation of ion channels/ substrates within the kidney, leading to renal pathology the below mentioned study was undertaken.

Fig 1.4 Structure and nephronal segments of the kidney. Anatomy of the kidney consisting of cortex, medulla, renal pelvis and ureter. Nephron and its tubular arrangement with expression of ion channels across the different parts of the nephron. TRPC6 (Ca^{2+}) expressed in glomerulus, TRPM6 expressed in distal convoluted tubule (Mg^{2+}), CLC5 expressed in proximal tubule (Cl^-/H^+), CLC-Kb (Barttin) expressed in loop of Henle (Cl^-), ROMK (KCNJ1) expressed in thick ascending loop of Henle, distal nephrons (K^+), ENaC expressed in the collecting duct (Na^+) and Polycystin-2 (TRPP2) is expressed throughout the nephron (predominant in convoluted tubules) (Ca^{2+}). Reproduced from (Kuo and Ehrlich, 2012).

Chapter 1: Introduction

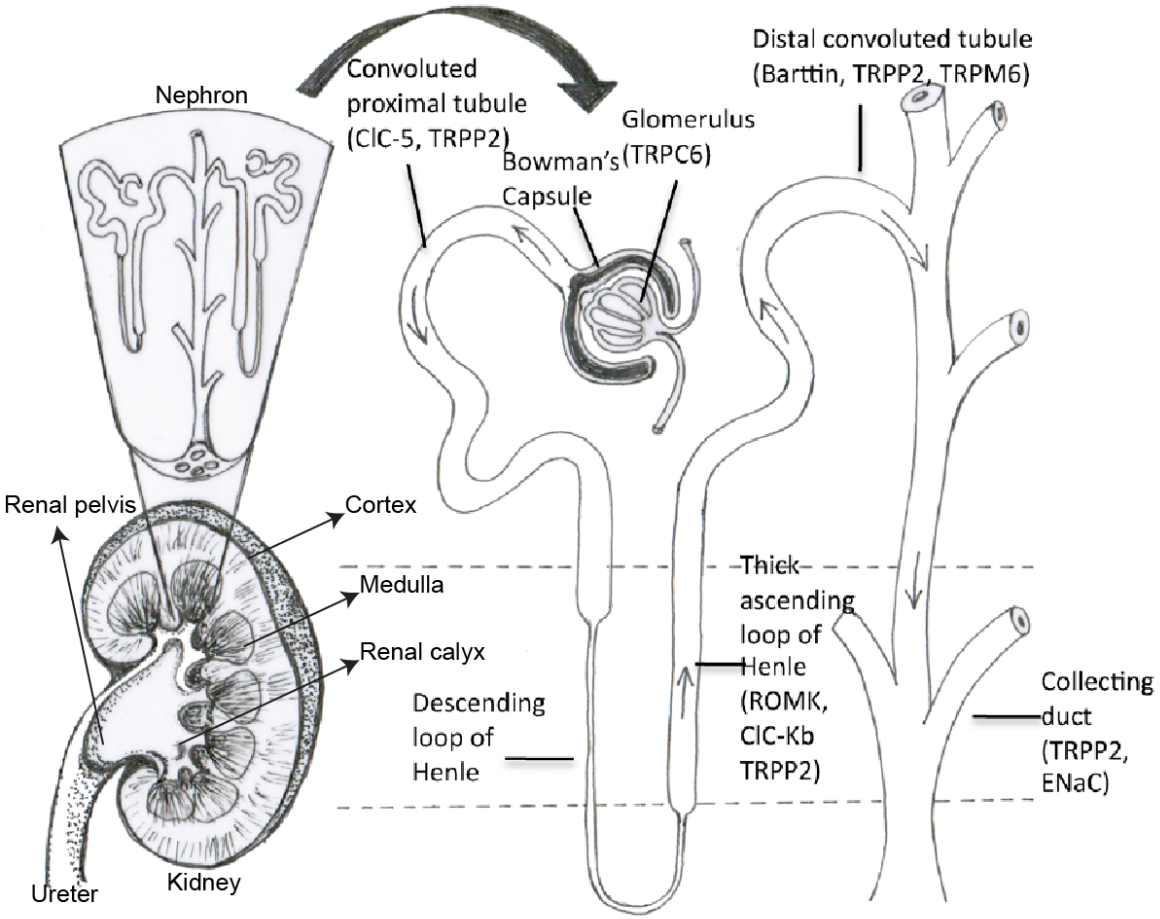

8. Project Aims

As discussed in **section 6**, recently generated *NEDD4-2* KO mouse models have been instrumental in providing novel insights into the biological functions of Nedd4-2. As part of the phenotypic characterisation of Nedd4-2 KO mice, we noticed a previously undescribed pathology in kidneys of mice deficient in Nedd4-2. The characterisation of this complex renal phenotype is the subject of this thesis.

Based on initial observations of the renal phenotype in *NEDD4-2* KO mice it was hypothesized that NEDD4-2 plays a critical role in renal homeostasis by either directly or indirectly regulating substrates involved in renal cysts and/or renal dysplasia.

The specific aims of this study were to:

1) Histologically and morphologically characterise the renal phenotype in *Nedd4-2*$^{-/-}$ mice.

2) Investigate a possible role for polycystins in the *Nedd4-2*$^{-/-}$ renal phenotype, especially with regards to renal cyst formation, and test whether the polycystin proteins are substrates of Nedd4-2.

3) Use differential gene expression study for understanding the transcriptional changes within the *Nedd4-2*$^{-/-}$ kidney phenotype to decipher the genetic processes and molecular pathways affected.

Chapter 2:

Characterization of the *Nedd4-2*$^{-/-}$ kidney phenotype

Statement of Authorship

Title of Paper	Characterization of the *Nedd4-2*$^{-/-}$ kidney phenotype
Publication Status	☐ Published ☐ Accepted for Publication ☐ Submitted for Publication ☑ Unpublished and Unsubmitted w ork w ritten in manuscript style
Publication Details	

Principal Author

Name of Principal Author (Candidate)	Pranay Goel
Contribution to the Paper	Wrote the manuscript, edited the manuscript, evaluated the data , made figures, experimental design Note: work included in this thesis has been solely done by me and the experiments otherwise have been duly acknowledged. The contribution of the work in this thesis chapter-2 with two figures taken from the co-author.
Overall percentage (%)	80%
Certification:	This paper reports on original research I conducted during the period of my Higher Degree by Research candidature and is not subject to any obligations or contractual agreements with a third party that would constrain its inclusion in this thesis. I am the primary author of this paper.
Signature	Date 2/12/15

Co-Author Contributions

By signing the Statement of Authorship, each author certifies that:

i. the candidate's stated contribution to the publication is accurate (as detailed above);

ii. permission is granted for the candidate in include the publication in the thesis; and

iii. the sum of all co-author contributions is equal to 100% less the candidate's stated contribution.

Name of Co-Author	Dr. Jantina Manning
Contribution to the Paper	Helped in data interpretation, experimental design for the below mentioned experiments and manuscript evaluation. (Fig2.12-cAMP assay,Fig2.5- Nephronal marker staining)
Signature	Date 2-12-15

Name of Co-Author	Dr. Tanya henshall
Contribution to the Paper	Helped in data interpretation, experimental design for the below mentioned experiments and manuscript evaluation. (Kidney dysplasia- Fig 2.15)
Signature	Date 2-12-15

Name of Co-Author	Prof.Sharad Kumar
Contribution to the Paper	Supervised development of work,, experimental design, co-wrote the manuscript
Signature	Date 2-12-15

Please cut and paste additional co-author panels here as required.

Chapter 2: Characterization of *Nedd4-2*$^{-/-}$ kidney

2.1 Introduction

Kidneys play a pivotal part in maintaining body homeostasis (Chmielewski, 2003). Abnormalities associated with kidney dysfunction and development are characterised into disorders like renal agenesis, renal dysplasia, renal hypoplasia, autosomal recessive polycystic kidney disease (ARPKD), autosomal dominant polycystic kidney disease (ADPKD), juvenile nephronophthisis and medullary cystic kidney disease (Wilson and Goilav, 2007, Schedl, 2007). Renal cystic kidney syndromes can be acquired due to ailments affecting other parts of the body. Tuberous sclerosis patients suffering from epilepsy, mental retardation and fleshy nodules underneath the skin also acquire cysts in the kidney (Shepherd *et al*., 1991). Von Hippel Lindau disease is an inherited condition that occurs in children born to affected parents that is associated with blood vessel abnormalities of the brain and eyes, with cysts formed in pancreas, kidney and epididymis. There are chances of cysts manifesting into cancer (Maher *et al*., 2011). Multicystic dysplastic kidneys are the most common type of paediatric renal cystic disease (Cramer and Guay-Woodford, 2015, Atiyeh *et al*., 1992). The kidneys look like a bunch of grapes from the outside but with little renal tissue the kidney contours are maintained (Schedl, 2007, Cramer and Guay-Woodford, 2015). Simple renal cysts occur in individuals between birth and age 18 years, and in 50% of the population by the age of 50 years (Cramer and Guay-Woodford, 2015). These cysts are no major problem until they develop into larger ones (Schedl, 2007, Cramer and Guay-Woodford, 2015). Medullary sponge kidneys are characterised by small but multiple cysts formed in the tubules that collect urine (Cramer and Guay-Woodford, 2015). Acquired renal cystic disease is another form of renal disease acquired in individuals undergoing dialysis for renal failure (Cramer and Guay-Woodford, 2015). The rate of kidney cancers is higher in such individuals (Cramer and Guay-Woodford, 2015).

Chapter 2: Characterization of *Nedd4-2*$^{-/-}$ kidney

Polycystic kidney disease (PKD) is one amongst many renal disorders with large fluid filled cysts leading to kidney dysfunction (Harris and Torres, 2009). These renal cysts arise from the renal tubules within the nephrons which undergo abnormalities in cell proliferation, apoptosis, and fluid secretion within the lumen of the tubules leading to cyst formation and causing downstream signalling alteration within the kidneys (Igarashi and Somlo, 2007, Chang and Ong, 2008). PKD has been well characterised in different mouse models of renal cysts and shows variations in disease onset, leading to progression and complications in the kidney incurred due to variance in cyst formation (Chang and Ong, 2008). PKD is further subdivided into autosomal dominant polycystic kidney disease (ADPKD) affecting the majority of the suffering population. 85% of APKD cases in humans are due to defects in the PKD1 (polycystin-1) gene, and 15% of cases are due to PKD2 (polycystin-2) mutations. The less common forms of PKD are caused by mutations in genes such as PKHD1 (fibrocystin) and NPHP1-6, which causes nephronophthisis (NPH) (Newby *et al*., 2002, Harris and Torres, 2009). The onset of disease varies based on the severity of cyst development within the kidney. Knock out mouse models of PKD1 and PKD2 are embryonic lethal with cyst onset initiated at embryonic stages within the kidneys of these mice (Wu *et al*., 1998, Lu *et al*., 1997). Conditional knock out studies with PKD1 and PKD2 mice have been undertaken to overcome the limitations of the previous studies, and suggest a crucial role for these genes in disease progression and post-natal kidney development (Wu *et al*., 1998, Lu *et al*., 1997). Spontaneous mouse models of PKD, such as *pcy* which results from mutation in encoding gene nephrocystin-3, have early cyst development and survive as late as 30 weeks (Woo *et al*., 1997, Omran *et al*., 2001). Nephrons within the kidney are essential for maintaining ion homeostasis and misregulation within leads to the origination of fluid filled cysts (Woudenberg-Vrenken *et al*., 2009). Previous studies in mice with mutations in Never in Mitosis Gene A (NimA) - related Kinase 8 (Nek8) have been reported to suffer from cyst

formation, with cysts originating from different segments of the nephrons (Cai and Somlo, 2008). One of the earliest reported models of kidney cysts associated with a ubiquitin ligase are the Transcriptional coactivator with PDZ-binding motif (TAZ) KO mice which suffer from PKD, where the transcription factor TAZ binds to F-box protein beta-transducin repeat containing protein (β-Trcp) to form the E3 ligase complex $SCF^{\beta\text{-}Trcp}$ (Tian *et al*., 2007). Renal cystic disorders are characterised by certain common features in studies undertaken to elucidate their clinical implications, the most important being imbalance between cell proliferation and apoptosis driven by an increase in upstream cAMP flux, leading to secretion of fluid in the cystic lumen, altering extracellular matrix and causing interstitial fibrosis (Blanco and Wallace, 2013). These alterations lead to downstream effector signalling changes such as Wnt, TGFβ and mTOR during cyst progression and development (Blanco and Wallace, 2013) (**Fig 2.1**). Apart from cellular factors, organelles like primary cilia and centrosomes are essential players in defects associated with mice suffering from PKD. Ciliary proteins involved in mechanosensation like polycystins, and motor proteins involved in ciliary transport and aiding in downstream effector signalling localise to cilia and are important for normal kidney function (Blanco and Wallace, 2013, Fliegauf *et al*., 2007, Yoder, 2007) (**Fig 2.1**).

Nedd4-2, a HECT domain ubiquitin ligase belonging to the Nedd4 family has been previously reported to function in ubiquitinating cell surface receptors, ion channels and transporters leading to their internalisation, altered trafficking or degradation through lysosomes/ proteasomes (Rotin and Kumar, 2009, Scheffner and Kumar, 2014). The current study was undertaken to understand the role Nedd4-2 plays in renal physiology and its regulation of ion channels or transporters involved in renal disorders. Previous studies have characterised the role Nedd4-2 plays in regulating epithelial sodium channel (ENaC) and sodium chloride transporter in the kidneys, important in maintaining salt and fluid balance.

Chapter 2: Characterization of *Nedd4-2*$^{-/-}$ kidney

Studies undertaken in mouse models to establish its pathophysiological significance, specifically in the kidneys, highlight the role of Nedd4-2 in hypertension (Boase *et al*., 2011, Kimura *et al*., 2011, Ronzaud *et al*., 2013, Shi *et al*., 2008). The *Nedd4-2*$^{-/-}$ mice generated in our laboratory are perinatal lethal, with 5% of mice surviving until post-natal day (P) 19-21, when they die due to respiratory distress (Boase *et al*., 2011). Initial observations of the kidneys collected from P19 *Nedd4-2*$^{-/-}$ mice identified renal cysts. This study was undertaken based on the initial hypothesis that *Nedd4-2*$^{-/-}$ survivor mice displayed multiple cysts in the kidneys at P19, and suffered from a renal cystic disorder with multiple cysts similar to PKD. The work undertaken in this chapter highlights the novel role Nedd4-2 plays in renal pathophysiolology and aids in our understanding of renal cystic disorders.

2.2 Materials and methods

2.2.1 *Nedd4-2*$^{-/-}$ mouse colony breeding and genotyping

Nedd4-2$^{-/-}$ mice were generated and maintained as described previously (Boase *et al*., 2011). All animals were kept under 12 hour light/dark cycles with free access to food and water. *Nedd4-2*$^{-/-}$, *Nedd4-2*$^{+/-}$ and *Nedd4-2*$^{+/+}$ post natal mice were obtained by breeding pairs of Nedd4-2 heterozygous mice with the pure C57/BL6 genetic background. The SA Pathology animal ethics committee and Adelaide University animal ethics committee approved all animal procedures used for the study. Mice displaying signs of respiratory distress or a hunched posture were humanely sacrificed by cervical dislocation and autopsy was performed.

2.1.1.1 Extraction of genomic DNA for genotyping

Genomic DNA (gDNA) was extracted from mouse tail tips after cervical dislocation using RED Extract-N-AMP tissue PCR kit (Sigma-Aldrich) according to manufacturer's protocol.

Fig 2.1 Overview of cyst formation in the kidneys. Cyst formation arises from the nephrons of the kidney. The pathophysiological mechanisms known to be involved in the kidney cyst formation are non-genetic factors and genetic factors. The non genetic factors are circulating factors in the fluid like vasopressin, cAMP, epidermal growth factor (EGF) and proto oncogene tyrosine-protein kinase (Src). Genetic factors include mutations and misregulation of genes Pkd1 (Polycystin-1) and Pkd2 (Polycystin-2). Pathophysiological factors associated with cyst formation are cell proliferation, alteration in cell polarity, extracellular matrix remodification and cell cilia malformation. (Taken from Wallace *et al;* 2011).

Chapter 2: Characterization of *Nedd4-2*$^{-/-}$ kidney

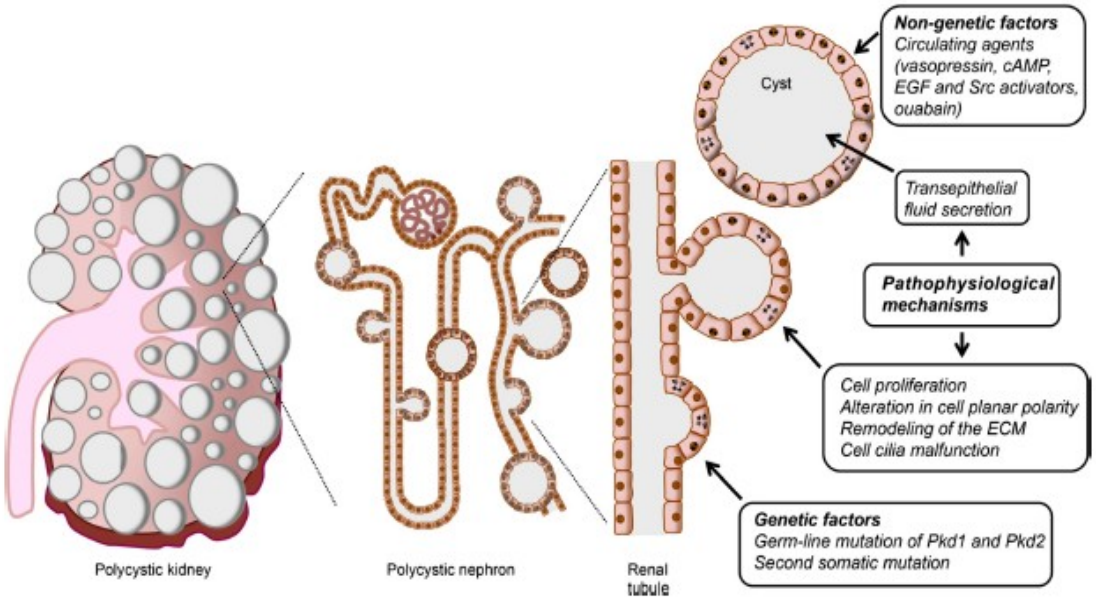

2.1.1.2 Polymerase chain reaction (PCR)

The thermo cycler conditions used for the wild type (WT) and *Nedd4-2*$^{-/-}$ (KO) genotyping PCR reactions are as indicated: A single initial denaturation step of 94^{o}C for 3 min, followed by 40 cycles of 94^{o}C for 30 sec, 53^{o}C for 45 sec, 72^{o}C for 1 min 30 sec and a final single elongation step of 72^{o}C for 5 min. Both WT and KO reactions were carried out separately to reduce background band overlap. PCR reactions were repeated to confirm *Nedd4-2*$^{-/-}$ after tissue collections using fresh tail tips. If genotyping reaction did not work reactions were repeated with less than 2ul gDNA.

2.1.1.3 Primer reaction preparation

Genotyping PCRs were performed using 2ul of gDNA, 100ng of each primer and 10ul of RED extract-N-AMP PCR mix in a final volume of 20ul. Reactions using distilled water were used as a negative control for each PCR run.

Table 2.1 Forward (F) and reverse (R) primer sequences for used for genotyping

Gene	Primer sequences (5'-3')	Detection	Band size
Nedd4-2$^{+/+}$ (WT)	1-TGGCAAGAATTGTAGCTG(F) 2-AGAAGGAACGCAAGGATT(R)	wild type	516 base pairs (bp)
Nedd4-2$^{-/-}$ (KO)	1-TGGCAAAGAATTGTAGCTG (F) 2-ATATCATGCCTCCAAAGG (R)	Targeted allele	900 base pairs (bp)

All primers used for genotyping were procured from Geneworks.

2.1.1.4 Gel electrophoresis

DNA fragments PCR amplified were analysed using agarose gel electrophoresis in 2% w/v agarose gels made in TAE buffer (40mM Tris, 20mM glacial acetic acid, 1mM EDTA, pH-8.0). 100 bp (New England Biolabs) ladder was used to measure amplicon sizes as control

molecular size standard. Samples were run at 90 Volts (v) for 40min. DNA was stained in ethidium bromide solution (2ug/ml) for 15 min and transilluminator (UVltec) was used to visualise DNA under UV light (254nm).

2.2.2 Nedd4-2 Mouse surgery, weighing and histology

For embryonic day post coitum (E) 18.5 mice, pregnant mice were cervically dislocated and the embryonic sac transferred to phosphate buffered saline (PBS). The embryos were removed and then euthanized by decapitation. After tail tipping for genotyping, embryos were dissected and organs were either snap frozen in liquid nitrogen or placed in 10% formalin at room temperature overnight. Fixed organs were then embedded in paraffin blocks and 10µm sections were cut. The procedure was repeated for mice collected at different post-natal days, from P1 to P22, which were cervically dislocated and decapitated and body parts collected. Left kidneys were set in fixative for immunohistochemistry work and right kidneys were snap frozen in liquid nitrogen and kept at -70^{o}C for biochemical analysis. Both kidneys were weighed along with the mice simultaneously before separation for histological and biochemical analysis. Fixed tissues were embedded and processed in paraffin and stained for haematoxylin/eosin by the Department of Surgical Pathology, SA Pathology (Adelaide, SA). Digital images were acquired using a nanozoomer (Hamamatsu) or wherever stated using an Olympus BL-X51 light microscope. The mouse and kidney images were taken using Samsung galaxy SIII 8 megapixel autofocus camera.

2.2.3 Immunohistochemistry and Immunofluoroscence

For DAB (3, 3` diaminobenzidine) staining, sections were washed in xylene for ten minutes and then rehydrated in a series of 100%, 95%, 80%, 50% ethanol/distilled water for 5 minutes each. Antigen retrieval was performed in 0.01 M sodium citrate (pH 6) for 10 minutes at 100% microwave power (300 W) followed by cooling for 30 min and rinsing in PBS. Endogenous peroxidase was quenched with 0.3% hydrogen peroxide in distilled water for 10

minutes. Sections were then washed in TBST (Tris-buffered saline/0.05% Tween 20) for 5 minutes and blocked with 10% donkey serum in TBST for 3 hours at room temperature. Primary antibodies for THP (1:50 sheep anti-human Tamm Horsfall Glycoprotein; AbD Serotec), PCNA (1:100 clone PC10; Cell Signalling Technology), cleaved caspase-3 (1:50; Abcam), Collagen-1 (1:100; rabbit antibody Rockland antibodies and assays), acetylated α-tubulin (1:1000; sigma Aldrich) were added in blocking solution overnight. Next day, sections were washed three times with TBST for 5 minutes each and then processed with the Vectastain ABC kit (Vector labs) according to the manufacturer's protocol. Staining was developed with DAB (Vector labs) as described by the manufacturer. Sections were finally washed in distilled water and mounted in Depex mounting media. For immunofluorescence secondary antibodies (1:1000 rabbit Alexa Fluor 488 and/or 1:1000 mouse Alexa Fluor 568 (Molecular Probes) were added in blocking solution for 2 hours at room temperature and sections were mounted in Prolong Gold Antifade reagent (Molecular Probes).

2.2.4 *Nedd4-2*$^{-/-}$ nephronal markers

For nephronal markers LTL (Lotus Tetragonolobus Lectin) and DBA (Dolichos Biflorus Agglutinin), staining was conducted as above with conjugated primary antibodies added for 2 h (1:200 Fluorescein Lotus Tetragonolobus Lectin or 1:50 Rhodamine Dolichos Biflorus Agglutinin; Vector Laboratories) and mounted using Prolong Gold Antifade reagent (Molecular Probes). Images were obtained using a confocal microscope (Radiance 2100, Bio-Rad Laboratories).

2.2.5 *Nedd4-2*$^{-/-}$ Picrosirius red staining (Collagen)

Picrosirius red dye staining was conducted on paraffin sections. Sections were deparaffinised and hydrated as described above and Picrosirius red stain (0.5 g direct red 80, Sigma Aldrich) in 1.3% picric acid (Sigma Aldrich) in water was added for 1 h. Sections were washed in two

changes of acidified water, dehydrated in three changes of 100% ethanol and cleared in xylene. The slides were mounted with permount (Puchtler *et al*., 1962).

2.2.6 *Nedd4-2*$^{-/-}$ Masson trichrome staining (Interstitial Fibrosis)

Paraffin embedded tissue sections were placed in distilled water. Then the nuclei were stained with Celestin blue [(5% ammonium ferric sulphate (iron alum) 100 mL in Celestin blue 0.5 g (CI 51050) was heated for 3 minutes. When cooled the solution was filtered, and 14 mL of glycerol added] for 5 minutes. Then sections were rinsed in distilled water. Haematoxylin was added for 5 minutes, and then sections were kept under running tap water. They were further rinsed in distilled water. Beibrich scarlet- acid fuchsin dye (which stains all tissue elements) was added for 8 minutes. These sections were briefly rinsed with distilled water and then phosphotungstic acid solution [Phosphotungstic acid-5 g and 100 mL distilled water] which selectively removes red stain from unwanted areas and acts as a mordant for the next step. The solution was drained from the tissue; aniline blue dye [2.5 g Aniline blue, 2 mL glacial acetic acid and 100mL distilled water] was added for 5 minutes before rinsing briefly in distilled water. These sections were further differentiated for colour briefly in 1% acetic acid solution [99 mL distilled water and 1ml glacial acetic acid]. (Luna, 1968, Masson, 1929). Tongue tissue sections were used as a positive control.

2.2.7 *Nedd4-2*$^{-/-}$ periodic acid Schiff (PAS) staining (Polysaccharide)

Paraffin embedded sections were placed in distilled water. They were treated with 1% periodic acid [50% periodic acid solution-10 mL in 500 ml distilled water] for 5 min. The sections were washed in distilled water and stained with Schiff reagent [Australian Biostain Pty ltd] for 10 min. Washed in running tap water for 5 min and stained for nuclei with haematoxylin for 1 minute and rinsed and differentiated with acid alcohol for a few seconds. The sections were dehydrated in 50%, 80%, 95%, and 100%, ethanol/distilled water for 5 min

each, cleared in xylene and then mounted using permount. Tongue tissue sections were used as a positive control.

2.2.8 cAMP measurements

cAMP levels were measured using the Cyclic AMP EIA (ELISA (Enzyme linked Immunosorbent Assay) Immuno absorbance Assay) Kit (Cayman Chemical Company) on dissected kidneys stored at -70° C. For E18.5 mice, 2 kidneys from each animal were used and for P19 mice one quarter of a kidney was used. Each kidney sample was weighed and dropped into 5 volumes of 5% TCA (Trichloroacetic acid). Kidneys were homogenised on ice, bath sonicated 3 times and vortexed. Samples were centrifuged at 1500x g for 10 minutes at 4° C and supernatant transferred to new tubes. TCA was extracted with water saturated ether 3 times before heating samples at 70° C for 5 minutes. Samples were then processed and analysed for cAMP levels according to the manufacturer's instructions.

2.2.9 Nedd4-2 mouse embryonic fibroblast (MEF) isolation and culture

Timed-matings were set to obtain pregnant female mice at E13.5/14.5. Pregnant females were humanely killed via cervical dislocation, and the embryonic sac harvested and transferred to petri dish with DMEM (GIBCO) media. The embryos were separated by cutting the border of each sac and placed individually in 24 well dishes in the tissue culture hood. The maternal membranes were detached from the embryos. The embryos were placed in a petri dish and the tail tips were removed and placed in eppendorf tubes for genotyping as described previously. The head was separated from the body and the liver (red lobe) teased out. The remaining body of the embryo was transferred to a clean eppendorf tube and MEF media was added [DMEM complete media (GIBCO) + HEPES + 1% pencillin/streptomycin + 2mM glutamine + 10% foetal calf serum, along with 250μm asparagine + 50μm β-mercaptoethanol]. The embryos were homogenised using a small tube homogeniser (ethanol washed, UV treated). The homogenate was added to the centre of petri dish with MEF media,

and the dish slowly swirled to disperse the cells. The MEF cells were incubated in 37^{o}C 5% CO_2 incubator and allowed to adhere overnight. The cells were washed next day with PBS and fresh MEF media was added. Once dish was confluent the cells were harvested with trypsin by washing and plated for cell staining.

2.2.9.1 Cilia formation in MEFs

2x10^5 MEF cells were seeded on glass coverslips. The cells were seeded for 24 hours and then serum starved with MEF media minus foetal calf serum for 36 hours. The cells were then fixed in 4% paraformaldehyde in methanol for 10min, washed in PBS, permeabilised in 0.1% TritonX-100/PBS for 2 minutes and incubated in blocking solution (1% FBS/PBS) for 2 hours. Primary antibodies acetylated alpha tubulin (1:1000; Sigma) and Nedd-1 (1:1000; (Manning *et al*., 2010)in blocking solution were added overnight for incubation at 4^{o}C. Cells were washed the next day with PBS and stained with secondary antibodies for two hours as stated earlier along with Hoechst 33342 (Molecular Probes). After washing coverslips were mounted using permount (Fisher Scientific). Cells were then blind counted for cilia and centrosomes. The cell percentages were evaluated using two independent experiments with values averaged from four replicates and images were obtained using confocal microscopy (LSM700, Zeiss laboratories).

2.2.10 Ribonucleic acid (RNA) isolation and Quantitative PCR (qPCR)

To isolate RNA, kidney tissue was lysed in 1ml of Trizol reagent (Life Technologies) and processed according to manufacturer's instructions. RNA extracted was resuspended in diethylpyrocarbonate-(DEPC) treated water. RNA was quantified using a Nanodrop1000^{TM} spectrophotometer (ThermoScientific). First strand cDNA synthesis was performed using the high capacity cDNA Reverse Transcription Kit (Applied Biosciences) with oligo-dT primers. Real time quantitative (q)PCR was performed on the samples in a rotor gene 3000 (Corbett Research) by using RT^2 Real time SYBR green/ROX PCR Master Mix (Qiagen) as per the

manufacturer's instructions. Each gene product was identified in independent PCR runs and normalized for expression to β-actin with the $2^{-\Delta\Delta ct}$ method. Quantification was performed in Microsoft Excel and the statistical analysis was performed using GraphPad Prism v5 using unpaired T-test assuming unequal variance, with statistical significance determined as being $p \leq 0.05$. Data were represented as mean ± SEM. The primer sequences used for gene amplification are stated in the table below.

Table 2.2 Primer sequences used for qPCR analysis of mouse genes

Gene	Forward primer (5'-3')	Reverse Primer (5'-3')
β-actin	GATCATTGCTCCTCCTGAGC	AGTCCGCCTAGAAGCATTTG
Collagen-1	ATCTCCTGGTGCTGATGGAC	ACCTTGTTTGCCAGGTTCAC
Matrix metalloproteinase-9	GGCCGCTCGGATGGTTAC	TCGCGTCCACTCGGGTAG
Smooth muscle actin	GAGGCACCACTGAACCCTAA	CATCTCCAGAGTCCAGCACA
Kinesin-3 subunitA	GAAGCCCAACAAGAGCATCAGT	CCAGTGGACGTAGTTTTCAATCAT
Dynactin-5	GATTGGGCGCCGTTGTGTATTG	GAACTGAACCTGGGTCCTCCTCTG

2.2.11 Processing for Scanning Electron Microscope (SEM) and Transmission Electron Microscope (TEM)

2.2.11.1 Transmission Electron micrscope

Tissues were collected from *Nedd4-2*$^{-/-}$ mice, cut into smaller sections and fixed overnight in 4% paraformaldehyde/1.25% glutaraldehyde (EM grade) in PBS, with 4% sucrose, pH7.2.

They were washed twice in PBS + 4% sucrose (washing buffer) for 10 minutes. Post fixation 2% osmium tetroxides (OSO_4) was added for 1 hour on a rotator. Dehydration was performed in 70%, 90%, 95% and 100% ethanol with two incubations each for 15 minutes. These were then treated with propylene oxide for 20-30 minutes. Resin infiltration was performed using 1:1 propylene oxide/resin- two incubations with one change of solution for one hour. The tissues were then kept overnight on rotator in 100% resin. Next day the resin was changed and fresh resin was added. Tissues were embedded the next day in fresh resin and kept in an oven at 70^{o}C for 24 hours for polymerisation. The tissues were further processed for microtome by Adelaide Microscopy staff (University of Adelaide, SA). The images were taken using FEI Tecnai G2 Spirit TEM at Adelaide Microscopy (University of Adelaide, SA).

2.2.11.2 Scanning electron microscopy

As described in section 2.2.11.1, tissues were fixed, washed and post fixation treated with OSO_4 (Osmium tetroxide) and dehydrated. Tissues were then taken for critical point dry for biological tissues via chemical drying (HMDS (Hexamethyldisilazane)) by two incubations for 20 minutes, and mounted on a stub. This experiment was performed under the supervision of Adelaide Microscopy staff (University of Adelaide). The images were taken using a FEI Quanta 450 FEG Environmental Scanning Electron Microscope (ESEM).

2.2.12 Quantification and statistical analysis

Statistical analyses was performed with Graphpad Prism (v5) or Microsoft® Excel using unpaired T-test assuming equal variance, with statistical significance determined as being $P \leq 0.05$. For grouped experiments in cilia and centrosomes Sidaks multiple comparison tests with two way Anova was used to calculate statistical significance with $P \leq 0.05$ deemed being significant.

2.3 Results

2.3.1 *Nedd4-2*$^{-/-}$ mice show renal cystic onset

To understand renal cyst onset and characterise the cystic progression in the *Nedd4-2*$^{-/-}$ kidneys, the initial working hypothesis was that these cysts could start at early post natal day stages in *Nedd4-2*$^{-/-}$ kidneys as the initial phenotype recapitulated a phenotype seen in P19 *Pkd*$^{+/-}$ mice, a less severe phenotype (Wilson, 2008) . In cystic mouse models, such as Pkd1 and Pkd2 null mice, the cyst initiation starts at early embryonic stages and progresses until these mice succumb to kidney failure due to kidney injury (Lantinga-van Leeuwen *et al*., 2007). The kidneys collected from the P19 *Nedd4-2*$^{-/-}$ mice showed multiple cysts in cortex and medulla, with dilation in the tubules of the cortex as shown in **Fig 2.2** (**D, J, P** and **V**). The *Nedd4-2*$^{-/-}$ mice were further staged for cystic onset and kidneys were collected from P2 and E18.5 mice. As shown in **Fig 2.2 (E and K)** the kidneys from post natal day 2 had cysts in the cortex whereas the medulla (**Fig 2.2 Q and W**) of these kidneys looked normal in comparison to their control littermates (**Fig 2.2 B, H, N** and **T**). The kidneys of E18.5 mice looked normal (**Fig 2.2 F, L, R** and **X)** with no cyst formation in the cortex and medulla as compared to *Nedd4-2*$^{+/+}$ control littermates (**Fig 2.2 C, I, O and U**). The 5% *Nedd4-2*$^{-/-}$ survivor mice were staged and collected at E18.5 to P19 to track the initial onset of kidney cysts and disease progression, and the results are summarised in **Table 2.3**. The kidneys collected for mice at P2 showed cystic onset (**Fig 2.2**). These *Nedd4-2*$^{-/-}$ survivor mice were further collected to understand disease progression cyst formation and variability in the later stages for consistency in the phenotype observed. Most of the mice at post natal day 19 showed cyst formation and progression in comparison to earlier stages as shown in representative images in **Fig 2.2**. However there were anomalies associated with the cyst formation and variability was observed in the mice collected at later stages. This variability observed in the cystic index was evaluated by the number of hollow spaces seen in the

kidneys of the surviving *Nedd4-2*$^{-/-}$ mice. This phenotypic variability is summarised in **Table 2.3,** where approximately 83% of mice which showed the cystic phenotype. The kidneys from Pkd null mice have a consistent phenotype of multiple cysts spread around the cortex and medulla of the kidney. In the *Nedd4-2*$^{-/-}$ mice cyst formation is observed in the cortex and medulla, although the size of cysts varied from large, medium to none as summarised in the **Table 2.3**.

Table 2.3 Cystic onset and frequency in *Nedd4-2*$^{-/-}$ survivor mice

Stage	Number of animals	Cystic kidneys	Non-cystic kidneys	Percentage of animals with cysts	Cyst Size
P17-P22	12	10	2	83.3%	Varied-large, medium and none
P14-15	6	6	0	100%	medium
P3-5	3	2	0	100%	small
P1-2	4	1	0	100%	initiation
EL18.5	4	0	4	0%	none

2.3.2 Nedd4-2$^{-/-}$ mice do not show alteration in body weight, kidney weight and cystic burden

To further understand the morphological changes due to renal cysts within the kidneys that could alter kidney function and lead to cystic burden, body weight, kidney weight, shape and size were examined. The kidneys from the *Nedd4-2*$^{-/-}$ mice were collected and weighed, and images taken at post natal day 19 to visualise any characteristic kidney architecture, colour

and shape differences. The kidneys from P19 *Nedd4-2*$^{-/-}$ were slightly smaller and paler (**Fig 2.3 A**) with no apparent cystic burden or kidney architecture alterations. The P19 *Nedd4-2*$^{-/-}$ mice appeared slightly smaller than wild-type littermates (**Fig 2.3 A**), although upon body weight measurement analyses there was a trend of lower body weights in the P19 *Nedd4-2*$^{-/-}$ the differences were not statistically significant (**Fig 2.3 B**). Further, to correlate this with cystic burden on the kidneys, individual left and right kidneys were measured and normalised with respect to body weight and showed no significant differences (**Fig 2.3 D**). In P19 *Nedd4-2*$^{-/-}$ the total weight of both kidneys were normalised to total body weight of the mice and showed no significant difference in comparison to the P19 *Nedd4-2*$^{+/+}$ control littermates (**Fig 2.3 C**). The sex was not considered in the initial study due to the small percentage of *Nedd4-2*$^{-/-}$ mice (5%) that survive birth.

Pkd is characterised by the formation of cysts not just in the kidney but in other body parts also, especially in liver, pancreas and spleen (Lu *et al*., 2001). Formation of cysts can affect tissue architecture leading to fibrosis in affected body parts. To assess tissue architecture, various body organs were collected from P19 *Nedd4-2*$^{-/-}$ mice for histological analyses and subjected to comparative analysis with P19 *Nedd4-2*$^{+/+}$ mice (**Fig 2.4**). As shown in **Fig 2.4** there were no significant differences found in the tissues of the mice collected. Organs commonly affected by mice afflicted with renal cysts, such as liver, pancreas and spleen, looked normal in *Nedd4-2*$^{-/-}$ (**Fig 2.4 D**, **F** and **H**) in comparison to the P19 *Nedd4-2*$^{+/+}$ (**Fig 2.4 C**, **E** and **G**) littermates. Additional tissues, such as thymus, colon and stomach, also showed no difference between *Nedd4-2*$^{+/+}$ (**Fig 2.5 I**, **A** and **K**) and *Nedd4-2*$^{-/-}$ (**Fig 2.5 J**, **B** and **L**). In summary, there was no cyst formation or pathological differences observed in the liver, colon, pancreas, spleen, thymus or stomach (**Fig 2.4**). **Table 2.4** summarises the fibrosis and cystic formation in all examined organs of P19 *Nedd4-2*$^{-/-}$ mice.

Table 2.4 Summary of cyst formation and fibrosis in organs of *Nedd4-2*$^{-/-}$ mice

Organs	Fibrosis	Cyst formation
Kidney	Y	Y
Liver	N	N
Pancreas	N	N
Spleen	N	N
Colon	N	N
Stomach	N	N
Thymus	N	N

2.3.3 *Nedd4-2*$^{-/-}$ kidney cysts originate from proximal and distal tubules, collecting ducts, and the loop of Henle

Nephrons are the building blocks of the kidneys, and different parts of the nephrons play a critical role in the regulation of ion channels and transporters. Previous studies on mice models of kidney cysts suggest the important role cyst origination plays within the nephrons of the kidney in identifying proteins involved in the phenotype (Lin *et al*., 2003). To ascertain where *Nedd4-2*$^{-/-}$ kidney cysts originate, *Nedd4-2*$^{-/-}$ P19 kidneys were stained with different nephronal segment markers. Cysts arise from within different segments of the nephrons within these kidneys as shown in **Fig 2.5**. The nephronal markers used were Lotus Tetragonolobus Lectin (LTL) to indicate proximal tubules, Dolichos Biflorus Agglutinin (DBA) to mark collecting ducts and Tamm Horsfall Protein (THP) to mark thick ascending loop of Henle. At early postnatal day 3 only a small number of cysts are present, but a few cysts stained positive for each marker (proximal tubules (**Fig 2.5 A**), collecting ducts (**Fig 2.5**

B), and the thick ascending loop of Henle (**Fig 2.5 C**)). In postnatal day P19, cysts were again detected in the different nephronal segments analysed (**Fig 2.5 D**, **E** and **F**). The larger cysts stained positive for THP, with their origin from the loop of Henle (**Fig 2.5 F**).

2.3.4 *Nedd4-2* $^{-/-}$ kidneys show increased cell proliferation

Cysts are formed due to imbalances in cell proliferation which could be driven by upstream non genetic factors like cAMP driving downstream pathophysiological mechanisms like cell proliferation and apoptosis (Blanco and Wallace, 2013) . To ascertain the pathophysiological mechanism important in cyst formation in the kidneys, proliferation cell nuclear antigen (pCNA) marker for cell proliferation was used to measure the level of cell proliferation in cystic kidneys, which is caused due to misregulation between proliferating cells surrounding cysts or apoptotic cells around the cysts (Takakura *et al*., 2008). In **Fig 2.6** increased pCNA staining in the kidney cortex and medulla of the P19 *Nedd4-2*$^{-/-}$ mice is observed in comparison to *Nedd4-2*$^{+/+}$ control littermates. The proliferating cells seem to be more in number in and around the cysts taken from different regions within the kidney medulla (**Fig 2.6 G** and **J**) and cortex (**Fig 2.6 H** and **K**).The tubules around the cysts (**Fig 2.6 H** and **J**) and collecting ducts (**Fig 2.6 K**,) within the *Nedd4-2*$^{-/-}$ kidneys seem to be undergoing hyper proliferation in comparison to the *Nedd4-2*$^{+/+}$ (**Fig 2.6** (**A** and **D**) cortex and (**B** and **E**) medulla). There was no proliferation difference seen around the glomeruli of *Nedd4-2*$^{+/+}$ and *Nedd4-2*$^{-/-}$ kidneys (**Fig 2.6 A, D, G** and **J**).

Fig 2.2 Morphology, cyst initiation and cyst progression in *Nedd4-2*$^{-/-}$ kidney. Representative sections of paraffin embedded kidney tissues (80x) stained with haematoxylin and eosin, at post natal day 19 (**P19**), post natal day 2 (**P2**) and embryonic day 18.5 (**E18.5**) with respective images taken from medulla and cortex region of the kidney with indicated genotypes. Images **A** and **G** represent P19 *Nedd4-2*$^{+/+}$ cortex. Images **M** and **S** represent P19 *Nedd4-2*$^{+/+}$ cortex. Images **B** and **H** represent P2 *Nedd4-2*$^{+/+}$ cortex. Images **N** and **T** represent P2 *Nedd4-2*$^{+/+}$ medulla. Images **C** and **I** represent E18.5 *Nedd4-2*$^{+/+}$ cortex. Images **O** and **U** represent E18.5 *Nedd4-2*$^{+/+}$ medulla. Images **D** and **J** represent P19 *Nedd4-2*$^{-/-}$ cortex**.** Images **P** and **V** represent P19 *Nedd4-2*$^{-/-}$ medulla**.** Images **E** and **K** represent P2 *Nedd4-2*$^{-/-}$ cortex**.** Images **Q** and **W** represent P2 *Nedd4-2*$^{-/-}$ medulla. Images **F** and **L** represent E18.5 *Nedd4-2*$^{-/-}$ cortex. Images **R** and **X** represent E18.5 *Nedd4-2*$^{-/-}$ medulla. The cysts (C) are marked by arrows. The dilated tubules are marked by asterisks (*).Glomeruli are represented as G. The images were taken using Hamamatsu nanozoomer view 2. Scale bar = 25μm.

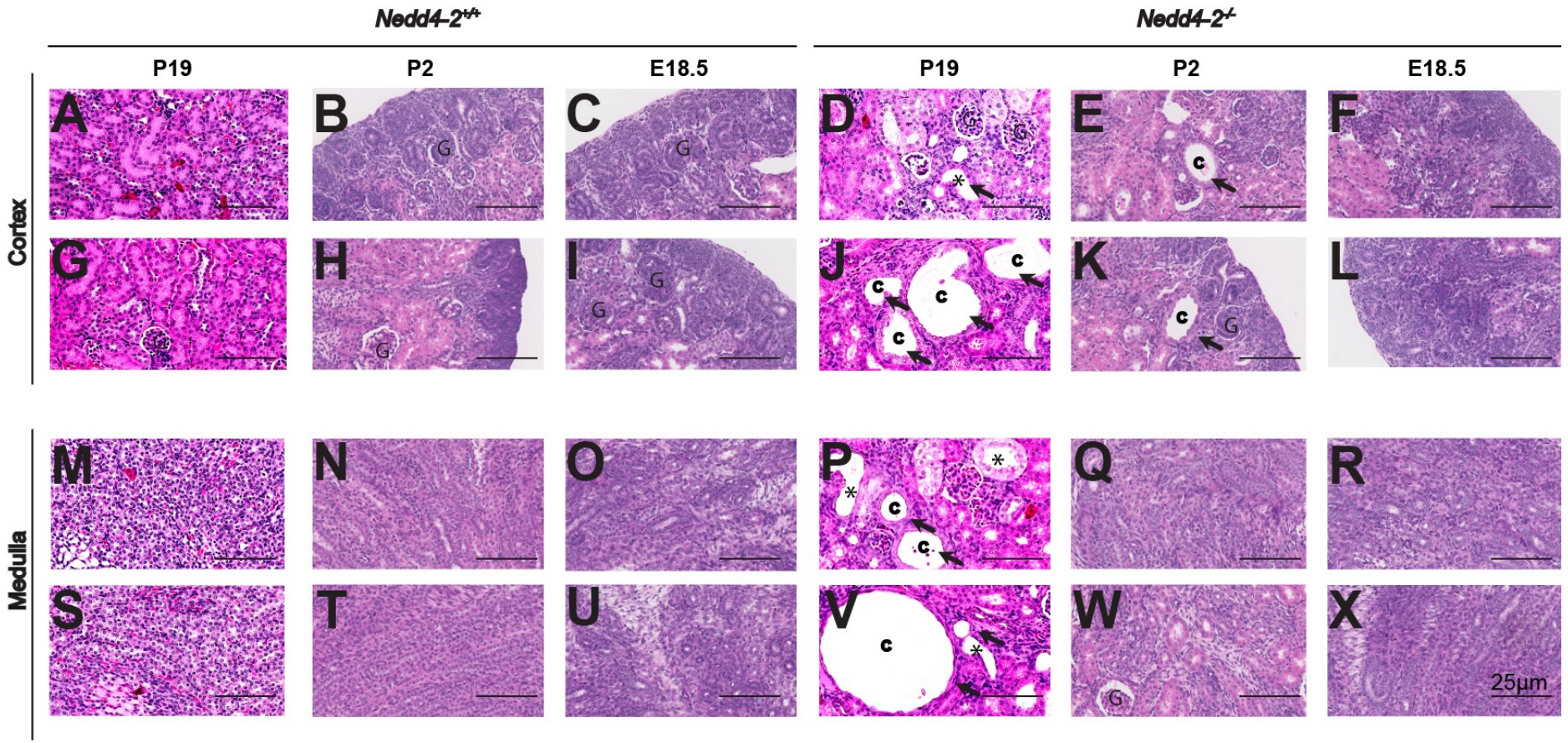
Nedd4-2+/+
Nedd4-2-/-
P19
P2
E18.5
P19
P2
E18.5
Cortex
Medulla
A
B
C
D
E
F
G
H
I
J
K
L
M
N
O
P
Q
R
S
T
U
V
W
X
G
c
*
25μm

Fig 2.3 Gross morphology of *Nedd4-2*$^{-/-}$ mice kidneys. A) Top image shows *Nedd4-2*$^{+/+}$ (WT) post natal day 19 and *Nedd4-2*$^{-/-}$ (KO) post natal day 19 mice. The bottom image represents WT (**L**eft and **R**ight) and KO (**L**eft and **R**ight) kidneys taken from post natal day 19 mice with indicated genotypes. **B)** Graphical representation of total body mass (grams) for collected P19 WT and KO mice. **C)** Graphical representation of total kidney weight (**L** and **R**) compared to total body weight at post natal day 19. **D)** Kidney weight measurement for cystic burden were undertaken for each individual (**L** and **R**) kidney at post natal day 19 represented by **L** and **R** respective kidney weight compared to total body weight. Data represented as mean ± SEM ($P>0.05$ not significant (n.s), unpaired T-test using Welch correction). BW = body weight. KW = kidney weight. The images were taken using Samsung galaxy SIII 8 megapixel autofocus camera.

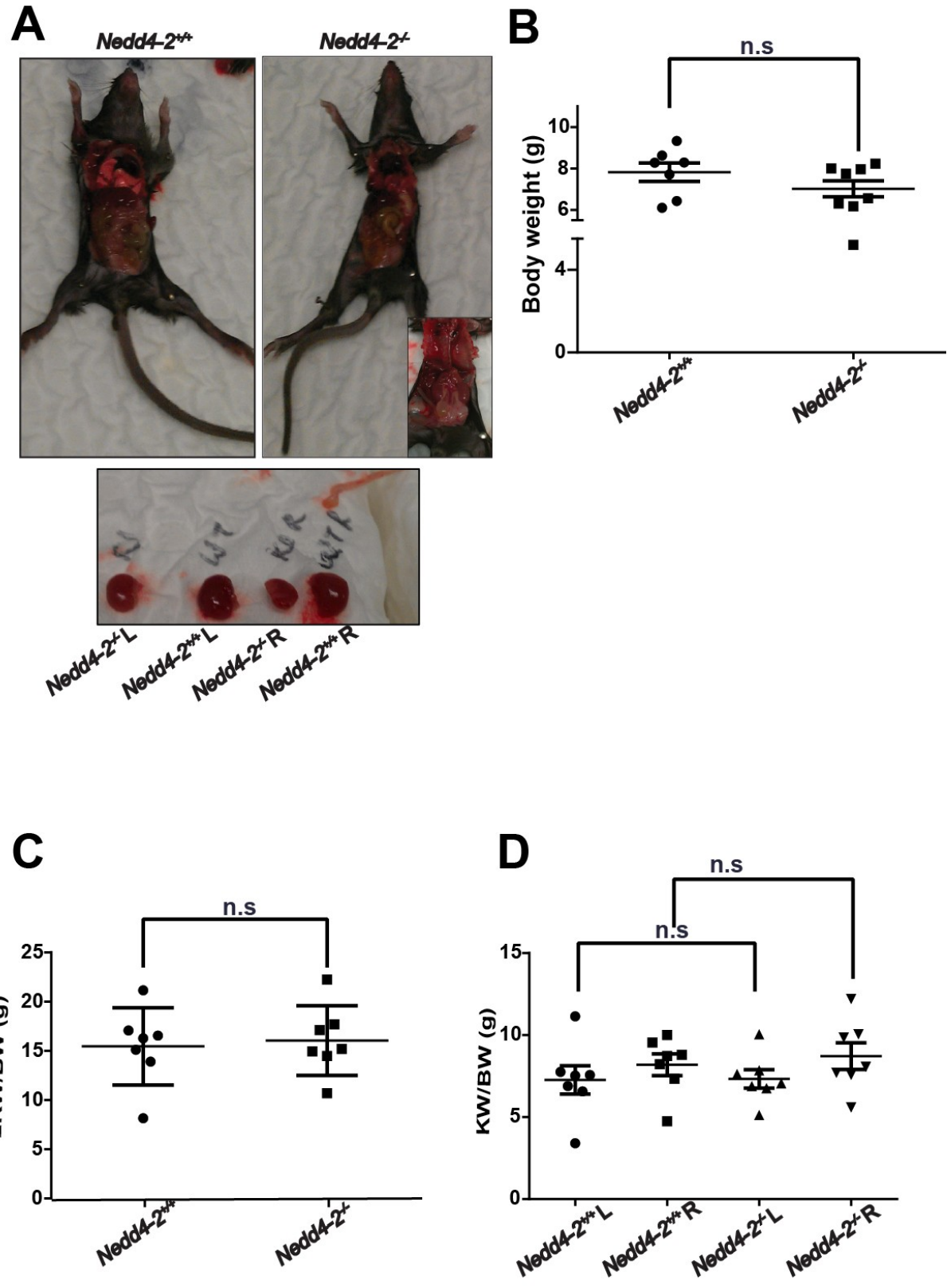
A
Nedd4-2+/+
Nedd4-2-/-
Nedd4-2-/- L
Nedd4-2+/+ L
Nedd4-2-/- R
Nedd4-2+/+ R
B
n.s
Body weight (g)
10
8
6
4
0
Nedd4-2+/+
Nedd4-2-/-
C
n.s
2KW/BW (g)
25
20
15
10
5
0
Nedd4-2+/+
Nedd4-2-/-
D
n.s
n.s
KW/BW (g)
15
10
5
0
Nedd4-2+/+ L
Nedd4-2+/+ R
Nedd4-2-/- L
Nedd4-2-/- R

Fig 2.4 Morphology of tissues from P19 *Nedd4-2*$^{-/-}$ mice. Representative 80x images are taken from sections of paraffin embedded colon, liver, pancreas, spleen, thymus and stomach of the indicated genotypes that have been stained with haematoxylin and eosin, at P19. Images **A** and **B** represent colon. Images **C** and **D** represent liver. Images **E** and **F** represent pancreas. Images **G** and **H** represent spleen. Images **I** and **J** represent thymus. Images **K** and **L** represent stomach. The images were taken using a Hamamatsu nanozoomer view 2. Scale bar=25µm.

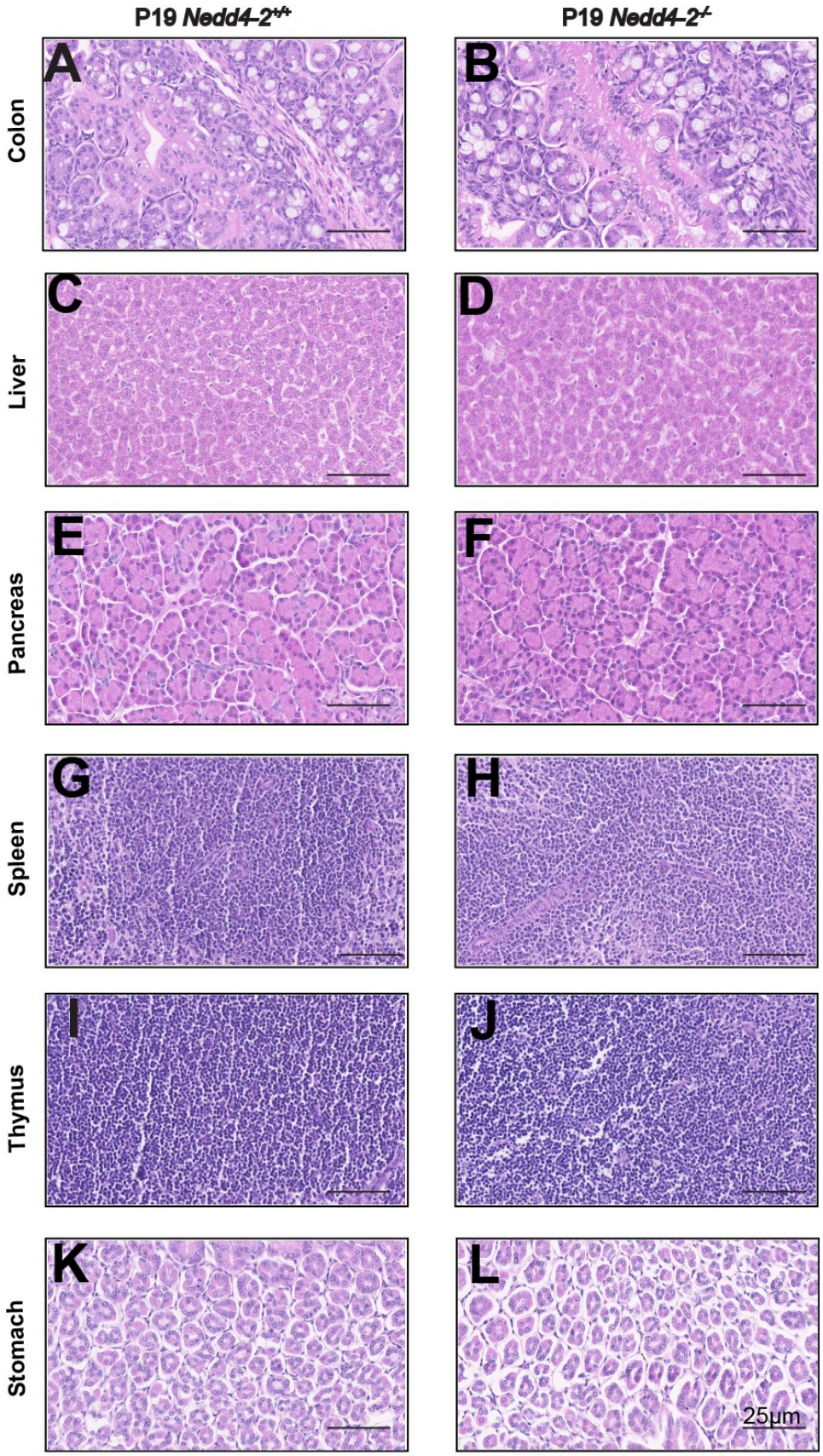
P19 Nedd4-2+/+
P19 Nedd4-2-/-
Colon
Liver
Pancreas
Spleen
Thymus
Stomach
A
B
C
D
E
F
G
H
I
J
K
L
25µm

Fig 2.5 *Nedd4-2*$^{-/-}$ cysts arise from multiple nephronal segments. Cysts within Post natal day 3 **(**P3**)** and Post natal day 19 **(**P19**)** kidneys of *Nedd4-2*$^{-/-}$ stain positive for **L**otus **T**etragonolobus **L**ectin (**LTL**), **D**olichos **B**iflorus **A**gglutinin (**DBA**) and **T**amm **H**orsfall **P**rotein (**THP**). Image **A** represents P3 *Nedd4-2*$^{-/-}$ kidney cysts staining positive for LTL in green indicates proximal tubules. Image **B** represents P3 *Nedd4-2*$^{-/-}$ kidney cysts staining positive for DBA in red indicates collecting ducts. Image **C** represents P3 *Nedd4-2*$^{-/-}$ kidney cysts staining positive for THP using DAB brown stain indicates thick ascending loop of Henle. Image **D** represents P19 *Nedd4-2*$^{-/-}$ kidney cysts staining positive for LTL in green indicates proximal tubules. Image **E** represents P19 *Nedd4-2*$^{-/-}$ kidney cysts staining positive for DBA in red indicates collecting ducts. Image **F** represents P19 *Nedd4-2*$^{-/-}$ kidney cysts staining positive for THP using DAB brown stain indicates thick ascending loop of Henle. The arrows in indicate cysts. The fluorescence images (**A**, **B**, **D** and **E**) were taken using LSM 700 confocal microscope. The DAB brown treated images (**C** and **F**) were taken using Hamamatsu nanozoomer view 2. Scale bar=100µm. This experiment was performed by **Dr. Jantina.A.Manning**.

Chapter 2: Characterization of *Nedd4-2*$^{-/-}$ kidney

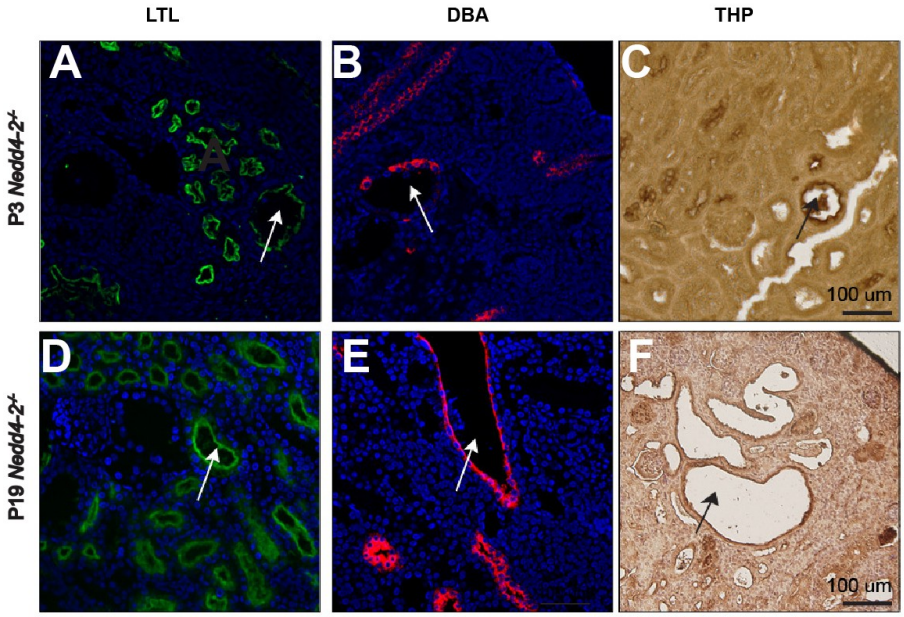

Fig 2.6 Increased cell proliferation in P19 *Nedd4-2*$^{-/-}$ cystic kidneys. Representative images (80x) of proliferating cell nuclear antigen (pCNA) immunohistochemistry performed on post natal day 19 *Nedd4-2*$^{+/+}$ and *Nedd4-2*$^{-/-}$ cystic kidneys images taken from medulla and cortex region of the kidney with indicated genotypes. Images **A** and **D** represent P19 *Nedd4-2*$^{+/+}$ cortex. Images **B** and **E** represent P19 *Nedd4-2*$^{+/+}$ medulla. Images **C** and **F** represent negative secondary only controls of P19 *Nedd4-2*$^{+/+}$ cortex and medulla respectively. Images **G** and **J** represent P19 *Nedd4-2*$^{-/-}$ cortex. Images **H** and **K** represent P19 *Nedd4-2*$^{-/-}$ medulla. Images **I** and **L** represent negative secondary only antibody controls of P19 *Nedd4-2*$^{-/-}$ cortex and medulla respectively. The cysts (C) are marked by arrows. Glomeruli are represented as G. The collecting ducts of the kidney are marked as CD. The images were taken using Hamamatsu nanozoomer view 2.Scale bar = 25μm.

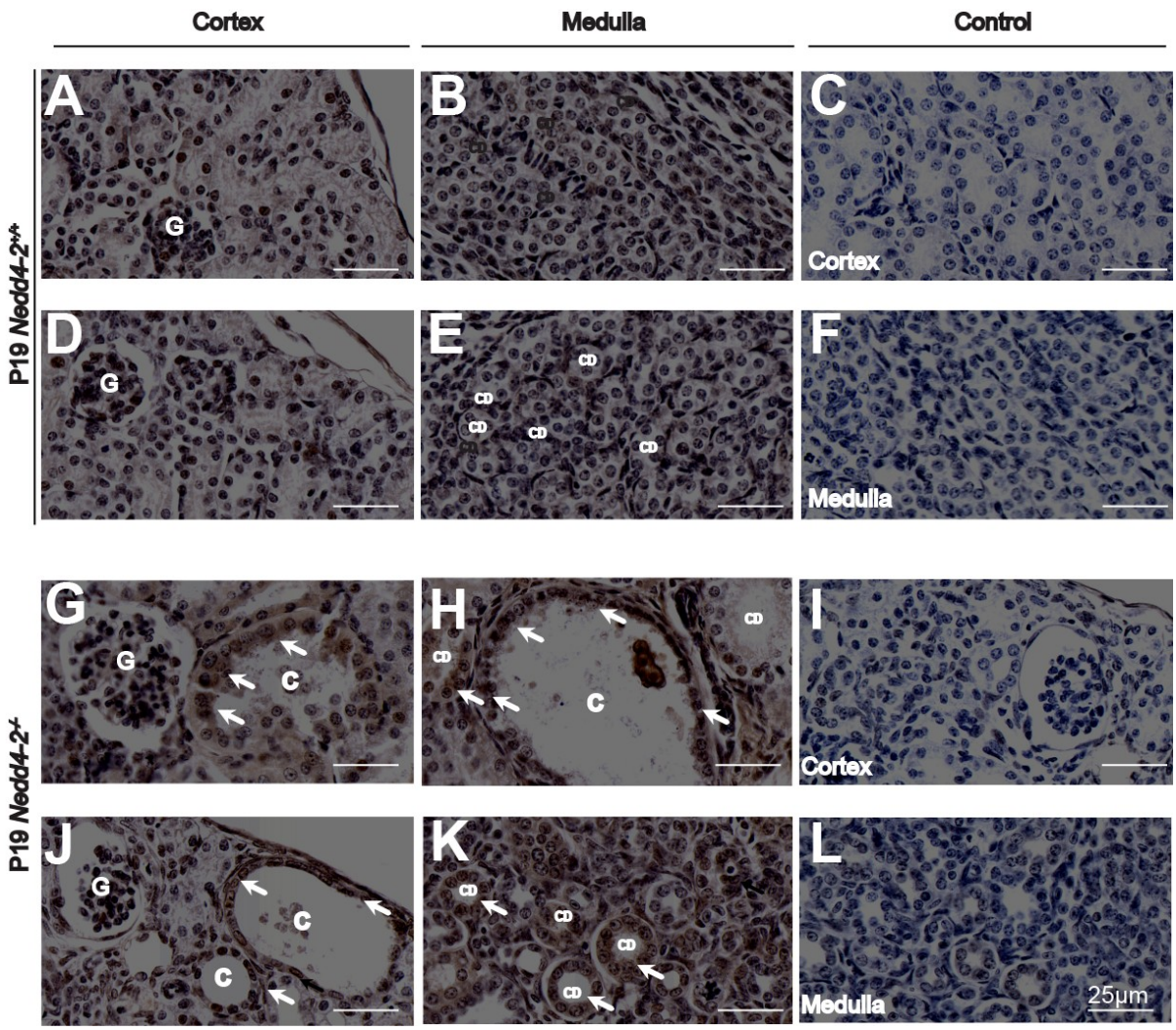
Cortex
Medulla
Control
P19 Nedd4-2+/+
P19 Nedd4-2-/-
A
B
C
D
E
F
G
H
I
J
K
L
G
CD
C
Cortex
Medulla
25µm

2.3.5 *Nedd4-2* $^{-/-}$ cystic kidneys do not show apoptotic difference

To further assess imbalance between cell proliferation and apoptosis, an important parameter in cyst formation and expansion, the *Nedd4-2*$^{-/-}$ kidneys were subjected to immuno histochemistry with the apoptosis marker cleaved caspase-3. Apoptosis is programmed cell death and is a hallmark for cystic kidney disorders, and un-programmed uncontrolled cell death (necrosis) is another mechanism for shedding of unwanted cells in the tissues (Woo, 1995, Goilav, 2011). The cell death process is important for normal kidney development and has been implicated in different animal models of PKD as well as in human cyst formation (Goilav, 2011). The cysts can undergo disturbances in cell death depending upon imbalance between intracellular pro and anti apoptotic factors, such as caspases and intracellular inhibitors of apoptosis respectively (Goilav, 2011). Cleaved caspase-3 is the active form of caspase-3, and antibody against active Caspase-3 is used as a marker for apoptotic caspases involved in executing cell death (Goilav, 2011). To evaluate the levels of apoptosis in *Nedd4-2*$^{-/-}$ P19 kidneys, sections were immunohistochemically treated with antibody to cleaved Caspase-3 with *Nedd4-2*$^{+/+}$ kidneys as control. There was no significant difference between *Nedd4-2*$^{-/-}$ and wild-type littermates in the staining pattern of apoptotic cells as seen in representative images of the *Nedd4-2*$^{-/-}$ cortex (**Fig 2.7 G, J**) and medulla (**Fig 2.7 H, K**) with *Nedd4-2*$^{+/+}$ kidneys as a control (**Fig 2.7** (**A, D**), cortex, (**B, E**), medulla). The secondary antibody was used as negative control for secondary antibody specificity (**Fig 2.7 F** and **L**) and a positive cancerous tissue stained with cleaved caspase-3 antibody was taken as a positive control (**Fig 2.7 C** and **I**).

2.3.6 *Nedd4-2* $^{-/-}$ cystic kidneys show increased renal fibrosis (due to extracellular matrix modification) and decreased polysaccharide accumulation

Collagen synthesis and degradation is important in the extracellular matrix protein metabolism, and structural changes caused by cyst formation in the kidneys lead to collagen

accumulation around the cysts. These changes could be driven by upstream regulators involved in renal cyst formation like cAMP and TGFβ (Yamamoto *et al*., 1994, Clarkson *et al*., 1999). To further assess the progression and changes associated with cyst formation leading to extracellular matrix modification and collagen accumulation in the cystic kidneys, kidney sections from *Nedd4-2*$^{-/-}$ post natal 2, 15 and 19 were stained with Sirius red dye to showcase fibrosis in these tissues as shown in **Fig 2.8**. Collagen accumulation around the cysts epithelial lining is considerably higher in *Nedd4-2*$^{-/-}$ kidneys compared with wild-type littermates, along with areas surrounding the cysts marked by arrows from different stages in the cortex and the medulla of *Nedd4-2*$^{-/-}$ kidney (**Fig 2.8** Post natal day 2 (**D,J**)(**P,V**), Postnatal day15(**E,K**)(**Q,W**), Post natal day19 (**F,L**)(**R,X**), cortex, medulla respectively) in comparison to *Nedd4-2*$^{+/+}$ (**Fig 2.8** Post natal day2(**A,G**)(**M,S**), Post natal day 15(**B,H**)(**N,T**), Post natal day 19 (**C,I**)(**O,U**), cortex, medulla respectively) littermates. There is considerable progression of collagen deposition/fibrosis observed in the *Nedd4-2*$^{-/-}$ kidneys affected by cystic burden (**Fig 2.8 D-F**) in comparison to control littermates (**Fig 2.8 A-C**). Further, quantification of transcript levels of Collagen-1 in P19 kidneys of *Nedd4-2*$^{+/+}$ (N=5) and *Nedd4-2*$^{-/-}$ (N=5) mice show an increasing trend in mRNA transcript levels of Collagen-1 in the *Nedd4-2*$^{-/-}$ kidneys but this is not a statistically significant difference (**Fig 2.8 Y**). Extracellular matrix proteins like matrix metalloproteinase-9 (MMP-9) belonging to the zinc metalloproteinase family are involved in degradation and remodelling of extracellular matrix as previously reported in other models of renal cystic disease (Obermüller *et al*., 2001). The transcript levels of MMP-9 were measured to investigate the proteinase activity in the kidneys of *Nedd4-2*$^{-/-}$ mice, and they did not show any significant difference to wild-type (**Fig 2.8 Y**). To further assess the role played by collagen in the kidney extracellular matrix, immunohistochemistry for Collagen-1 was undertaken. Previous studies had pointed to the important role Collagen-1 plays in kidney fibrosis through its interaction with polycystin-1.

Chapter 2: Characterization of *Nedd4-2*$^{-/-}$ kidney

Polycystin-1 a cystoprotein interacts via its extra cellular domain on the plasma membrane with extracellular matrix proteins has been reported to have a potential role in cyst formation (Zeisberg *et al*., 2001, Weston *et al*., 2001). The relative abundance of collagen-1 could be seen in the *Nedd4-2*$^{-/-}$ cystic kidney cortex and medulla in cells lining the cysts (arrows), collecting ducts (CD) and tubules (*) as seen in **Fig 2.9** (**C, K** and **L**) and contrast adjusted images in **Fig 2.9** (**G**, **H, O** and **P**) relative to *Nedd4-2*$^{+/+}$ in **Fig 2.9** (**A**, **I** and **J**) with contrast adjusted images in **Fig 2.9** (**E, F, M** and **N**). To confirm the specificity and binding of the secondary antibody, a control lacking primary antibody was used for both *Nedd4-2*$^{+/+}$ (**Fig 2.9 B**) and *Nedd4-2*$^{-/-}$ (**Fig 2.9 D**) cystic kidneys. This collagen accumulation could also be corroborated by some of the transmission electron micrographs seen in **Fig 2.16 C, D** and **E** in the *Nedd4-2*$^{-/-}$ cystic kidneys marked by arrows suggesting accumulation of collagen fibres in comparison to *Nedd4-2*$^{+/+}$ (**Fig 2.16 A** and **B**).

To corroborate the above findings and understand the role of interstitial fibrosis in the *Nedd4-2*$^{-/-}$ cystic kidneys, Masson trichrome staining was performed. This staining, in conjunction with Sirius red staining, is essential for pathological cross verification for interstitial fibrosis to avoid artefacts and assure reproducibility. The blue colouration and grey colouration in phase contrasted images represents collagen deposition in **Fig 2.10**. There was a significant increase in interstitial fibrosis in P19 *Nedd4-2*$^{-/-}$ cystic kidney medulla and cortex as compared to wild-type (**Fig 2.10),** showing increased staining (blue/grey) colouration around the cysts with accumulation of collagen adjacent to the disturbed renal parenchyma (**Fig 2.10** *Nedd4-2*$^{-/-}$ cortex (**C**, **G),** (**D, H**), and medulla (**K, O**), (**L, P**) and *Nedd4-2*$^{+/+}$ cortex (**A, E**), (**B, F**), and medulla (**I, M**), (**J, N**) medulla). This further highlights the importance of extracellular matrix remodelling due to cyst formation or tubular injury leading to increased renal/interstitial fibrosis. The renal interstitium ECM contains sulphated and non-sulphated glycosaminoglycans such as biglycan and decorin, as well as collagen types I and III, and

fibronectin (Lemley and Kriz, 1991). Tubular atrophy is caused by specialised transport and metabolic loss in kidneys due to cystic formation (Thomas *et al*., 1999). To assess the role of polysaccharides such as glycogen and mucosubstances in *Nedd4-2*$^{-/-}$ cystic kidney tissue, periodic acid Schiff (PAS) staining was undertaken. PAS stains for carbohydrate macromolecules found in connective tissues, mucus and basal laminae. This stain is also used to detect disease associated with glycogen storage (diabetes) and adenocarcinomas (Chen and Burchell, 1998). The magenta/blue colouration in phase contrasted images represents polysaccharide accumulation in **Fig 2.11**. The *Nedd4-2*$^{-/-}$ cystic kidneys displayed a significant decrease in PAS staining (magenta/blue colouration) around the cysts, with no accumulation adjacent to the disturbed renal parenchyma as seen in representative images from medulla and cortex of *Nedd4-2*$^{-/-}$ kidney sections (**Fig 2.11** (**C**, **G),** (**D, H**), cortex, (**K, O**), (**L, P**) medulla) in comparison to the *Nedd4-2*$^{+/+}$ kidney (**Fig 2.11** (**A, E**), (**B, F**) cortex, (**I, M**), (**J, N**) medulla). A positive control tissue (tongue) was used for obtaining relative understanding of the colour patterns and accumulation of glycoprotein's and mucus (data not shown). These results highlight the decreased accumulation of polysaccharides and mucosubstances such as glycolipids, glycoproteins and mucins in the P19 *Nedd4-2*$^{-/-}$ kidneys.

Fig 2.7 *Nedd4-2*$^{-/-}$ cystic kidneys show wild-type levels of cell death. Representative images (80x) of cleaved caspase-3 immunohistochemistry performed on post natal day 19 *Nedd4-2*$^{+/+}$ (N=3) and *Nedd4-2*$^{-/-}$ (N=3) cystic kidneys with respective images taken from medulla and cortex region of the kidney with indicated genotypes. Images **A** and **D** represent P19 *Nedd4-2*$^{+/+}$ cortex. Images **D** and **E** represent P19 *Nedd4-2*$^{+/+}$ medulla. Image **C** represents positive control from cancerous tissue undergoing apoptosis and image **F** represents negative secondary antibody control of P19 *Nedd4-2*$^{+/+}$ medulla. Images **G** and **J** represent P19 *Nedd4-2*$^{-/-}$ cortex. Images **H** and **K** represent P19 *Nedd4-2*$^{-/-}$ medulla. Image **I** represents positive control from cancerous tissue undergoing apoptosis and image **L** represents negative secondary antibody only control of P19 *Nedd4-2*$^{-/-}$ cystic kidney medulla. The cysts (C) are marked by arrows. Glomeruli are represented as G. The collecting ducts of the kidney are marked as CD. The images were taken using Hamamatsu nanozoomer view 2. Scale bar = 25μm.

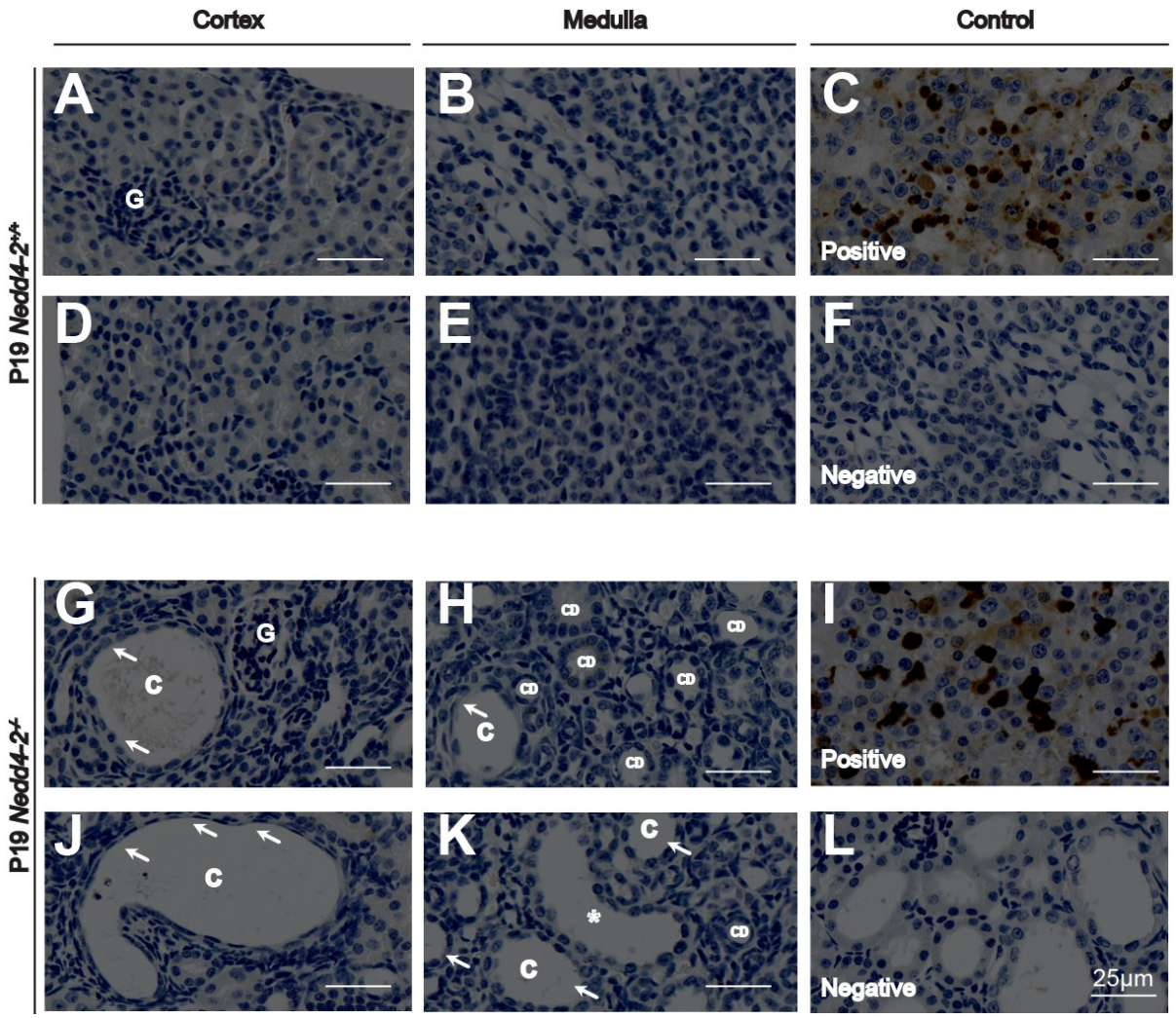
Cortex
Medulla
Control
P19 Nedd4-2+/+
A
B
C
G
Positive
D
E
F
Negative
P19 Nedd4-2-/-
G
G
C
H
CD
C
I
Positive
J
C
K
C
*
C
L
Negative
25µm

Fig 2.8 Increased renal fibrosis in *Nedd4-2*$^{-/-}$ kidneys. Representative Picrosirius red dye stained images (80x) at different post natal stages from day 2, day 15 and day 19. *Nedd4-2*$^{+/+}$ and *Nedd4-2*$^{-/-}$ cystic kidneys with images taken from medulla and cortex region of the kidney with indicated genotypes. Images **A** and **G** represent P2 *Nedd4-2*$^{+/+}$ cortex. Images **M** and **S** represent P2 *Nedd4-2*$^{+/+}$ medulla. Image **B** and **H** represent P15 *Nedd4-2*$^{+/+}$ cortex. Images **N** and **T** represent P19 *Nedd4-2*$^{+/+}$ medulla. Image **C** and **I** represent P19 *Nedd4-2*$^{+/+}$ cortex. Images **O** and **U** represent P19 *Nedd4-2*$^{+/+}$ medulla. Images **D** and **J** represent P2 *Nedd4-2*$^{-/-}$ cortex. Images **P** and **V** represent P2 *Nedd4-2*$^{-/-}$ medulla. Image **E** and **K** represent P15 *Nedd4-2*$^{-/-}$ cortex. Images **Q** and **W** represent P15 *Nedd4-2*$^{-/-}$ medulla. Image **F** and **L** represent P19 *Nedd4-2*$^{-/-}$ cortex. Images **R** and **X** represent P19 *Nedd4-2*$^{-/-}$ medulla. Images **G-L** and **S-X** represent threshold adjusted images using Image J software. The dark red colour in images (**A-X**) indicates collagen accumulation. The cysts are marked by arrows. The images were taken using Hamamatsu nanozoomer view 2. **Y** represents quantitative real time PCR analysis of collagen-1 and Matrix metalloproteinase-9 (MMP-9) expression in *Nedd4-2*$^{+/+}$ (N=5) and *Nedd4-2*$^{-/-}$ (N=5) P19 kidneys. Expression is measured relative to β-actin levels. Data represented as mean ± SEM ($P>0.05$, n.s=not significant, unpaired T-test using Welch correction). Scale bar = 25μm.

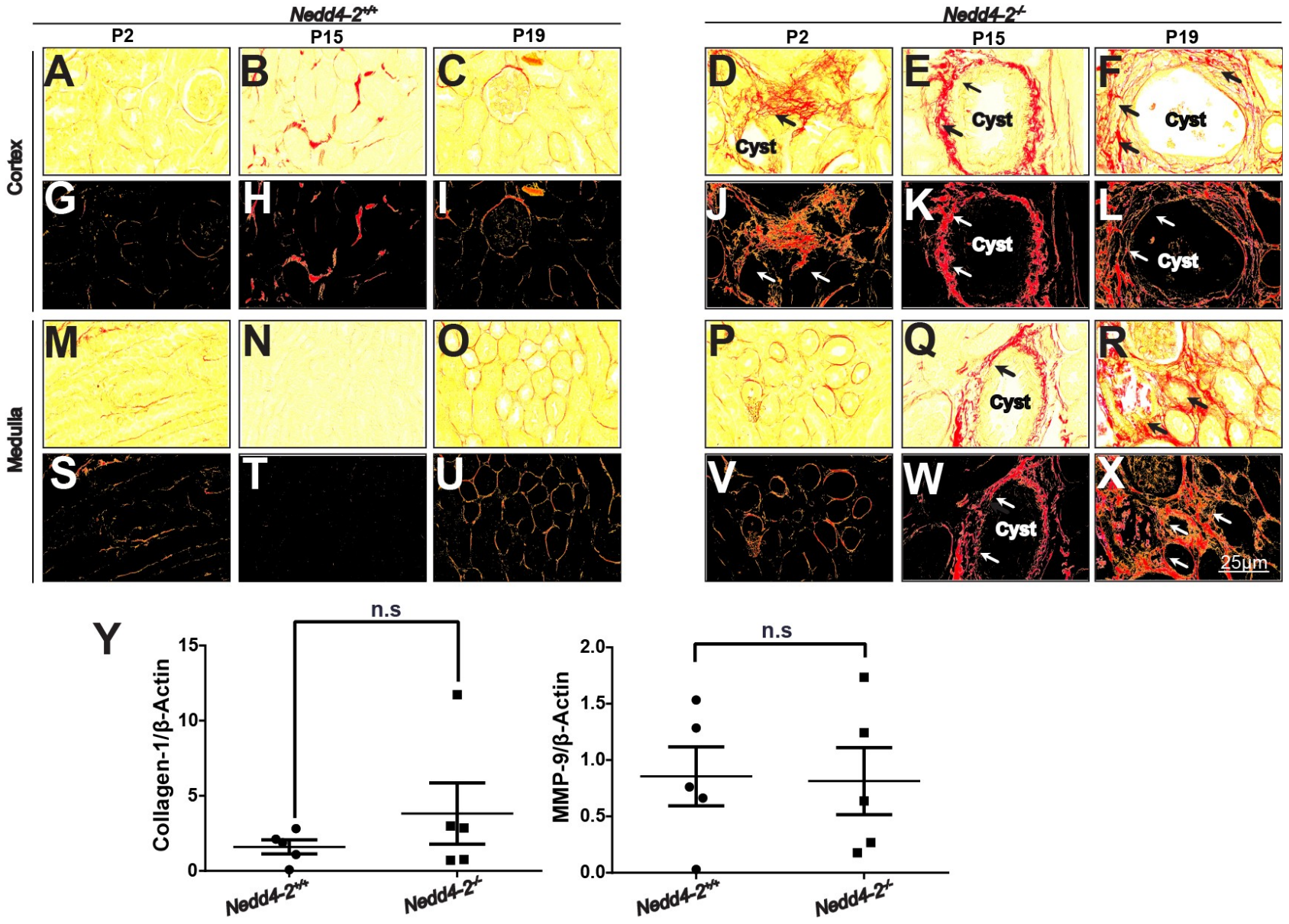
Nedd4-2+/+
Nedd4-2-/-
P2
P15
P19
Cortex
Medulla
A
B
C
D
E
F
G
H
I
J
K
L
M
N
O
P
Q
R
S
T
U
V
W
X
Cyst
25μm
Y
n.s
Collagen-1/β-Actin
MMP-9/β-Actin
Nedd4-2+/+
Nedd4-2-/-

Fig 2.9 *Nedd4-2*$^{-/-}$ cystic kidneys show increased collagen-1 expression and collagen-1 accumulation around the cysts and tubules. Representative Collagen-1 stained images (80x) of post natal day 19 *Nedd4-2*$^{+/+}$ (N=4) and *Nedd4-2*$^{-/-}$ (N=4) cystic kidneys with images taken from medulla and cortex region of the kidney with indicated genotypes. Images **A**, **E** and **F** represent P19 *Nedd4-2*$^{+/+}$ cortex. Images **I, J, M** and **N** represent P19 *Nedd4-2*$^{+/+}$ medulla. Images **C, G** and **H** represent P19 *Nedd4-2*$^{-/-}$ cortex. Images **K, L, O** and **P** represent P19 *Nedd4-2*$^{-/-}$ medulla. Images **B** and **D** represent P19 *Nedd4-2*$^{+/+}$ cortex and *Nedd4-2*$^{-/-}$ cortex from kidney treated with secondary antibody only as a negative control. Images **E-H** and **M-P** represent threshold adjusted images using Image J software. The dark brown colour in images (**A, C** and **I-L**) and black colour in images (**E-H and M-P**) is indicative of collagen accumulation in kidneys. The cysts (C) are marked by arrows. Glomeruli are represented as G. The collecting ducts of the kidney are marked as CD. The images were taken using Hamamatsu nanozoomer view 2. Scale bar = 25µm.

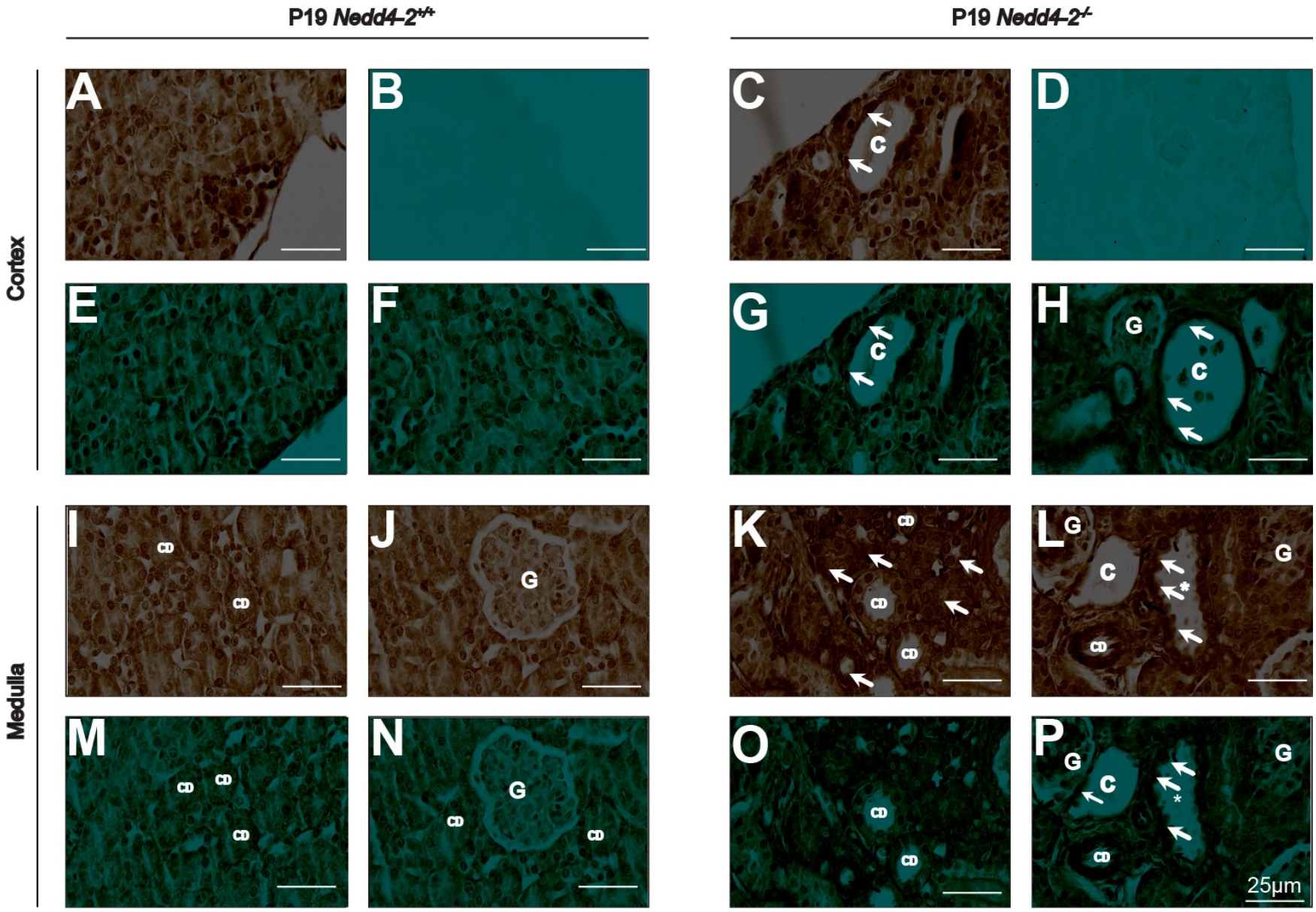
P19 Nedd4-2+/+
P19 Nedd4-2-/-
Cortex
Medulla
A
B
C
D
E
F
G
H
I
J
K
L
M
N
O
P
c
G
*
25µm

Fig 2.10 *Nedd4-2*$^{-/-}$ cystic kidneys show increased interstitial fibrosis. Representative Masson trichrome stained images (80x) of post natal day 19 *Nedd4-2*$^{+/+}$ (N=3) and *Nedd4-2*$^{-/-}$ (N=3) cystic kidneys with images taken from medulla and cortex region of the kidney with indicated genotypes. Images **A**, **E, B** and **F** represent P19 *Nedd4-2*$^{+/+}$ cortex. Images **I, J, M** and **N** represent P19 *Nedd4-2*$^{+/+}$ medulla. Images **C, D, G** and **H** represent P19 *Nedd4-2*$^{-/-}$ cortex. Images **K, L, O** and **P** represent P19 *Nedd4-2*$^{-/-}$ medulla. Images **E-H** and **M-P** represent threshold adjusted images using Image J software. The dark blue colour in images (**A-D** and **I-L**) and grey colour in images (**E-H and M-P**) represents interstitial fibrosis and damage in the kidneys. The cysts (C) are marked by arrows. Glomeruli are represented as G. The collecting ducts of the kidney are marked as CD. The images were taken using Hamamatsu nanozoomer view 2. Scale bar = 25µm. This experiment was done with the help of Anatomical Pathology at SA Pathology.

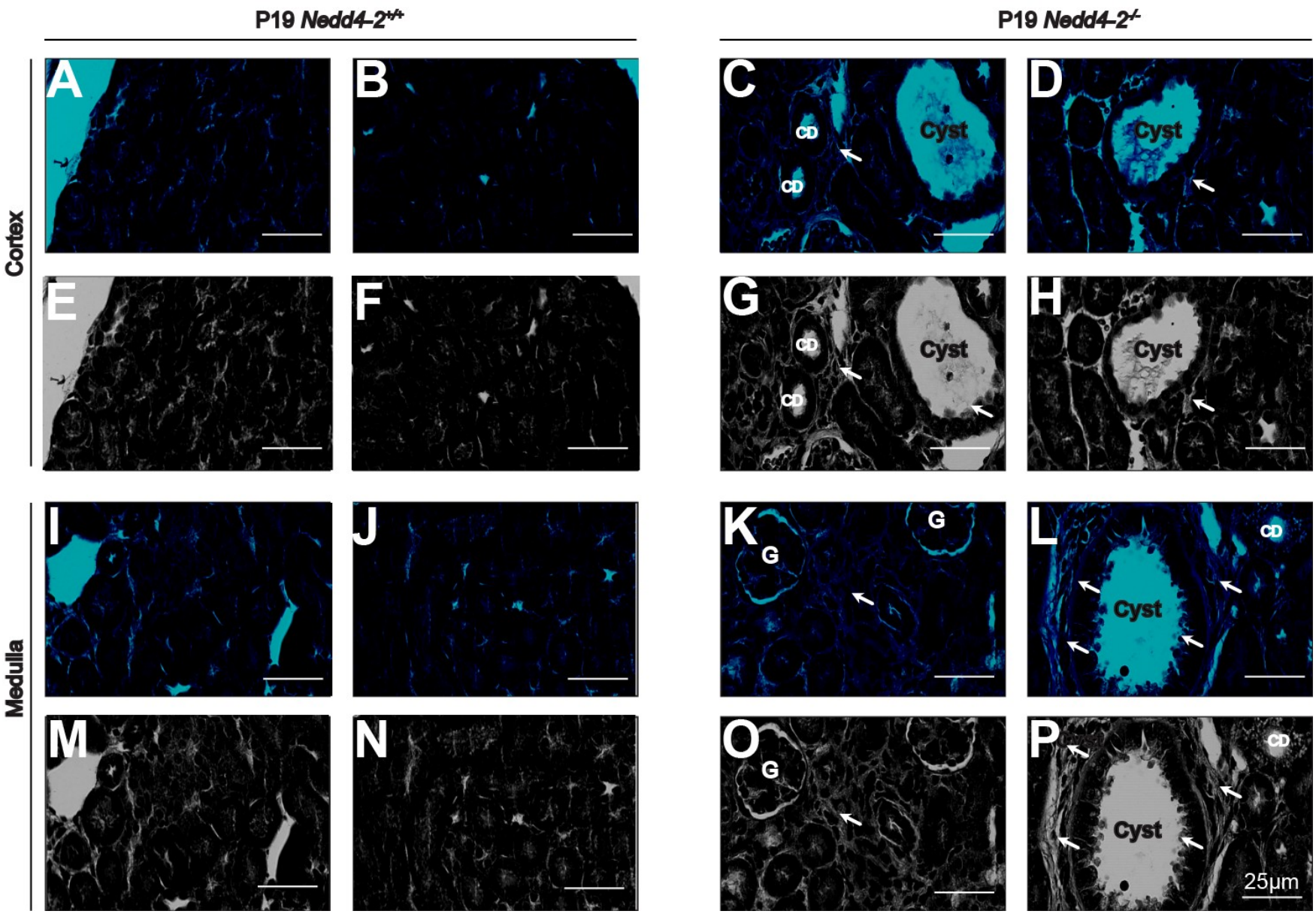
P19 Nedd4-2+/+
P19 Nedd4-2-/-
Cortex
Medulla
A
B
C
D
E
F
G
H
I
J
K
L
M
N
O
P
CD
Cyst
G
25μm

Fig 2.11 *Nedd4-2*$^{-/-}$ cystic kidneys show decreased accumulation of polysaccharides and mucosubstances. Representative periodic acid Schiff stained images (80x) of post natal day 19 *Nedd4-2*$^{+/+}$ (N=3) and *Nedd4-2*$^{-/-}$ (N=3) cystic kidneys with images taken from medulla and cortex region of the kidney with indicated genotypes. Images **A**, **B, E** and **F** represent P19 *Nedd4-2*$^{+/+}$ cortex. Images **I, J, M** and **N** represent P19 *Nedd4-2*$^{+/+}$ medulla. Images **C, D, G** and **H** represent P19 *Nedd4-2*$^{-/-}$ cortex. Images **K, L, O** and **P** represent P19 *Nedd4-2*$^{-/-}$ medulla. Images **E-H** and **M-P** represent threshold adjusted images using Image J software. The magenta colour in images (**A-D** and **I-L**) and dark blue colour in images (**E-H and M-P**) represents accumulation of polysaccharides such as glycogen, and mucosubstances such as glycolipids, glycoproteins and mucins in the kidneys. The cysts (C) are marked by arrows. Glomeruli are represented as G. The tubules in the kidneys are marked by asterisks (*). The collecting ducts of the kidney are marked as CD. The images were taken using Hamamatsu nanozoomer view 2. Scale bar = 25μm. This experiment was done with help of Anatomical Pathology at SA Pathology.

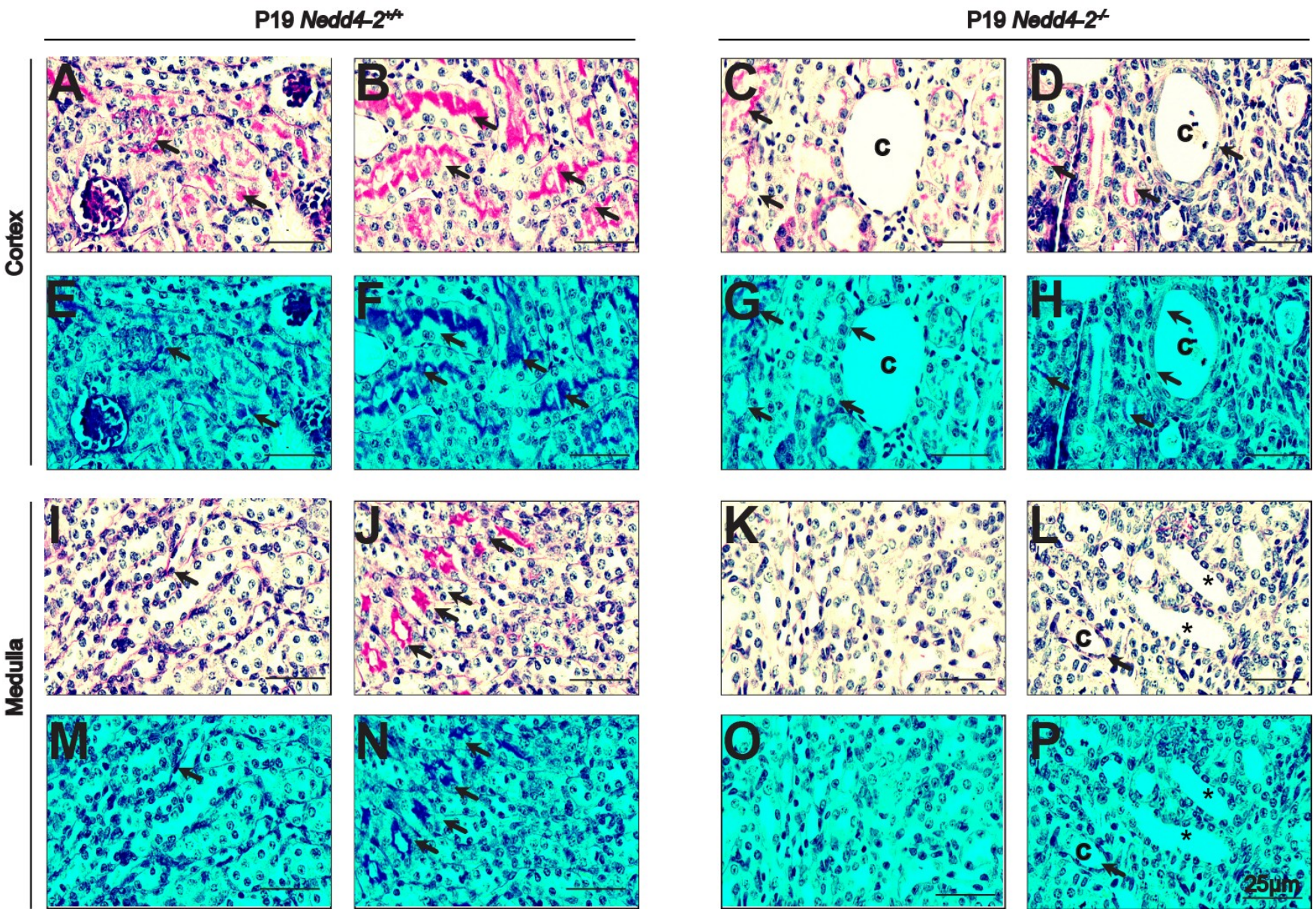
P19 Nedd4-2+/+
P19 Nedd4-2-/-
Cortex
Medulla
A
B
C
D
E
F
G
H
I
J
K
L
M
N
O
P
c
25μm

2.3.7 Increase in cAMP levels drives cyst formation.

Cell proliferation and fluid secretion within cystic kidneys are hallmarks of kidney cyst disorders, and both of these features of cyst formation are stimulated by cyclic AMP flux (cAMP) and interstitial fibrosis (Blanco and Wallace, 2013, Clarkson *et al*., 1999). Therefore, the levels of cAMP were measured, as cAMP is an upstream regulator of pathophysiological mechanisms reported in earlier sections of this thesis to be associated with *Nedd4-2*$^{-/-}$ cystic kidneys. **Fig 2.12** shows that levels of cAMP were similar in wild type and *Nedd4-2*$^{-/-}$ kidneys before birth at embryonic day 18.5 (E18.5). As reported earlier in **Fig 2.2,** these E18.5 *Nedd4-2*$^{-/-}$ kidneys looked normal with no major aberration in the renal parenchyma. However post natal day 19 (P19) *Nedd4-2*$^{-/-}$ kidneys usually have cystic growth, and *Nedd4-2*$^{-/-}$ cystic kidneys were used to measure cAMP levels, and showed a significant increase in cAMP levels (**p = 0.03**). This confirms our previous understanding of cAMP, which is known to drive cyst expansion and formation within the kidneys affected with cystic disorders.

2.3.8 Role of Nedd4-2 in ciliogenesis

As we have tried to establish the pathophysiological characteristics associated within *Nedd4-2*$^{-/-}$ cystic kidneys, cell cilia malfunction is another primary aspect of renal cystic disorders. Cilia are specialized dynamic structures with cytoplasm, cell membranes and longitudinal microtubules (Satir and Christensen, 2007). Centrosomes are organelles that are microtubule organising centres and regulate cell cycle progression, and defects in centrosomes have been associated with renal cyst formation (Satir and Christensen, 2007, Hildebrandt and Otto, 2005). Centrosomes are composed of two orthogonally directional centrioles per cell (Satir and Christensen, 2007). The lengthening of cilium across the microtubules via intraflagellar transport is important in maintaining cilia structure. When disrupted through defects in transporter motor proteins like kinesin-2 (anterograde) and dyenins (retrograde), these play an important role in renal cyst development (Satir and Christensen, 2007, Zariwala *et al*., 2007).

Chapter 2: Characterization of *Nedd4-2*$^{-/-}$ kidney

To understand the role Nedd4-2 plays in ciliogenesis and renal cystic disorder, also characterised as ciliopathies, *Nedd4-2*$^{-/-}$ post natal kidneys were stained with the ciliary marker acetylated α-tubulin and viewed for cilia in comparison to control *Nedd4-2*$^{+/+}$ littermates (**Fig 2.13 A-F**). The ciliary structure within the cysts looked different in *Nedd4-2*$^{-/-}$ (**Fig 2.13 E** and **F**) kidneys in comparison to *Nedd4-2*$^{+/+}$ littermates (**Fig 2.13 B** and **C**). In *Nedd4-2*$^{-/-}$ (**Fig 2.13 D)** kidney cortex there is more ciliary growth present around the collecting duct in comparison to *Nedd4-2*$^{+/+}$ littermates (**Fig 2.13 A)**. It is easier to distinguish the *Nedd4-2*$^{-/-}$ (**Fig 2.13 D**) kidney ciliary structure since the lumens of the tubules and overall kidney architecture seem to be more dilated and cilia do not overlap, contrary to the control *Nedd4-2*$^{+/+}$ (**Fig 2.13 A**). Due to the dilation of the tubules, the number of cilia in the *Nedd4-2*$^{-/-}$ kidneys (**Fig 2.13 D**) appear to be greater in comparison to the control *Nedd4-2*$^{+/+}$ (**Fig 2.13 A**). Higher magnification images highlight distinctive differences in the cilia structure of *Nedd4-2*$^{-/-}$ (**Fig 2.13 F**) in comparison to *Nedd4-2*$^{+/+}$ (**Fig 2.13 C**), and *Nedd4-2*$^{-/-}$ cystic cilia lacks in the lumen overall, another hallmark of renal cyst formation. To further investigate this structural difference, transmission electron microscopy and scanning electron microscopy techniques were undertaken. In image **Fig 2.16** (**H-J)** we highlight protruding ciliary structure, which was quite difficult to locate in the cross sections taken of the *Nedd4-2*$^{+/+}$ kidney (**Fig 2.16 F-G**). The centrosome structure located in *Nedd4-2*$^{-/-}$ kidneys (**Fig 2.16 M-N**) did not show any attached cilia, and it looked different in comparison to the *Nedd4-2*$^{+/+}$ centrosome (**Fig 2.16 K-L**). To investigate further, scanning electron microscopy images were taken as reported in **Fig 2.17** but no significant ciliary image was visualised (**Fig 2.17A-D**). To understand the role of motor proteins localised to the cilia which aid in formation and function of the cilia, ciliary proteins like anterograde motor protein Kinesin-2 subunit KIF3A, Dynactin-5 retrograde transport motor protein subunit in cilia, and smooth muscle actin (SMA) involved in microtubule maintenance and known to be affected during

cystic kidney disease were checked via quantitative real time PCR (**Fig 2.13 G**). There was no significant difference found in *Nedd4-2*$^{-/-}$ kidney in comparison to *Nedd4-2*$^{+/+}$ littermates at the transcript level. Nedd4-2 has previously not been reported to be involved in ciliogenesis. To understand the role of Nedd4-2 in cilia formation, mouse embryonic fibroblasts (MEF) were isolated from embryonic day 13.5 mice, cultured, plated and stained with the ciliary marker acetylated α- tubulin, and the centrosome marker Nedd-1 after serum starvation for 36 hours. Cilia and centrosome numbers were observed and blind counted for two independent experiments. The average percentage of MEF cells showing cilia number and centrosome number are shown in **Fig 2.14 A** and **B**. There was no significant difference found between the control isolated cells and Nedd4-2 deficient cells (**Fig 2.14 A** and **B**).

Fig 2.12 Increased cAMP levels in *Nedd4-2*$^{-/-}$ mice. cAMP measurements were made from embryonic day 18.5 (N=3), Post natal day 19 (N=3) *Nedd4-2*$^{+/+}$ and *Nedd4-2*$^{-/-}$ cystic kidneys. At E18.5, the levels of cAMP in *Nedd4-2*$^{+/+}$ and *Nedd4-2*$^{-/-}$ kidneys were the same. At P19 there is a statistically significant increase in cAMP levels (pmol/ml) in *Nedd4-2*$^{-/-}$ kidneys in comparison to *Nedd4-2*$^{+/+}$ as indicated by P value=0.03. Data represented as mean ± SEM ($P \leq 0.05$ deemed statistically significant, unpaired T-test assuming equal variance). This experiment was performed by **Dr. Jantina. A. Manning.**

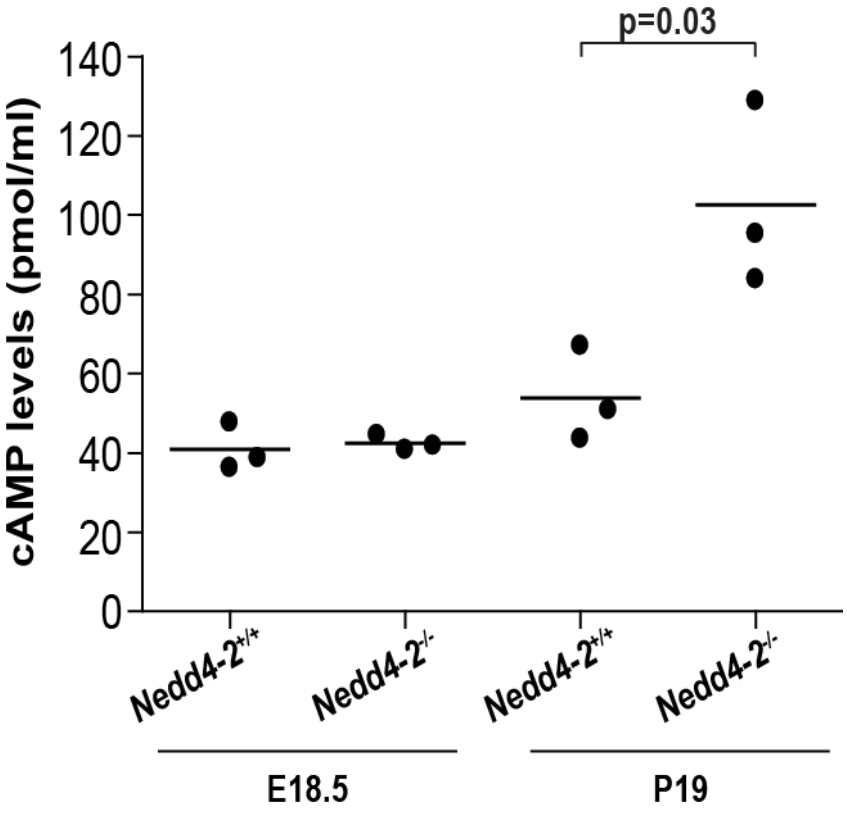
p=0.03
cAMP levels (pmol/ml)
140
120
100
80
60
40
20
0
Nedd4-2+/+
Nedd4-2-/-
Nedd4-2+/+
Nedd4-2-/-
E18.5
P19

Fig 2.13 Ciliary abnormalities in *Nedd4-2*$^{-/-}$ cystic kidneys. Representative immunofluoroscence images from paraffin embedded kidney sections stained with acetylated α-tubulin ciliary marker in green (N=3). Images **A-C** from Post natal day 15 *Nedd4-2*$^{+/+}$ kidneys. Images **A** and **B** at lower magnification. Image **C** inset of box indicated in Image **B**. Image **D** and **E** represent P15 *Nedd4-2*$^{-/-}$ cystic kidney. Images **D** and **E** are represented at lower magnification and **F** at higher magnification zoomed in image. Image **F** inset of box indicated in Image **E**. The cysts are marked in images **E** and **F**. The tubules and cilia (green) in the kidneys are marked by arrows indicated in images (**A, C, D and F**). The images were taken using LSM700 confocal microscope. **G** represents quantitative real time PCR analysis of Smooth Muscle Actin (SMA), Dynactin-5 (DCTN5) and Kinesin subunit 3A (KIF3A) expression in post natal day 19 *Nedd4-2*$^{+/+}$ (N=3) and *Nedd4-2*$^{-/-}$ (N=3) kidneys. Expression is relative to β-actin levels. Data represented as mean ± SEM ($P>0.05$, n.s=not significant, unpaired T-test using Welch correction). Images (A, B, D and E) Scale bar = 100µm, Images (C and F) Scale bar = 50µm.

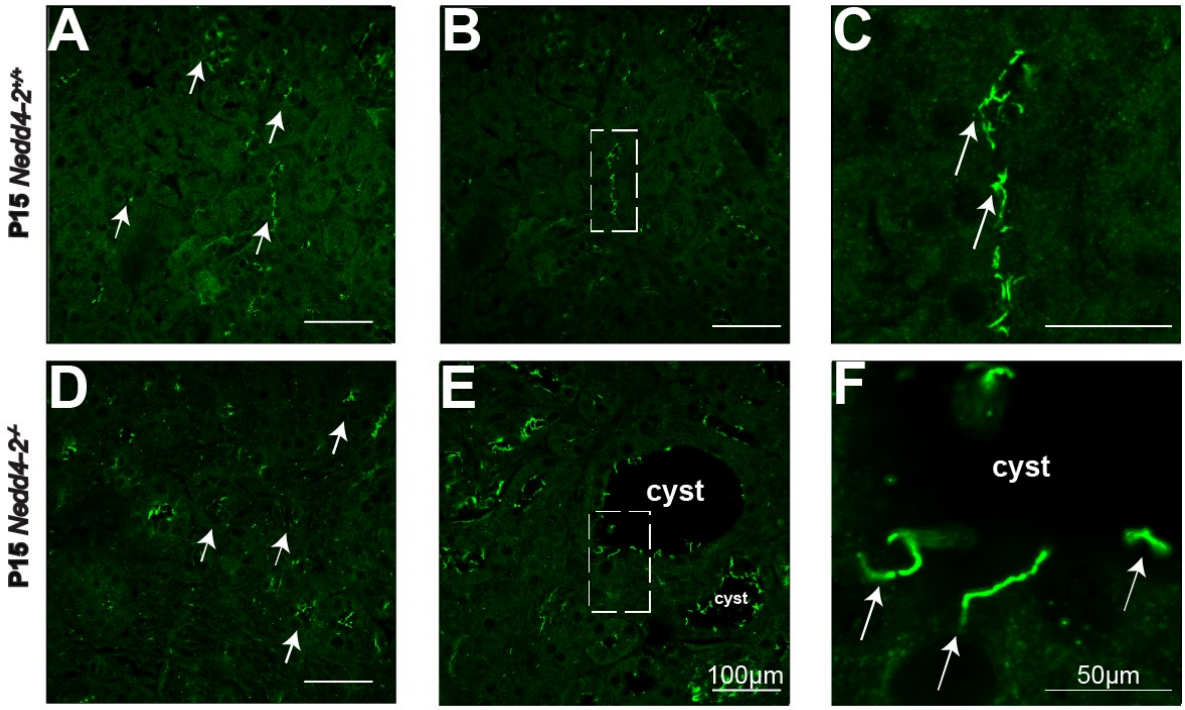
A
B
C
D
E
F
P15 Nedd4-2+/+
P15 Nedd4-2-/-
cyst
cyst
100μm
cyst
50μm

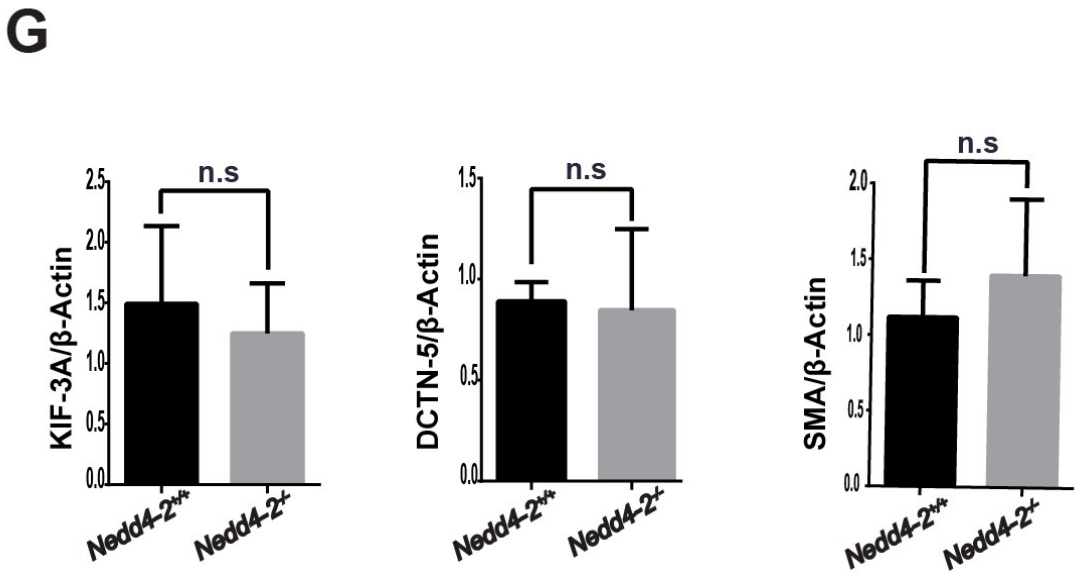
G
n.s
KIF-3A/β-Actin
2.5
2.0
1.5
1.0
0.5
0.0
Nedd4-2+/+
Nedd4-2-/-
n.s
DCTN-5/β-Actin
1.5
1.0
0.5
0.0
Nedd4-2+/+
Nedd4-2-/-
n.s
SMA/β-Actin
2.0
1.5
1.0
0.5
0.0
Nedd4-2+/+
Nedd4-2-/-

Fig 2.14 Role of Nedd4-2 in cilia formation. Immunofluoroscence images of *Nedd4-2*$^{-/-}$ mouse embryonic fibroblasts stained with acetylated α- tubulin (ciliary marker) and Nedd-1 (centrosomal marker) were counted from isolated cells of *Nedd4-2*$^{+/+}$ and *Nedd4-2*$^{-/-}$ embryonic day 13.5 mice. The cells were blind-counted in two independent experiments using confocal LSM700 microscope. **A)** Quantitation of number of cilia/cell percentage between *Nedd4-2*$^{+/+}$ and *Nedd4-2*$^{-/-}$ **B)** Quantitation of centrosome number/cell percentage comparison between *Nedd4-2*$^{+/+}$ and *Nedd4-2*$^{-/-}$. This calculation was done in Microsoft excel for percentage cells per experiment. Data represented as mean ± SEM for N=2 independent experiments ($P>0.05$, n.s=not significant, two way ANOVAs using Sidaks multiple comparison test for grouped experiments).

A

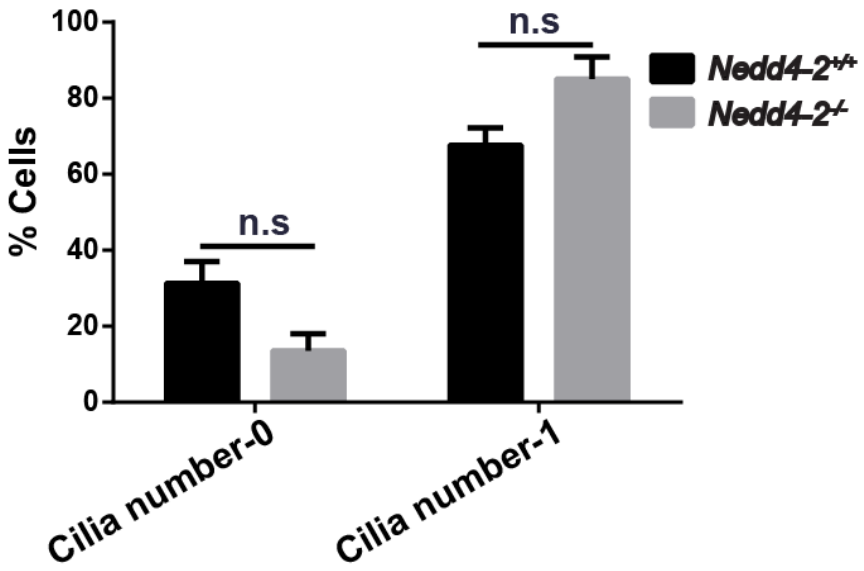
100
80
60
40
20
0
% Cells
n.s
n.s
Nedd4-2+/+
Nedd4-2-/-
Cilia number-0
Cilia number-1

B

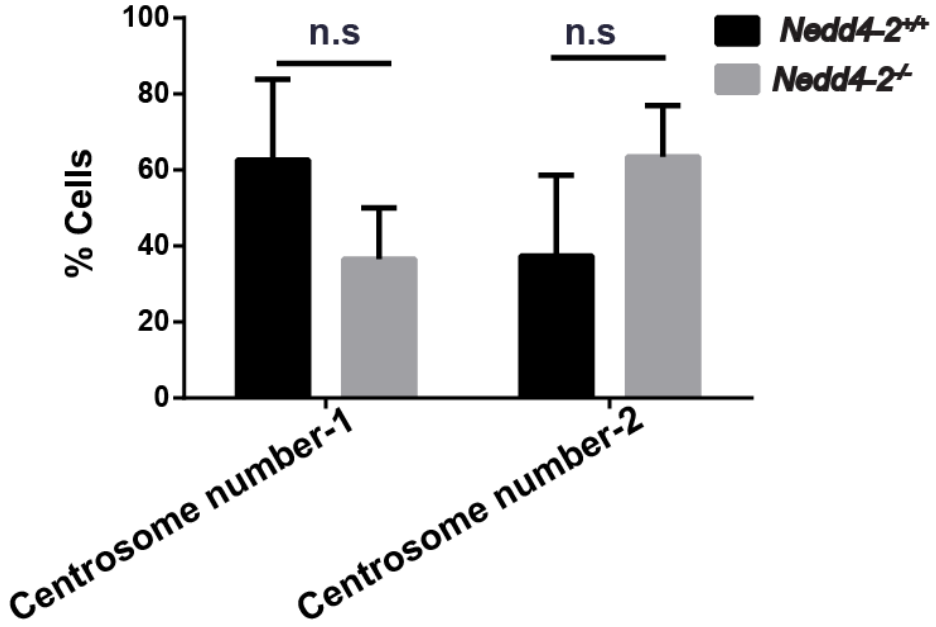
100
80
60
40
20
0
% Cells
n.s
n.s
Nedd4-2+/+
Nedd4-2-/-
Centrosome number-1
Centrosome number-2

2.3.9 *Nedd4-2*$^{-/-}$ kidneys show renal dysplasia, not PKD

To further understand the differences seen in the *Nedd4-2*$^{-/-}$ cystic kidneys in comparison to previous studied mouse models of PKD, it became important to evaluate the pathological characteristics in finer detail for the *Nedd4-2*$^{-/-}$ cystic kidneys. To aid in this understanding, a detailed pathology report was prepared by mouse pathologist Dr. John Finnie, SA Pathology.

As shown in **Fig 2.15 C-J**, *Nedd4-2*$^{-/-}$ kidney sections examined at postnatal day 17 showed histological changes consistent with renal dysplasia resulting in the cystic phenotype, which is defined by the presence of poorly differentiated, foetal/immature glomeruli and tubules with persistent mesenchyme, inappropriate to the stage of development of the animal, due to anomalous differentiation. These changes were not found in age-matched, wild-type mice **(Fig 2.15 A-B)**.

Microscopically, dysplastic changes are characterised, in the cortex, by persistence of aggregates of small, immature, hyper cellular glomeruli with unapparent capillaries and, in the intervening interstitium, persistent mesenchyme. There were sometimes small, primitive tubules with scant cytoplasm or large tubules lined by cuboidal to columnar, sometimes vacuolated and multilayered, epithelium; in some dilated ducts, the epithelium was markedly attenuated (**Fig 2.15 E-G**). Many medullary tubules and collecting ducts were hyper cellular by numerous poorly differentiated epithelial cells, sometimes without detectable lumina, and a few epithelial cells were undergoing mitotic division (**Fig 2.15 I**). These are all characteristics of renal dysplasia rather than polycystic kidney disease.

The dysplastic areas, particularly at postnatal day 17, occupied a large portion of the cortex, sometimes being disposed in radial segments extending from the sub capsular surface to the corticomedullary junction and sometimes more circumscribed within the cortex; adjacent cortical tissue was more normally developed (**Fig 2.15 J**).

2.4 Discussion

Renal cystic disorders are human kidney ailments, inherited or acquired depending on the disease pathology, leading to kidney dysfunction causing alteration in body homeostasis, an endpoint being human death. Recent studies undertaken to recapitulate these human kidney cyst disorders have been focussed on a variety of mouse models linked to genetic manipulations, spontaneously acquired mutations in genes involved in cyst formation and development within the kidneys (Schedl, 2007).

However factors responsible for cyst progression and disease development are still not very well characterised. To investigate the novel role played by Nedd4-2 the initial observation reported in this study, we highlight upon deletion of Nedd4-2, renal cysts were observed in the *Nedd4-2*$^{-/-}$ kidneys **(Fig 2.2)**. It became evident from this renal model that the cysts arising in the kidney had a pathological significance correlative of other mouse models of renal cyst formation (Schedl, 2007). To understand this we initially hypothesized this model of cyst formation to be similar to mouse models of polycystic kidney disease, a leading cause of renal cystic abnormalities. The multiple cysts in medulla and cortex at Post natal day19 (**Fig 2.2 J, P** and **V**) observed in these mice are shown to initiate at Post natal day 2 (**Fig.2.2 E** and **K**). Previous findings in renal mouse models of PKD suggested that the rate of progression of disease varies with age of onset in ADPKD, with genetic or environmental modifying factors (Reeders, 1992). The two hit theory is the most widely accepted one for cyst formation in ADPKD, where mutated single PKD gene allele by itself is not sufficient for cyst formation this could only occur by somatic inactivation of the non-mutated PKD allele (Qian *et al*., 1997). The progression of renal cysts is also characterised by outgrowth into other parts of the body, along with developmental defects within the kidney (Wilson, 2008, Wilson and Goilav, 2007). Loss of Nedd4-2 generated renal cysts with variability and an inconsistent phenotype as reported in **Table 2.3**. This cystic progression is also absent in

the organs prevalent of cystic growth like spleen, liver and pancreas reported to be affected in earlier models of PKD for cysts, as shown in **Fig 2.4.** This could be argued to be due to either a difference in the protein regulation of cyst development in the *Nedd4-2*$^{-/-}$ kidneys, or due to the variability of the phenotype seen from earlier reported models of PKD in disease progression. This progression in the *Nedd4-2*$^{-/-}$ animals could not be studied beyond day 19 since these mice die due to respiratory distress caused by the lung phenotype, as reported by Boase *et al*. (2011). These findings, though contrary to earlier reported models of PKD, pointed towards a milder form of cystic kidney disease in the *Nedd4-2*$^{-/-}$ animals or an altered pathology.

To dissect this pathology we sought clarification on the role variable cyst generation plays in *Nedd4-2*$^{-/-}$ kidneys to alter renal function. Renal cyst formation previously has been reported to increase cystic burden causing alterations in body weight and kidney size (Tao *et al*., 2005). These *Nedd4-2*$^{-/-}$ kidneys seemed to be paler, and slightly smaller but showed no significant kidney size difference compared to their control littermates **(Fig 2.3)**. The kidney cyst formation also had no significant difference on the body weight of these animals, suggesting that kidney cyst formation by P19 does not lead to any alteration in kidney function causing body weight changes as reported in earlier models of PKD (Tao *et al*., 2005). These initial findings further indicated a milder form of PKD since the cystic growth reported in conditional model of PKD is severe at post natal stages, leading to alterations in kidney function and body weight (Piontek *et al*., 2004). To identify the origin of these cysts within the different nephronal segments of the kidneys, crucial for understanding ion regulation within the different segments of the nephrons, *Nedd4-2*$^{-/-}$ kidneys were stained for nephronal markers (Starremans *et al*., 2008). The renal cysts in the *Nedd4-2*$^{-/-}$ kidneys originated from different regions of nephrons as reported in **Fig 2.5.** The origin of smaller cysts occurred from within the proximal tubule and collecting ducts, with the larger cysts

originating from the loop of Henle. Prior reports in other mouse models of PKD, like Cpk, Orpk and Bpk, showed cyst formation arising specifically from the collecting ducts unlike *Nedd4-2*$^{-/-}$ mice where cysts arise from multiple segments within the nephron (Devuyst *et al*., 1996). This could be due to specific expression of ion channels and transporters within different regions of the nephronal segments within the *Nedd4-2*$^{-/-}$ kidney being regulated by Nedd4-2.

Different mechanisms are proposed for cyst formation and growth such as changes in cell polarity, altered matrix composition, and imbalance between cell proliferation and apoptosis. One mechanism is increased cAMP concentration, a common finding in various models of ADPKD, which stimulates cyst fluid and electrolyte secretion within the cyst and also involves stimulation of the chloride channel cystic fibrosis transmembrane conductance regulator (CFTR) (Hanaoka *et al*., 1996). Previous reports showed increased levels of cAMP inhibit Nedd4-2 (Snyder *et al*., 2004a), suggesting upon deletion of Nedd4-2 in the kidney there is increase in levels of cAMP as reported in P19 *Nedd4-2*$^{-/-}$ cystic kidneys (**Fig 2.12**). Cystic dilations occur in PKD kidneys in response to cAMP as shown previously in the *Pkd1*$^{m1Bei-/-}$ embryonic kidneys, which when treated with 8-Br-cAMP were found to form cysts. This suggested that cAMP treatment in early renal tubule formation could stimulate fluid secretion, when cysts are formed for the very first time in PKD kidneys (Magenheimer *et al*., 2006). Further changes in intracellular cAMP could alter transcriptional and protein expressions of cAMP responsive proteins like vasopressin receptor (V2R) and aquaporin-2 (Starremans *et al*., 2008).

cAMP flux upstream is known to drive downstream signalling involved in cystic phenotypes by mediating imbalances in cell proliferation and cell death. In the majority of cases increased proliferation leads to cystogenesis (Zheng *et al*., 2008). In the *Nedd4-2*$^{-/-}$ cystic kidneys we report increased number of proliferating cells as demonstrated by staining around

cyst lining epithelia, tubules and the collecting ducts, contributing to cyst progression **(Fig 2.6).** In contrast there seems to be no such alteration in the number of apoptotic cells lining the cysts, shown via active caspase-3 staining for cell death **(Fig 2.7).**

Extracellular matrix modification and accumulation is also termed as interstitial fibrosis. This is key to correlate progressive kidney cystic disease due to alteration in adjacent renal parenchyma to cyst development or tubular atrophy (Morrissey *et al*., 2002). The interstitial volume is around 5 to 20% in normal kidneys which increases with age (Morrissey *et al*., 2002). Following extracellular matrix also includes sulphated and non-sulphated glycosaminoglycans along with type I and Type III collagen (Zeisberg *et al*., 2001). This composition aids in determining protease degradation susceptibility upon kidney damage (Zeisberg *et al*., 2001). In *Nedd4-2*$^{-/-}$ cystic kidneys we show an increase in renal fibrosis with age **(Fig 2.8, 2.9).** Also, other components of renal interstitium involved in fibrosis, including polysaccharides, showed an overall decrease in accumulation in and around the cystic epithelia in *Nedd4-2*$^{-/-}$ cystic kidneys **(2.11).**

During fibrosis tubular epithelial to mesenchymal transition (EMT), T cell and macrophage infiltration plays a crucial role (Zeisberg *et al*., 2001). During this transition process there is expression of alpha smooth muscle actin, along with interstitial components such as collagen-1 (Zeisberg *et al*., 2001). We show here that in the *Nedd4-2*$^{-/-}$ cystic kidneys there is an increased expression of collagen-1, specifically in the tubules and cysts lining epithelial cells. Also alpha smooth muscle transcript levels in the kidneys of *Nedd4-2*$^{-/-}$ did not show any major difference, nor did collagen-1 and MMP-9 transcripts (**Fig 2.8Y, Fig 2.9, Fig 2.13G**). It needs to be further ascertained using immunohistochemistry whether smooth muscle actin, also involved in EMT, is a major contributor to renal damage within the kidney (Yamamoto *et al*., 1994). TGFβ signalling upstream has been implicated in the progression of renal fibrosis and EMT in renal damage (Yamamoto *et al*., 1994). Of importance is the

involvement of Nedd4-2 *in vitro* studies suggesting Nedd4-2 regulation of TGFβR1 (Kuratomi *et al*., 2005). However this needs to be further explored to determine the pathophysiological implications in the *Nedd4-2*$^{-/-}$ kidney.

Another pathophysiological mechanism involved in renal cyst formation is cell primary cilia. Malfunctioning of this organelle leads to major alteration in mechanosensation causing cysto protein mislocalisation, leading to alteration in ion homeostasis downstream leading to formation of cysts (Blanco and Wallace, 2013). Cilia also aids in cell-cell communication and cell-junction recognition within the kidney (Hildebrandt and Otto, 2005). To investigate this role upon Nedd4-2 ablation in renal cyst development within the kidney, our findings show renal cysts in the *Nedd4-2*$^{-/-}$ mice display ciliary anomalies around the cysts with formation of abnormal cilia (**Fig 2.13 F**). There seems to be increased cilia in the renal tubules of the *Nedd4-2*$^{-/-}$ kidneys due to the dilation of the renal tubules. Given the pathology of the *Nedd4-2*$^{-/-}$ kidneys, this could not be quantitated due to the difference in the tissue morphology and lack of similar dilation patterns in the kidneys of control littermates (**Fig 2.13 A-F**).

To assess structural changes in the cilia preliminary electron microscopy was performed, and our data suggests no obvious differences although a more detailed study with increased sample size needs to be further undertaken (**Fig 2.16**). *In vitro* studies to compensate for the lack of cilia number and centrosome measurement in *Nedd4-2*$^{-/-}$ kidneys was undertaken in mouse embryonic fibroblasts and showed no major differences in cilia formation and centrosome number within the cells (**Fig 2.14 A, B**); however it needs to be further ascertained in kidney specific cells contributing to the development of cysts. The role of ciliary motor proteins involved in cilia formation within the cilia and cilia maintenance was assessed, and no major differences were seen at the transcript levels. This study further highlights the importance of cilia formation in renal cyst pathology, and the morphological

role cilia plays in regulation of renal cyst development upon Nedd4-2 depletion within the kidneys **(Fig 2.14 A and B).**

To summarize these findings and understand the anomalies associated with the given model of renal cystic disease, it became imperative to pathologically distinguish the renal cystic disease given there were both similarities and dissimilarities seen in the *Nedd4-2*$^{-/-}$ renal phenotype and PKD. Pathological reports from kidneys of *Nedd4-2*$^{-/-}$ mice in **Fig 2.15** suggested the phenotype is due to kidney dysplasia, which is an anomaly to polycystic kidney disease. In renal dysplasia the cyst size varies, with cysts being smaller or absent in comparison to polycystic kidney disease (Woolf *et al*., 2004). Renal dysplastic kidneys at early post natal days show no major differences in kidney weight, shape and size unlike PKD (Woolf *et al*., 2004). The developmental defects as reported in earlier studies could be correlated with *Nedd4-2*$^{-/-}$ dysplastic kidneys as associated with poorly differentiated tissue largely undergoing aberration during development, along with cell proliferation and abnormalities in the collecting duct system (**Fig 2.6, Fig 2.15**) (Woolf *et al*., 2004). The *Neddd4-2*$^{-/-}$ kidneys also show primitive development of tubular formation including renal hypoplasia and renal atrophy compared to renal dysplastic kidneys (**Fig 2.15**) (Woolf *et al*., 2004). Further, dysplastic kidneys are associated with multiple cysts and renal agenesis, where primitive ducts are cystic due to undifferentiated columnar to cuboidal epithelium also seen in *Neddd4-2*$^{-/-}$ (**Fig 2.15**) (Woolf *et al*., 2004). The cysts in dysplastic kidneys could originate from multiple segments within the ducts which could be large or small also reported in *Neddd4-2*$^{-/-}$ (**Fig 2.5**) (Woolf *et al*., 2004). In the case of *Neddd4-2*$^{-/-}$ nephronal development and collecting duct formation (known to arise from ureteric bud in the early stages) there is epithelial transformation leading to renal fibrosis due to defects in adjacent renal parenchyma causing extra cellular matrix modification (**Fig 2.8, Fig 2.10**) and enhanced accumulation of collagen (**Fig 2.9**) consistent with renal dysplasia (Woolf *et al*., 2004).

However, decreased expression of the extracellular matrix component of glycoproteins was observed (**Fig 2.11**), but this could be due to altered levels of other regulators of ion homeostasis regulated by Nedd4-2 like glucose transporters or lipid binding proteins like polycystin-1, known to interact with extracellular matrix proteins in the kidney (Malhas *et al*., 2002, Weston *et al*., 2001).

The current results have uncovered the crucial role Nedd4-2 plays in the development of renal dysplasia in the kidneys of *Nedd4-2*$^{-/-}$ mice, where cyst formation occurs due to key potential factors regulated by Nedd4-2. Nedd4-2 is also likely to be involved through its function either in protein degradation or localisation of some of the important, well characterised cystoproteins like polycystin-1 and polycystin-2 involved in renal cyst development. Nedd4-2 interaction leads to alteration in the levels of proteins via binding to a PPxY motif of the substrates involved in protein homeostasis. Polycystin-1 and polycystin-2, both involved in renal cyst development caused via extracellular matrix interactions as reported in other models of renal cysts, lack a canonical PPxY motif. The present results prompt further investigation into the role of polycystins as potential substrates of Nedd4-2, a potential post-translational modulator in renal cyst development.

Fig 2.15 *Nedd4-2*$^{-/-}$ cystic kidneys show renal dysplasia. Representative images of haematoxylin and eosin stained kidney sections derived from *Nedd4-2*$^{+/+}$ and *Nedd4-2*$^{-/-}$ post natal day 17 mice. *Nedd4-2*$^{+/+}$ mouse kidney show a normal pattern of differentiation at P17 including glomeruli (arrows) and tubules (asterisks) (**A** and **B**). *Nedd4-2*$^{-/-}$ kidneys show renal dysplastic cortical tissue, with immature glomeruli, atypical tubules and persistent mesenchyme (m) (**C** and **D**). **E-G** are higher magnification images of *Nedd4-2*$^{-/-}$ dysplastic cortical kidney tissue. Glomeruli (arrows) are immature. Tubular lumina in the cortex are distended and lined by atypical epithelium with pale nucleus and cytoplasm. Mitotic figures are observed (arrows, image **E**). Asterisks in **F** and **G** indicate atypical tubules. Tubular lumen in **G** appears hyper cellular with atypical epithelium partially (left) and completely occluding the lumen (right). Tubular lumina in the cortex in **H** are distended and lined by atypical epithelium. Left tubule, epithelium is degenerate and distended into the lumen, resulting in the attenuation of the lining epithelium. Right tubule is lined by atypical epithelium with possible mitotic figures being present (arrows). **I** represent hyper cellular collecting ducts without discernible lumina. Numerous mitotic figures are present (arrows). In **J** medullary tubules are hypercellular and poorly differentiated. Tubules lined by large epithelia (asterisks) and mitotic figures (cells) (arrows). This experiment was done with help of Anatomical Pathology at SA Pathology. The images were taken using Olympus BX-51 light microscope. Images **A** and **C** were taken at lower magnification of 10x (final images 10*10=100x). Images **B, D** and **E-J** were taken at higher magnification of 20x (final images 20*10= 200x). The images and pathological report was performed by Dr. John Finnie/Dr.Tanya Henshall, SA Pathology. Images (**A** and **C**) Scale bar = 50µm, Images (B, D, E and J) Scale bar = 25µm.

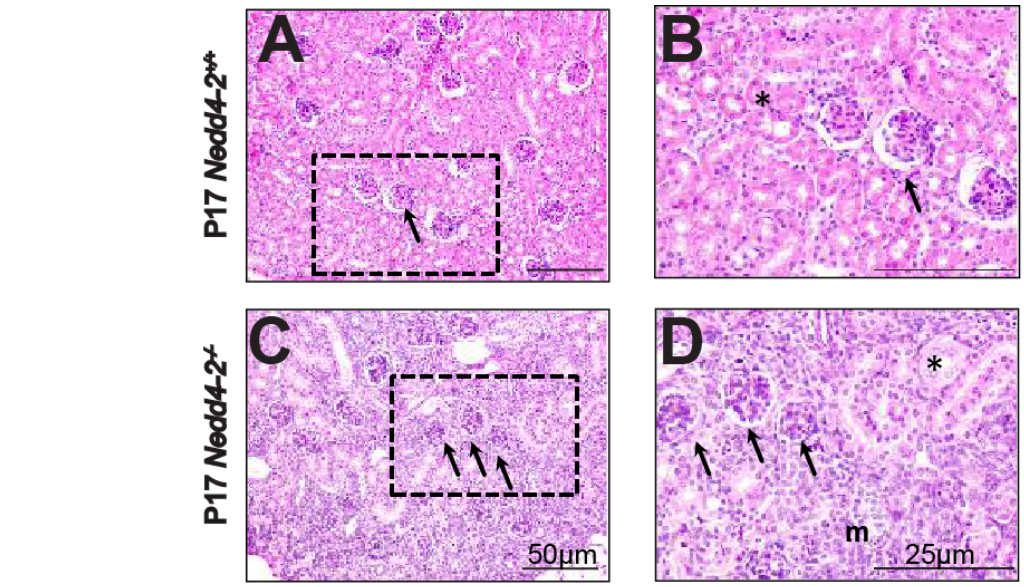
P17 Nedd4-2+/+
P17 Nedd4-2-/-
A
B
C
D
50µm
m
25µm

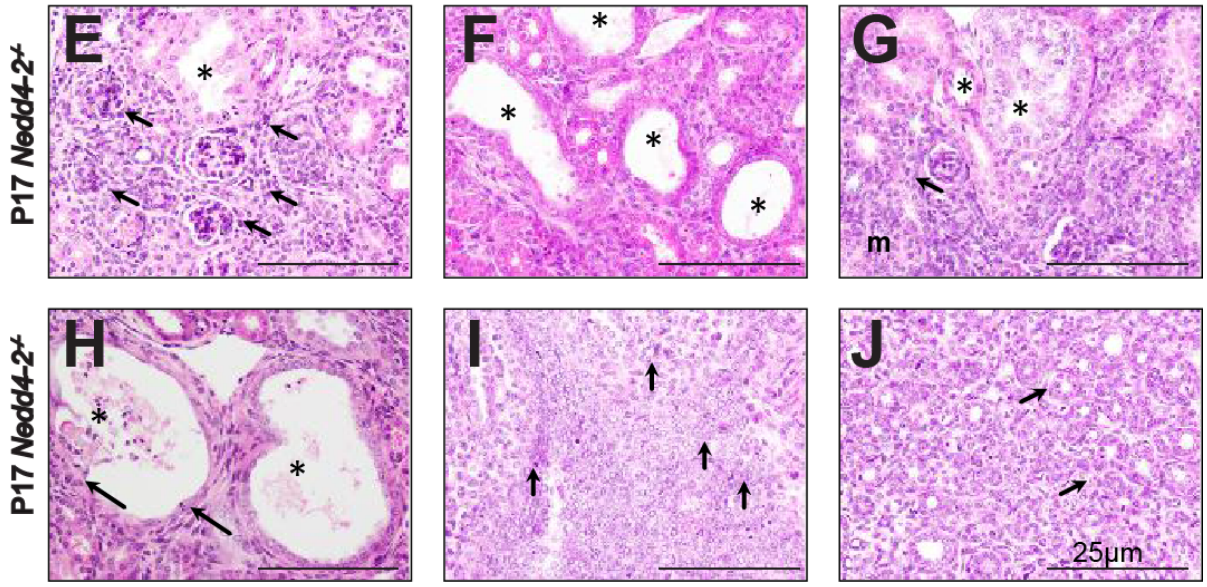
P17 Nedd4-2-/-
P17 Nedd4-2-/-
E
F
G
H
I
J
m
25µm

Fig 2.16 Transmission electron microscopy of *Nedd4-2*$^{-/-}$ cystic kidneys. Representative images for P19 kidney cilia, centrosome structure and morphology. Images **A-B, F-G** represents *Nedd4-2*$^{+/+}$ kidney overview of morphology as control kidney. Image **K** represents centrosome structure within *Nedd4-2*$^{+/+}$ kidneys. Image **L** is a higher magnification inset of image **K.** Images **C-E** represent accumulation of collagen fibres in *Nedd4-2*$^{-/-}$ dysplastic kidney tissue marked by arrows. Image **H** and **I** represent cilium within the *Nedd4-2*$^{-/-}$ dysplastic kidney tissue with image **I** at higher magnification than image **H.** Image **J** highlights both cilia and centrosome structure in the *Nedd4-2*$^{-/-}$ kidneys marked by arrows. Image **M** and **N** are higher magnification images of *Nedd4-2*$^{-/-}$ dysplastic cortical kidney tissue highlighting centrosome structure in the kidney. Image **N** indicates a transverse section of centrosome at higher magnification from image **M.** Image **O** represent cilia structure in transverse section along the end of the cilia structure marked by arrows. The images were taken using FEI Tecnai G2 Spirit TEM at Adelaide Microscopy, University of Adelaide. Image (C) Scale bar = 2 µm, Images (**A, D, E and J**) Scale bar = 1µm, Images (B **and K**) Scale bar = 200nm, Images (N,I,F and G) Scale bar = 100nm, Images (M,O and H) Scale bar = 50nm.

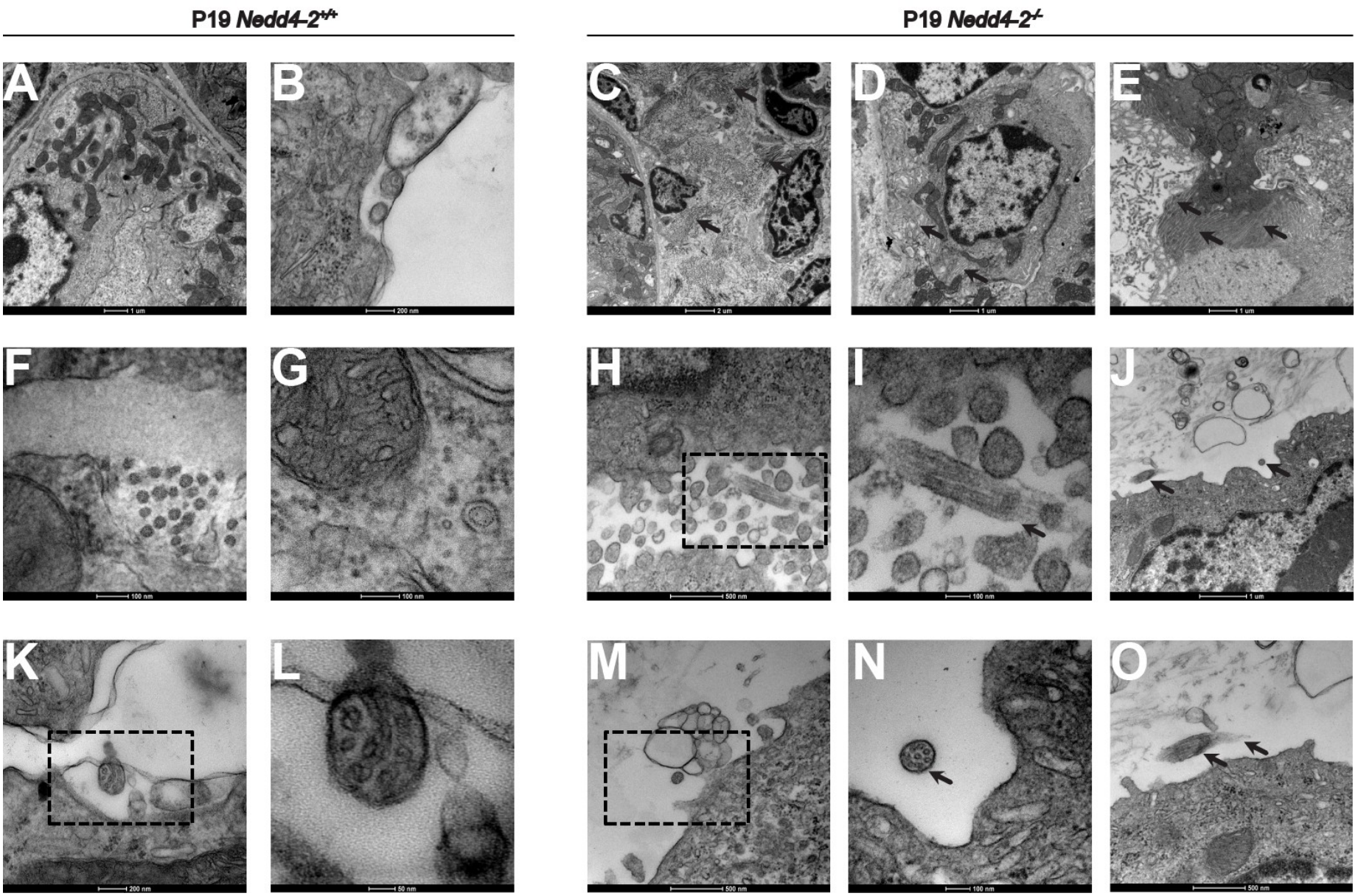
P19 Nedd4-2+/+
P19 Nedd4-2-/-
A
B
C
D
E
F
G
H
I
J
K
L
M
N
O

Fig 2.17 Scanning electron microscopy (SEM) of *Nedd4-2*$^{-/-}$ cystic kidneys. Images of cilia structure and morphology from P19 *Nedd4-2*$^{-/-}$ kidneys. Image **A** and **B** represent overview of P19 *Nedd4-2*$^{-/-}$ dysplastic kidneys that show tissue overview for SEM. Image **C** and **D** represent P19 *Nedd4-2*$^{-/-}$ dysplastic cortical kidney tissue at higher magnification to see cilia formation and structure. The images were taken using FEI Quanta 450 FEG Environmental Scanning Electron Microscope (ESEM). Image (A) Scale bar = 400µm, Images (**B**) Scale bar = 100µm, Images (C) Scale bar = 10 µm and Images (**D**) Scale bar = 10µm.

Chapter 2: Characterization of *Nedd4-2*$^{-/-}$ kidney

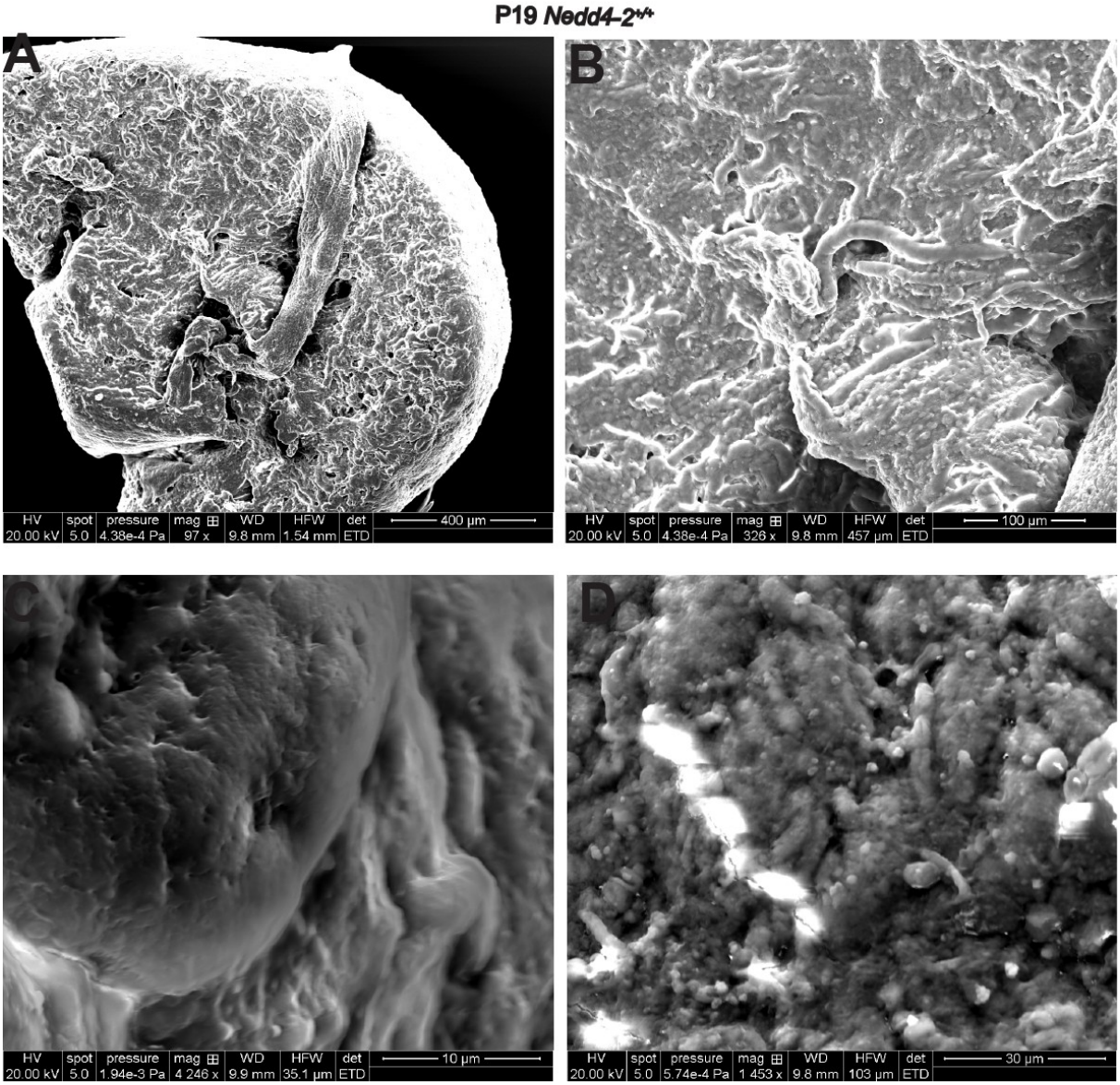

CHAPTER 3:

Role of polycystins in Nedd4-2 mediated renal cyst development

Statement of Authorship

Title of Paper	Role of polycystins in Nedd4-2 mediated renal cyst development
Publication Status	☐ Published ☐ Accepted for Publication ☐ Submitted for Publication ☑ Unpublished and Unsubmitted work written in manuscript style
Publication Details	

Principal Author

Name of Principal Author (Candidate)	Pranay Goel
Contribution to the Paper	Wrote the manuscript, edited the manuscript, evaluated the data , made figures, experimental design Note: The work included in this thesis has been solely done by me and the experiments otherwise have been duly acknowledged. The contribution of the work in this thesis chapter-3 with one figure taken from the co-author
Overall percentage (%)	80%
Certification	This paper reports on original research I conducted during the period of my Higher Degree by Research candidature and is not subject to any obligations or contractual agreements with a third party that would constrain its inclusion in this thesis. I am the primary author of this paper.
Signature	Date 4/12/15

Co-Author Contributions

By signing the Statement of Authorship, each author certifies that:

the candidate's stated contribution to the publication is accurate (as detailed above);

permission is granted for the candidate to include the publication in the thesis; and

the sum of all co-author contributions is equal to 100% less the candidate's stated contribution.

Name of Co-Author	Dr. Kimberly Mackenzie
Contribution to the Paper	Helped in data interpretation, experimental design for the below mentioned experiments and manuscript evaluation (Polycystin-1 ubiquitination assay) (Fig 3.11)
Signature	Date 4/12/15

Name of Co-Author	Prof Sharad Kumar
Contribution to the Paper	Supervised development of work., experimental design, co-wrote the manuscript
Signature	Date 2./2./15

Chapter 3: Role of polycystins in Nedd4-2 mediated renal cyst development

3.1 Introduction

In the previous chapter we reported the novel role Nedd4-2 plays in development of kidney dysplasia associated with renal cysts. To further investigate the role Nedd4-2 plays in cystogenesis or cyst development, polycystins were identified as potential substrates due to their previous established function in renal cyst development. The current understanding based on the various mouse models of renal cysts studied have suggested the existence of a dosage dependent or threshold model associated with polycystins, which explains cystogenic growth in the kidneys like in ADPKD (Hopp *et al*., 2012). In humans there is a 50% reduction in functional polycystin-1 or polycystin-2 if affected with renal cysts (Hopp *et al*., 2012). The cysts are formed if there is lower functional polycystin expression than the cystogenic threshold (Hopp *et al*., 2012). This occurrence can be due to cellular variability of polycystin expression (Raphael *et al*., 2009). Factors such as renal damage are also reported to promote cystogenesis, and may influence cystic onset (Bastos *et al*., 2009, Happé *et al*., 2009). Previous studies have reported the minimum cystogenic threshold required for cystic development taking into consideration factors such as the variability between animals, nephronal segment expression, developmental stages studied, cell and tissue expression type (Piontek *et al*., 2007, Fedeles *et al*., 2011, Raphael *et al*., 2009).

In mice models a slow progression of kidney disease occurs if polycystin-1 levels are around 40%, but this progression is rapidly enhanced when there is only 20% functional polycystin-1, again highlighting the importance of the dosage of polycystins (Hopp *et al*., 2012). The level of functional activity of polycystin-1(PC-1) is linked to the severity of renal disease (Hopp *et al*., 2012). Genetic events similar to tumour development in cancer and environmental factors also influence the survival of cystic growth (Leonhard *et al*., 2014). Other factors which influence cyst development include the paracrine cytogenetic factors, which are secreted from developed cysts to influence cystic clustering in comparison to early

cyst development, a slow process (Leonhard *et al*., 2014). In genetic mouse models it has been reported the non- randomness of Cre inactivation could also play an important role in cyst onset (Leonhard *et al*., 2014).

Polycystin-1, a 460 kDa glycoprotein, consists of a G protein coupled receptor (GPCR) auto proteolysis inducing regulatory domain (GAIN), a polycystic kidney disease (PKD) domain, a Polycystin-1 lipoxygenase alpha-toxin (PLAT) domain and a C- terminal tail region (Yu *et al*., 2007, Araç *et al*., 2012) **(Fig 3.1).** The polycystin-1 3D structure is still an enigma for scientists given the large size and complex structure of the protein. The crystal structure of the regulatory domains has a 320 residue region which includes a proteolysis site within the G-protein coupled receptor (GPS) motif of 50 residues, and this site mediates polycystin-1 cleavage and generates an unglycosylated 320 kDa N-terminal protein product and a 140 kDa C-terminal protein product (Araç *et al*., 2012). This GPS motif is a highly conserved domain present in 33 cell adhesion GPCR's along with Polycystin-1 like proteins (Araç *et al*., 2012). The cleavage of polycystin-1 and the important role it plays in protein function is still not very clear, but it has been postulated that the mechanism leading to polycystin-1 protein folding and trafficking is dependent on the extent of cleaved protein product, which varies in different cells (Chapin *et al*., 2010). The interaction of polycystin-1 and polycystin-2 is suggested to be necessary for efficient GPS cleavage (Chapin *et al*., 2010). However, recent data suggested polycystin-1 was efficiently cleaved in Pkd2 deficient cells (Gainullin *et al*., 2015, Kim *et al*., 2014). *In vivo* studies on polycystin-1 have suggested cleaved N-terminal surface over expressed polycystin-1 to be detached from C-terminal region providing further evidence for efficient GPS cleavage (Kurbegovic *et al*., 2014).

The extracellular region of Polycystin-1 has 16 copies of the PKD domain which is topologically comparable to domain structures of immunoglobulin and fibronectin like domains (Bycroft *et al*., 1999). This arrangement is similar to structural proteins involved in

mechanical roles like neural cell adhesion molecules (Bycroft *et al*., 1999). The PKD domain is important in surface layered proteins for mediation with multicellular structures (Bastos *et al*., 2009, Jing *et al*., 2002). Polycystin-1 mechanical studies on cells have suggested the role these domains play in maintaining normal tubular structure under fluid flow (Streets *et al*., 2009). Further, these are essential for formation of cell adhesion and cell junctions in mammalian cells (Streets *et al*., 2003, 2009, Ibraghimov-Beskrovnaya *et al*., 2000). The PLAT domain is an integral part of proteins structurally similar to PC-1 (Bateman and Sandford, 1999, Ponting *et al*., 1999). Previous work by others have highlighted the importance of the polycystin-1 PLAT domain in binding lipids on the membrane and scaffolding protein binding to aid in cell signalling downstream and polycystin-1 trafficking (Bateman and Sandford, 1999, Xu *et al*., 2015). The most well characterised domain of polycystin-1 is the 200 amino acid C-terminal region (**Fig 3.1**). This consists of a coiled–coil domain (aa4220-4251) which aids in binding polycystin-2 and activating heterotrimeric G proteins (Parnell *et al*., 2012, Streets *et al*., 2013). Previous reports show that this C-terminal region can be phosphorylated *in vitro* and regulates both polycystin-1 and polycystin-2 phosphorylation (Parnell *et al*., 2012, Streets *et al*., 2013). Key signalling proteins in cystogenesis such as Wnt, mTOR and transcription factor activation can also be regulated through the C-termini end (Shillingford *et al*., 2006, Lal *et al*., 2008, Bhunia *et al*., 2002).

Polycystin-2 is a highly conductive non selective calcium permeable channel that consists of two coiled-coil domains, an EF-hand domain, six transmembrane domains and two polycystin homologous motifs **(Fig 3.1)** (Koulen *et al*., 2002, González-Perrett *et al*., 2001, Ma *et al*., 2005). The sequence homology suggests its similarity to transient receptor potential (TRP) channels henceforth polycystin-2 is also known as TRPP2 (Montell *et al*., 2002). The primary site of polycystin-2 regulation by polycystin-1 directly affects polycystin-2 channel opening along with calcium binding and phosphorylation, although the mechanism by which

this occurs is still not clear (Yu *et al*., 2009). The two coiled-coil domains of polycystin-2, coiled coil-1 and coiled coil-2, aid in its oligomerization via its binding to its own C–termini end to form oligomers, an important function necessary to allow the PC-1 C-terminus to bind and form the PC-1/PC-2 complex (Giamarchi *et al*., 2010). The EF-hand a structural domain has a helix-loop-helix topology, and vertebrate homolog's of polycystin-2 all share a single functional EF-hand calcium binding motif (EF2) (Petri *et al*., 2010). The effect the EF2 domain has on calcium binding is to favour monomer rather than dimer formation in case of polycystin-2, and thereby regulates the calcium dependent interaction for open channel probability (Schumann *et al*., 2009, del Rocío Cantero and Cantiello, 2013). Membrane targeting motifs are distinct motifs within polycystin-2 which have been proposed for detection in cilia (^{6}RVxP^{9}) and plasma membrane (^{572}KxxxF^{576}) (Geng *et al*., 2006, Hoffmeister *et al*., 2011). Polycystin-2 has been proposed to be directed from cis-golgi to cilia or plasma membrane independent of interaction with polycystin-1 (Hoffmeister *et al*., 2011). Polycystin-1 surface expression can be regulated by pathways like calcium/calmodulin dependent kinase, protein kinase A and glycogen synthase kinase 3 although the mechanism by which they regulate surface expression of polycystin-1 is still not clear (Streets *et al*., 2013, Streets *et al*., 2006, Miyakawa *et al*., 2013). Multiple studies have pointed to an important role of phosphorylation of polycystin-2 leading to regulation of its retrograde trafficking, surface localisation and calcium permeability (del Rocío Cantero and Cantiello, 2013, Streets *et al*., 2006, Cai *et al*., 2004, Köttgen *et al*., 2005). The S829 residue was reported to be a PKA activated site on polycystin-2 which remains phosphorylated even in the absence of polycystin-1, and could be a link between the reported bindings of polycystin-2 with receptor phosphatases (Parnell *et al*., 2012, Streets *et al*., 2013, Boucher *et al*., 2011). Ubiquitination and proteasomal degradation of PC-1 has been reported via binding with E3 ubiquitin ligase Siah-1, and polycystin-2 through its interaction with the SCF$^{\beta\text{-Trcp}}$ E3 ligase

complex (Kim *et al*., 2004, Tian *et al*., 2007). TAZ mutant mice have also been reported to develop glomerular cysts with polycystin-2 levels being lower (Makita *et al*., 2008). Polycystin-1 is also known to play an integral role in cell matrix interaction and cell-cell interaction (Streets *et al*., 2003). This is supported by reports suggesting ablation of β1-integrin leads to suppression in the *Pkd1*$^{-/-}$ cystic phenotype (Lee *et al*., 2014). Abnormalities in cell-cell junction formation are consistently reported in studies involving polycystin-1 and polycystin-2 (Natoli *et al*., 2008). Polycystin-1 has a conceivable role in cell-cell adhesion and in establishing apicobasal polarity (Fogelgren *et al*., 2011, Lee *et al*., 2014). The intercellular changes to adhesion cause alteration in cell-matrix adhesion, especially Collagen-1 (Fogelgren *et al*., 2011, Lee *et al*., 2014).

The Nedd4-2 ubiquitin ligase binds via its WW domains to proline rich motifs in its substrates. Previous *in vitro* studies have shown Nedd4-2 binds to cell junction proteins like occludin *in vitro* through its PY motif (Raikwar *et al*., 2010). The lack of canonical binding motifs (LPxY/PPxY) in polycystin-1 and polycystin-2 is identified from a sequence motif search (**Fig 3.2 A** and **B)**. However, non-canonical proline rich regions which could act as potential Nedd4-2 binding sites were identified in polycystin-1 **(Fig 3.2 A)** which needs to be explored further, whereas sequence analysis of polycystin-2 revealed no such potential interaction sites **(Fig 3.2 B)**. As reported in chapter 2, increased levels and the accumulation of extracellular matrix protein collagen-1 in *Nedd4-2*$^{-/-}$ cystic kidneys led us to the current hypothesis that polycystins are involved in the *Nedd4-2*$^{-/-}$ renal phenotype. Polycystin-1 is known to interact with extracellular proteins on the cell membrane via its extracellular domain, and could aid in renal cyst development in *Nedd4-2*$^{-/-}$ dysplastic kidneys (Weston *et al*., 2001). This study is focussed on understanding the potential role polycystin-1/polycystin-2 could play in renal cystogenesis due to post translational modifications mediated via Nedd4-2. The initial working hypothesis was since there are potential non-canonical proline

rich motifs within polycystin-1 (**Fig 3.2 A**), and *Nedd4-2*$^{-/-}$ cystic kidneys display increased levels of the extracellular matrix protein collagen-1, Nedd4-2 could be directly or indirectly mediating the regulation of polycystin-1 in complex formation with polycystin-2, which are known to form a complex for downstream effector signalling required in cyst onset.

Chapter 3: Role of polycystins in Nedd4-2 mediated renal cyst development

Fig 3.1 Structure and domain architecture of polycystin1 and polcystin-2. The Polycystin-1 glycoprotein structure consists of N-terminal region leucine rich repeats, sixteen polycystic kidney disease (PKD) domains, a C-type lectin binding domain, a receptor egg jelly domain, G recpetor autoproteolysis domain A and B (GAIN), a G receptor auto proteolysis binding site (GPS), G protein activating peptide domain, a polycystin-1 lipooxygenase alpha toxin (PLAT) domain, 11 transmembrane domains and a coiled-coil domain and polycystin-2 binding region in the C-terminus. Polycystin-2 N-terminus consists of cilia targeting region, two polycystin homologous regions, six transmembrane domains, and a C-termini containing an ER targeting motif along and two coiled-coil domains. Diagram taken from Chebib, F. T. *et al.* (2015).

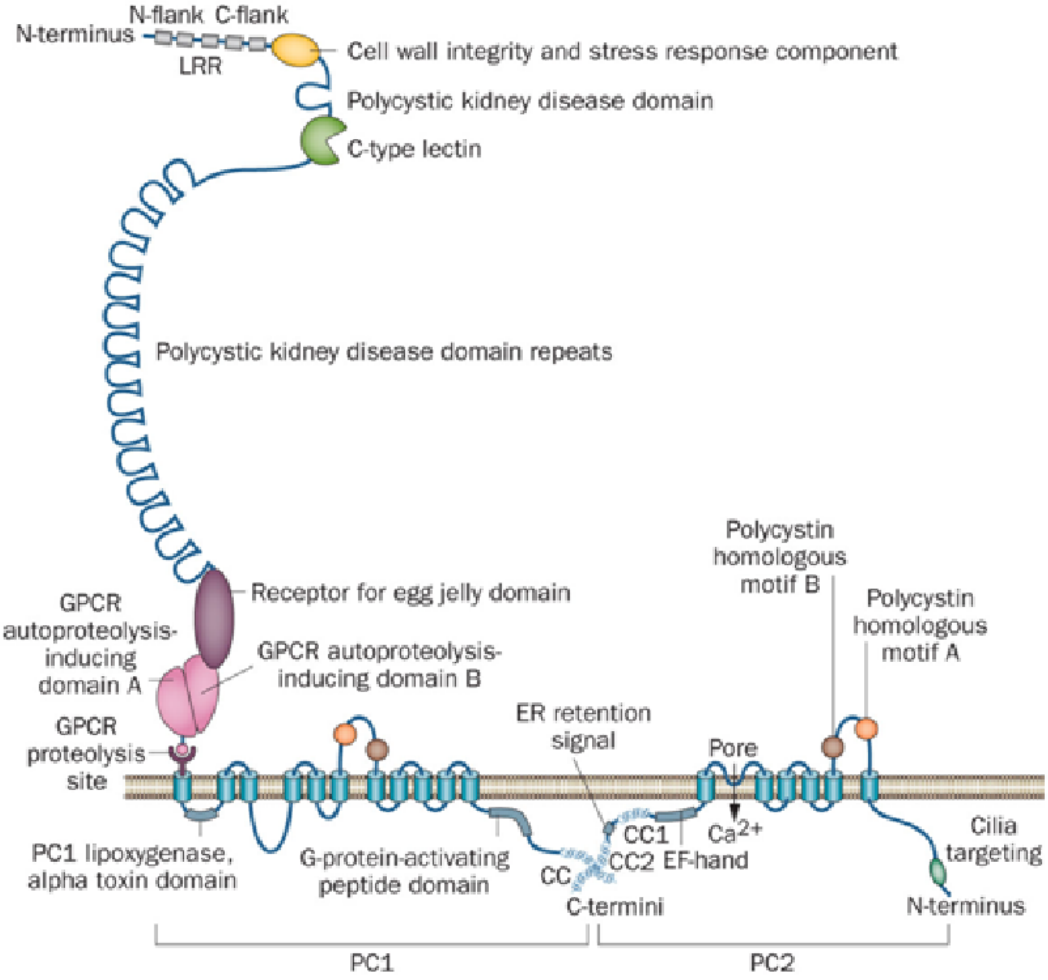
N-flank C-flank
N-terminus
LRR
Cell wall integrity and stress response component
Polycystic kidney disease domain
C-type lectin
Polycystic kidney disease domain repeats
Receptor for egg jelly domain
GPCR autoproteolysis-inducing domain A
GPCR autoproteolysis-inducing domain B
GPCR proteolysis site
Polycystin homologous motif B
Polycystin homologous motif A
ER retention signal
Pore
Ca^{2+}
CC1
CC2
EF-hand
CC
Cilia targeting
PC1 lipoxygenase, alpha toxin domain
G-protein-activating peptide domain
C-termini
N-terminus
PC1
PC2

.

Fig 3.2 Potential non-canonical Nedd4-2 WW domain binding motifs in polycystin-1 and polycystin-2. A) Amino acid sequence of mouse polycystin-1 [Pubmed accession number >gi|124487380|ref|NP_038658.2| polycystin-1 precursor (*Mus musculus*)]. **B)** Amino acid sequence of mouse polycystin-2 [Pubmed accession number >gi|164519057|ref|NP_032887.3| polycystin-2 (*Mus musculus*). Highlighted in red and bold in **A)** are potential PY like motifs (similar to LPxY and PPxY) identified in polycystin-1. In **B)** polycystin-2 sequence there are no such potential proline rich binding motifs to Nedd4-2 WW domains.

A Polycystin-1

MPLGAPALLALALGLGLWLGALAGDPGRGCGPCPLPCFCGPAPDAACRVNCSGRWLQTLGPSLRIPADATALDLSHNLLQTLDIGLLVNLSAL
VELDLSNNRISTLEEGVFANLFNLSEINLSGNPFECNCGLAWLPRWAKEHQVHVVQSEATTCRGPIPLAGQPLLSIPLLDNACGEEYVACLPDN
SSGAVAAVPFYFAHEGPLETEACSAFCFSAGEGLAALSEQNQCLCGAGQASNSSAACSSWCSSISLSLNSACGGPTLLQHTFPASPGATLVGPH
GPLASGQPADFHITSSLPISSTRWNFGDGSPEVDMASPAATHFYV**LPGSY**HMTVVLALGAGSALLETEVQVEATPTVLELVCPSFVHSNESLEL
GIRHRGGSALEVTYSILALDKEPAQVVHPLCPLDTEIFPGNGHCYRLVAEKAPWLQAQEQCRTWAGAALAMVDSPAIQHFLVSKVTRSLDVWI
GFSSVEGTEGLDPRGEAFSLESCQNWLPGEPHPATAEHCVRLGPAGQCNTDLCSAPHSYVCELRPGGPVWDTENFVMGMSGGGLSGPLHPLA
QQETVQGPLRPVEVMVFPGLSPSREAFLTAAEFSTQKLEEPAQMRLQVYRPSGGAAAVPEGSSEPDNRTEPAPKCVPEELWCPGANVCIPFDA
SCNSHVCINGSVSRLGLSRASYTLWKEFFFSVPAG**PPTQY**LVTLHSQDVPMLPGDLIGLQHDAGPGTLLQCPLASSCPGQALYLSTNASDWMT
NLPVHLEEAWAGPVCSLQLLLVTERLTPLLGLGPNPGLQHPGHYEVRATVGNSVSRQNLSCSFSVVSPIAGLRVIHPIPLDGHIYVPTNGSVLVL
QVDSGANATATAQWFGGNISAPFEDACPPEVDFLKQDCTEEANGTLFSVLMLPRLKEGDHTVEIVAQNGASQANLSLRVTAEEPICGLRAVPS
PEARVLQGILVRYSPMVEAGSDVAFRWTIDDKQSLTFHNTVFNVIYQSAAIFKLSLTASNHVSNITVNYNVTVERMNKMHGLWVSAVPTVLPP
NATLALTGGVLVDSAVEVAFLWNFGDGEQVLRQF**KPPY**DESFQVPDPTVAQVLVEHNTTHIYTTPGEYNLTVLVSNTYENLTQQVTVSVRTV
LPNVAIGMSSNVLVAGQPITFSPYPLPSTDGVLYTWDFGDGSPVLIQSQPVLNHTYSMTGAYRITLEVNNTVSSVTAHADIRVFQELHGLTVYL
SPSVEQGAPMVVSASVESGDNITWTFDMGDGTVFTGPEATVQHVYLRAQNFTVTVEAANPAGHLSQSLHVQVFVLEVLHIEPSTCIPTQPSAQ
LMAHVTGDPVHYLFDWTFGDGSSNVTVHGHPSVTHNFTRSGIFPLALVLSSHVNKAHYFTSICVEPEIRNITLQPERQFVKLGDEARLVAYSW**P**
PFPYRYTWDFGTEDTTHTQTGGSEVKFIYREPGSYLVIVTVSNNISSTNDSAFVEVQEPVLVTGIRINGSHVLELQQPYLLSAMGSGSPATYLWE
LGDGSQSEGPEVTHIYSSTGDFTVRVSGWNEVSRSEAQLNITVKQRVRGLTINASRTVVPLNGSVSFSTLLEVGSDVHYSWVLCDRCTPIPGGP
TISYTFRSVGTFNIIVTAENEVGSAQDSIFIYVLQFIEGLQVAGGDNGCCFPTNYTLQLQAAVRDGTNISYSWTAQQEGSLITLFGSGKCFSLTSL
KASTYYVHLRATNMLGSAAANRTIDFVEPVESLILSASPNPAAVNMSLTLCAELAGGSGVVYTWYLEEGLSWKTSMPSTTHTFAAPGLHLVR
VTAENQLGSVNATVEVAIQVPVGGLSIRTSEPDSIFVAAGSTLPFWGQLAEGTNVTWCWTLPGGSKDSQYIAVRFSTAGSFSLQLNASNAVSW
VSAMYNLTVEEPIVNLMLWASSKVVAPGQPVHFEILLAAGSALTFRLQVGGSVPEVLPSPHFSHSFFRVGDHLVNVQAENHVSHAQAQVRILV
LEAVVGLQVPNCCEPGMATGTEKNFTARVQRGSRVAYAWYFSLQKVQGDSLVILSGRDVTYTPVAAGLLEIHVRAFNELGGVNLTLMVEVQ
DIIQYVTLQSGRCFTNRSARFEAATSPSPRRVTYHWDFGDGTPVQKTEEFWADHYYLRPGDYHVEVNATNLVSFFVAQATVTVQVLACREPE
VEVALPLQVLMRRSQRNYLEAHVDLRNCVSYQTEYRWEIYRTASCQRPGRMAQMVLPGVDVSRPQLVVPRLALPVGHYCFVFVVSFGDTPL
ARSIQANVTVAAERLVPIIEGGSYRVWSDTQDLVLDGSKSYDPNLEDGDQTPLNFHWACVASTQSETGGCVLNFGPRGSSVVTIPLERLEAGV
EYTFNLIVWKAGRKEEATNQTVLIRSGRVPIVSLECVSCKAQAVYEVSRSSYVYLEGHCHNCSRGYKQGCWAARTFSNKTLVLNETTTSTGST
GMNLVVRPGALRDGEGYIFTLTVLGHSGEEEGCASIRLSPNRPPLGGSCRLFPLDSVRGLTTKVHFECTGWRDAEDGGAPLVYALLLKRCRQS
YCENFCIYKGSLSTYGAVLPPGFQPLFVVSLAVVVQDQLGAAVVALNRSLTIVLPEPSGNPADLVPWLHSLTASVLPGLLKQADPQHVIEYSLA
LITVLNEYEQAPDVSEPNVEQQLRAQMRKNITETLISLRVNTVDDIQQITAALAQCMVSSRELMCRSCLKKMLQKLEGMMRILQAETTEGTLT
PTTIADSILNITGDLIHLASLDMQGPQPLELGVEPPSLMVASKAYNLSSALMRILMRSRVLNEEPLTLAGEEIVALGKRSDPLSLLCYGKALGPSC
HFSIPEAFSGALSNLSDVVQLIFLVDSNPFPFGYISNYTVSTKVASMAFQTQTGTQIPIEQLAAERAITVKVPNNSDQAAQSSHNPVGSTIVQPQT
SVSAVVTADNSNPQAGLHLRITYTVLNERYLSAEPEPYLAVYLHSVSQPNEYNCSASRRISLEVLEGADHRLYTFFIAPGTGTLDRSYYLNLTSH
FHWSALEVSVGLYTSLCQYFSEEMMMWRTEGIVPLEETSPSQAVCLTRHLTAFGASLFVPPSHVQFIFPEPSASINYIVLLTCVICLVTYVVMA
MILRKLDQLDVSRVRVIPFCGKGGRFKYEILVKTGWSRGSGTTAHVGIMLYGEDNRSGHRHLDGDRAFHRNSLDIFQIATPHSLGSVWKIRVW
HDNKGLSPAWFLQHIIVRDLQSARSTFFLVNDWLSVETEANGGLVEKEVLAANEAALWQFQRLLVAELQRGFFDKHIWLSIWDRPPRSRFTRV
QRVTCCVLLLCLFLAANAVWYGVVRDTTYSMGPVSSLISPGVDTVAIGLVSSVVVYPVYLAVLFLFRMSRSKVSGDQNPTPTGQQALDVDSY
LDPSVLDSSLLTLSGLTEAFAGQVKNDLFLEDAKSLVCWPSSEGTLSWPDLLSDPSVVSSTLQRLTQGRPGCMLGSEEDGASLVSPS**LPAKY**LS
ASDEDLIHQVLADGANNLVPTQDTLLETDLLTSLSSVPGEKTETLILQTVGEERPASMGLSWEQSPVTRLSRTGLVEGFQKRLLPAWCAPLAHG
LSLLLVAVAVAVSGWIGASFPPSVSVMWLLSSSSSFLASFLGWEPLKVLLEALYFSLVAKRLHPDEDDTLVESPAVTPVSERVPRVRPPHGFAL
FLAKEEARKVKRLHDMLKRLLVYMLFLLVTLLANYGDASCHGHAYRLQSAIKQELDSQAFLAITRSDEFWPWMSHV**FLPY**VHGNQSSPELGP
PRLRQVRLQEAFCPDPSSSEHMCSAAGSLSTSDYGIGWQSVVQNGSETWAYSAPDLLGAWYWGYCAVYDSGGYIQELGLSLEESRARLGFLQ
LHNWLDSRSRAVFVELTRYSPAVGLHAAVTLRLEFPVAGHALAAFSVRPFALRRLSTGLSLPLLTSVCLLLFALYFSMAEVQTWRKDGCACT
ARPDTWARCLLVILTAATGLVRLAQLGIADRQWTHFVQDHPRHFTSFDQVAQLGSVARGLAASLLFLLLVKAAQQLRFVRQWSVFGKTLCR
ALPELMGATLGLVLLGVAYAQMAILLISSGADTLYNMARAFLVLCPGARVPTLCPSESWYLSPLLCVGLWALRVWGALRLGAILLRWRYHAL
RGELYRPAWEPQDYEMVELFLRRLRLWMGFSKVKEFRHKVRFEGMDPLPSRSSRGSKSSPVVLPPSSGSEASHPSTSSSQPDGPSASLSRSTLK
LEPEPSRLHAVFESLLVQFDRLNQATEDVYQLEQQLQSLQGHGHNGPPSSPSPGCFPGSQPALPSRLSRASQGLDQTVGPNRVSLWPNNKVHPS
ST

B Polycystin-2

MVNSRRVQPQPPGDAGRSPAPRASGPGRLVAGGAGLAVPGGLGEQRGLEIEMERIRQAAARDPPAGASASPSPPLSSCSRQAWSRDNPG
FEAEEDDDDDEVEGEEGGMVVEMDVEWRPGSRRSASSSAVSSVGARGRGLGSYRGAAHLSGRRRRLEDQGAQCPSPAGGGDPLHRHLP
LEGQPPRVAWAERLVRGLRGLWGTRLMEESNANREKYLKSVLRELVTYLFFLVVLCILTYGMMSSNVYYYTRTLSQLFIDTPVSKTEKT
NFKTLSSMEDFWKFTEGSFLDGLYWKAQTSNHTQADNRSFIFYENLLLGVPRLRQLRVRNGSCSIPQDLRDEIKECYDVYSVSSEDRAPF
GPRNGTAWMYTSEKELNGSSHWGIIASYSGAGYYLDLSRTREETAAQLAGLRRNFWLDRGTRAAFIDFSVYNANINLFCVVRLLAEFPA
TGGVVPSWQFQPVKLIRYVTAFDFFLAACEIIFCFFIIYYVVEEILEIRIHRLSYFRSFWNCLDVVIVVLSVVAMVINIYRMSNAEGLLQFLE
DQNSFPNFEHVAYWQIQFNNISAVMVFLVWIKLFKFINFNRTMSQLSTTMSRCAKDLFGFTIMFSIIFLAYAQLAYLVFGTQVDDFSTFQE
CIFTQFRIILGDINFAEIEEANRVLGPLYFTTFVFFMFFILLNMFLAIINDSYSEVKSDLAQQKAEMELSDLIRKGCQKALVKLKLKRNTVDAI
SESLRQGGGKLNFDELRQDLKGKGHTDAEIEAIFTKYDQDGDQELTEREHQQMRDDLEKEREDLDLEHSSLPRPMSSRSFPRSLDDSEEE
DDEDSGHSSRRRGSISSGVSYEEFQVLVRRVDRMEHSIGSIVSKIDAVIVKLEIMERAKLKRREVLGRLLDGVAEDARLGRDSEIHREQME
RLVREELERWESDDAASQTGHGVSTQVGLGGQPHPRNPRPPSSQSAEGLEGGGGNGSANVHA

3.2 Materials and Methods

3.2.1 *Nedd4-2*$^{-/-}$ mouse colony breeding

As mentioned in Section 2.2.1.

3.2.2 Plasmid preparation.

3.2.2.1 Preparation and transformation of competent *Escherichia coli*

Chemically competent *E. coli* DH5α (Invitro Life Technologies) were prepared. *E. coli* cultures were grown overnight at 37^{o}C with vigorous shaking in super broth (2%w/v Bacto™ tryptone (Sigma), 0.5%w/v Bacto™ yeast extract (Sigma), 0.5%w/v $MgSO_4$, pH 7.6). These were further subcultured 1:10 into 100ml ψ broth until OD (Optical Density) values range between 0.4-0.6 at 600nm. Cultures were pelleted after chilling on ice with gentle mixing for 15 minutes at 4000g at 4^{o} C. The bacterial pellets were transformed into 40ml cold Tfb1(Transformation buffer 1) (30mM KOAc (Potassium actetate), 100mM KCl, 10mM $CaCl_2.2H_2O$, and 50mM $MnCl_2.4H_2O$, 15% glycerol, pH 5.8) incubated on ice for 5 minutes then centrifuged for 10 minutes at 4000g at 4^{o}C temperature. These pellets were further resuspended in 40ml cold Tfb2 (Transformation buffer 2) (10mM MOPS (3-(*N*-morpholino) propanesulfonic acid), 75mM $CaCl_2.2H_2O$, 10mM KCl, 15% glycerol, pH 6.5) incubated on ice for 15 minutes and then divided into 50µl aliquots in ice chilled tubes and stored at -70^{o}C. The competent cells from DH5α *E. coli* were further transformed with plasmids for purpose of obtaining high quality transfection grade plasmid constructs for mammalian cell expression. The competent *E.coli* cells were thawed on ice, mixed with 1µl of 100ng of DNA constructs on ice for 30 minutes. The mixed reactions were heat shocked in a water bath at 42^{o}C for 40 sec, then kept on ice for 2 minutes before adding 150µl Luria- Bertani (LB) broth (1% w/v Bacto™ tryptone, 0.5% w/v Bacto ™ yeast extract, 1% w/v NaCl). The cells were incubated on a shaker at 37^{o}C for 45 min and then pelleted before plating onto LB agar plates

(LB broth+1.5%w/v Bacto™ agar (Sigma)) containing ampicillin (100µg/ml ampicillin) overnight in 37°C incubator.

3.2.2.2 Plasmid purification

The plasmids were inoculated in LB media with ampicillin (1mg/ml) and cultured at 37°C overnight. DNA was extracted from the 200ml culture via Qiagen midi-prep extraction (Qiagen) as per the manufacturer's protocol, and used for DNA sequencing, cell transfection experiments and ubiquitination assays as detailed below.

3.2.2.3 Plasmid sequencing

Big Dye sequencing was performed on extracted plasmids Flag-Polycystin-1-HA and Myc-Polycystin-2. The plasmids were procured from Prof. Stefan Somlo (Yale University). The M13 Forward and Reverse primers specific to the pcDNA3.1 vector backbone were used in conjunction with gene specific primers as reported in the table below. The Flag-Nedd4-2 and Flag-Nedd4-2 cysteine (cys) catalytically inactive mutant construct was laboratory generated by Dr. Andrew Fotia. The plasmid pcDNA3.1 is a commercially available control construct (Invitrogen).

The sequencing reaction mix is as below:

2.0ul Big Dye Sequence Terminator Ready Reaction mix (2.5x)

1.0 ul 5x Big Dye Sequencing buffer

0.5ul primer (100ng/ul)

X ul DNA template (500-1000ng/Xul of plasmid DNA)

Y ul water (Y- remaining amount of water)

Total = 10ul

The sequencing reaction was subjected to 25 cycles in the thermocycler with the following conditions: 96°C for 30 sec, 50°C for 15 sec and 60°C for 4 minutes. The DNA PCR reaction product was precipitated by addition of 75% isopropanol, vortexing and incubation at 37°C

for 15 minutes. After centrifugation for 20 minutes at 15000g the supernatant was discarded. The precipitated DNA was washed with 75% isopropanol, vortexed and pelleted at 15000xg for 5 minutes. The supernatant was removed and pellet allowed to air-dry at room temperature. The purified sequencing reaction was sent to the Institute for Medical and Veterinary Sciences (IMVS) Sequencing Centre for sequencing. The output sequences were analysed using BioEdit 7.1 software.

3.2.3 Maintenance of cell culture

3.2.3.1 Human embryonic kidney cells (HEK)

The HEK cells were cultured in RPMI media (GIBCO) with 10% foetal calf serum (GIBCO), 1% glutamine and penicillin/streptomycin (50 units/ml/ 0.05 mg/ml respectively). The cells were plated 24 hours prior to transfection in 6 well plates and incubated at 37°C in 5% CO_2 overnight to adhere. Cells were transfected the next day for expression and ubiquitination assay (protocols as below (section 3.7).

3.2.3.2 Mouse pyruvate kidney collecting duct cells (mpkCCD)

Mouse pyruvate kidney collecting duct (mpkCCD) cells were obtained from Prof. Ming-Jiun Yu (Institute of Biochemistry and Molecular Biology, National Taiwan University College of Medicine) and cultured in 50% Dulbecco's Modified Eagle's Medium/50% F12 (GIBCO) supplemented with 2% foetal bovine serum (FBS, GIBCO), 50 units/ml penicillin, 0.05 mg/ml streptomycin, 1x insulin/transferrin/selenium (ITS, Gibco), 50 nM dexamethasone and 10 ng/ml epidermal growth factor, and incubated at 37°C in 5% CO_2.

3.2.3.3 Inner medullary cortical collecting duct cells (IMCD)

Inner medullary cortical collecting duct (IMCD) cells were obtained from Prof. Ian Smyth (Monash University) and cultured in 50% Dulbecco's Modified Eagle's Medium/50% F12 (GIBCO) supplemented with 2% fetal bovine serum (FBS, GIBCO), 50 units/ml penicillin,

0.05 mg/ml streptomycin, 1x insulin/transferrin/selenium (ITS, Gibco), 50nM dexamethasone and 10 ng/ml epidermal growth factor at 37°C in 5% CO_2.

3.2.3.4 Isolation of Nedd4-2 kidney collecting duct cells

Nedd4-2 mice of age Post natal day 19 were humanely killed by cervical dislocation and then decapitated. The kidneys were then flushed with phosphate buffer saline using 0.5ml syringe and sliced into small pieces and placed in a 10 ml tube filled with a mixture of collagenase (5mg/ml, Worthington Biochemical Corporation) and DMEM/F12 (GIBCO). The kidney/enzyme mixture was then incubated for 5 minutes at 37^{o}C, and then moved to a rocker for 20 minutes at 37^{o}C and vortexed gently after every 10 minutes. The tube was then centrifuged at 90xg for 5 min on a table top centrifuge. The supernatant was removed and the pellet was resuspended into fresh primary media (DMEM/F12, 10% FBS, streptomycin/penicillin). The resuspended mix was then passed through a 106µm sieve and collected at the bottom of a 10ml tube. This process was repeated twice to get rid of debris. The final mix was collected in a fresh 10ml tube at the bottom of the sieve. This was centrifuged for 5min at 90xg. The supernatant was discarded and the cell pellet resuspended in the primary media. The mix was vortexed gently and kept at room temperature for 10 minutes to allow cells to settle. The supernatant was then gently decanted from the top. The bottom cellular pellet was resuspended in fresh primary media, distributed into 6 well plates with cover slips for cell staining and kept overnight in 37^{o}C incubator in 5% CO_2. The cells were washed with PBS the next day to remove any residual debris.

3.2.4 Ribonucleic acid (RNA) isolation and quantitative PCR (qPCR)

Ribonucleic acid (RNA) isolation and quantitative PCR (qPCR) were carried out as in section 2.2.10. The primer sequences used for qPCR are described below in Table 3.1.

3.2.5 Immunoblotting

3.2.5.1 Protein concentration and quantification

Protein quantification for cell lysates and whole kidney lysates were performed using the BCA (Bicinchoninic acid assay) protein quantification kit (Thermo Fisher Scientific) in 96 well plates. The standard curve was made using Bovine serum albumin (BSA, Sigma-Aldrich) as standards (0.1mg/ml). The BCA dye reagent (Thermo Fisher Scientific) 200ul was added to 10ul of BSA standard or 10ul of diluted cell/kidney lysates (1: 5 diluted cell lysates, 1:100 kidney lysates). A Fluostar optima plate reader (BMG Labtek) was used to measure OD at 595nm. All the samples and standards were assayed in triplicate for protein concentration and the final concentration calculated from the standard curve.

3.2.5.2 Protein extraction.

Proteins were extracted from cell pellets/kidney lysates after homogenisation in RIPA (Radioimmunoprecipitation assay buffer) lysis buffer (150 mM NaCl, 1% NP-40 (Nonyl phenoxypolyethoxylethanol), 0.5% DOC (Deoxycholate), 0.1% SDS, 50 mM Tris-HCl pH7.4, 5 mM EDTA) with addition of Halt™ protease/ phosphatase inhibitor cocktail (Thermo Fisher Scientific). The cell/kidney lysates were incubated for 60 minutes at 4^{o}C on rotating mixer (Nutator) and centrifuged at 13000xg for 10 minutes. Protein lysates were transferred after centrifugation to fresh Eppendorf tubes and stored at -70^{o}C. Protein lysates were analysed by SDS polyacrylamide gel electrophoresis (PAGE).

3.2.5.3 SDS PAGE and electrotransfer

In preparation for sodium dodecyl sulfate–polyacrylamide gel electrophoresis (SDS-PAGE) 100µg protein samples were incubated at 37^{o} C for 30 min in protein loading buffer (50mM Tris pH 6.8, 100mM DTT (Dithiothreitol), 1%w/v SDS, 0.5% w/v bromophenol blue and 10% v/v glycerol). Mini Protean TGX™ precast gradient polyacrylamide gels (BIORAD) were used for gel electrophoresis. The polyacrylamide gels were placed in a Hoefer mini gel

tank (Amersham biosciences) with protein electrophoresis running buffer (25mM Tris, 250mM glycine and 0.01%w/v SDS). The gel electrophoresis was performed at 200V (Volts) at 100mA (Milliamperes) for 40 minutes. Precision plus Protein Kaleidoscope™ standard (Bio-Rad) or HiMark™ Pre-stained Protein Standard (Thermo Fisher Scientific) were used to size the proteins.

Electrophoresed proteins were then transferred onto the 0.45µm methanol soaked polyvinylidene fluoride (PVDF) membrane (GE Healthcare) using Hoefer wet transfer apparatus (Amersham Biosciences) and Whatmann filter paper soaked in transfer buffer (49mM Tris, 39mM Glycine, pH 8). Proteins were electrotransferred onto the PVDF membrane for 60 minutes 100V at 350mA.

After transfer, PVDF membrane was blocked while gently rocking at room temperature for 1 hour in blocking buffer consisting of 5% w/v skim milk in TBS-T (25mM Tris pH 7.5, 140mM NaCl, 2.7mM KCl and 0.05%v/v Tween 20). After blocking the PVDF membrane was incubated with primary antibodies rabbit anti polycystin-1 (1:500, Santa Cruz), rabbit anti polycystin-2 (1:500, Millipore) and mouse anti β-Actin (1:2000, Sigma Aldrich) in blocking buffer overnight gently rocking at 4^{o}C. The membrane was washed 3 times for 15 minutes each in TBS-T. The membrane was then incubated with species specific secondary antibody diluted 1:2000 in blocking buffer or Rabbit IgG alkaline phosphatase (AP)-conjugated antibody (Millipore). AP-conjugated secondary antibodies were detected using ECF™ substrate (Enhanced chemifluoroscence, GE healthcare). Proteins were detected using AP and Cy5 – conjugated antibody on a Typhoon 9410 (Molecular Dynamics). Immunoblots were further quantified using Image Quant software (GE Healthcare).

3.2.5.4 Coomassie staining

Polyacrylamide gels were stained using 0.25%w/v coomassie brilliant blue solution for 1 hour after electrotransfer, and then destained in destain solution (40%w/v methanol, 10% v/v glacial acetic acid) 3 times for 20 min each.

3.2.6 siRNA in IMCD cells

IMCD cells ($2x10^5$) were seeded on 60mm dish (BD Falcon) in 2ml of DMEM/FBS medium and allowed to adhere. siRNA were diluted to 20µM in DEPC (Diethylpyrocarbonate water) and 10µl of both Nedd4-2 siRNA constructs (below) along with 10ul of RNAi Max transfection reagent (Invitrogen) were pooled with 100µl of Opti-mem (Gibco) and incubated for 20 minutes at room temperature. The control siRNA was also used in same amount as the Nedd4-2 siRNA for transfection as a negative control. The siRNAs were then added dropwise to cells. After 48hrs at 37^oC in transfection media, the cells were harvested for protein extraction, or processed further for cell staining. The siRNAs were purchased from Genepharma:

control siRNA- 5'UUCUUCGAACGUGUCACGUTT'3

mouse Nedd4-2 L -5'GGAGACAGCAUUCUAUUUATT'3

mouse Nedd4-2 LP -5'AACCACAACACAAAGUCACACTT3'

Mouse siRNA against Nedd4-2 and control siRNA (Cat No- 1027416, Qiagen) was used to check for off target effects of Nedd4-2 knock down.

3.2.6.1 Cell staining of siRNA treated IMCD cells

IMCD cells after siRNA transfection above were left to adhere on coverslips for 48 hours in transfection media. For staining the cells were washed three times with PBS for 5 minutes each, fixed with 4% paraformaldehyde for 10 minutes and washed with PBS thrice more. After washing, the cells to be permeabilized were incubated with 0.1% triton X-100 for 10 minutes, and the non- permeabilized cells were incubated with PBS alone. These cells were

then washed further with PBS for 10 minutes and blocked with 5% FBS/PBS (Blocking solution) for 1 hour. After 1 hour the cells were washed with PBS and incubated overnight in primary antibodies against rabbit Polycystin-1 (1:100, Santa Cruz), rabbit Polycystin-2 (1:100, Santa Cruz) and mouse Nedd4-2 (1:100, Santa Cruz) respectively in PBS. The next day the incubated cells were washed with PBS three times for 10 minutes and then incubated with secondary fluorescent antibodies (1:1000 rabbit Alexa Fluor 488) or (1:1000 rabbit Alexa Fluor 568) respectively for two hours at room temperature. These cells on coverslips were washed with PBS before mounting with Prolong Gold Antifade (Molecular Probes) and incubated for two minutes either with Hoechst 33342 or DAPI (1:400, Molecular Probes) for two minutes. Images were taken at the IMVS Confocal Microscopy Facility (Detmold imaging centre) using LSM 700 Carl Zeiss microscope.

3.2.6.2 Immunoblotting for Nedd4-2 siRNA treated IMCD cells

Cells after treatment with Nedd4-2 siRNA were pelleted and then protein was extracted as specified in section 3.2.5.2. After extraction the protein was quantitated and equal amounts of the cell extract was loaded onto the gradient gel, and electrophoresis, transfer and immunoblotting was carried out as stated in section 3.2.5.3.

3.2.6.3 Isolation of RNA from siRNA treated IMCD cells and qPCR

Cells were treated with Nedd4-2 siRNA as stated above. After incubation the cells were pelleted with PBS and RNA extraction was performed using Ambion RNAqueous Micro Kit (Life Technologies, #AM1931) according to the manufacturer's protocol. The RNA extracted from the cells was resuspended in DEPC treated water. RNA was further quantified using a Nanodrop1000TM spectrophotometer (Thermoscientific). The cDNA was generated using the High Capacity cDNA Reverse Transcription Kit (Applied Biosciences) with oligo-dT primers. The primer sets in Table 3.1 below were used for quantitative analysis for real time PCR as stated in section 2.2.10 for further analysis.

Table 3.1 qPCR analysis of mouse genes: primer sequences

Gene	Forward primer (5'-3')	Reverse Primer (5'-3')
β-actin	GATCATTGCTCCTCCTGAGC	AGTCCGCCTAGAAGCATTTG
PKD-1	GACAAGCATCTCTGGCTCTCC	ACGACCCCGTACCACACAG
PKD-2	CCACGTCCGATGAGCAGAAGT	ACCCAGTCGCGCATCCTCAGC
Nedd4-2	CTCTGATTCAGAGAGAGCCCTCG	GCATCCTTTCTTTCTTCCCAGCC

The quantitative real time PCR primers were ordered from GeneWorks.

3.2.7 Polycystin ubiquitination assay

For ubiquitination assays HEK293T cells were transfected with the indicated plasmids using Fugene HD transfection reagent (Promega) according to the manufacturer's instructions. After 24 hrs incubation, cells were treated for 4 hrs prior to lysis with 50 μM MG132 (Boston Biomedical, Boston, MA) and 400 μM chloroquine (Sigma-Aldrich) to block proteasomal and lysosomal degradation. Inhibition of deubiquitination enzymes was carried out by the addition of 5 mM NEM (Sigma-Aldrich) to the lysis buffer (RIPA) containing protease inhibitor cocktail (Sigma-Aldrich). Immunoprecipitations were performed as previously described (Foot *et al*., 2008). Briefly, cells were lysed at 4ºC, centrifuged at 15,000g to remove cellular debris and the supernatant was collected. For analysis of input levels of proteins 5% of the protein lysate was denatured with Laemmli buffer to be used as input. 30ul of protein G sepharose beads were washed and allowed to equilibrate with the lysis buffer prior to addition of the remaining protein supernatant. Immunoprecipitation with 1ul of rabbit polycystin-1 antibody (Santa Cruz) was carried out overnight on a rotating mixer (Nutator) at 4ºC. The following day the beads were washed 2x lysis buffer and 1x PBS to remove unbound proteins. After the addition of 20ul of 4x protein load buffer bound proteins were

released from the beads and denatured at 37ºC for 30 min. Protein samples were separated through 10% SDS-PAGE gel electrophoresis, transferred to PVDF membrane and blocked in 5%BSA/TBST (Blocking buffer). Immunoblotting was carried out with primary antibodies [(mouse ubiquitin (1:500, Covance), (rat anti-Flag clone 6F7, Sigma), (mouse β-actin clone AC-15, Sigma), (mouse c-Myc clone 9E10, Roche)] diluted in blocking buffer overnight at 4°C, followed by incubation with an alkaline phosphatase (AP), horse radish peroxidase (HRP) or Cy5-conjugated secondary antibody. Visualization of AP and Cy5 signals was carried out on a Typhoon FLA Biomolecular Imager (GE Healthcare) and HRP signals were detected on an ImageQuant LAS 4000 (GE Healthcare).

3.2.8 Immunofluorescence

For Immunofluoroscence staining, paraffin embedded sections were washed in xylene for ten minutes and then rehydrated in a series of 100%, 95%, 80%, 50% ethanol/distilled water for 5 minutes each. Antigen retrieval was performed in 0.01 M sodium citrate (pH-6) for 10 minutes at 100% microwave power (300 W) followed by cooling for 30 min and rinsing in PBS. Endogenous peroxidase was quenched with 0.3% hydrogen peroxide in distilled water for 10 minutes. Sections were then washed in TBST (Tris-buffered saline/0.05% Tween 20) for 5 minutes and blocked with 10% donkey serum in TBST for 3 hours at room temperature. Primary antibodies for goat polycystin-1 (1:100, Santacruz) were added in blocking solution overnight. For immunofluoroscence secondary antibodies (1:1000, rabbit Alexa Fluor 488, Molecular Probes) were added in blocking solution for 2 hours at room temperature and sections were mounted in Prolong Gold Antifade reagent (Molecular Probes).

3.2.9 Statistical significance

Statistical analyses were performed with GraphPad Prism (v6) or Microsoft® Excel using unpaired t-test assuming equal variance, with statistical significance determined as being $P \leq 0.05$.

3.3 Results

3.3.1 Polycystin-1 expression and transcript levels in *Nedd4-2*$^{-/-}$ kidney

Previous studies on PKD1 transgenic mice suggested over expression of polycystin-1 in the kidneys had links to renal cystogenesis (Kurbegovic *et al*., 2010). Based on the same I hypothesized that polycystin-1 could be over expressed in the *Nedd4-2*$^{-/-}$ kidneys. To evaluate the expression levels of polycystin-1 in Nedd4-2 kidneys, P19 *Nedd4-2*$^{+/+}$ (N=4) and P19 *Nedd4-2*$^{-/-}$ (N=4) whole cystic kidney lysates where prepared and evaluated. As a polycystin-1 antibody control, the over-expressed dual tagged polycystin-1 plasmid construct was simultaneously expressed in HEK293T cells and lysed in the same lysis buffer as the whole kidney lysates for use in size detection since antibodies specific to polycystin-1 have been known to detect non-specific bands of higher molecular weight. **Fig 3.3 A** shows the polycystin-1 protein is expressed in both P19 *Nedd4-2*$^{+/+}$ and *Nedd4-2*$^{-/-}$ kidney, with the endogenous polycystin-1 protein band slightly around the expected 450kDa. The over-expressed polycystin-1 expression construct resulted in a slightly fainter protein band at the same size than expressed endogenously in the kidney. Also seen are protein bands as compared to over expressed protein are cleaved products of polycystin-1. Alpha tubulin was used as a loading control, and quantitation of polycystin-1 was performed with normalization to alpha tubulin. **Fig 3.3 B** shows that after normalization there was no significant difference observed in the expression levels of polycystin-1 in the kidneys of P19 *Nedd4-2*$^{+/+}$ and P19 *Nedd4-2*$^{-/-}$ using the unpaired T-test. To corroborate the protein expression data the transcript levels of polycystin-1 were measure in the kidney. Whole kidney samples from P19 *Nedd4-2*$^{+/+}$ (N=5) and P19 *Nedd4-2*$^{-/-}$ (N=5) mice were used for RNA extraction and quantitative real time PCR was performed using primers specific to the N terminal exon region of PKD1, with β-actin used as a loading control. As shown in **Fig 3.3 C** there was no significant

difference seen in the levels of polycystin-1 transcript levels in the *Nedd4-2* $^{+/+}$ and *Nedd4-2* $^{-/-}$ kidneys using unpaired T-test.

3.3.2 Polycystin-2 expression and transcript levels in *Nedd4-2*$^{-/-}$ kidney

Lower levels of polycystin-2 in the TAZ mutant mice kidneys have been linked to the onset of glomerular cysts, and polycystin-2 has been reported to form a multimeric complex with polycystin-1 in the regulation of renal cystogenesis (Makita *et al*., 2008, Tian *et al*., 2007, Giamarchi *et al*., 2010). To further evaluate the protein expression levels of polycystin-2 in Nedd4-2 kidneys, P19 *Nedd4-2*$^{+/+}$ (N=6) and P19 *Nedd4-2*$^{-/-}$ (N=6) whole cystic kidney lysates were evaluated. The Myc-tagged polycystin-2 over expression plasmid was simultaneously expressed in HEK293T cells and lysed in the same lysis buffer as the whole kidney lysates to be used as a positive size control for the polycystin-2 antibody. **Fig 3.4 A** shows detection band of polycystin-2 with the expected size of 110 kDa compared to the over expressed polycystin-2 construct which has a slightly higher molecular weight, possibly due to the presence of the Myc tag. Alpha tubulin was used as a loading control and **Fig 3.4 B** shows that upon quantitation of polycystin-2 normalized to alpha tubulin there was no significant difference observed in the polycystin-2 protein levels between P19 *Nedd4-2*$^{+/+}$ and P19 *Nedd4-2*$^{-/-}$ kidneys. To corroborate the protein expression levels of polycystin-2 as reported earlier transcriptional changes were measured for polycystin-2 in whole kidney samples. The P19 *Nedd4-2*$^{+/+}$ (N=5) and P19 *Nedd4-2*$^{-/-}$ kidneys (N=5) were used for RNA extraction and the quantitative real time PCR was performed using primers specific to PKD2 and β-actin was used as a loading control . As shown in Fig 3.4 C there was no significant difference in polycystin-2 transcript levels seen between P19 *Nedd4-2*$^{-/-}$ and *Nedd4-2*$^{+/+}$ kidneys, using unpaired T-test.

Fig 3.3 Polycystin-1 protein expression and transcript levels in *Nedd4-2*$^{-/-}$ kidneys. A) Whole cystic kidney lysates were subjected to polycystin-1 immunoblot analysis for P19 *Nedd4-2*$^{+/+}$ (N=4) and P19 *Nedd4-2*$^{-/-}$ mice (N=4). Dual tagged polycystin-1(HA-FLAG) was over-expressed in HEK cells and used as a size control **B)** The immunoblot from A was to quantify polycystin-1 protein levels, using α-tubulin as a loading control **C)** Whole cystic kidney RNA was extracted and qPCR analysis of polycystin-1 (PKD1) transcription performed from P19 *Nedd4-2*$^{+/+}$ (N=5) and *Nedd4-2*$^{-/-}$ cystic kidneys. Expression of polycystin-1 transcript was measured relative to β-actin transcript. Data is represented as mean ± SEM ($P \geq 0.05$, not significant (n.s), using unpaired T-test).

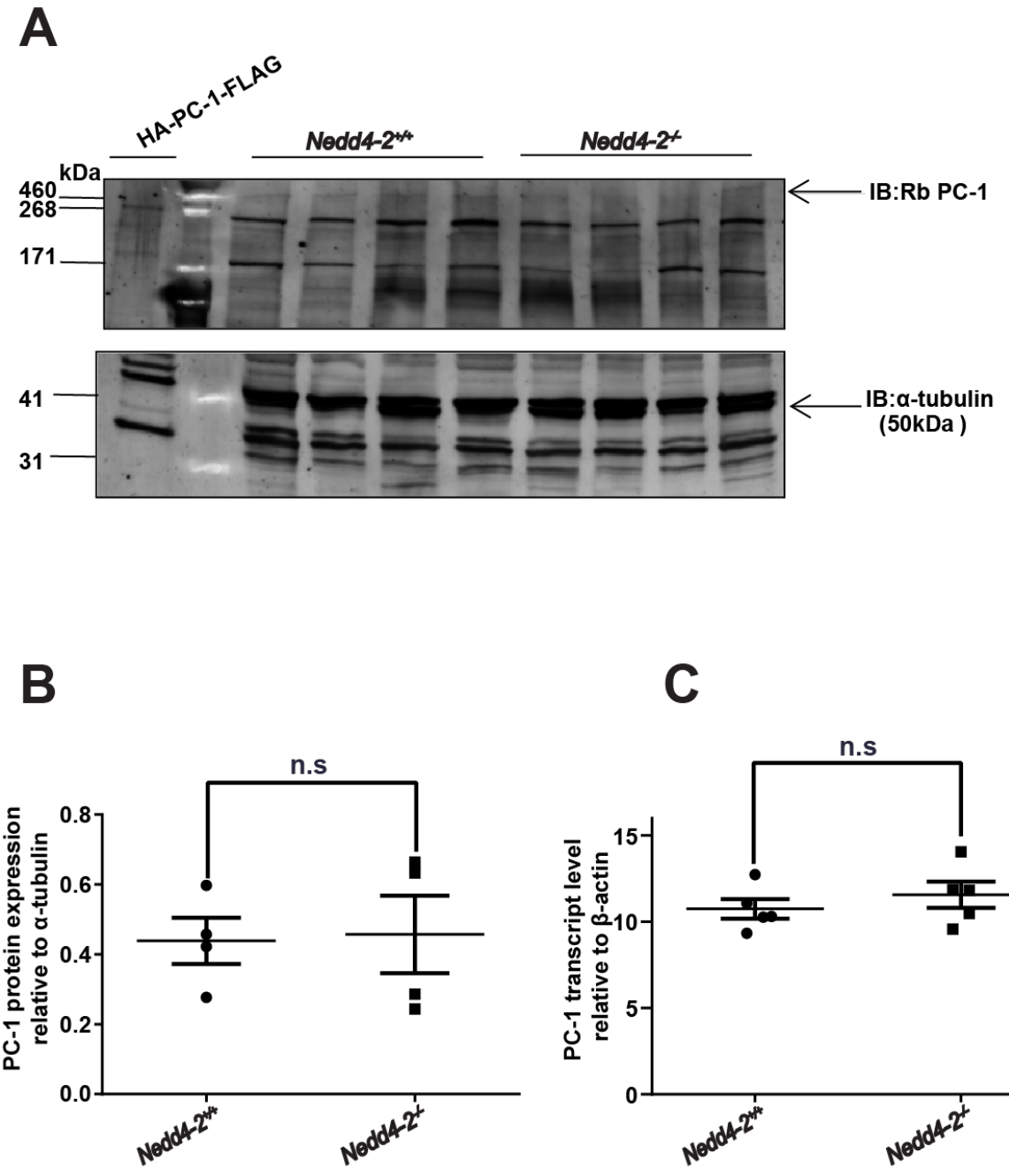
A
HA-PC-1-FLAG
Nedd4-2+/+
Nedd4-2-/-
kDa
460
268
171
IB:Rb PC-1
41
31
IB:α-tubulin
(50kDa)
B
n.s
PC-1 protein expression
relative to α-tubulin
0.8
0.6
0.4
0.2
0.0
Nedd4-2+/+
Nedd4-2-/-
C
n.s
PC-1 transcript level
relative to β-actin
15
10
5
0
Nedd4-2+/+
Nedd4-2-/-

Fig 3.4 Polycystin-2 protein expression and transcript levels in *Nedd4-2*$^{-/-}$ kidneys. A) Whole kidney lysates at P19 day were subjected to polycystin-2 immunoblot analysis for (N=6) *Nedd4-2*$^{+/+}$ kidneys and (N=6) *Nedd4-2*$^{-/-}$ cystic kidneys, and α-tubulin was used as loading control. Over expressed polycystin-2 (myc-PC-2) in HEK cells was used as a size control. **B)** The immunoblot from A was used to quantify polycystin 2 protein expression using α-tubulin as a loading control. **C)** Whole kidney RNA was extracted and qPCR analysis of polycystin-2 (PKD2) transcription performed from (N=5) *Nedd4-2*$^{+/+}$ and (N=5) *Nedd4-2*$^{-/-}$ kidneys. Expression was polycystin-2 transcript was measured relative to β-actin transcript levels. Data is represented as mean ± SEM ($P \geq 0.05$, not significant (n.s), using unpaired T-test)**.**

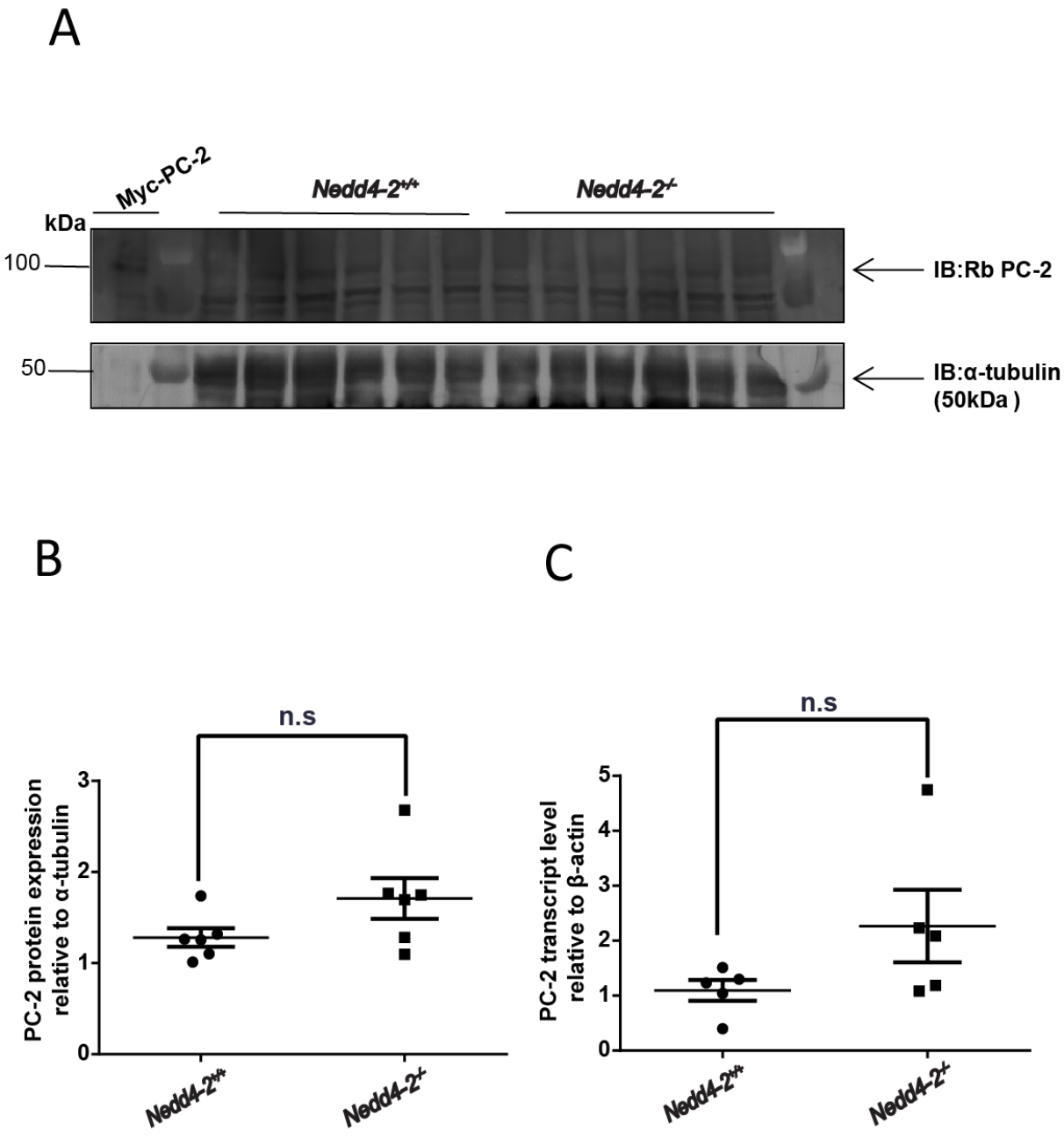
A
Myc-PC-2
Nedd4-2+/+
Nedd4-2+/-
kDa
100
50
IB:Rb PC-2
IB:α-tubulin
(50kDa)
B
n.s
PC-2 protein expression
relative to α-tubulin
0
1
2
3
Nedd4-2+/+
Nedd4-2+/-
C
n.s
PC-2 transcript level
relative to β-actin
0
1
2
3
4
5
Nedd4-2+/+
Nedd4-2+/-

3.3.3 Isolation and characterisation of cortical collecting duct cells (CCD)

I further hypothesized that polycystin expression could be dependent upon Nedd4-2 expression within specific regions of the kidney. Previous reports in mice suggested Nedd4-2 is expressed throughout the kidney nephrons, but higher expression in the collecting duct with lower Nedd4-2 expression levels in the late convoluted tubule and early connecting tubules (Loffing-Cueni *et al*., 2006). It became imperative to isolate kidney cells from *Nedd4-2*$^{-/-}$ mice to understand the role ablation of Nedd4-2 plays in the regulation of polycystins in these cells. Cortical collecting duct cells were isolated from P19 *Nedd4-2*$^{-/-}$ kidney, as seen in **Fig 3.5 A, B** and **C,** and the mouse pyruvate kinase cortical collecting duct (mpkCCD) cell line was used as control for characterising these cells (**Fig 3.5 C**, **D** and **E)**. The morphology of the CCD cells isolated looked very similar in shape and size in comparison to the control cell line. However, the cells isolated from the P19 *Nedd4-2*$^{-/-}$ kidneys showed a milieu of different other cell types since the nephron of the kidney is subdivided into different segments and technically difficult to micro-dissect. As different nephronal segments have different levels of Nedd4-2 expression, polycystin expression could also be expected to be differentially regulated and therefore it was necessary to demonstrate the pattern of polycystin expression within these cells. As suggested from previous reports, polycystin localisation and expression varies between different kidney cell types (Newby *et al*., 2002). These primary CCD cells (**Fig 3.5 A, B** and **C)** showed very similar morphology to the control cell line, however there were a lot of different cell types with different morphological features around the isolated cells despite several washes to get rid of the debris. These CCD cells could not further be passaged and stained for kidney nephronal markers due to the primary nature of the isolated cells, with no further propagation feasible once plated on the cover slips for immunocytochemisty. With very few cells available we further proceeded to investigate the localisation and expression of polycystins within cells isolated from the

kidneys of *Nedd4-2*$^{-/-}$ mice to understand the role Nedd4-2 mediated regulation of polycystins could play in renal cystic onset in these mice.

3.3.4 Polycystin-1 and polycystin-2 expression and localisation in isolated primary cells.

To investigate the possible regulation of polycystins by Nedd4-2, the isolated primary kidney cells CCD like as mentioned above from P19 *Nedd4-2*$^{+/+}$ and P19 *Nedd4-2*$^{-/-}$ mice were utilised. These primary kidney cells isolated from the P19 *Nedd4-2*$^{-/-}$ (N=2) and P19 *Nedd4-2*$^{+/+}$ (N=2) mice were subjected to cell staining with antibodies specific to Nedd4-2, polycystin-1 (Leucine Rich Repeat region on N-terminal) and polycystin-2 and were used to understand the role constitutive abrogation of Nedd4-2 in the kidney cells in polycystins surface expression and localisation as previous reports had suggested to Nedd4-2 being highly expressed in the cortical collecting ducts (Loffing-Cueni *et al*., 2006). The initial working hypothesis was that in these few isolated CCD like cells expression of Nedd4-2 could be regulating surface expression of polycystin-1 on the membrane, necessary for polycystin-1 interaction with extracellular microenvironment and for polycystin-2 functioning and channel properties (Giamarchi *et al*., 2010, Weston *et al*., 2001). To firstly assess the Nedd4-2 expression, Nedd4-2 specific immunostaining was performed on isolated P19 *Nedd4-2*$^{-/-}$ kidney cells, with P19 *Nedd4-2*$^{+/+}$ isolated kidney cells used as control. *Nedd4-2*$^{-/-}$ isolated kidney cells showed no staining for Nedd4-2 (**Fig 3.6 C, D**), in comparison to P19 *Nedd4-2*$^{+/+}$ control cells that show clear Nedd4-2 expression (**Fig 3.6 A** and **B,** Nedd4-2 staining (green) and DAPI (blue) merged images). To assess polycystin-1 surface expression in these cells, polycystin-1 specific N-terminal region antibody was used. As seen in **Fig 3.6 G** and **H** (polycystin-1 staining (green) and DAPI (blue) merged images), increased expression of polycystin-1 predominantly cytosolic was observed in primary kidney cells from P19 *Nedd4-2*$^{-/-}$ mice in comparison to P19 *Nedd4-2*$^{+/+}$ controls (**Fig 3.6 G** and **H**). To ascertain the specificity of the anti-rabbit secondary antibody, merged cell stained

images with no primary antibody added were taken as negative control (**Fig 3.6 M** and **N**) and show no non-specific staining.

To further examine the expression of polycystin-2 in context to the above findings, isolated kidney cells were simultaneously stained for polycystin-2 expression (**Fig 3.6**). Polycystin-2 expression was greatly increased in P19 *Nedd4-2*$^{-/-}$ (**Fig 3.6 K** and **L)** in comparison to P19 *Nedd4-2*$^{+/+}$ control cells (**Fig 3.6 I** and **J)**.

3.3.5 Polycystin expression and localisation upon Nedd4-2 knock down in inner medullary collecting duct (IMCD) cells.

To corroborate the increased polycystin expression seen in primary kidney cells lacking Nedd4-2 (**Fig 3.6)** it was necessary to investigate the localisation and expression of the polycystins in a stable cell line known to express requisite amounts of Nedd4-2. To this end, inner medullary collecting duct (IMCD) cells that were isolated and stabilised from the kidney collecting duct were procured (Ono *et al*., 1994). The primary kidney cells did highlight the variability and changes in expression of the polycystins, but to focus on the role Nedd4-2 plays in regulating polycystins *in vitro,* Nedd4-2 depletion studies were undertaken in the IMCD cell line as these cells are easily transfected and maintain similar ion channel properties to cortical collecting duct cells (Ono *et al*., 1994). Therefore IMCD cells were transfected with Nedd4-2 siRNA or control siRNA and cells were examined for expression of polycystin-1 and polycystin-2. The initial hypothesis was that by knocking down Nedd4-2 in the IMCD cells it could alter the surface localisation and expression of polycystin-1, a potential direct target of Nedd4-2 with proline rich motifs predominantly localised on the membrane (Giamarchi *et al*., 2006). This could be either polycystin-2 dependent or independent, and could also be affected by the altered expression and localisation of polycystin-2 seen in Nedd4-2 deficient cells (**Fig 3.6 K** and **L**). The IMCD cells were plated and transfected the next day with Nedd4-2 and control siRNA and left for 48 hours. These

cells were then stained with same antibodies used in **Fig 3.6** for Nedd4-2, polycystin-1 and polycystin-2 to confirm the above findings. In **Fig 3.7 F** we further report increased expression of polycystin-1 (red - polycystin-1, blue - Hoechst 333458) predominantly localised on the membrane upon treatment with Nedd4-2 siRNA in comparison to negative control siRNA treated cells (**Fig 3.7 C**). In **Fig 3.7 L** we confirm the effective knock down of Nedd4-2 by the Nedd4-2 siRNA construct, in comparison to the control siRNA stained cells where Nedd4-2 expression is predominantly cytoplasmic (**Fig 3.7 I** (red - Nedd4-2; blue - Hoechst 333258)). To examine the expression and localisation of polycystin-2 upon Nedd4-2 depletion, IMCD cells were treated as above. In **Fig 3.8 F** (red, blue-Hoechst 333458) we report slightly decreased expression levels of polycystin-2 around the membrane in Nedd4-2 depleted cells in comparison to the control siRNA treated cells (**Fig 3.8 C)**, contrary to our previous findings in isolated primary kidney cells (**Fig 3.6**).

To confirm the increased expression of polycystin-1 observed upon Nedd4-2 depletion in IMCD cells, immunoblotting was performed to detect total polycystin-1 protein, and transcript levels of both polycystin-1 and polycystin-2 in these cells were analysed. The protein lysates prepared from Nedd4-2 siRNA treated IMCD cells were immunoblotted for polycystin-1 and Nedd4-2 (to confirm knock down). Higher protein expression of polycystin-1 was observed (Cleaved product) in Nedd4-2 siRNA treated cells in comparison to control treated cells (**Fig 3.9 A**), with β-actin used as a loading control. The Nedd4-2 immunoblot confirmed an effective knock down of Nedd4-2 in the Nedd4-2 siRNA treated cells. To quantitate the effectiveness of the knockdown and measure the changes in transcript levels of polycystin-1 and polycystin-2 upon Nedd4-2 depletion in IMCD cells, qPCR was performed on Nedd4-2 siRNA treated cells along with control siRNA treated cells in two independent experiments. **Fig 3.9 B** and **C** show the transcript levels of Nedd4-2 are significantly down regulated ($P<0.05$) in Nedd4-2 siRNA treated cells in comparison to control siRNA treated

cells. The effectiveness of the Nedd4-2 knockdown was roughly 85% in the Nedd4-2 siRNA treated cells in comparison to control siRNA treated cells. To measure the transcript levels of both polycystin-1 and polycystin-2 in these cells the same set of qPCR primers were used as in **Fig 3.3 C** and **3.4 C.** Upon Nedd4-2 depletion in IMCD cells, polycystin-1 transcript levels showed an increasing trend, although this was not statistically significant in comparison to control siRNA treated cells (**Fig 3.9 B**). There was also no statistically significant difference seen in polycystin-2 transcript levels upon Nedd4-2 depletion in siRNA treated cells in comparison to the control (**Fig 3.9 C**), although there was a similar increasing trend comparable to polycystin-1 (**Fig 3.9 B**), which was contrary to the reduced expression of polycystin-2 observed in these cells via immunofluoresence (**Fig 3.8 F**).

3.3.6 Polycystin-1 is ubiquitinated by Nedd4-2 independent of polycystin-2

Given the above findings, that upon Nedd4-2 knockdown in IMCD cells there is an increase in expression levels of polycystin-1 but not polycystin-2; further investigation was required to determine whether polycystin-1 is indeed a substrate for Nedd4-2 mediated ubiquitination. Previous studies suggest polycystin-1 is ubiquitinated by the RING ubiquitin ligase Siah-1 (Kim *et al*., 2004). To determine whether polycystin-1 is ubiquitinated by Nedd4-2, and dissect the role polycystin-2 plays in altering the stability of the interaction between polycystin-1 and Nedd4-2, the following ubiquitination assay was designed. Tagged polycystin-1 construct was co-transfected in HEK293T cells with either active Nedd4-2 or catalytically inactive Nedd4-2 cysteine mutant (Nedd4-2 CM) in the absence or presence of polycystin-2 (as indicated in **Fig 3.10)**. The addition of Ub-HA in the presence of Nedd4-2 and polycystin-1 (and absence of polycystin-2) resulted in a laddering pattern indicative of polycystin-1 ubiquitination. The observed ubiquitination of polycystin-1 by Nedd4-2 in the absence of polycystin 2 was inhibited upon addition of the catalytically inactive Nedd4-2 CM. Previous studies have highlighted the role of polycystin-2 in interacting with polycystin-

1 that forms a proper functioning PC-1/PC-2 complex (Giamarchi *et al*., 2010). To assess the role polycystin-2 plays in Nedd4-2 mediated ubiquitination of polycystin-1, polycystin-2 was co-expressed with polycystin-1 in the presence of either Nedd4-2 or Nedd4-2 CM as indicated in **Fig 3.10**. Upon addition of polycystin-2, Nedd4-2 mediated ubiquitination of polycystin-1 was clearly abrogated (**Fig 3.10**). and catalytically inactive Nedd4-2 was unable to ubiquitinate polycystin-1 in presence and absence of polycystin-2. This data further indicated that polycystin-1 is a novel substrate for Nedd4-2 mediated ubiquitination.

3.3.7 Polycystin-1 over expression in collecting ducts of *Nedd4-2*$^{-/-}$ kidneys

To further understand the physiological relevance of the above findings, the localisation of polycystin-1 in the *Nedd4-2*$^{-/-}$ kidneys was assessed to validate the novel role it plays in renal cystogenesis in these mice. To evaluate polycystin-1 expression immuno- staining was performed on P19 kidney sections from *Nedd4-2*$^{-/-}$ mice and *Nedd4-2*$^{+/+}$ control littermates. Confocal images in **Fig 3.11 A, B** and **C (**PC-1-Red, Hoechst 33342-blue**)** represent merged images taken from different regions of the *Nedd4-2*$^{+/+}$ kidneys and **Fig 3.11 E, F** and **G** represent different regions within *Nedd4-2*$^{-/-}$ kidneys respectively. To confirm specificity of binding of the secondary antibody, a negative control that lacked primary antibody and contained only the species specific secondary antibody was used on P19 *Nedd4-2*$^{-/-}$ and P19 *Nedd4-2*$^{+/+}$ kidney sections (**Fig 3.11 D** and **H**). In the kidneys of P19 *Nedd4-2*$^{-/-}$ mice (**Fig 3.11 E, F** and **G**) there is an increased expression of polycystin-1 in the distal convoluted tubules (DCT) and the collecting ducts (CD) in comparison to P19 *Nedd4-2*$^{+/+}$ control littermates (**Fig 3.11 A, B** and **C**). This further confirmed the important role polycystin-1 plays in the pathophysiological context of the P19 *Nedd4-2*$^{-/-}$ kidneys to aid in renal cystogenesis.

Fig 3.5 Isolated kidney collecting duct cells from *Nedd4-2*$^{-/-}$ mice. Isolated cortical collecting kidney duct cells from P19 *Nedd4-2*$^{-/-}$ mice were plated in 6 well dishes. Images **A, B** and **C** were taken at 4x, 10x, 20 x magnifications respectively. Images **D**, **E** and **F** were taken at 4x, 10x, 20x magnification of the mouse pyruvate kinase cortical collecting duct (mpkCCD) cell line in a T75 culture flask. The morphology of the cell line was compared to the isolated cells as control. The images (**A-C**) are representative of the field of interest of the cells showing similar characteristics to control cell line. The cortical collecting kidney duct cells were isolated from two independent mice to show consistency in the isolation protocol. Images were taken using an Olympus inverted light microscope.

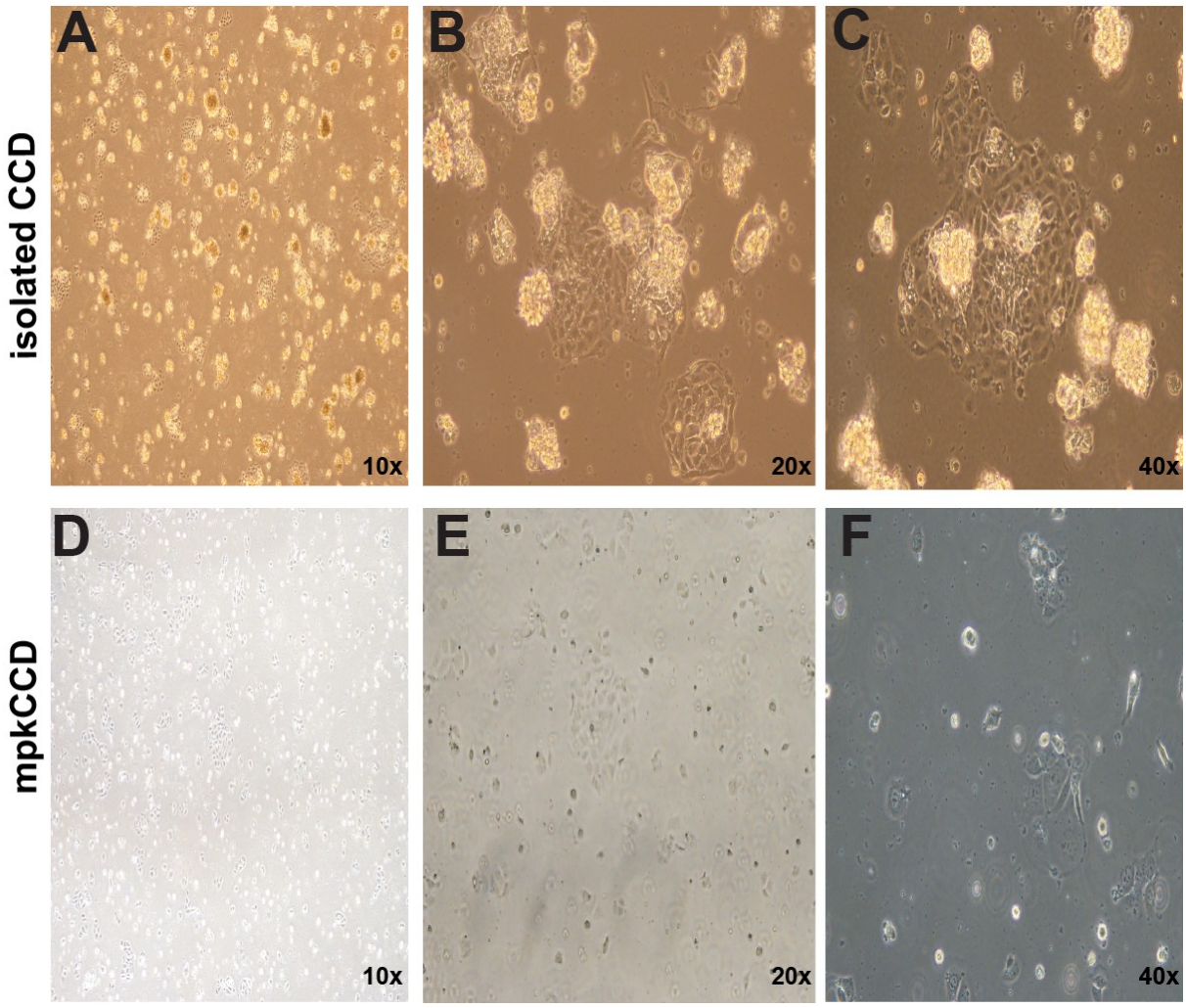
isolated CCD
mpkCCD
A
B
C
D
E
F
10x
20x
40x
10x
20x
40x

Fig 3.6 Polycystin-1 and polycystin-2 expression and localisation in isolated kidney cells. Confocal microscopy images of endogenous levels of polycystin-1 (green), polycystin-2, Nedd4-2 (green) and DAPI (blue) in *Nedd4-2*$^{+/+}$ and *Nedd4-2*$^{-/-}$ cortical collecting kidney cells isolated from P19 kidneys. Images **A-N** represents merged channels (green/blue). Image **A** and **B** represent Nedd4-2 staining in P19 *Nedd4-2*$^{+/+}$ isolated cells in comparison with Images **C** and **D** in P19 *Nedd4-2*$^{-/-}$ cells. Image E and **F** represent polycystin-1 staining in P19 *Nedd4-2*$^{+/+}$ isolated cells in comparison with images **G** and **H** in P19 *Nedd4-2*$^{-/-}$ cells. Image I and **J** represent polycystin-1 staining in P19 *Nedd4-2*$^{+/+}$ isolated cells in comparison with images **K** and **L** in P19 *Nedd4-2*$^{-/-}$ cells. Images M and **N** represent secondary antibody control in P19 *Nedd4-2*$^{+/+}$ and P19 *Nedd4-2*$^{-/-.}$ isolated cells respectively. This experiment was performed on N=2 animals independently. Images were taken using LSM 700 confocal microscope. Scale bar= 50µm.

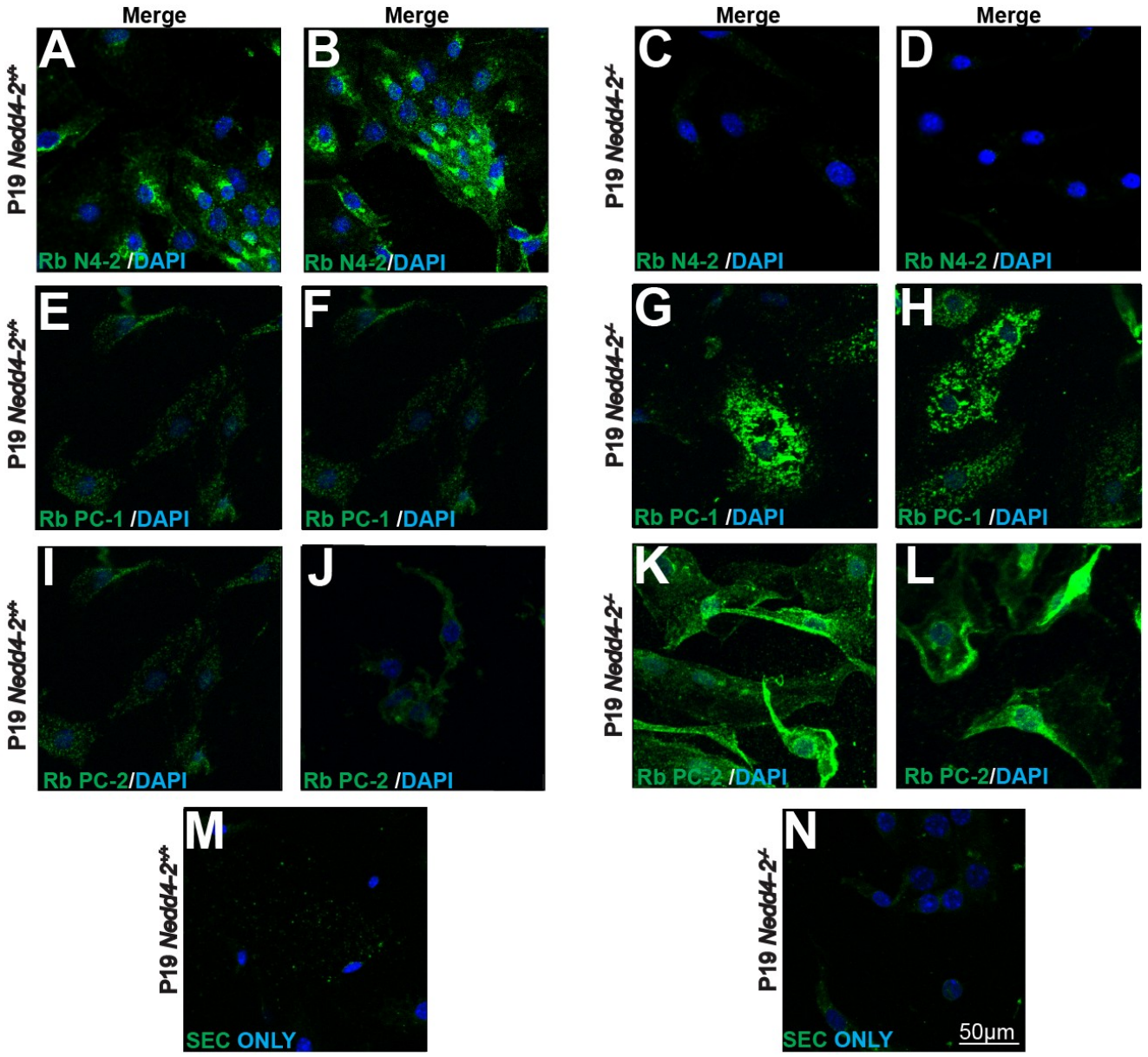
Merge
Merge
Merge
Merge
A
B
C
D
P19 Nedd4-2+/+
P19 Nedd4-2-/-
Rb N4-2 /DAPI
Rb N4-2/DAPI
Rb N4-2 /DAPI
Rb N4-2 /DAPI
E
F
G
H
Rb PC-1 /DAPI
Rb PC-1 /DAPI
Rb PC-1 /DAPI
Rb PC-1 /DAPI
I
J
K
L
Rb PC-2/DAPI
Rb PC-2 /DAPI
Rb PC-2 /DAPI
Rb PC-2/DAPI
M
N
SEC ONLY
SEC ONLY
50µm

Fig 3.7 Increased expression of polycystin-1 upon Nedd4-2 knock down. Confocal microscopy images of endogenous levels of polycystin-1 (red), Nedd4-2 (red) and Hoechst 3358 (blue) in control siRNA and Nedd4-2 siRNA treated IMCD cells. Images **C**, **F**, **I** and **L** represent merged channels (red/blue). Image **G** (red) represents Nedd4-2 (red) staining in control siRNA treated cells in comparison with Image **J** (red) of Nedd4-2 siRNA treated cells. Image **A** (red) represents polycystin-1 (red) staining in control siRNA treated cells in comparison with Image **B** (red) of Nedd4-2 siRNA treated cells. Images **B**, **E**, **H** and **K** show Hoechst 33342 staining. This staining is representative of N=2 independent experiments. Images were taken using LSM 700 confocal microscope. Scale bar= 50µm.

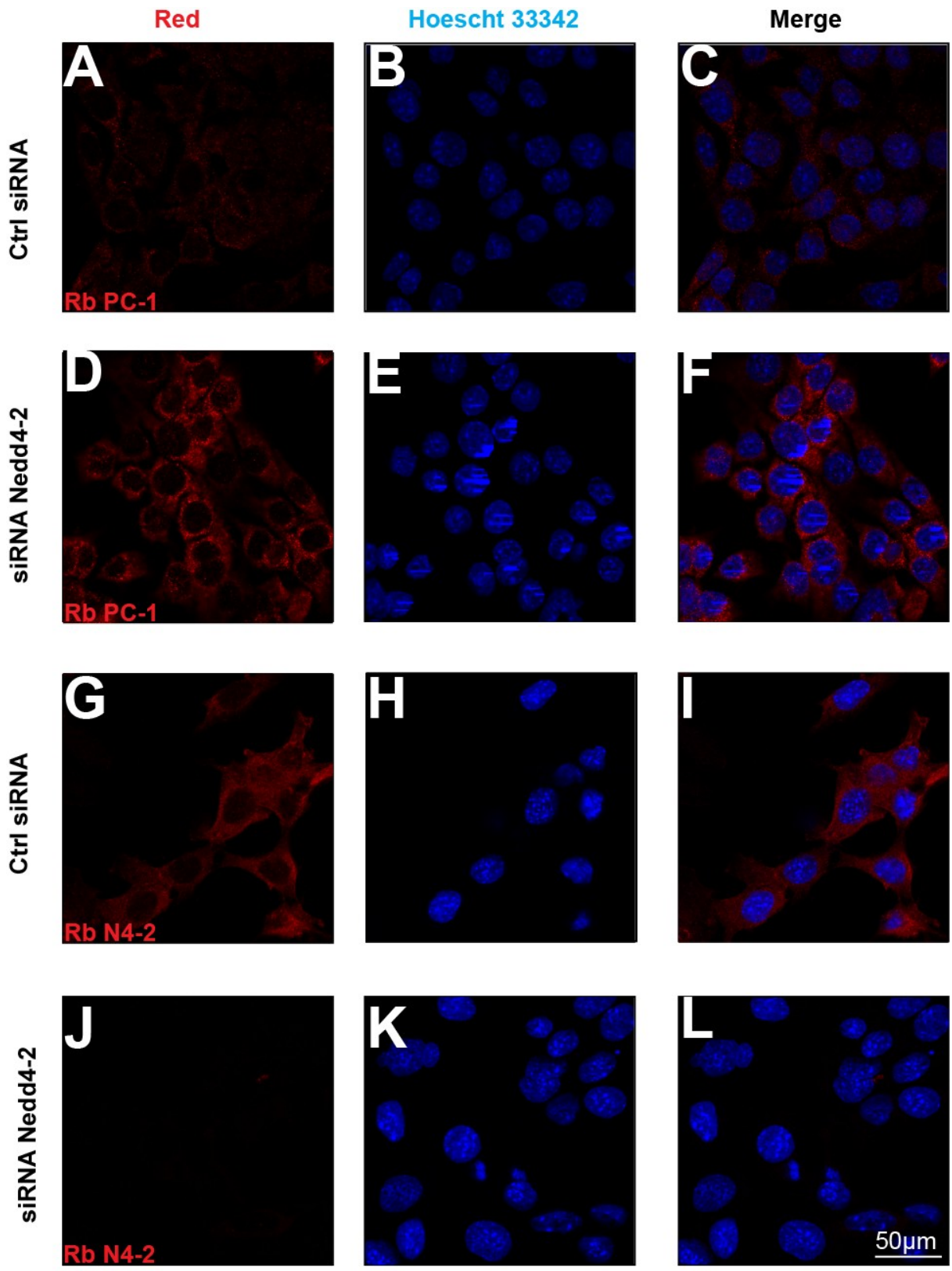
Red
Hoescht 33342
Merge
Ctrl siRNA
siRNA Nedd4-2
Ctrl siRNA
siRNA Nedd4-2
A
B
C
D
E
F
G
H
I
J
K
L
Rb PC-1
Rb PC-1
Rb N4-2
Rb N4-2
50µm

Fig 3.8 Decreased expression of polycystin-2 upon Nedd4-2 knock down. Confocal microscopy images of endogenous levels of polycystin-2 (red), Nedd4-2 (red) and Hoechst 33358 (blue) in control siRNA and Nedd4-2 siRNA treated IMCD cells. Images **C**, **F**, **I** and **L** represent merged channels (red/blue). Image **G** (red) represent Nedd4-2 (red) staining in control siRNA treated cells in comparison with Image **J** (red) of Nedd4-2 siRNA treated cells. Image **A** (red) represent polycystin-2 (red) staining in control siRNA treated cells in comparison with Image **B** (red) of Nedd4-2 siRNA treated cells. Images **B**, **E**, **H** and **K** show Hoechst 33342 staining. This staining is representative of N=2 independent experiments. Images were taken using LSM 700 confocal microscope. Scale bar= 50µm.

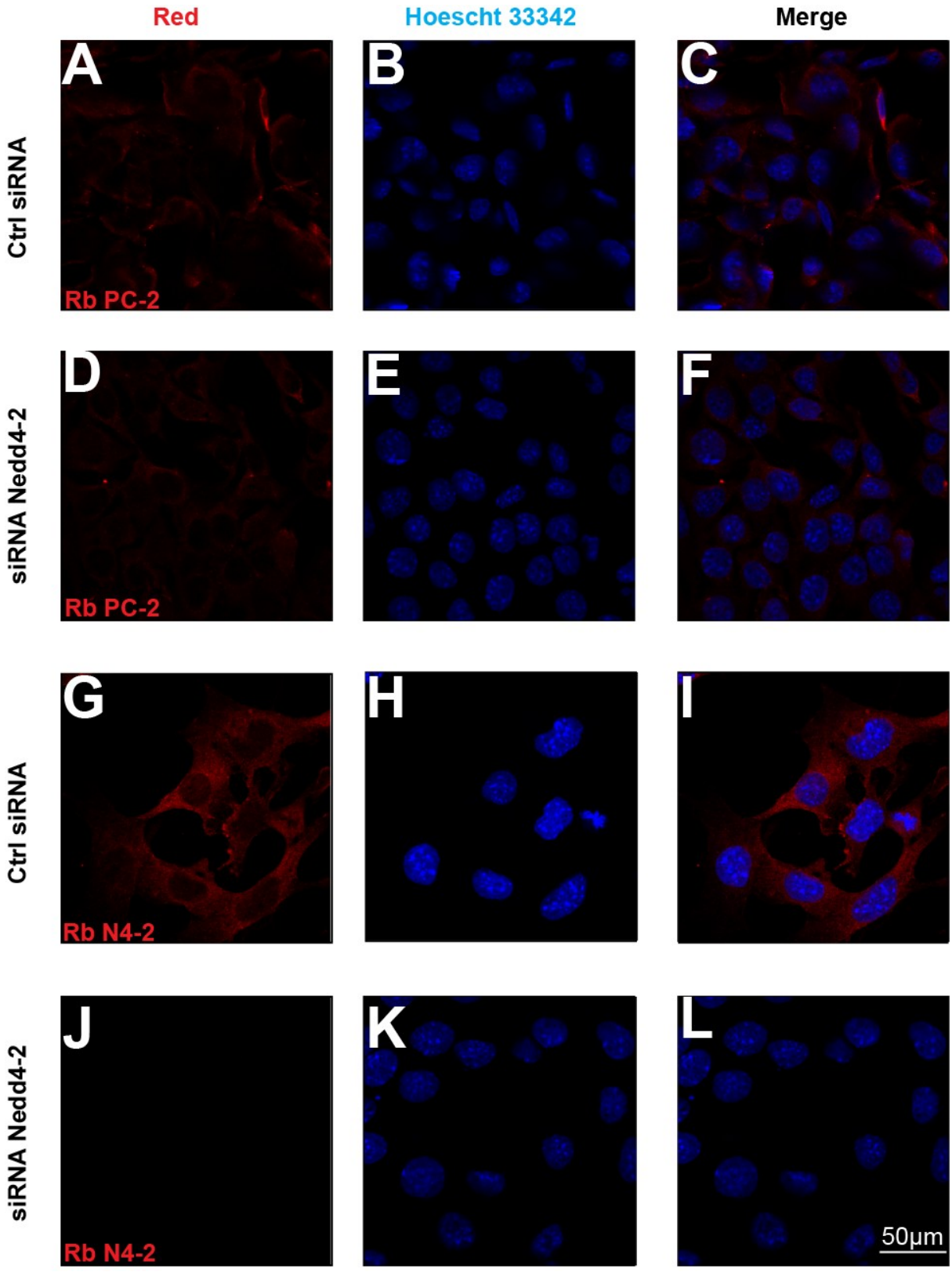
Red
Hoescht 33342
Merge
Ctrl siRNA
siRNA Nedd4-2
Ctrl siRNA
siRNA Nedd4-2
A
B
C
D
E
F
G
H
I
J
K
L
Rb PC-2
Rb PC-2
Rb N4-2
Rb N4-2
50µm

Fig 3.9 Polycystin-1 over expression upon Nedd4-2 depletion. A) Western blot analysis of Nedd4-2 siRNA and control siRNA treated IMCD cells using antibodies specific to Nedd4-2, polycystin-1 and β-actin a loading control. A 250kDa molecular weight marker was used as a size control. **B)** Real time quantitative PCR analysis of Nedd4-2 and polycystin-1 upon Nedd4-2 depletion in IMCD cells and control siRNA treated cells. Expression was determined relative to β-actin transcript levels. **C)** Real time quantitative PCR analysis of Nedd4-2 and polycystin-2 upon Nedd4-2 depletion in IMCD cells and control siRNA treated cells. Expression was relative to β-actin transcript levels. Data represented as mean ± SEM for two independent experiments done in triplicates (*$P<0.05$, $P>0.05$, not significant (n.s), unpaired t-test was used to measure significance assuming equal variance. NC stands for negative control. KD stands for knock down).

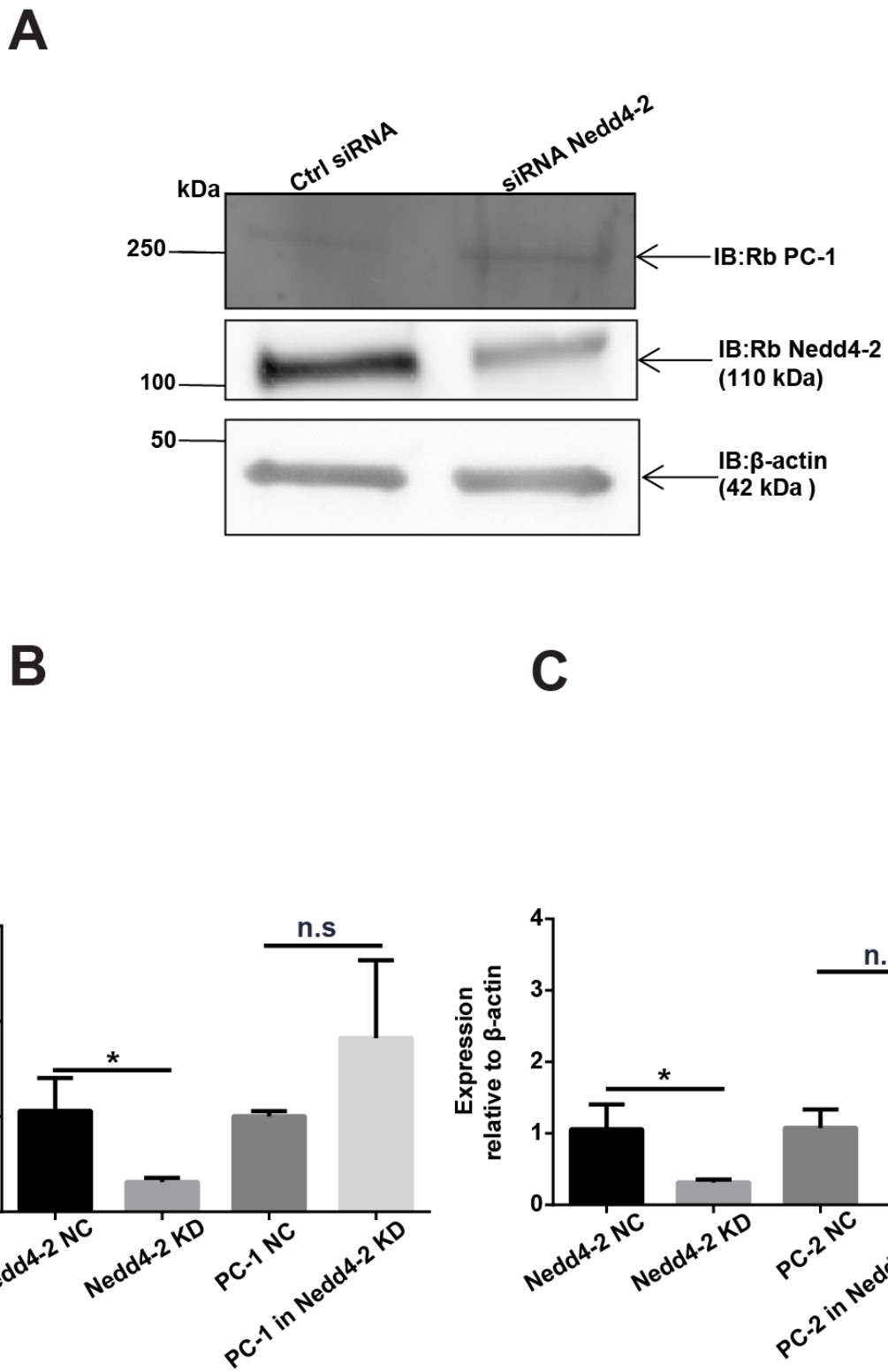
A
kDa
Ctrl siRNA
siRNA Nedd4-2
250
IB:Rb PC-1
100
IB:Rb Nedd4-2
(110 kDa)
50
IB:β-actin
(42 kDa)
B
Expression relative to β-actin
n.s
*
Nedd4-2 NC
Nedd4-2 KD
PC-1 NC
PC-1 in Nedd4-2 KD
C
Expression relative to β-actin
n.s
*
Nedd4-2 NC
Nedd4-2 KD
PC-2 NC
PC-2 in Nedd4-2 KD

Fig 3.10 Nedd4-2 mediated polycystin-1 ubiquitination is independent of polycystin-2. As indicated polycystin-1 construct (PC1-HA/Flag), Nedd4-2 constructs (Nedd4-2 Flag, or the catalytically inactive cysteine mutant Nedd4-2 Flag CM), polycystin-2 construct (PC2-Myc) and pcDNA 3.1 (control) constructs were transfected along with a tagged ubiquitin construct (Ub-HA) in HEK293T cells for 24 hours. After 24 hrs incubation, cells were treated for 4 hrs prior to lysis with MG132 and chloroquine to block proteasomal and lysosomal degradation. Inhibition of deubiquitination enzymes was carried out by the addition of NEM to the lysis buffer containing protease inhibitor cocktail**.** The cells were lysed and overnight incubated with rabbit polycystin-1 antibody for immunoprecipitation. Expression of respective constructs was measured using equal volumes of input lysates used for immunoprecipitation. The respective lysates eluted after immunoprecipitation were further immunoblotted and probed with anti-ubiquitin antibody. Input lysates were immunoblotted with tag specific antibodies for Nedd4-2, polycystin-1 and polycystin-2 as specified and β-actin was used as a loading control. This experiment was performed by **Dr. Kimberly Mackenzie**.

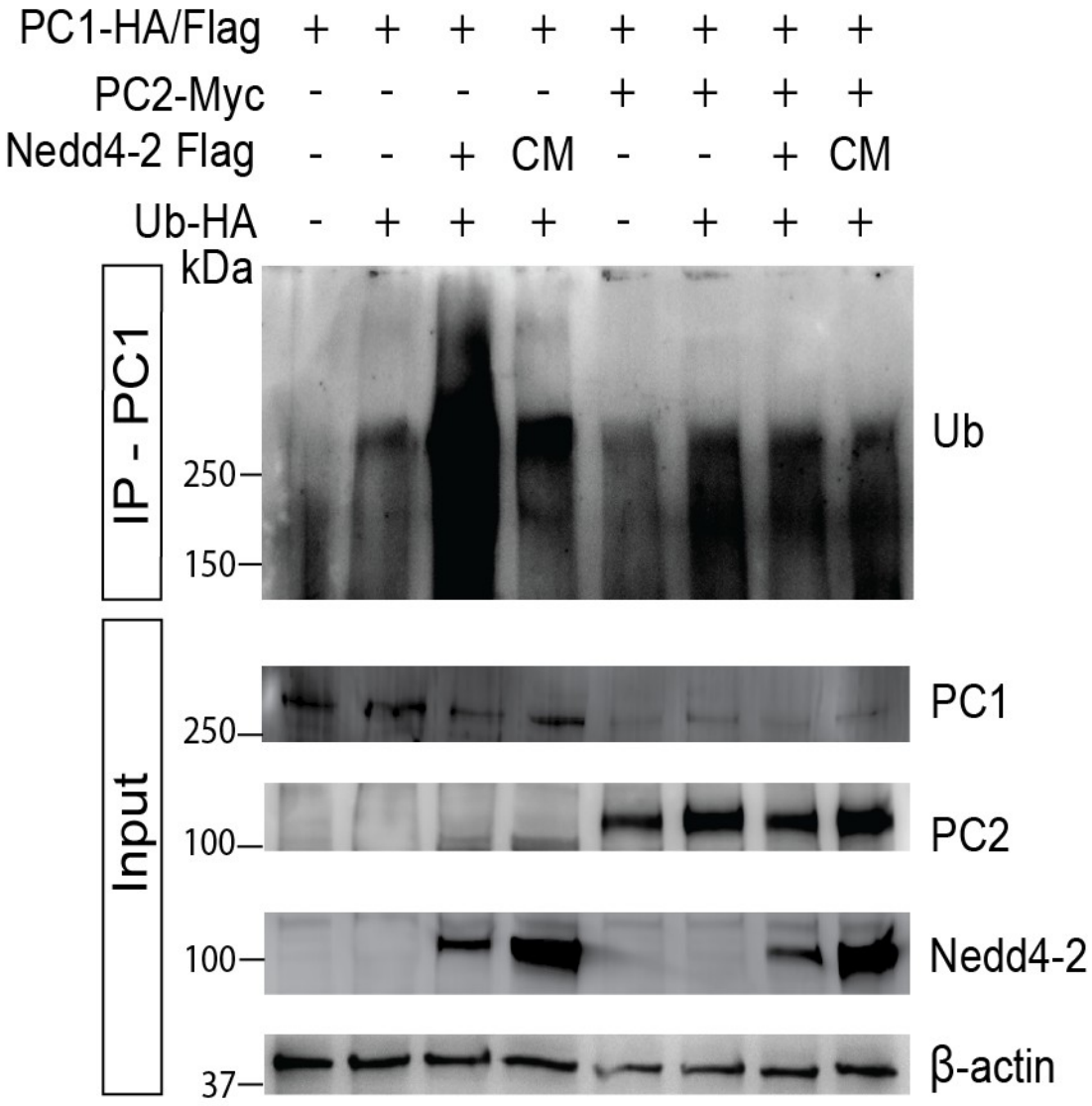
PC1-HA/Flag + + + + + + + +
PC2-Myc - - - - + + + +
Nedd4-2 Flag - - + CM - - + CM
Ub-HA - + + + - + + +
kDa
IP - PC1
250
150
Ub
Input
250
PC1
100
PC2
100
Nedd4-2
37
β-actin

Fig 3.11 Polycystin-1 over expression in *Nedd4-2*$^{-/-}$ kidneys. Polycystin-1 staining of P19 *Nedd4-2*$^{+/+}$ and P19 *Nedd4-2*$^{-/-}$ kidneys. Paraffin embedded (5µm) sections from P19 kidneys were incubated with antibody specific to polycystin-1 diluted in PBS. Primary antibody binding was detected using an Alexa flour 488 (Green) antibody and to detect cell nuclei staining with Hoechst 33342 (blue) prior to analysis on the LSM700 confocal microscope. Images **A**, **B** and **C** represent different regions within the P19 *Nedd4-2*$^{+/+}$ kidneys. Images **E**, **F** and **G** represent different regions within the P19 *Nedd4-2*$^{-/-}$ cystic kidneys. Images **D** and **H** represent secondary antibody control for P19 *Nedd4-2*$^{+/+}$ kidney and P19 *Nedd4-2*$^{-/-}$ cystic kidney respectively. The arrows indicate different regions within the nephron. CD indicates collecting duct and DCT indicates distal convoluted tubules. Scale bar = 50µm.

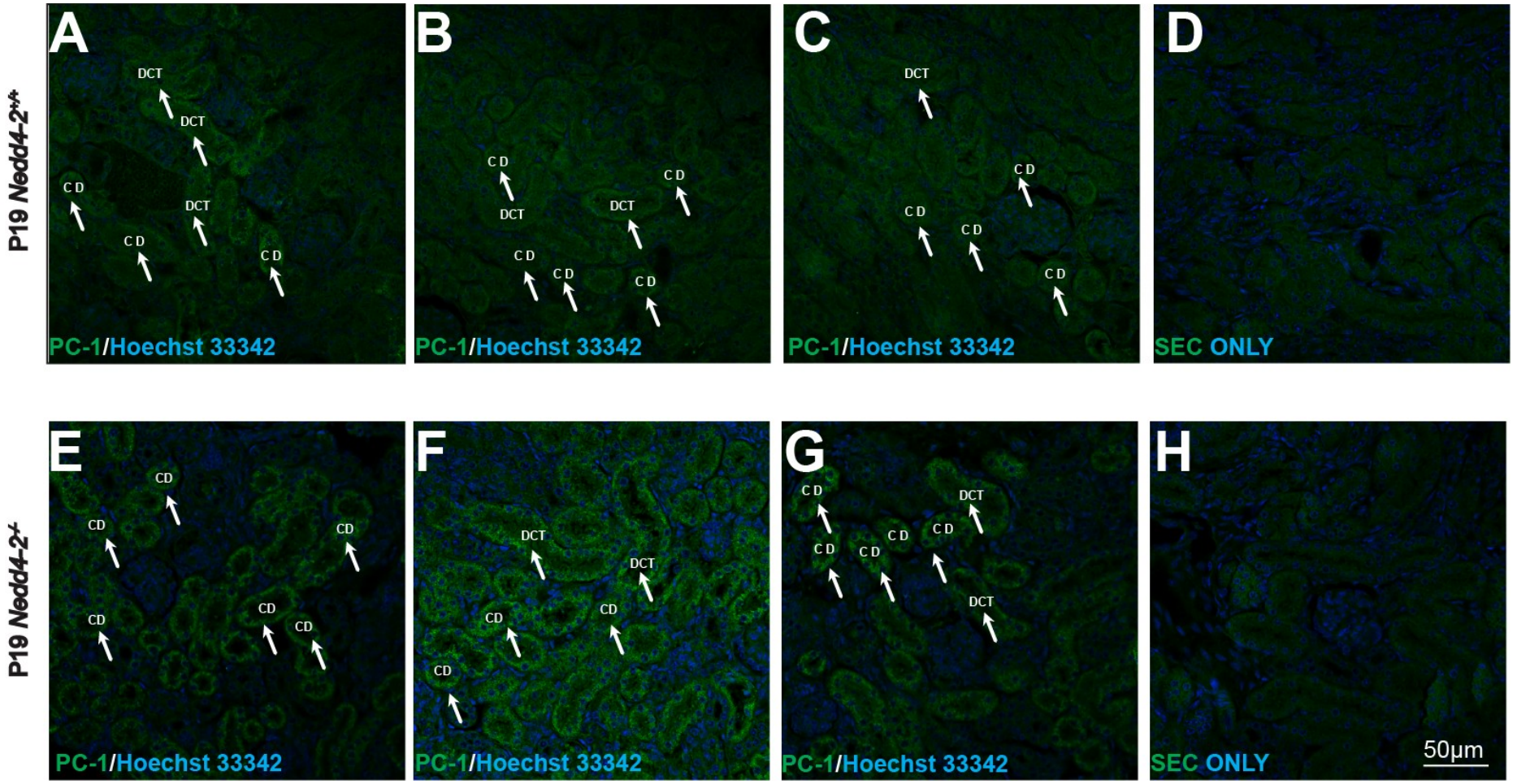
P19 Nedd4-2+/+
P19 Nedd4-2-/-
A
B
C
D
E
F
G
H
DCT
CD
PC-1/Hoechst 33342
SEC ONLY
50µm

3.4 Discussion

Polycystins play an integral role in maintaining renal structure and are necessary during kidney formation. Aberrant expressions of polycystins can lead to renal aberrations like renal cysts. Polycystins complex (PC-1/PC-2) steady state expression plays an important role in renal development (Van Adelsberg *et al*., 1997). Alteration in the expression and localisation of polycystin-1 and polycystin-2 has been previously reported in mouse models of renal cysts (Cai *et al*., 2014). Firstly to understand the role polycystins play in renal cyst development in the *Nedd4-2*$^{-/-}$ cystic kidneys, total protein expression and transcript levels in the *Nedd4-2*$^{-/-}$ cystic kidneys for both polycystin-1 and polycystin-2 were analysed. As reported earlier in **Fig 3.3** and **Fig 3.4,** the *Nedd4-2*$^{-/-}$ postnatal day 19 cystic kidneys show no significant difference in the transcript levels (via qPCR analysis) and protein levels (via Western analysis) of both polycystin-1 and polycystin-2 in comparison to wild-type. These results suggested that overall polycystin expression in the kidneys of these mice could not be regulated by Nedd4-2. However the kidneys are complex tissues with 25 different cell types and they are known to have dissimilar protein expression profile throughout the nephron for ion channels and membrane proteins (Piontek *et al*., 2007, Fedeles *et al*., 2011, Raphael *et al*., 2009). Since polycystin expression could be dependent on the expression profile of Nedd4-2 within the kidney nephron it became imperative to focus on the nephronal region specific cell types previously shown to express Nedd4-2. Previous work on understanding ENaC regulation, one of the first substrates of Nedd4-2, suggested increased expression of Nedd4-2 in the collecting duct and the distal nephrons (Loffing-Cueni *et al*., 2006). Therefore it was crucial to investigate expression and localisation of polycystins within these cell types. To aid in our understanding of localisation and trafficking of polycystin-1 and polcysytin-2, of crucial importance in understanding renal cyst development, kidney collecting duct cells were isolated from P19 *Nedd4-2*$^{-/-}$ mice (**Fig 3.5)** (Cai *et al*., 2014). Since these isolated

primary cells tended to undergo cell death after passaging rather than proliferation, the nephronal marker staining to characterise and distinguish their origin within the nephron was unclear due to inability to propagate the isolated kidney cells. To overcome this limitation mouse pyruvate kinase collecting duct cells (mpkCCD) were procured and used as a morphological control. As reported in **Fig 3.5** some of the kidney cortical collecting duct cells isolated showed similar morphological characteristics as stable mpkCCD cells, however there were other kidney cell types present. The isolated primary kidney cells from *Nedd4-2*$^{-/-}$ mice showed increased expression of polycystin-1 and polycystin-2 in comparison to wild-type, with majorly cytoplasmic distribution of polycystin-2 and increased expression of polycystin-1 on the membrane (**Fig 3.6)**. Concurrently to verify and validate the above results it was imperative to undertake a similar approach under stable conditions in an *in vitro* model system. To undertake this, inner medullary collecting duct cells showcasing similar channel properties as cortical collecting ducts were procured for validation of the above findings upon depletion of endogenously expressed Nedd4-2. Upon Nedd4-2 depletion in IMCD cells polycystin-1 expression around the plasma membrane was shown to increase (**Fig 3.7 F)** consistent with expression data in isolated primary *Nedd4-2*$^{-/-}$ kidney cells (**Fig 3.6 G** and **H**). However, polycystin-2 levels are decreased upon Nedd4-2 depletion in IMCD cells (**Fig 3.8 F),** contrary to the increased expression of polycystin-2 observed in isolated primary *Nedd4-2*$^{-/-}$ kidney cells (**Fig 3.6 K** and **L**). Previous studies on IMCD cells suggest endogenous polycystin-2 localisation to the plasma membrane, contrary to the predominant localisation around the endoplasmic reticulum shown in the canine kidney cells (Luo *et al*., 2003). This further highlights the controversies surrounding polycystin-2 localisation accrued in the field in comparison to polycystin-1 which is predominantly thought to be plasma membrane localised, with the activated C-terminal end localised to the endoplasmic reticulum for interaction with polycystin-2 before being trafficked to the membrane for its activated

channel conformation (Foggensteiner *et al*., 2000). The conflicting results seen in **Fig 3.6** and **Fig 3.8** could be attributed to the milieu of uncharacterised cells staining positive for both the polycystins in the primary kidney cell culture, and limitations faced in characterising these cell types comprehensively for nephronal origin.

To further confirm over expression of polycystin-1 in the absence of Nedd4-2, lysates from Nedd4-2 siRNA treated IMCD cells showed an increase in expression levels of polycystin-1(Cleaved product) (**Fig 3.9 A)**. There were no significant transcript changes for either polycystin-1 or polycystin-2 upon significant depletion of Nedd4-2 in IMCD cells (**Fig 3.9 B** and **C**). Since the unchanged gene transcription levels did not correlate to the increased expression levels of polycystin-1 in Nedd4-2 depleted IMCD cells (as ascertained from immunofluorescent analysis), the regulation of polycystin-1 could be post translational rather than post transcriptional. This is crucial to understanding the misregulation of polycystin-1/polycystin-2, reported to form a multimeric complex with alterations leading to renal cyst development (Grimm *et al*., 2003). Previous studies on polycystin-1 ubiquitination through the RING finger ubiquitin ligase Siah-1 had suggested Siah-1's role in mediating the protein degradation process of polycystin-1 through the ubiquitin-proteasome pathway via Siah-1 interaction dependent on the intracellular C-terminal region of polycystin-1. To ascertain whether Nedd4-2 is directly responsible for the regulation of polycystin-1 in IMCD cells it was necessary to demonstrate that polycystin-1 is indeed ubiquitinated by Nedd4-2 *in vitro,* and examine the affect polycystin-2 could have on the direct regulation of polycystin-1 mediated through Nedd4-2. The *in vitro* ubiquitination assay in **Fig 3.10** demonstrated that polycystin-1 could be directly ubiquitinated by Nedd4-2, and that this ubiquitination did not occur in the presence of catalytically inactive Nedd4-2. To further elaborate the role polycystin-2 could be playing in this ubiquitination, in the presence and absence of both active/inactive form of Nedd4-2 there is complete abrogation of polycystin-1 ubiquitination

in the presence of polycystin-2. This indicated that Nedd4-2 could aid in polycystin-1 ubiquitination via its sequestration which could be independent of its interaction with polycystin-2 on the membrane. Since there are predicted non canonical proline rich motifs in the C-terminal end of polycystin-1 (**Fig 3.2 A**), it could be predicted that Nedd4-2 binds to polycystin-1 via this domain, which is supported by **Fig 3.9.** This protein-protein interaction could be dependent on a threshold model with increased levels of polycystin-2 translocation, affecting the binding between Nedd4-2 and polycystin-1 which could be hindered, stabilising this interaction on the membrane could aid in an open channel activity, again dosage dependent for both polycystin-1 and polycystin-2 (Xu *et al*., 2015). This data further validates the importance of both polycystin-1 and polycystin-2 in complex formation and any disturbance in the stoichiometry of these two proteins alter the stability in binding of these proteins (Giamarchi *et al*., 2010). Interestingly recent reports suggested that polycystin-1 membrane localisation was inhibited upon addition of polycystin-2, affecting the C-terminal site of PKA phosphorylation necessary for plasma membrane localisation and stability of polycystin-1 (Xu *et al*., 2015). This binding between polycystin-1 and polycystin-2 is aided through polycystin-2 forming an oligomer through its coiled coiled domains and sequestering interaction with polycystin-1 C-terminal region (Giamarchi *et al*., 2010). From data presented here it could be suggested that the binding of polycystin-1 with polycystin-2 and Nedd4-2 could be competitive, and the stabilization of polycystin-1 on the membrane could aid in binding with polycystin-2 for channel activity, though Nedd4-2 interaction could lead to its lysosomal or proteasomal degradation which still remains to be validated.

To further ascertain the physiological relevance in context to our previous findings, it became imperative to evaluate polycystin-1 localisation within the *Nedd4-2*$^{-/-}$ kidneys. Previous reports had suggested that both polycystin-1 and Nedd4-2 are highly expressed in the collecting ducts and the early parts of the distal nephrons (Foggensteiner *et al*., 2000,

Loffing-Cueni *et al*., 2006). Therefore, as reported earlier in **Fig 3.11 E**, **F** and **G,** the expression of polycystin-1 is seen to be increased in the collecting ducts and the distal convoluted tubules in *Nedd4-2*$^{-/-}$ kidneys in comparison to *Nedd4-2*$^{+/+}$ control littermates. As reported in Chapter **2 Fig 2.2,** cysts in the *Nedd4-2*$^{-/-}$ kidneys are variable, and cysts arise from different parts in the cortex and medulla, specifically from the collecting duct. This further highlights the crucial role Nedd4-2 could be playing in renal cyst growth by regulating the localisation of polycystin-1 in the *Nedd4-2*$^{-/-}$ kidneys. These results are also consistent with the findings from chapter-2 where collagen-1 was seen to be up regulated in renal cystic tissues in the *Nedd4-2*$^{-/-}$ mice (**Fig 2.9)**. Previous published reports have highlighted the importance of the polycystin-1 extracellular domain in interaction with extracellular matrix proteins (Malhas *et al*., 2002). These further increased the validity of our findings where Nedd4-2 plays a crucial role in ubiquitinating polycystin-1. However further work needs to be performed to identify the specific region of interaction mediated between polycystin-1 and Nedd4-2 that leads to its sub cellular trafficking, and either aids in its internalisation/ degradation. In the future, it needs to be ascertained *in vivo* whether suggesting mis-localisation of polycystin-1 could be further validated physiologically by undertaking co-localisation studies in *Nedd4-2*$^{-/-}$ mice with both polycystin-1 and polycystin-2 specific robust antibodies targeting specific regions involved in their interaction. Since previous reports in other models of renal cysts suggest not all the cysts stain positive for both polycystin-1 and polycystin-2, and cyst progression is dependent upon the tissue expression pattern and cell type, corroborated from studies conducted in human patients suffering from renal cysts with variability of polycystin expression (Foggensteiner *et al*., 2000, Yoder *et al*., 2002).

In conclusion this study highlights the novel role Nedd4-2 plays in regulating polycystin-1 via ubiquitination, and provides the first physiological evidence of role for Nedd4-2 in renal

cyst formation. It also aids in our better understanding of polycystins regulation in the kidneys, since polycystin-1 is known to aid in cell matrix and cell-cell adhesion on the membrane for kidney structure maintenance. To elucidate the downstream signalling pathways aided by the up-regulation of polycystin-1, and simultaneously aid in our understanding of differential changes in gene transcriptional profiles associated with renal dysplasia, differential gene expression studies were further undertaken as detailed in chapter 4.

Chapter 4:

Differential gene expression of *Nedd4-2*$^{-/-}$ kidneys

Statement of Authorship

Title of Paper	Differential gene expression of *Nedd4-2*$^{-/-}$ kidneys
Publication Status	☐ Published ☐ Accepted for Publication ☐ Submitted for Publication ☑ Unpublished and Unsubmitted work written in manuscript style
Publication Details	

Principal Author

Name of Principal Author (Candidate)	Pranay Goel
Contribution to the Paper	Wrote the manuscript, edited the manuscript, evaluated the data , made figures, experimental design Note: work included in this thesis has been solely done by me and the experiments otherwise have been duly acknowledged.
Overall percentage (%)	90%
Certification:	This paper reports on original research I conducted during the period of my Higher Degree by Research candidature and is not subject to any obligations or contractual agreements with a third party that would constrain its inclusion in this thesis. I am the primary author of this paper.
Signature	Date 2/12/15

Co-Author Contributions

By signing the Statement of Authorship, each author certifies that:

i. the candidate's stated contribution to the publication is accurate (as detailed above);

ii. permission is granted for the candidate in include the publication in the thesis; and

iii. the sum of all co-author contributions is equal to 100% less the candidate's stated contribution.

Name of Co-Author			
Contribution to the Paper			
Signature		Date	

Name of Co-Author	Prof.Sharad Kumar
Contribution to the Paper	Supervised development of work,, experimental design, co-wrote the manuscript
Signature	Date 2.12.15

Please cut and paste additional co-author panels here as required.

Chapter 4: Differential gene expression of *Nedd4-2*$^{-/-}$ kidneys

4.1 Introduction

Renal dysplasia is a severe developmental disorder of the kidneys associated with renal obstruction and urological developmental phenotypes (Ichikawa *et al*., 2002, Loirat, 2001). Patients suffering from renal dysplastic hereditary syndromes are caused by genetic defects as reported in cases affected by mutations in SAL-like 1 (SALL1) in Towns Brock syndrome, glypican-3 in Simpson Golabi Behmel syndrome and AGTR2 in CAKUT(Congential anomalies of the kidney and urinary tract) (Kohlhase *et al*., 1998, Nishimura *et al*., 1999, Pilia *et al*., 1996). Recent studies point to the involvement of transcription factors in renal development to cause renal dysplasia, and patients with mutations in Paired box gene-2 (PAX-2) have all been reported to suffer from renal dysplasia (Porteous *et al*., 2000). Transcription factor-2 (TCF-2), eyes absent 1 (EYA1) or sineoculis homeobox 1 (Six1) gene mutations in patients have also been associated with renal dysplastic kidneys (Weber *et al*., 2006). Renal development and renal abnormalities are well studied in animal models in which disruption of genes like Wilms tumor 1 (WT1), Pax-2, glial cell line derived neurotrophic factor (GDNF), angiotensin receptor 1 (AT1R), glypican-3 (GPC-3), wingless gene 4 (WNT4) and bone morphogenetic protein (BMP-4, 7) have all been shown to cause renal agenesis, hydronephrosis or dysplastic kidneys (Lipschutz, 1998, Jain *et al*., 2006, Woolf *et al*., 2004). Kidneys in renal dysplasia have a common histology suggesting a mechanism universal to renal dysplasia pathogenesis (Woolf *et al*., 2004, Liapis, 2003).

The disease itself is driven whether diagnosed after birth or in embryonic developmental stages by kidney transcriptional changes during development (Singer, 1991, Woolf *et al*., 2004, Liapis *et al*., 2002). However the molecular processes are not very well characterised, due to the limited human tissue samples from kidneys of affected patients, and the variability found in mouse models of kidney dysplasia (Jain *et al*., 2007). The mammalian kidneys are complex, with 25 distinct cell lineages based on function of cell types (Saxén and Sariola,

1987, Al-Awqati and Oliver, 2002). Kidneys grow rapidly during embryogenesis and early post natal stages, but this decreases as the organism reaches adulthood (Chang *et al*., 2008). Embryonically the kidney metabolic waste is excreted out from foetus through maternal circulation, but after birth this process is taken over by the neonatal kidney for excretion of nitrogenous waste, maintenance of electrolytes and fluid regulation (Chang *et al*., 2008). During embryonic development kidneys undergo differential changes in gene expression patterns for developmental processes (Chang *et al*., 2008). Transgenic mice have previously been used to identify key regulatory pathways in urinary tract development like GDNF, Ret and GFRA1 for ureter induction, Wnt 9b and Wnt 4 for nephrogenesis and DLL1, LIM1 and BRN1 for nephron patterning (Costantini and Shakya, 2006, Basson *et al*., 2005, Stark *et al*., 1994, Kispert *et al*., 1998, Carroll *et al*., 2005, Grieshammer *et al*., 2005, Kobayashi *et al*., 2005). Microarrays have been used to understand gene expression changes for kidney development in mouse and rat models (Stuart *et al*., 2001, Schwab *et al*., 2003, Challen *et al*., 2005). These provide good evidence for our understanding of early kidney development, though post natal kidney development has not been very well characterised in context of studies in renal dysplasia other than to understand transcriptional changes in normal post natal kidneys (Wu *et al*., 2013). Also of importance is gene expression patterns for kidney organogenesis and function, again not very well characterised (Wu *et al*., 2013). To enhance our understanding of neonatal renal development and link it to renal diseases such as renal dysplasia, and given the availability of next generation sequencing platforms it was imperative to undertake gene expression profiling of *Nedd4-2*$^{-/-}$ dysplastic kidneys post natally. Nedd4-2, a HECT domain ligase has previously been reported to affect transporter and ion channel protein levels. Given the novel phenotype in kidney of *Nedd4-2*$^{-/-}$ mice, it became important to integrate novel techniques to understand the role Nedd4-2 plays in renal disorder, associated with transcriptional changes of genes involved in kidney development, as

previously reported. To evaluate and understand this transcriptional signature upon Nedd4-2 depletion, this study was undertaken at the transcriptional level in post natal *Nedd4-2*$^{-/-}$ dysplastic kidneys. The initial hypothesis underlying this study was to confirm the involvement of genes previously reported to be involved in kidney dysplasia, and also extract some of the other novel genetic changes not reported previously which could aid in our understanding of renal dysplasia. This study highlights the transcriptional changes in *Nedd4-2*$^{-/-}$ kidneys and elucidates some of the major novel pathways involved in the development of kidney dysplasia. This is highly important in renal pathology for disease diagnosis, with the affects aiding in understanding the disease mechanism of kidney dysplasia.

4.2 Materials and methods

4.2.1 *Nedd4-2*$^{-/-}$ mouse colony breeding

As mentioned in Section 2.2.1

4.2.2 Total RNA isolation from kidneys

As mentioned in section 2.2.10, RNA isolation was performed from whole kidneys. The quality of RNA was analysed using Agilent 2100 Bioanalyser (Agilent technologies, USA).

4.2.3 RNA library preparation

Single end reads of 51bp (base coverage of the cDNA sequence) were sequenced on a HiSeq 2500 at the Centre for Cancer Biology, Australian Cancer Research Foundation and Cancer Genomics Facility using the New England Biolabs (NEB) Stranded RNA library preparation kit according to manufacturer's instructions (NEB). With the exception of the fragmentation step as per manufacturer's protocol and 1µg of starting total RNA input was used for RNA library preparation.

4.2.4 Bioinformatics analysis for differential gene expression

Reads (cDNA fragments) were trimmed for the NEB adapter

AGATCGGAAGAGCACACGTCTGAACTCCAGTCAC

Using Cutadaptv1.3 with an error rate of 20%, overlap of 2 bases, and discarding reads of shorter than 18nt and quality below 28. Reads were mapped to the UCSC mm10 mouse genome using Top Hat v2.0.9 with default parameters except for enabling strandedness: library-type=fr-firststrand.

Gene counts were obtained with HTSeq-count v0.5.3p9 using the UCSC mm10 genes.gtf. Differential expression was calculated with both edgeR v3.0.8 (using limma 3.14.4) and Cuffdiff v2.1.1.

(Martin, 2011, Kim *et al*., 2013, Anders *et al*., 2014, Robinson *et al*., 2010, Trapnell *et al*., 2013).Differential expression results per gene were combined from Cuffdiff and EdgeR and genes that were identified as significantly differentially expressed after adjusting for multiple testing by both programs were considered for further analysis and verification. For EdgeR, this was the False Discovery Rate ≤ 0.05 and for Cuffdiff the q_value column being ≤ 0.05.

4.2.5 Generation of heat map for differential gene expression

Heat maps were prepared for genes significantly differentially expressed with fold change ≥ 0 and ≥ 2 using R script with add on software packages colour brewer and pheatmap for visualization.

4.2.6 Singular value decomposition (SVD) plot

The singular value decomposition (SVD) plot was obtained by uploading the raw gene counts to BioGraphServ (http://biographserv.com). This removes low/no expression genes-removing genes where no sample has $\geq 0.1\%$ of total reads in that sample. Counts are normalized to reads per million, converted to natural log then passed to the SVD function in the Numpy Linear Algebra library (Jones *et al*., 2014).

4.2.7 Venn diagram

Differentially expressed genes significantly up-regulated and down-regulated were represented as Venn diagrams using Biovenn (http://www.cmbi.ru.nl/cdd/biovenn/) online software. Ingenuity pathway analysis (Ingenuity® Systems, www.ingenuity.com, Qiagen) software was used for making Venn diagrams for representation of genes specifically involved in the kidney disease and function.

4.2.8 Database for Annotation, Visualization and Integrated Discovery (DAVID) analysis

The Database for Annotation, Visualization and Integrated Discovery (DAVID) (https://david.ncifcrf.gov) bioinformatics resource was used to obtain enriched pathways from Enrichment of Kyoto Encyclopaedia of Genes and Genomes (KEGG). For the current analysis genes greater than $\log_2$ fold >1.1 (increased) or $\log_2$ fold <0.9 (decreased) showing 10% fold change were used. With pathways selected based on FDR (False Discovery Rate) p-values ≤0.05. Completed sequenced gene list from the sequencing data was used as background for enrichment. The DAVID software was also used for Gene Ontology (GO) to identify genes in biological processes, molecular function and cellular component enrichment.

4.2.9 Ingenuity pathway analysis

Ingenuity pathway analysis (IPA) (Ingenuity® Systems, www.ingenuity.com, Qiagen) was used for differentially expressed gene annotation. The software was used for identifying differentially expressed genes up-regulated and down-regulated in the kidney using mouse refseq Id's as input. The genes involved in kidney disease and function pathways were also generated using the software. For input analysis gene list including significantly expressed gene list were uploaded with log ratio≥1, p value≤0.05, False discovery rate<0.01, using benjamini-hochberg multiple testing correction p-values for pathway analysis.

4.2.10 Transcription factor regulation

The TFactS (www.tfacts.org) Transcription factor database, accumulated from published literature and other data sources (Essaghir *et al*., 2010), was used to understand transcription signatures of genes and their target genes in the database.

4.2.11 Quantitative real time PCR for validation

The RNA isolation and cDNA preparation for quantitative real time PCR was performed from fresh kidney samples as described in **section 2.2.10**.

Table 4.1 List of primer sets used for validation of genes identified by RNA sequencing

Gene	Forward primer (5'-3')	Reverse primer (5'-3')
β-actin	GATCATTGCTCCTCCTGAGC	AGTCCGCCTAGAAGCATTTG
Col1a1	CAGACGTGCTTCTTTTCCTTGG	TGACTGGAAGAG-CGGAGAGTACT
TGFβ$_1$	TAAAGAGGTCACCCGCGTGCTAAT	ACTGCTTCCCGAATGTCTGACGTA
ADAM23	TATGAGCAGCTGTCCACTCG	CCCCAGCCTGTGCCCCCAAG
HB-EGF	TTT GGA GAG TCC TTT GCA GA-	TGT GAC AAT GAG ATT CCT TGT
FGA	TGTGGAGAGACATCAGAGTCAATG	CGTCAATCAACCCTTTCATCC
ITGAM	ATGGACGCTGATGGCAATACC	TCCCCATTCACGTCTCCCA
ICAM-1	CAACTGGAAGCTGTTTGAGCTG	GTGTTCACAGTCTTGC TCCAT
BMP-1	CGCCTGTGCTGGTATGACTA	ACGTGGAAACCCTCAGACAC

4.2.12 Statistical analysis

Statistical analyses were performed for quantitative real time PCR using Graphpad Prism (v6) and Microsoft® Excel. Statistical significance determined as $P \leq 0.05$, using unpaired T-test assuming equal variance. For evaluation of DAVID KEGG pathway analysis and Ingenuity pathway analysis, statistical significance was determined using Benjamini correction (Number of false discoveries rejected to validate findings, based on the null hypothesis correction) with values ≤ 0.05 considered significant.

4.3 Results

4.3.1 Gene expression variability in the *Nedd4-2*$^{-/-}$ kidneys

Firstly to understand the differential gene expression between *Nedd4-2*$^{+/+}$ and *Nedd4-2*$^{-/-}$, whole kidney tissue RNA extracts were analysed on a bioanalyser for RNA integrity and the samples with the best qualitative assessment were selected for further analysis. The RNA samples selected were run on a HiSeq 2500 sequencer after 51bp single end reads NEB stranded library preparation. The sequenced samples were then extracted for gene expression using Cuffdiff and edgeR as described in **Section 4.2.4.** The extracted genes with gene counts from the gene library were used to prepare a list of significant genes that were then input into BioGraphServ for preparation of a SVD plot to understand the gene expression variation in the samples between the cohorts of *Nedd4-2*$^{+/+}$ and *Nedd4-2*$^{-/-}$. As seen in **Fig 4.1,** there is more variability observed in *Nedd4-2*$^{-/-}$ samples (KO, N=7) in comparison to *Nedd4-2*$^{+/+}$ (WT, N=5), which shows closer resemblance between the WT group. This could be attributed to the differences seen in the severity of the *Nedd4-2*$^{-/-}$ kidney phenotype in comparison to their WT littermates. The *Nedd4-2*$^{-/-}$ kidney samples selected to take into account this variability were selected at the same post natal day ages for gene expression studies.

4.3.2 Renal genes involved in kidney disease and function

To further understand the differential gene expression between the *Nedd4-2*$^{+/+}$ and *Nedd4-2*$^{-/-}$ samples all the significant listed genes were annotated using ingenuity pathway analysis software and then input into the R script software for preparation of heat maps. To analyse the hierarchical clustering pattern between genes and understand the variability in between the samples as seen through the colour codes by level of log fold expression change, with an increased expression marked in red and the decreased expression marked in green heat maps of significant differentially expressed genes with fold change >0 and >2 were prepared. **Supplementary Fig 1** summarises the data set obtained through cuffdiff and edgeR software of differential gene expression between *Nedd4-2*$^{+/+}$ and *Nedd4-2*$^{-/-}$ at postnatal day 19. In the *Nedd4-2*$^{-/-}$ kidney samples, 167 genes were significantly down-regulated (fold change > 0 and p-value < 0.05) as shown in green, and 370 genes were significantly up-regulated (fold change > 0 and p-value < 0.05) as shown in red**.** To further ascertain the variability between the sample patterns of expressed genes, those that were considered significantly different with a greater than 2 fold change were analysed. A hierarchically clustered heat map between the *Nedd4-2*$^{-/-}$ and *Nedd4-2*$^{+/+}$ kidneys (prepared using Supplementary Table **1**) highlights the differential pattern of the same genes between the *Nedd4-2*$^{-/-}$ and *Nedd4-2*$^{+/+}$ (**Fig 4.2**). There are two sets of differentially expressed gene sets as shown from the hierarchical clustering in **Fig 4.2,** with one gene set significantly up-regulated in the *Nedd4-2*$^{-/-}$ and the other significantly down-regulated in the *Nedd4-2*$^{-/-}$ kidney, highlighting the variable pattern of expression between the WT and KO, as well as the variability in between the *Nedd4-2*$^{-/-}$ samples in comparison to the WT. This data further validates the studies undertaken in **Chapter 2**, highlighting the phenotypic variation differences seen between the same genotype only in the case of *Nedd4-2*$^{-/-}$.

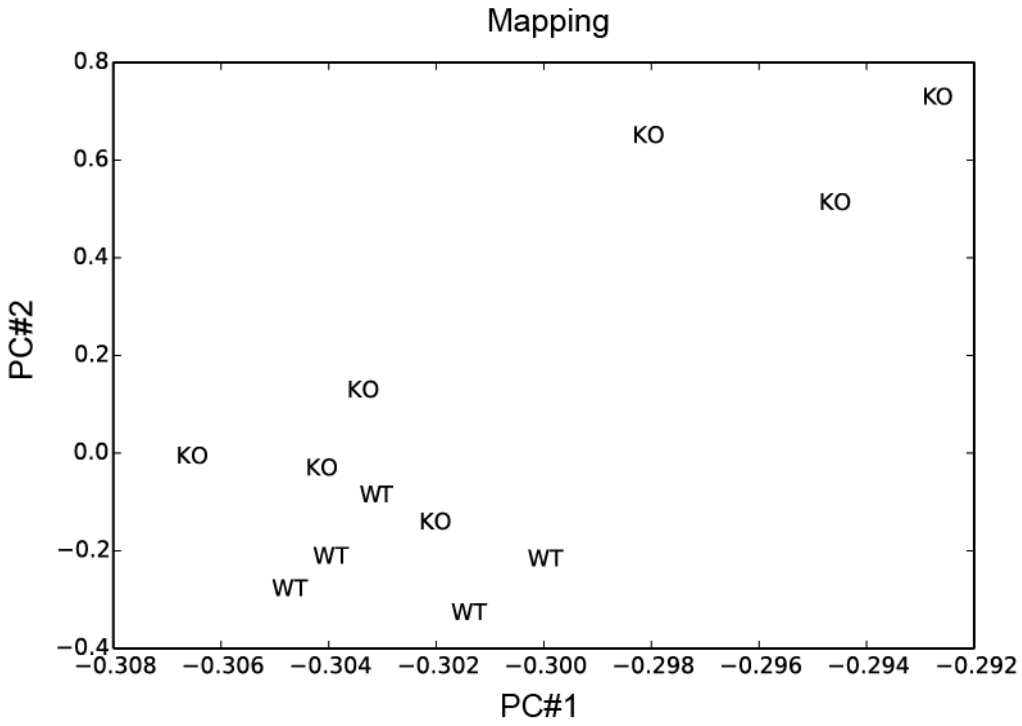

Fig 4.1 SVD plotting for differentially expressed genes in *Nedd4-2*$^{+/+}$ and *Nedd4-2*$^{-/-}$ kidneys. The plot shows variability in the gene expression from kidneys (FDR (False discovery rate) p-value <0.05) in *Nedd4-2*$^{-/-}$ (N=7) versus *Nedd4-2*$^{+/+}$ (N=5). KO in plot indicates *Nedd4-2*$^{-/-}$ (N=7) kidney gene expression, and WT indicates *Nedd4-2*$^{+/+}$ (N=5) kidney gene expression. The plot is designed against two dimensional gene components using natural log of genes with Numpy linear algebra library as shown by PC#1on X axis and PC#2 on Y axis (made using Supplementary Table **1**).

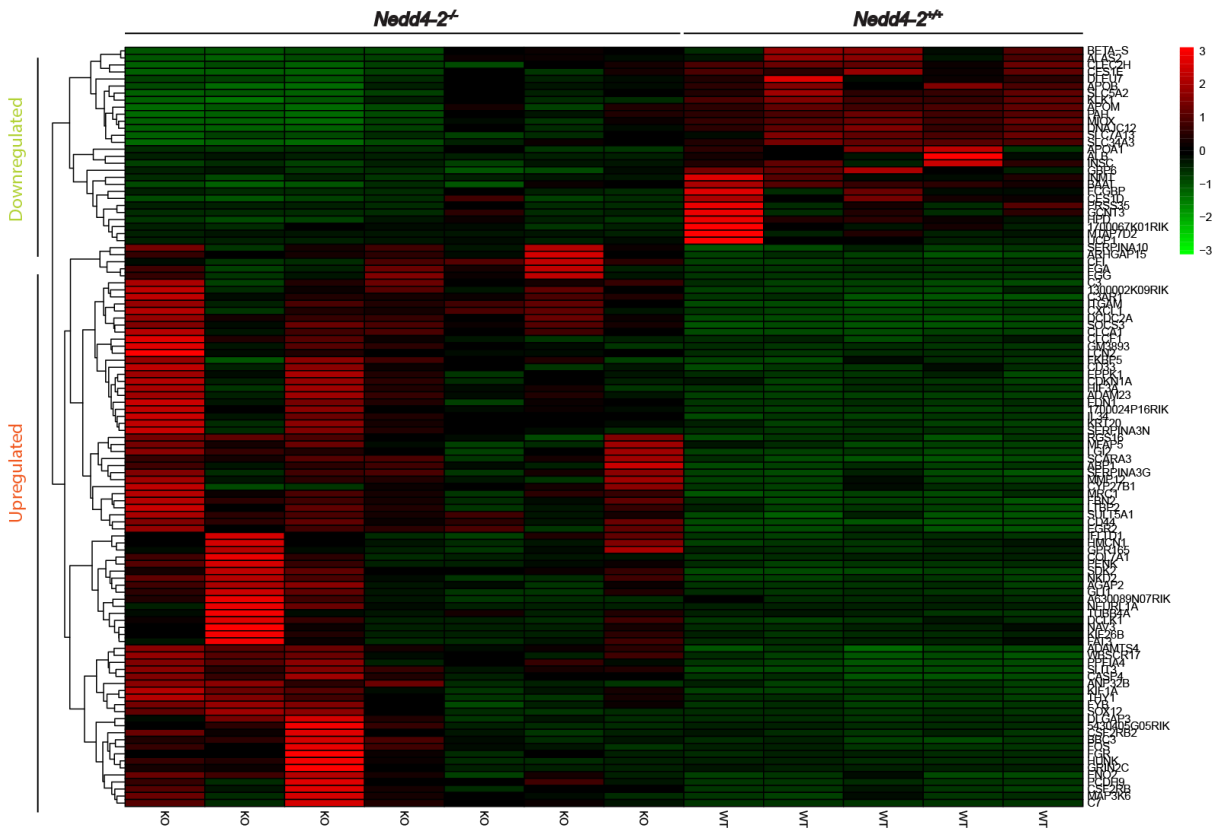

Fig 4.2 Hierarchical clustering of differentially expressed genes in *Nedd4-2*$^{-/-}$ kidneys. Heat map shows Log_2 expression mean of > 2 fold change of significantly differentially expressed genes (FDR (False discovery rate) p-value <0.05) in *Nedd4-2*$^{-/-}$ (N=7, KO) versus *Nedd4-2*$^{+/+}$ (N=5, WT) kidneys. Red in heat map indicates up-regulated expression and green indicates down-regulated expression. Unannotated genes are indicated by their refseq numbers. The red pattern in the KO shows increased variability among samples as compared to WT. On the right is indicated colour code for green to red for increased gene fold change expression values. Genes differentially regulated are written next to the respective lane on the right (made using data from Supplementary Table **1**).

To further investigate our initial aim of identifying genes differentially expressed in the dysplastic kidneys and understand the differential pattern of gene expression in *Nedd4-2*$^{-/-}$, it was imperative to understand the overlap of genes expressed within the kidney involved in disease and their functions, where either up regulation or down regulation could result in the *Nedd4-2*$^{-/-}$ dysplastic kidneys. Ingenuity pathway analysis software was predominantly used for this study as it is a database of genes obtained through experimental and published research highlighting the latest findings in diagnostics, with research undertaken to validate *in vitro* studies (Werner, 2008). **Fig 4.3A** summarises in a Venn diagram the number of genes with a significant fold change > 0, with significance observed with p-value <0.05. There is no overlap between the up-regulated and the down-regulated gene sets highlighting the robustness of the obtained dataset for further analysis. The significant gene sets were further input into ingenuity pathway analysis (Supplementary Table **1**) and a separate gene set of renal genes differentially expressed in the kidneys involved in disease and their functions were obtained (Supplementary Table**s 5** and **6**). As seen in **Fig 4.3B**, there were 39 (blue) significantly differentially expressed genes involved in the kidney in comparison to the whole data set of 509 annotated genes obtained through ingenuity pathway analysis software with fold change > 0. **Fig 4.3C** Venn diagram further highlights the important 11 (blue) significantly down-regulated genes obtained from the whole data set with fold change > 0 to be involved in the kidney phenotype (Supplementary Table **6**). 29 (blue) significantly up-regulated renal genes involved in kidney disease and function were identified (**Fig 4.3D)**; with one of the renal genes not involved in the annotated list but obtained through the significant gene list (Supplementary Table **5**). To understand the overlap between the genes listed in both up-regulated and down-regulated renal gene lists involved in disease and function both the separated lists were input as shown in **Fig 4.3E** Venn diagram, highlighting no overlap between the significant genes involved in kidney disease and function showcasing

the robustness of the obtained analysis. The importance of these genes in context of disease and function will be further discussed in **Fig 4.8 - 4.13**.

4.3.3 DAVID pathway analysis in *Nedd4-2*$^{-/-}$ Kidneys

To understand the canonical pathways which are significantly affected in the *Nedd4-2*$^{-/-}$ dysplastic kidneys, the DAVID online database was utilised (Dennis Jr *et al*., 2003). The database is a visual tool for annotation, integrated with visualisation of significant pathways using the KEGG (Kyoto Encyclopaedia for Genes and Genomes) database as a graphical model of current knowledge of manually curated biological networks (Zhang and Wiemann, 2009). This software also integrates gene ontology (GO), a database attributing functional representation across different species of genes and gene products with enrichment analysis obtained through experimental data giving functional interpretation (Ashburner *et al*., 2000, Consortium, 2004). The ontology of the gene and its product properties could be further subdivided into the cellular component, identifying where the availability of the gene product is within the cellular parts and also in terms of its extracellular environment (Consortium, 2004, Ashburner *et al*., 2000). The molecular function defines the gene product elemental properties at a molecular level stating its binding and role in catalysis, and the biological processes specifies the role of molecular events undertaken in the functioning of a living cell, tissue, organ and organism as an integrated event from start to end (Consortium, 2004, Ashburner *et al*., 2000).

KEGG pathways significantly up-regulated and down-regulated in *Nedd4-2*$^{-/-}$ kidneys using DAVID were obtained using genes with $\log_2$ fold change >1.1 (increased) or $\log_2$ fold change <0.9 (decreased) showing 10 % percent fold change (**Fig 4.4A** and **B)**. **Fig 4.4A** (Benjamini corrected p-value<0.05, black dashed line) summarises the major pathways up-regulated in *Nedd4-2*$^{-/-}$ dysplastic kidneys, highlighting genes listed in Supplementary Table **2A** in each individual process**.** The significant genes up-regulated in *Nedd4-2*$^{-/-}$ kidneys are involved in

pathways like complement and coagulation cascades, JAK-STAT signalling, chemokine signalling, focal adhesion, extracellular matrix interaction, MAPK signalling pathway, ErbB signalling pathway, calcium signalling pathway, cell adhesion molecules, Wnt signalling pathway, phosphoinositol signalling, Gap junction, axonal guidance, cell-cell communication, Toll like receptor signalling, mTOR signalling, vascular smooth muscle contraction, TGF beta signalling and the cell cycle. Some of the up-regulated pathways involved in prostate cancer, melanoma, glioma, colorectal cancer, small cell lung cancer, acute myeloid leukaemia, chronic myeloid leukaemia, prion diseases and endometrial cancer show up due to the overlap in expression of up-regulated genes like phosphatidylinositol-4,5-bisphosphate 3- kinase catalytic subunit Δ (PIK3CD), phosphoinositide-3-kinase regulatory subunit 5 (PIK3R5), phospholipase C β2 (PLCB2) kinases involved in cancer along with transcription factors like MYC (Liu *et al*., 2009, Katso *et al*., 2001, Dang *et al*., 2009).

The major pathways down-regulated in *Nedd4-2*$^{-/-}$ dysplastic kidneys are summarised in **Fig 4.4B** (Benjamini corrected p-value<0.05, black dashed line), highlighting genes listed in Supplementary Table **2B** in each individual process**.** Some of the significantly down-regulated pathways associated with amino acid metabolism like tryptophan, glycine, serine, threonine along with glutathione metabolism and glycolysis/gluconeogenesis highlight a possible role in mitochondrial dysfunctioning leading to metabolic disorders which could be driven by PPaR signalling upstream (significantly down-regulated in *Nedd4-2*$^{-/-}$ kidneys), a potential driver of downstream amino acid metabolism (Kersten *et al*., 2001, Liang and Ward, 2006, Rolo and Palmeira, 2006).

Fig 4.3 Venn diagram of differential expressed genes in *Nedd4-2*$^{+/+}$ and *Nedd4-2*$^{-/-}$ kidneys. Venn diagrams show Log_2expression mean of > 0 fold change of significantly differentially expressed genes (FDR (False Discovery Rate) p-value <0.05) in *Nedd4-2*$^{-/-}$ (N=7) versus *Nedd4-2*$^{+/+}$ (N=5) kidneys. **A)** Dataset in red in Venn diagram indicates up-regulated (370) expression and green dataset indicates down-regulated (167) expression in fold change ≥ 0 made through Biovenn. **B)** Genes annotated through ingenuity software with significant data set A (509, all differential genes annotated through IPA (Ingenuity pathway analysis)) vs genes regulated in the kidney significant data set B (39, differential expressed genes in kidney). Overlap shown in blue is intersection between two datasets. **C)** Genes annotated through ingenuity software with significant data set A (509, all differential genes annotated through IPA) vs significant genes down-regulated in the kidney data set B (11, differential down-regulated genes in kidney). Overlap shown in blue is intersection between two datasets. **D)** Genes annotated through ingenuity software with significant data set A (509, all differential genes annotated through IPA) vs significant genes up-regulated in the kidney data set B (30, differential up-regulated in kidney). Overlap shown in blue is intersection between two datasets. **E)** Genes annotated through ingenuity software with significant genes up-regulated in the kidney data set A (30, differential up-regulated genes in kidney) vs significant genes down-regulated in the kidney data set (11, differential down-regulated genes in kidney). Overlap shown in blue is intersection between two datasets. The following genes involved in the analysis are denoted in Supplementary Table **1.**

A

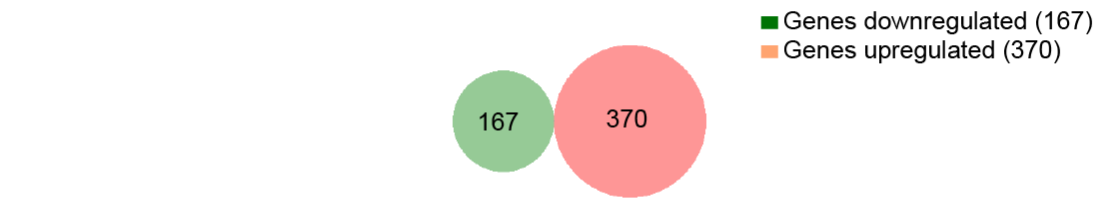
Number of genes differentially regulated in kidney
Genes downregulated (167)
Genes upregulated (370)
167
370

B

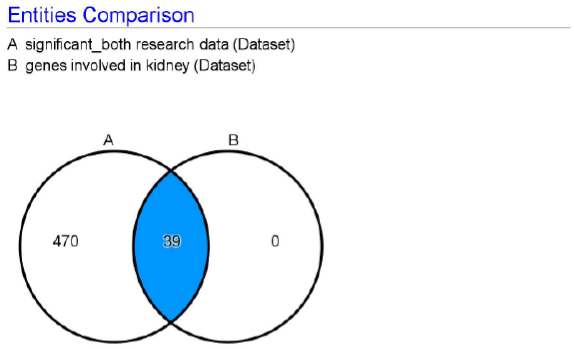
Entities Comparison
A significant_both research data (Dataset)
B genes involved in kidney (Dataset)
A
B
470
39
0

C

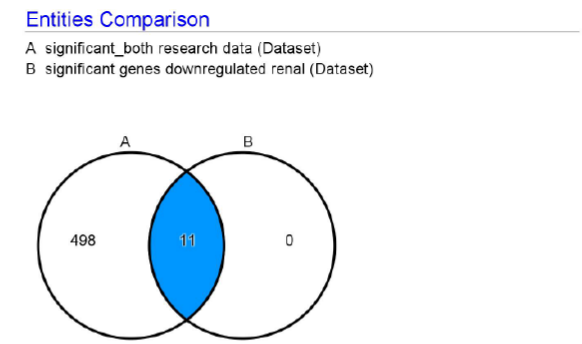
Entities Comparison
A significant_both research data (Dataset)
B significant genes downregulated renal (Dataset)
A
B
498
11
0

D

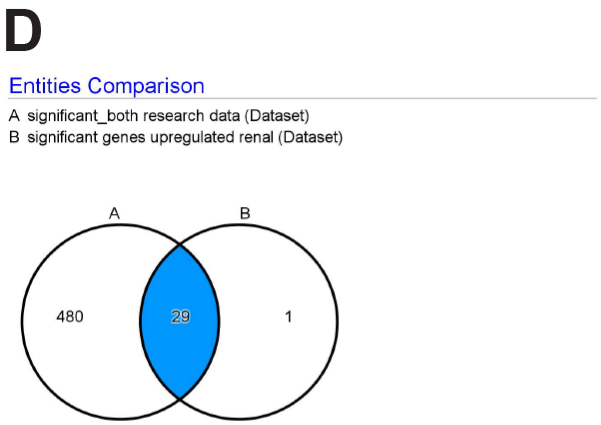
Entities Comparison
A significant_both research data (Dataset)
B significant genes upregulated renal (Dataset)
A
B
480
29
1

E

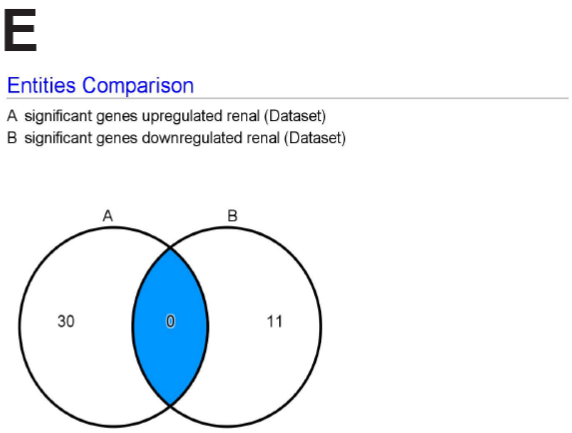
Entities Comparison
A significant genes upregulated renal (Dataset)
B significant genes downregulated renal (Dataset)
A
B
30
0
11

Fig 4.4 DAVID analyses for up-regulated and down-regulated canonical pathways in *Nedd4-2*$^{-/-}$ kidneys. Red colour represents increased genes and green colour represents decreased genes. Black vertical lines represents cut off for significance with benjamini correction for (–log10 (P-value)). The enrichment analysis was performed for Enrichment of Kyoto Encyclopaedia of Genes and Genomes (KEGG) using DAVID bioinformatics resource **A)** Pathways significantly up-regulated in *Nedd4-2*$^{-/-}$ kidneys (red)**.** Significant pathways involved in extracellular matrix interaction, cell adhesion, gap junction and cell communication are up-regulated **B)** Pathways significantly down-regulated in *Nedd4-2*$^{-/-}$ kidneys (green). Significant pathways involved in metabolic and mitochondrial pathways are down-regulated. The genes involved in individual pathways are specified in Supplementary Table**s 2A** (up-regulated) and **2B** (down-regulated).

A

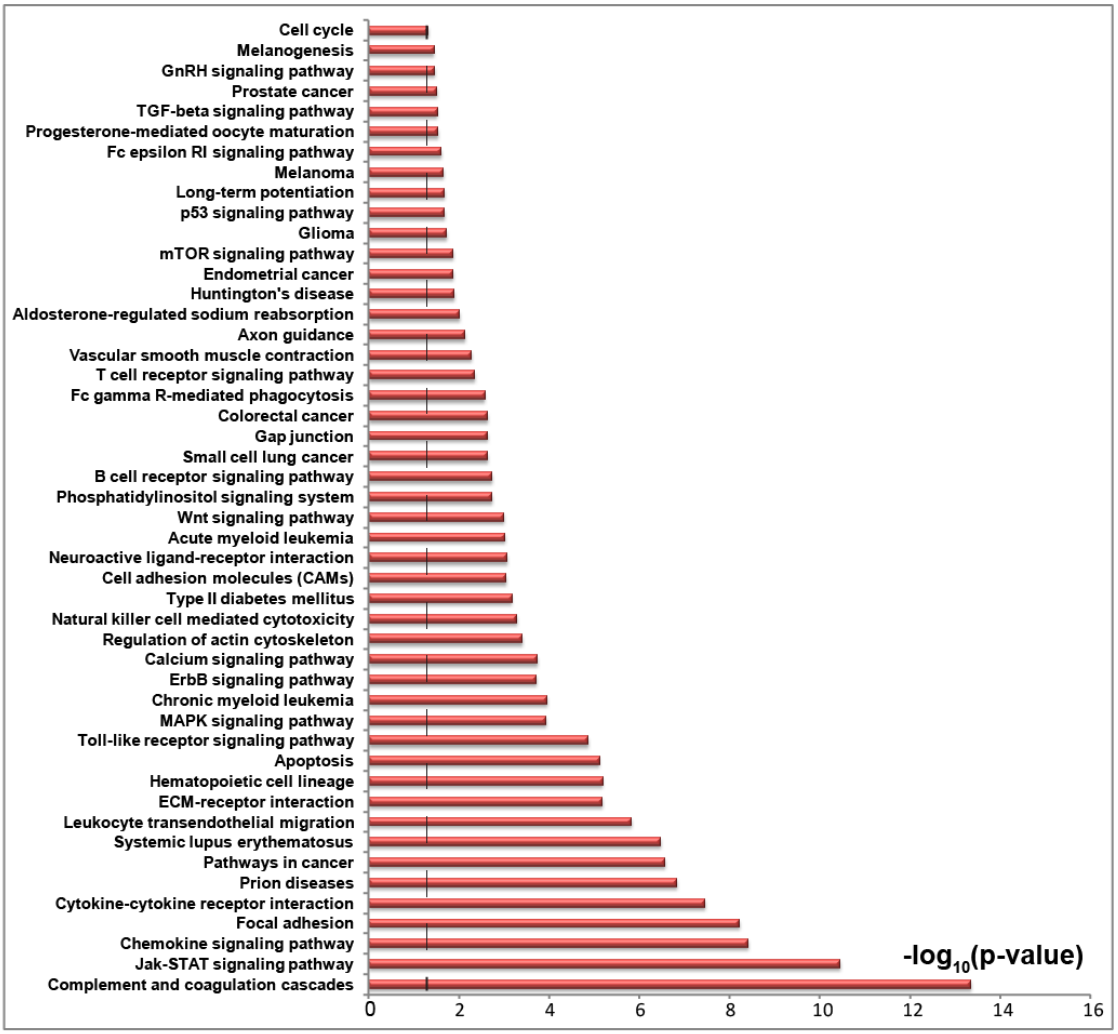
Cell cycle
Melanogenesis
GnRH signaling pathway
Prostate cancer
TGF-beta signaling pathway
Progesterone-mediated oocyte maturation
Fc epsilon RI signaling pathway
Melanoma
Long-term potentiation
p53 signaling pathway
Glioma
mTOR signaling pathway
Endometrial cancer
Huntington's disease
Aldosterone-regulated sodium reabsorption
Axon guidance
Vascular smooth muscle contraction
T cell receptor signaling pathway
Fc gamma R-mediated phagocytosis
Colorectal cancer
Gap junction
Small cell lung cancer
B cell receptor signaling pathway
Phosphatidylinositol signaling system
Wnt signaling pathway
Acute myeloid leukemia
Neuroactive ligand-receptor interaction
Cell adhesion molecules (CAMs)
Type II diabetes mellitus
Natural killer cell mediated cytotoxicity
Regulation of actin cytoskeleton
Calcium signaling pathway
ErbB signaling pathway
Chronic myeloid leukemia
MAPK signaling pathway
Toll-like receptor signaling pathway
Apoptosis
Hematopoietic cell lineage
ECM-receptor interaction
Leukocyte transendothelial migration
Systemic lupus erythematosus
Pathways in cancer
Prion diseases
Cytokine-cytokine receptor interaction
Focal adhesion
Chemokine signaling pathway
Jak-STAT signaling pathway
Complement and coagulation cascades
-log10(p-value)
0
2
4
6
8
10
12
14
16

B

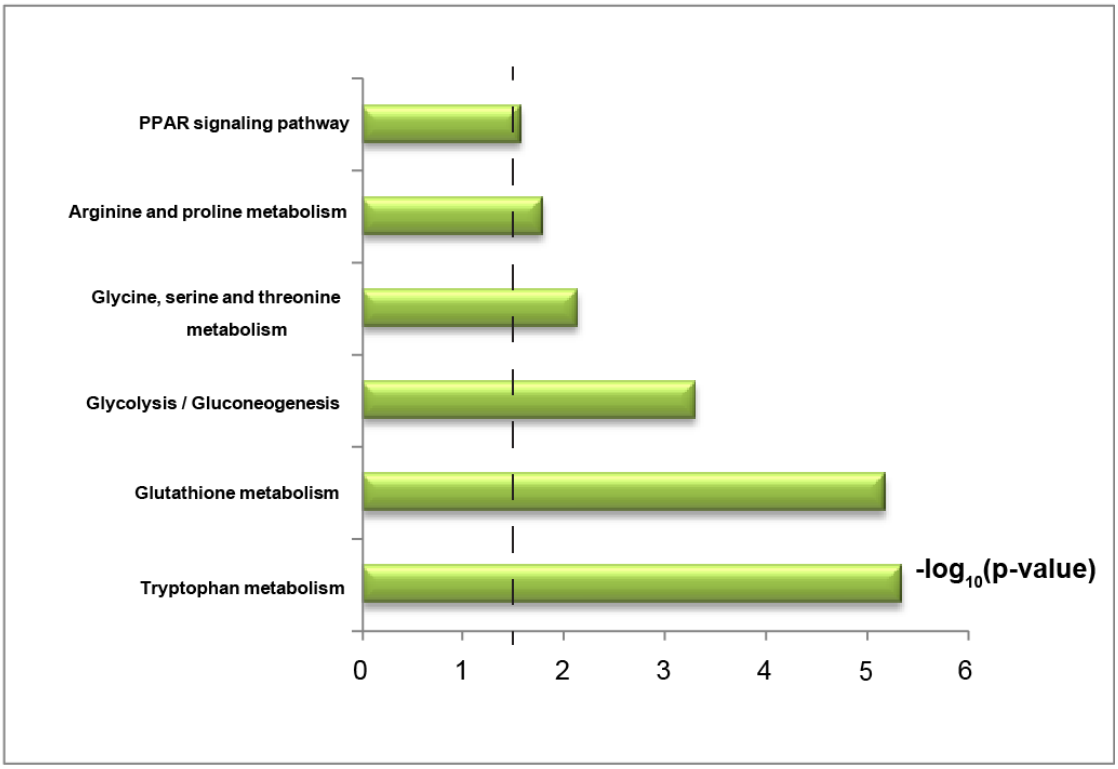
PPAR signaling pathway
Arginine and proline metabolism
Glycine, serine and threonine metabolism
Glycolysis / Gluconeogenesis
Glutathione metabolism
Tryptophan metabolism
-log10(p-value)
0
1
2
3
4
5
6

To further validate the GO (Gene Ontology) term pathways involved in biological processes identified above, cellular component analysis and molecular function for significantly up-regulated and down-regulated pathways genes $\log_2$ fold change >1.1 (increased) or $\log_2$ fold change <0.9 (decreased) showing 10 % percent fold change were used. **Fig 4.5 A** (Benjamini corrected p-value<0.05, black dashed line) summarises up-regulated genes from *Nedd4-2*$^{-/-}$ kidneys in biological processes involved in cell adhesion, inflammatory response, extracellular structure organisation, complement activation and response to wound healing (genes listed in Supplementary Table **3A** in each individual process). **Fig 4.5 B** (Benjamini corrected p-value<0.05, black dashed line) summarises down-regulated genes in biological processes such as oxidation/ reduction (genes listed in Supplementary Table **3B** in each individual process). **Fig 4.5 C** (Benjamini corrected p-value<0.05, black dashed line) summarises *Nedd4-2*$^{-/-}$ up-regulated genes and their cellular localisation involved along the extracellular region, in the extracellular matrix and around the plasma membrane (genes listed in Supplementary Table **3C** in each individual process). **Fig 4.5 D** (Benjamini corrected p-value<0.05, black dashed line) summarises down-regulated genes and their cellular localisation involved in mitochondrion and inside the membrane (genes listed in Supplementary Table **3D** in each individual process). **Fig 4.5 E** (Benjamini corrected p-value<0.05, black dashed line) summarises up-regulated genes and their molecular function predominantly involved in heparin binding, metal ion binding, polysaccharide binding, carbohydrate binding, glycosaminoglycans binding and calcium ion binding (genes listed in Supplementary Table **3E** in each individual process). **Fig 4.5 F** (Benjamini corrected p-value<0.05, black dashed line) summarises down-regulated genes and their molecular function predominantly involved in symporter activity necessary for solute transport across the membrane of two or more solutes together along with sodium ion binding (genes listed in Supplementary Table **3F** in each individual process). The findings in **Fig 4.5 A-F** further

Fig 4.5 DAVID component analysis for biological processes, cellular component and molecular function in *Nedd4-2*$^{-/-}$ kidneys. Red represents increased expression of genes, and blue represents decreased expression of genes *Nedd4-2*$^{-/-}$ kidneys. Black vertical lines represents cut off for significance with Benjamini correction for (–log10 (P-value)). The enrichment analysis was performed using DAVID bioinformatics resource for GO (Gene Ontology) enrichment of genes **A)** Genes significantly up-regulated in *Nedd4-2*$^{-/-}$ kidneys (red) in biological processes. Significant genes involved in cell substrate adhesion, extracellular structure organisation, defence response and wounding. **B)** Genes significantly down-regulated in *Nedd4-2*$^{-/-}$ kidneys (green) in biological processes. Significant genes involved in oxidation/ reduction are down-regulated. **C)** Cellular localisation of genes significantly up-regulated in *Nedd4-2*$^{-/-}$ kidneys (red). Significant genes expressed in the extracellular matrix are up-regulated. **D)** Cellular localisation of genes significantly down-regulated in *Nedd4-2*$^{-/-}$ kidneys (green). Significant genes expressed in the integral and intrinsic membrane and mitochondria are down-regulated. **E)** Genes significantly up-regulated in *Nedd4-2*$^{-/-}$ kidneys (red) in molecular function. Significant genes involved in calcium ion binding, heparin binding and glycosaminoglycan part are up-regulated. **F)** Genes significantly down-regulated in *Nedd4-2*$^{-/-}$ kidneys (green) in molecular function. Significant genes involved in sodium ion binding and symporter activity are down-regulated. The genes involved in individual pathways are specified in Supplementary Table **3A** (Biological process up-regulated), **3B** (Biological process down-regulated) **3C** (Cellular component up-regulated), **3D** (Cellular component down-regulated) **3E** (Molecular function up-regulated) and **3F** (Molecular function down-regulated).

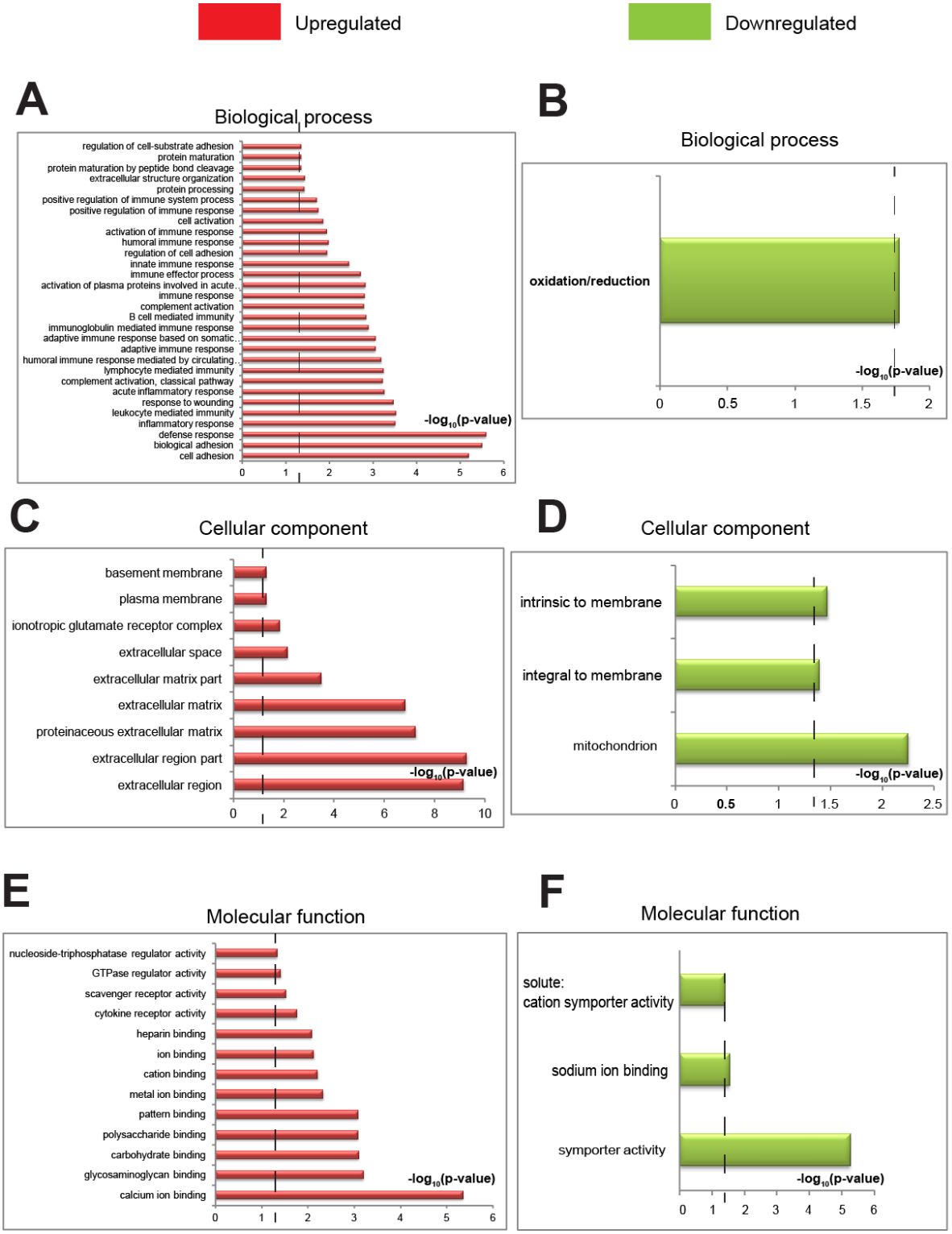
Upregulated
Downregulated
A
Biological process
regulation of cell-substrate adhesion
protein maturation
protein maturation by peptide bond cleavage
extracellular structure organization
protein processing
positive regulation of immune system process
positive regulation of immune response
cell activation
activation of immune response
humoral immune response
regulation of cell adhesion
innate immune response
immune effector process
activation of plasma proteins involved in acute...
immune response
complement activation
B cell mediated immunity
immunoglobulin mediated immune response
adaptive immune response based on somatic...
adaptive immune response
humoral immune response mediated by circulating...
lymphocyte mediated immunity
complement activation, classical pathway
acute inflammatory response
response to wounding
leukocyte mediated immunity
inflammatory response
defense response
biological adhesion
cell adhesion
-log10(p-value)
0 1 2 3 4 5 6
B
Biological process
oxidation/reduction
-log10(p-value)
0 0.5 1 1.5 2
C
Cellular component
basement membrane
plasma membrane
ionotropic glutamate receptor complex
extracellular space
extracellular matrix part
extracellular matrix
proteinaceous extracellular matrix
extracellular region part
extracellular region
-log10(p-value)
0 2 4 6 8 10
D
Cellular component
intrinsic to membrane
integral to membrane
mitochondrion
-log10(p-value)
0 0.5 1 1.5 2 2.5
E
Molecular function
nucleoside-triphosphatase regulator activity
GTPase regulator activity
scavenger receptor activity
cytokine receptor activity
heparin binding
ion binding
cation binding
metal ion binding
pattern binding
polysaccharide binding
carbohydrate binding
glycosaminoglycan binding
calcium ion binding
-log10(p-value)
0 1 2 3 4 5 6
F
Molecular function
solute:
cation symporter activity
sodium ion binding
symporter activity
-log10(p-value)
0 1 2 3 4 5 6

support that genes altered in *Nedd4-2*$^{-/-}$ kidneys are involved in extracellular matrix organisation, cell adhesion and cell- communication, and therefore to confirm these further some of the selected genes in the above processes were validated using quantitative real time PCR. **Fig 4.6** highlights the hierarchical clustering of genes in *Nedd4-2*$^{-/-}$ kidneys presented in the heat map obtained through RNA sequencing, identifying significantly up-regulated in processes described in **Fig 4.4A** with the exception of epidermal growth factor (EGF), which is down-regulated in response to complementation signalling and heparin binding being up-regulated as heparin binding-EGF (HB-EGF) was used for the study **(**genes listed in Supplementary Table **4** were used to obtain the heat map with fold change values obtained through RNA sequencing**).** The following genes were chosen for qPCR validation due to their involvement in processes involving extracellular matrix modification, reorganisation, cell- cell communication and cell adhesion also involved in tight junction formation. To measure the transcript levels of bone morphogenetic protein 1 (BMP-1), transforming growth factor beta-induced (TGFβ1), ADAM metallopeptidase domain 23 (ADAM23), fibrinogen alpha chain (FGA), intercellular adhesion molecule 1 (ICAM1), integrin alpha M (ITGAM), collagen I alpha 1 (COL1A1), and heparin binding epidermal growth factor (HB-EGF), whole kidney samples from P19 *Nedd4-2*$^{+/+}$ (N=4) and P19 *Nedd4-2*$^{-/-}$ (N=4) were used for RNA extraction (different from the kidney samples used for RNA sequencing), and quantitative real time PCR was performed using primers specific to the genes and β-actin as a loading control. As shown in **Fig 4.7** there was no significant difference seen in the levels of these genes at the transcript levels in the *Nedd4-2*$^{+/+}$ and *Nedd4-2*$^{-/-}$ P19 whole kidneys using unpaired T test but they showed a similar increased trend in comparison to the data obtained from RNA sequencing, highlighting their consistency in context to the given study. To further assess the involvement of the renal genes which are significantly up-regulated and down-regulated involved in

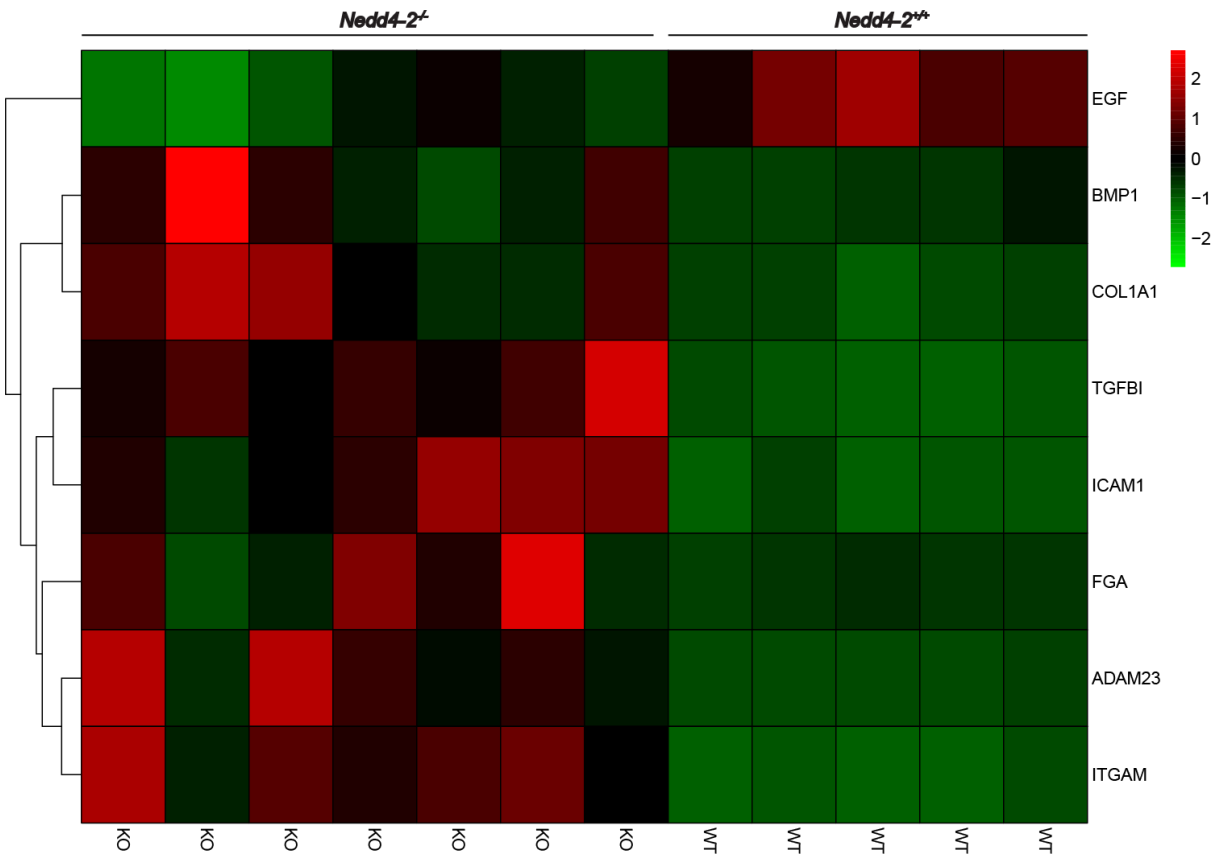

Fig 4.6 Hierarchical clustering heat map of quantitative real time PCR genes in *Nedd4-2*$^{+/+}$ and *Nedd4-2*$^{-/-}$ kidneys selected for validation. Heat map shows Log_2expression mean of > 1 fold change of significantly differentially expressed genes (FDR p-value <0.05) in P19 *Nedd4-2*$^{-/-}$ (N=7, KO) versus *Nedd4-2*$^{+/+}$ (N=5, WT) kidneys selected for validation. Red in heat map indicates up-regulated expression and green indicates down-regulated expression. The red pattern in the KO shows increased variability among samples as compared to WT. On the right is a colour code key, for green to red for increased gene fold change expression values. Gene names are indicated on the right of the respective lane. Individual gene fold changes for *Nedd4-2*$^{-/-}$ and *Nedd4-2*$^{+/+}$ are summarised in Supplementary Table **4**.

Fig 4.7 Quantitative real time PCR validation of genes in *Nedd4-2*$^{-/-}$ kidneys. Whole cystic kidney RNA was extracted and quantitative real time PCR validation of gene expression in P19 *Nedd4-2*$^{+/+}$ (N=4) and *Nedd4-2*$^{-/-}$ (N=4) cystic kidneys was performed. Expression was measured relative to β-Actin levels. Data is represented as mean ± SEM ($P \geq 0.05$, not significant (n.s), using unpaired T test). The following genes Col1a1: collagen-1, TGFβ1: transforming growth factorβ1, ADAM23: ADAM metallopeptidase domain 23, FGA: Fibrinogen, HB-EGF: heparin binding EGF (inhibits EGF), BMP-1: Bone morphogenetic protein-1 were quantitated, and *Nedd4-2*$^{-/-}$ kidneys showed an increasing trend similar to the increase observed from RNA sequencing on different samples.

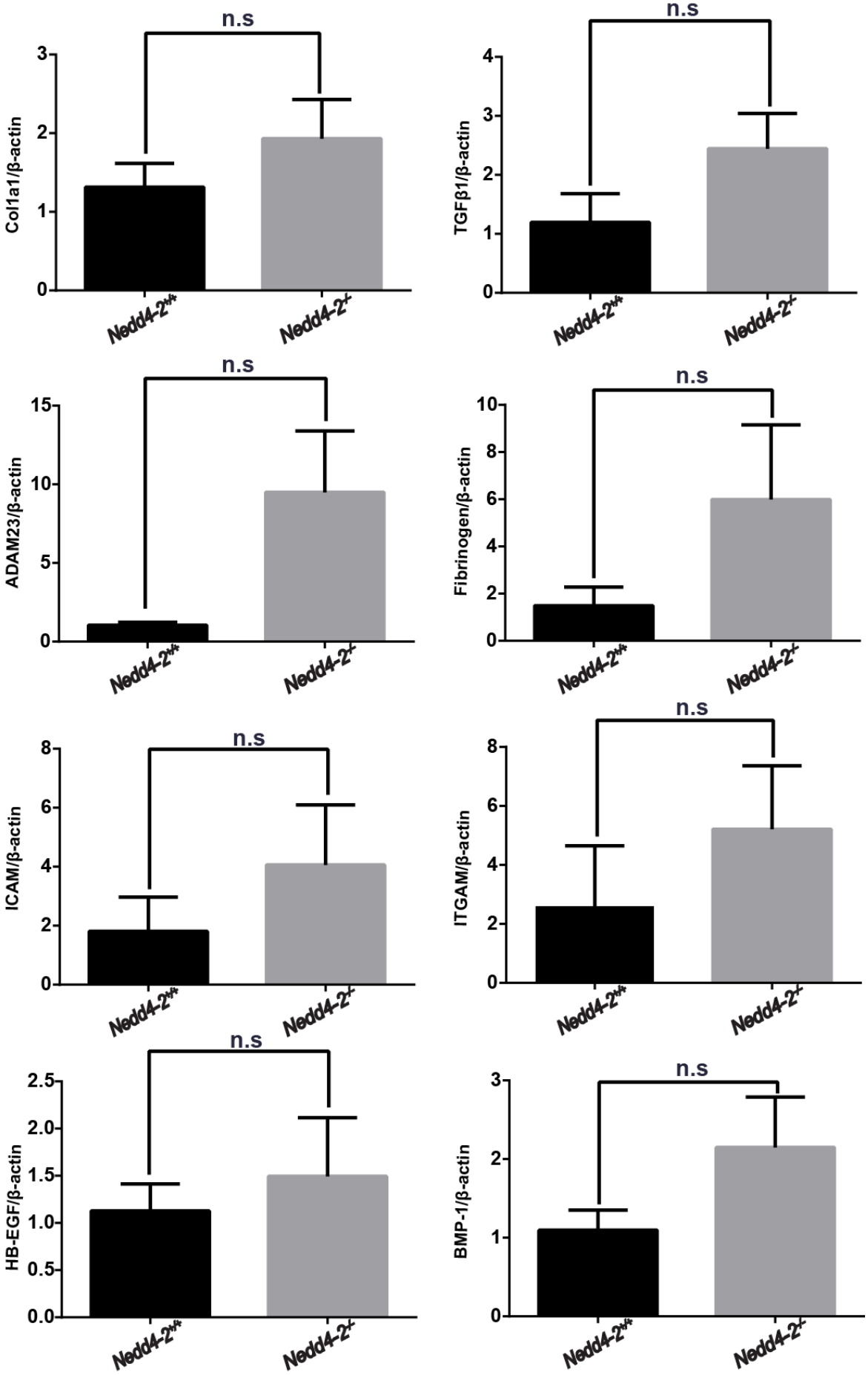
n.s
Col1a1/β-actin
TGFβ1/β-actin
ADAM23/β-actin
Fibrinogen/β-actin
ICAM/β-actin
ITGAM/β-actin
HB-EGF/β-actin
BMP-1/β-actin
Nedd4-2+/+
Nedd4-2-/-

disease and their respective function, further assessment was done using ingenuity pathway analysis as described previously for Venn diagrams **Fig 4.3 C** and **D.**

4.3.4 Ingenuity pathway analysis of renal genes in disease and function

To further elucidate the genes involved in kidney abnormalities associated with renal dysplasia and conditions associated with its anomalies, ingenuity pathway analysis of renal genes in disease and function was performed. It was imperative to understand the functional relevance of genes reported earlier (**Section 4.3.2),** where there were 30 up-regulated genes and 11 down-regulated genes in diseased conditions specifically. **Fig 4.8** summarises the list of 30 significantly up-regulated genes in renal diseases represented as a heat map obtained from a gene list generated through ingenuity pathway analysis software (Supplementary Table **5**). The heat map was hierarchically clustered to showcase the similarities associated between different genes (represented on the left of **Fig 4.8**) along with the variability of expression between the *Nedd4-2*$^{+/+}$ and *Nedd4-2*$^{-/-}$ P19 kidney samples. Interestingly, most of these 30 up-regulated genes were localised in the extracellular space, cytoplasm or the plasma membrane as reported in **Fig 4.9.** Previous reports on human foetal renal dysplastic kidneys have reported increases in transcript levels of transforming growth factor β1, extracellular matrix genes collagen-1 and -2, Slit homolog 3 (SLIT3), Fibrillin (FBLN1), adhesion molecules like (CD44) and complement system genes (C3, C1QB) (Jain *et al*., 2007). In the P19 *Nedd4-2*$^{-/-}$ kidneys some of the above mentioned genes (C3, C1QA, ALDH1A2, FBLN1, SLIT3, COL6A1, ITGAM and CD44) are seen to be significantly up-regulated in the heat map representing genes in renal disease, corroborating previous studies. Genes not previously reported to be up-regulated in the list are ATPase H+/K+ transporting non gastric alpha peptide (ATP12A), decorin (DCN), deltex4 E3 ubiquitin ligase (DTX4), signal transducer and activator of transcription 3 (acute-phase response factor) (STAT3), FRAS1 related extracellular matrix 1 (FREM1), protein tyrosine phosphatase receptor type S (PTPRS5),

SPARC related modular calcium binding 2 (SMOC2), dishevelled-binding antagonist of beta-catenin 3 (DACT3), FGR proto-oncogene Src family tyrosine kinase (FGR), lipocalin 2 (LCN2), sulfatase 1 (SULF1), poly (ADP-ribose) polymerase family member 3 (PARP3), complement component 3a receptor 1 (C3AR1), integrin alpha M (complement component 3 receptor 3 subunit) (ITGAM), collagen, type VI alpha 1 (COL6A1), matrix metallopeptidase 14 (membrane-inserted) (MMP14), biglycan (BGN), and colony stimulating factor 1 (macrophage) (CSF1). To further understand the altered up-regulated genes in renal abnormalities associated with renal dysplasia the above genes are summarised in the pathway map represented in **Fig 4.9.** The genetic disorders in the kidney pertaining to some of the above mentioned genes are coloured in orange, and show activation of the up-regulated genes (in red) leading to hypoplasia of kidney, congenital anomalies of kidney and urinary tract, proliferation of kidney cells, growth of kidney, kidney failure, kidney injury, kidney damage, nephritis, kidney formation, development of urinary tract and quantity of renal glomerulus. To further understand the role of these genes based on the predicted experimental and theoretical interactions predicted through ingenuity software, a genetic network model of the most up-regulated genes in kidney disease was made and their cellular localisation was shown as seen in **Fig 4.10,** with genes in red being up-regulated and genes in grey being predicted to be involved in the molecular cascade. Most of the genes in the pathway are regulated in the extracellular space and concentrated around genes involved in extracellular matrix modification and renal interstitial fibrosis, like collagens and fibrillin driven in response to cytokine transforming growth factor β1.

Fig 4.11 summarises the list of 11 significantly down-regulated genes in *Nedd4-2*$^{-/-}$ P19 renal disease represented as a heat map obtained from gene list generated through ingenuity pathway analysis software (Supplementary Table **6**). The heat map was hierarchically clustered to showcase the similarities associated between different genes (represented on the

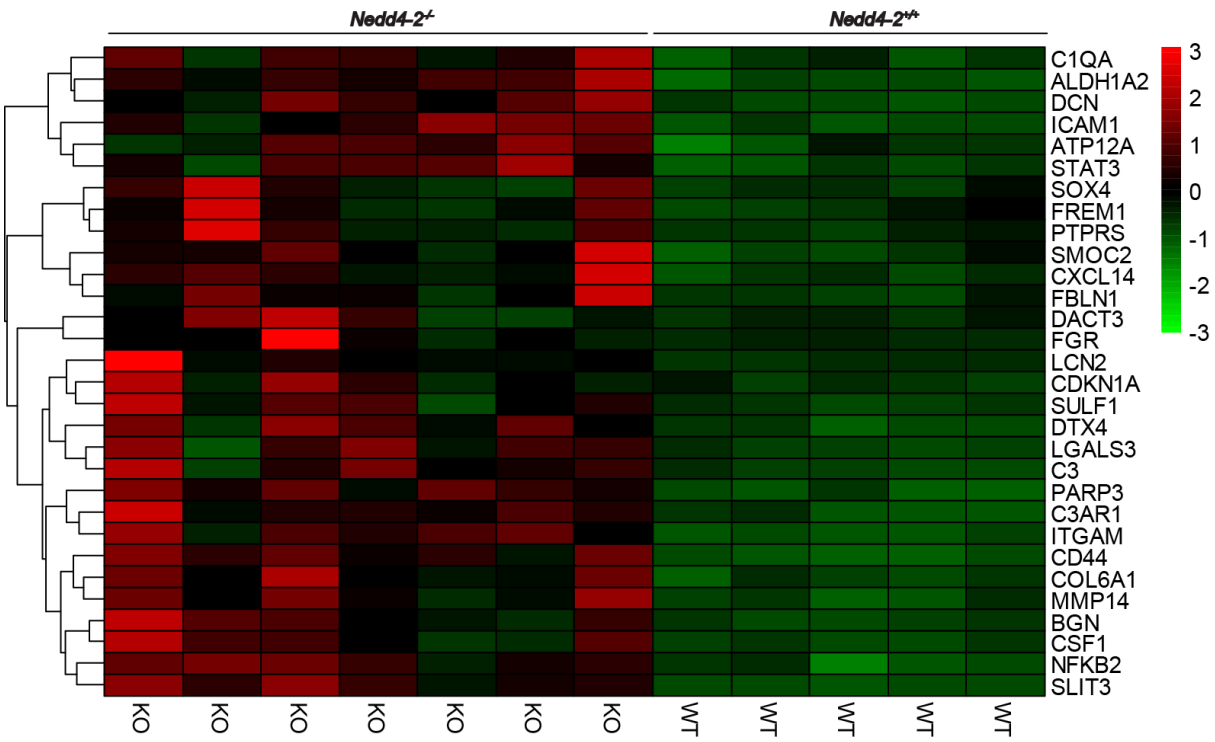

Fig 4.8 Hierarchical clustering of differential expressed renal genes up-regulated in *Nedd4-2*$^{-/-}$ kidneys involved in disease and function. Heat map shows Log_2expression mean of > 1 fold change of significantly differentially expressed genes (FDR p-value <0.05) in *Nedd4-2*$^{-/-}$ (N=7, KO) versus *Nedd4-2*$^{+/+}$ (N=5, WT) kidneys. Red in heat map indicates up-regulated expression and green indicates down-regulated expression. The red pattern in the KO shows increased variability among samples as compared to WT. On the right is indicated colour code for green to red for increased gene log fold change expression values. Genes differentially regulated are indicated next to the respective lane on the right. Individual gene fold changes for *Nedd4-2*$^{-/-}$ and *Nedd4-2*$^{+/+}$ are summarised in Supplementary Table **5**.

Fig 4.9 Differentially expressed renal genes up-regulated in *Nedd4-2*$^{-/-}$ kidneys involved in disease and function. The pathway map from top to bottom indicates genes localisation from extracellular space to plasma membrane to cytoplasm to nucleus. From left to right are the genes involved in the different diseases and function, and the disease and function are represented on the right. The prediction legend is on the left showing genes up-regulated in red, with predicted activation of disease and function in orange, and inhibition represented in blue. The dashed lines in orange represent predicted activation, dashed lines in blue are predicted to lead to inhibition. Yellow lines highlight inconsistent correlations between findings with downstream molecules. Dashed grey lines represent no potential prediction for candidate genes on disease and function. Individual gene fold changes for *Nedd4-2*$^{-/-}$ and *Nedd4-2*$^{+/+}$ renal genes are summarised in Supplementary Table **5**.

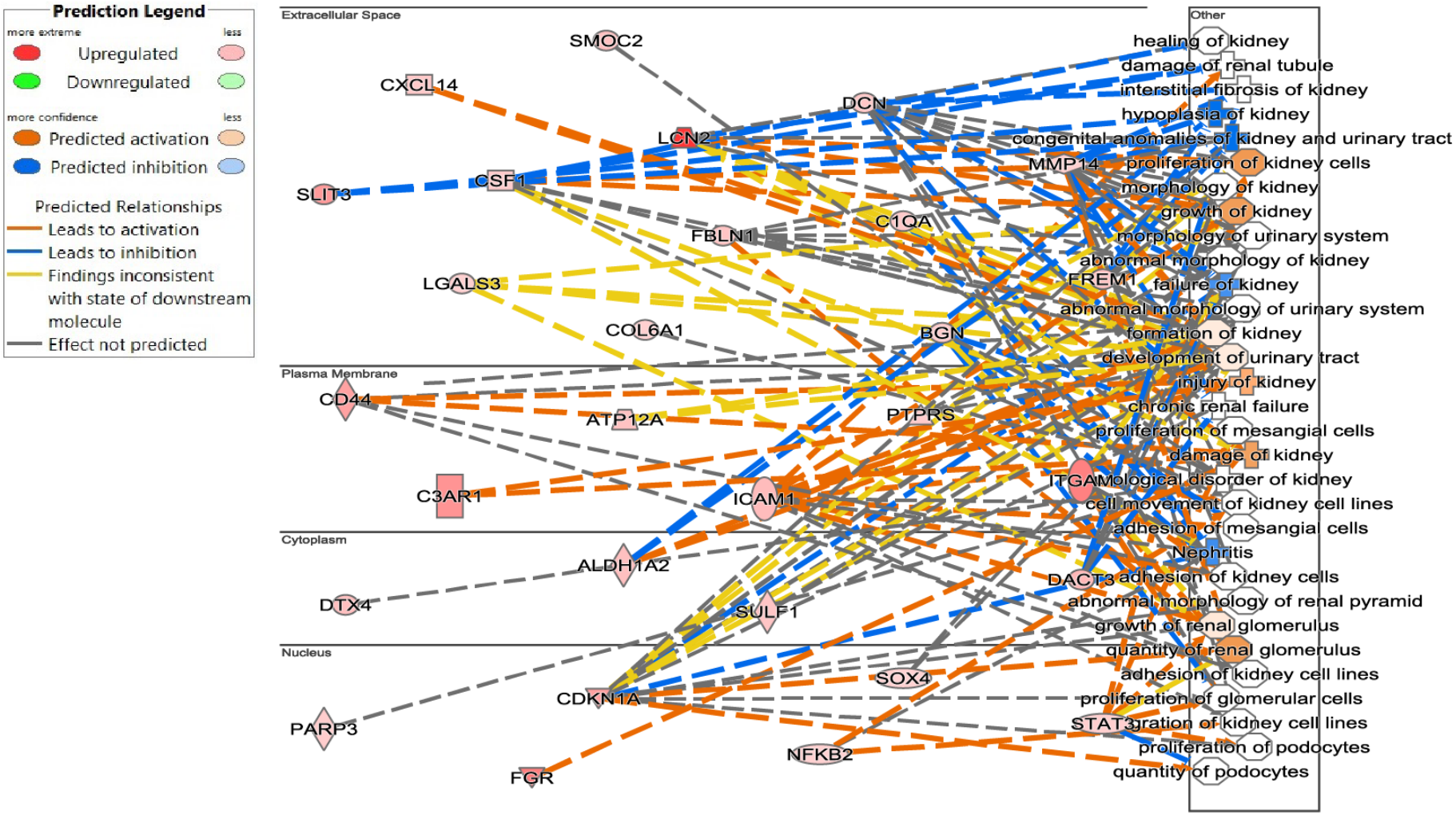
Prediction Legend
more extreme
less
Upregulated
Downregulated
more confidence
less
Predicted activation
Predicted inhibition
Predicted Relationships
Leads to activation
Leads to inhibition
Findings inconsistent with state of downstream molecule
Effect not predicted
Extracellular Space
Plasma Membrane
Cytoplasm
Nucleus
Other
SMOC2
CXCL14
SLIT3
CSF1
LCN2
DCN
FBLN1
C1QA
LGALS3
COL6A1
BGN
CD44
ATP12A
PTPRS
C3AR1
ICAM1
ALDH1A2
DTX4
SULF1
PARP3
CDKN1A
SOX4
FGR
NFKB2
MMP14
FREM1
ITGAM
DACT3
STAT3
healing of kidney
damage of renal tubule
interstitial fibrosis of kidney
hypoplasia of kidney
congenital anomalies of kidney and urinary tract
proliferation of kidney cells
morphology of kidney
growth of kidney
morphology of urinary system
abnormal morphology of kidney
failure of kidney
abnormal morphology of urinary system
formation of kidney
development of urinary tract
injury of kidney
chronic renal failure
proliferation of mesangial cells
damage of kidney
Mological disorder of kidney
cell movement of kidney cell lines
adhesion of mesangial cells
Nephritis
adhesion of kidney cells
abnormal morphology of renal pyramid
growth of renal glomerulus
quantity of renal glomerulus
adhesion of kidney cell lines
proliferation of glomerular cells
gration of kidney cell lines
proliferation of podocytes
quantity of podocytes

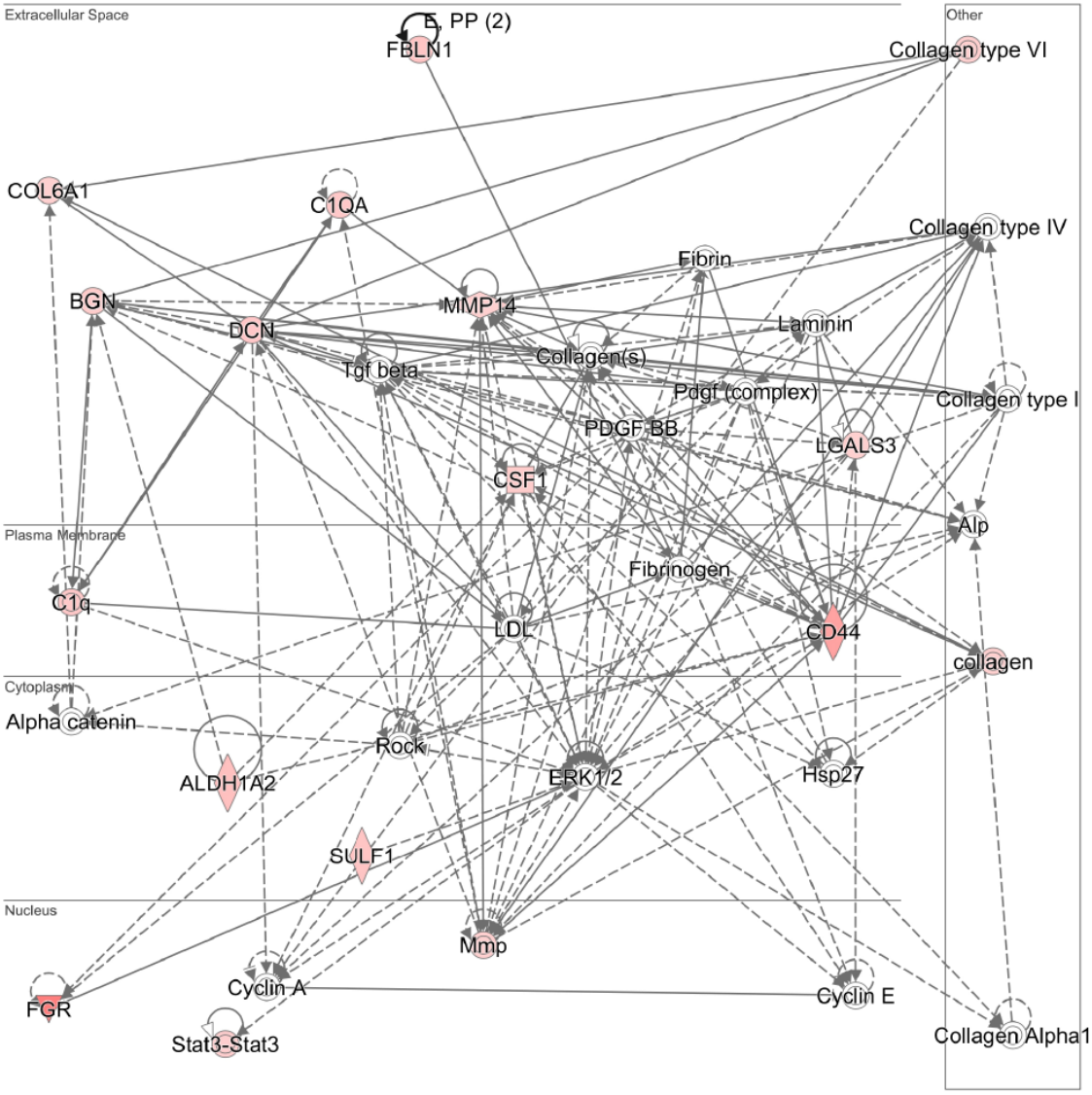

Fig 4.10 Differentially expressed renal gene potential pathways up-regulated in *Nedd4-2*$^{-/-}$ kidneys involved in disease and function. The pathway map from top to bottom indicates gene localisation from extracellular space to plasma membrane to cytoplasm to nucleus. The genes that are up-regulated are indicated in red with predicted activation. The straight lines in grey represent activation; dashed lines in grey indicate predicted activation. Genes represented in grey are genes predicted to be involved in the pathway not present in the differentially expressed genes list.

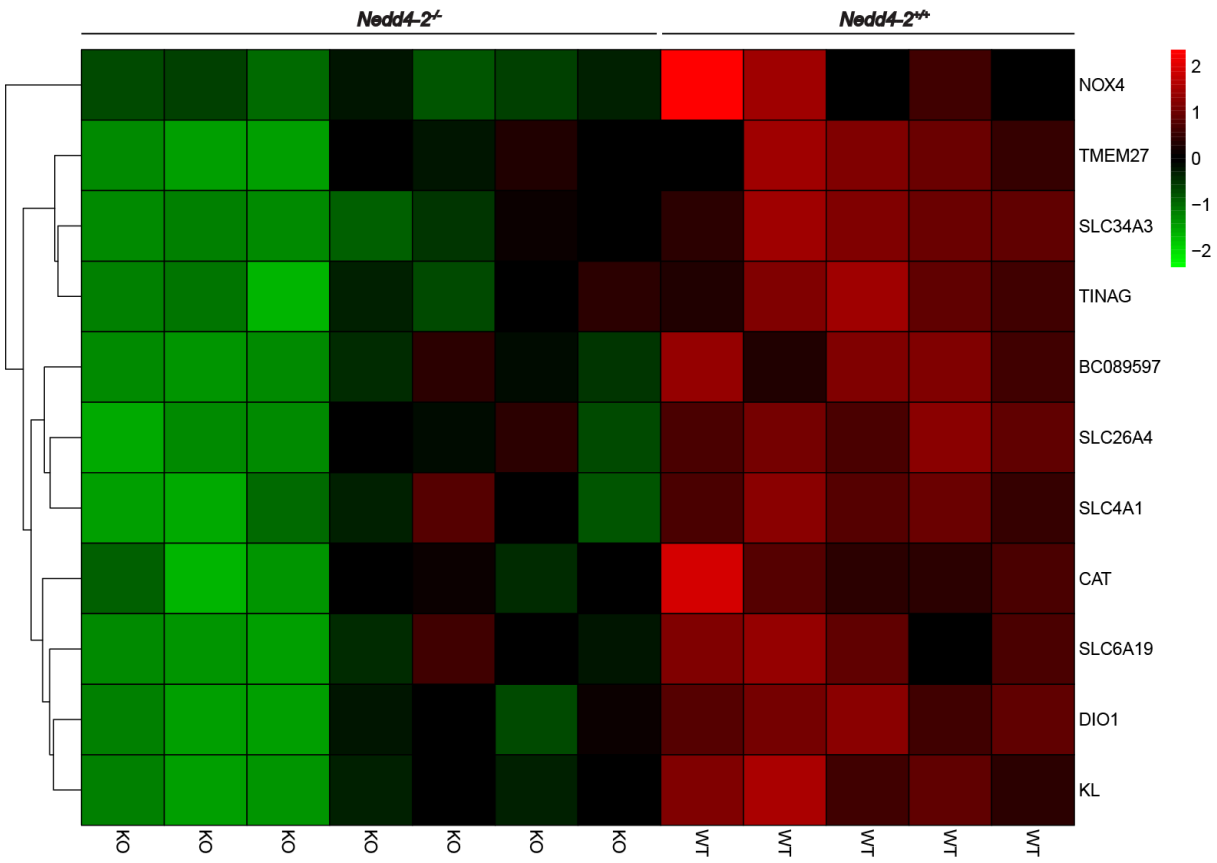

Fig 4.11 Hierarchical clustering of differential expressed renal genes down-regulated in *Nedd4-2*$^{-/-}$ kidneys involved in disease and function. Heat map shows Log_2expression mean of > 1 fold change of significantly differentially expressed genes (FDR p-value <0.05) in *Nedd4-2*$^{-/-}$ (N=7, KO) versus *Nedd4-2*$^{+/+}$ (N=5, WT) kidneys. Red in heat map indicates up-regulated expression and green indicates down-regulated expression. Unannotated genes are indicated by their refseq numbers. The red pattern in the KO shows increased variability among samples as compared to WT. On the right is indicated colour code for green to red for increased fold expression values of genes. Genes differentially regulated are indicated next to the respective lane on the right. Individual gene fold changes for *Nedd4-2*$^{-/-}$ and *Nedd4-2*$^{+/+}$ are summarised in Supplementary Table **6**.

Genes down-regulated in the *Nedd4-2*$^{-/-}$ dysplastic kidneys previously reported in human mid gestational foetal dysplastic kidneys include SLC4A1 solute carrier family 4 (anion exchanger) member 1 (Diego blood group), further confirming the validity of our findings (Jain *et al*., 2007). Genes not reported elsewhere in models of renal dysplasia which are significantly down-regulated in *Nedd4-2*$^{-/-}$ kidneys are NADPH oxidase 4 (NOX4), retinol dehydrogenase 16 (all-trans) (BC089597), transmembrane protein 27 (TMEM27), solute carrier family 34 member 3 (SLC34A3) (type II sodium/phosphate co transporter), solute carrier family 26 member 4 (SLC26A4) (anion exchanger), solute carrier family 6 member 19 (SLC6A19) (neutral amino acid transporter), tubulointerstitial nephritis antigen (TINAG), catalase (CAT), DIO1 (deiodinase iodothyronine type I) and KL (klotho).

To further understand the relationship of down-regulated genes in specific renal abnormalities and renal dysplasia, pathway mapping was performed as summarised in **Fig 4.12.** The genetic disorders in the kidney pertaining to some of the above mentioned genes are coloured in orange, showing activation of the down-regulated genes in green leading to urination disorder involving SLC34A1, SLC4A1, SLC6A19, and SLC26A4. Further SLC4A1 reported previously in human renal dysplasia to be down-regulated, is shown in the current down-regulated gene set to be involved in polyuria in the *Nedd4-2*$^{-/-}$ kidney (Jain *et al*., 2007). The following down-regulated genes involved in renal disease conditions were further used to obtain a potential activation cascade in form of a molecular pathway, with the top molecular pathway represented in **Fig 4.13** with genes down-regulated indicated in green, and genes in grey predicted to be involved in the molecular activation in the kidney. In **Fig 4.13,** the pathway is stimulated by PPAR (peroxisome proliferators activated receptor) gamma activation of CTNNB1 (Catenin (Cadherin-Associated Protein), Beta 1) which induces a downstream cascade of other proteins either predicted or shown in the down-regulated gene list mentioned above.

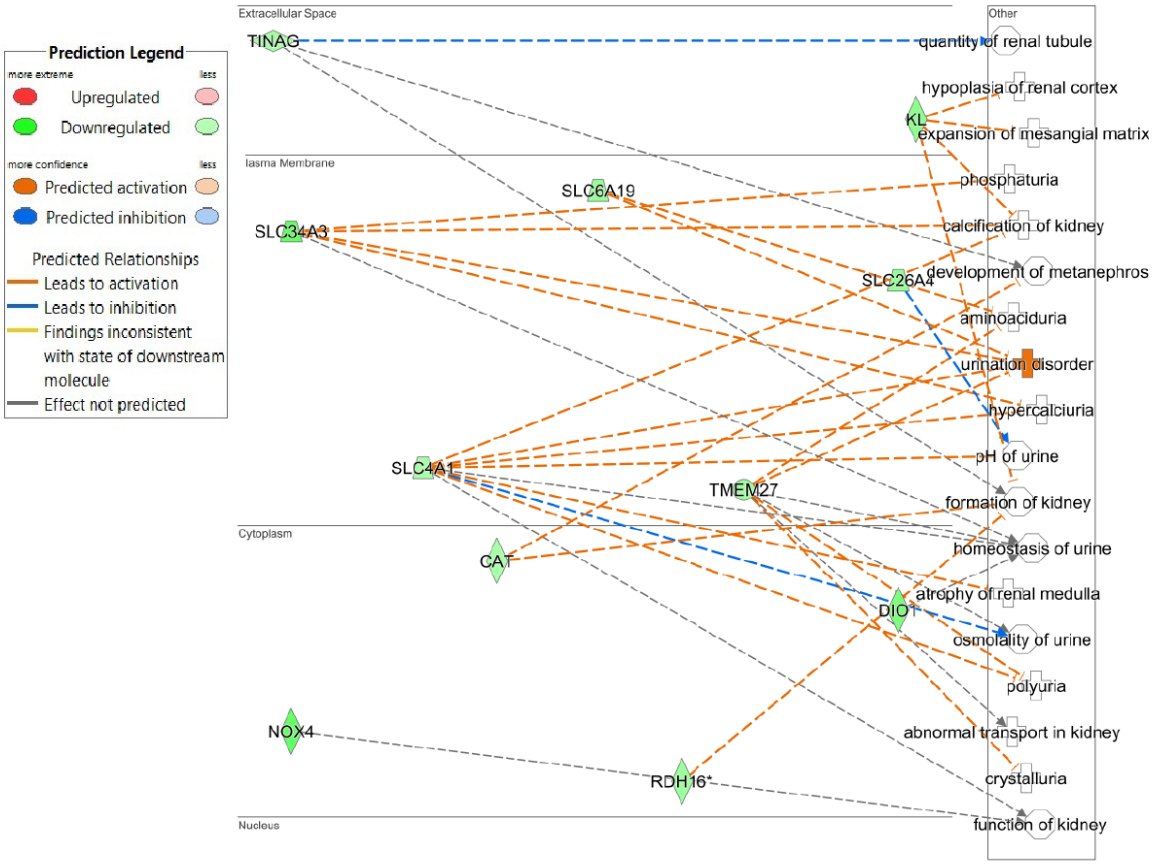

Fig 4.12 Differentially expressed renal genes down-regulated in *Nedd4-2*$^{-/-}$ kidneys involved in disease and function. The pathway map from top to bottom indicates genes localisation from extracellular space to plasma membrane to cytoplasm to nucleus. The disease and function are represented on the right, and the prediction legend on the left show genes being down-regulated in green, genes up-regulated in red, with predicted activation of disease and function in orange, and inhibition represented in blue. The dashed lines in orange represent predicted activation, and dashed lines in blue are predicted to lead to inhibition. Yellow lines highlight inconsistent correlations between findings with downstream molecules. Dashed grey lines predicting no potential prediction for candidate genes on disease and function. Individual gene fold changes for *Nedd4-2*$^{-/-}$ and *Nedd4-2*$^{+/+}$ are summarised in Supplementary Table **6**.

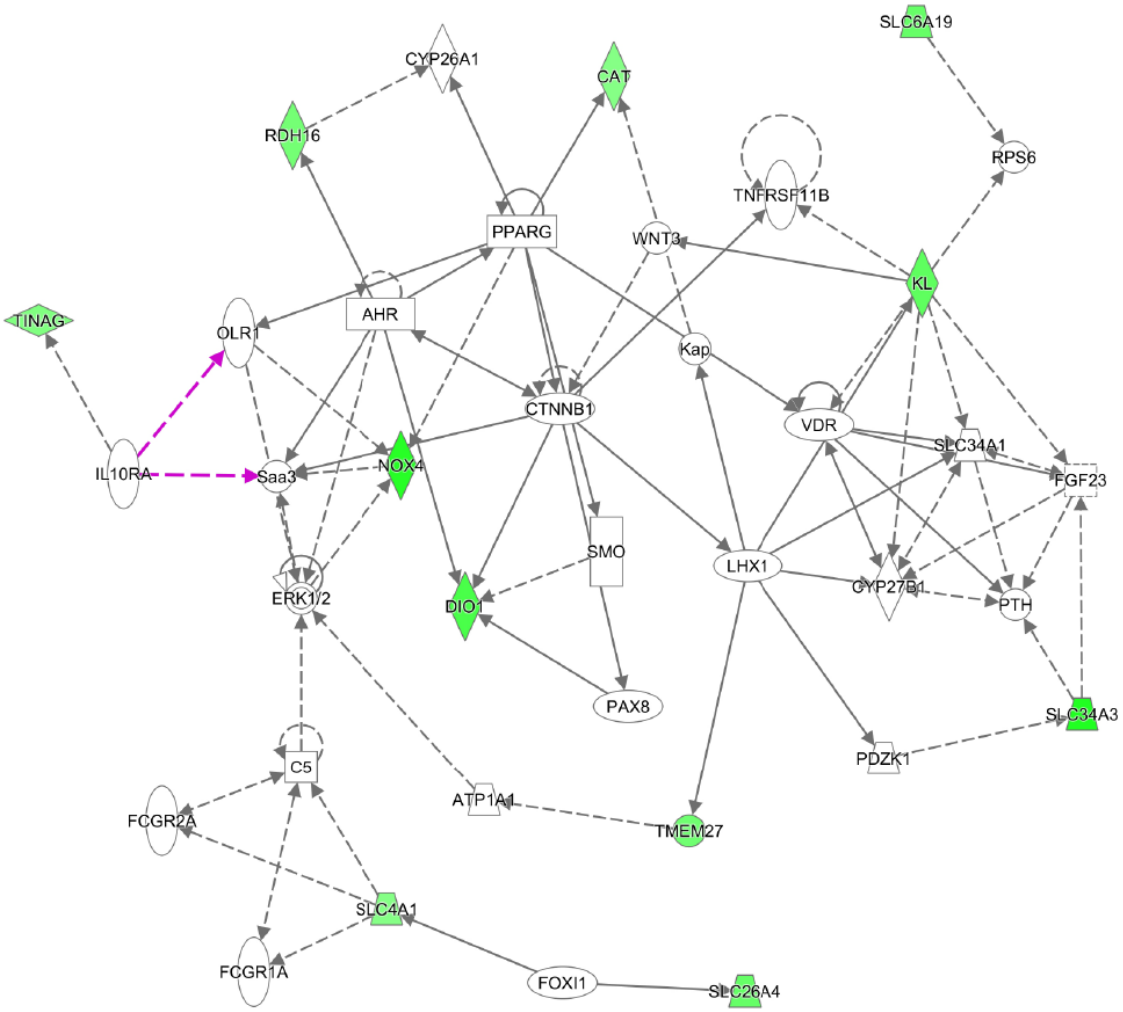

Fig 4.13 Differentially expressed renal gene potential pathways down-regulated in *Nedd4-2*$^{-/-}$ kidneys involved in disease and function. The genes in green are shown to be down-regulated and represent the list of renal genes down-regulated significantly in *Nedd4-2*$^{-/-}$ kidney. The straight lines in grey represent activation; dashed lines in grey indicate predicted activation. Dashed lines in pink indicate potential activation. Genes represented in grey are genes predicted to be involved in the pathway not present in the differentially expressed genes list.

left) along with the variability of expression between the P19 *Nedd4-2* $^{+/+}$ and *Nedd4-2*$^{-/-}$ kidneys. As renal dysplasia, previously described as renal developmental abnormality, is associated with the misregulation of transcriptional control within the kidney, to further aid in our understanding of transcriptional regulation of *Nedd4-2*$^{-/-}$ kidneys it was necessary to determine the transcription factors expressed in the *Nedd4-2*$^{-/-}$ kidneys and their downstream targets (Woolf *et al*., 2004).

4.3.5 Transcription control in *Nedd4-2*$^{-/-}$ dysplastic kidneys

Transcription factor regulation based on the downstream targets signature, and the transcription factors within the list of significant genes identified by RNA sequencing (Supplementary Table **1)** was uploaded in the TFacTS database. This database consists of transcription signatures of genes and their target genes from published literature and other data sources based on human and mouse annotated genes. As seen in **Fig 4.14,** there were a number of significantly regulated transcription factors based on the downstream targets and their representation in the respective input gene list, as indicated on the x-axis and plotted against the -log $_{10}$ fold change represented as e-value for significance. E-value <0.05 was considered as significant for the list of transcription factors significantly regulated. The overlap of target genes between the represented transcription factors is shown as a percentage of intersection by the orange line. Prior studies on renal dysplasia highlights the role of transcription factors like ESR1 (Estrogen receptor 1), TCF7/L2 (T-cell specific), WT1 (Wilms tumor), HNF4A (Hepatocyte nuclear factor 4 alpha) and JUN (c-Jun proto oncogene), which are highlighted in **Fig 4.14,** corroborating findings from previous studies on transcriptional control in kidney dysplasia (Jain *et al*., 2007). Some of the other novel transcription factors to be involved in P19 *Nedd4-2*$^{-/-}$ kidneys are SP1 (Specificity protein 1), GLI1(GLI family zinc finger 1), SPI1(Transcription factor PU.1), STAT3 (signal transducer and activator of transcription 3), SMAD 1/ 3 (Mothers against decapentaplegic homolog 1/3)

EGR1(Early growth response 1), TP53 (Tumor protein 53), ETS1(Protein C-ets-1), TFAP2A (Transcription factor activating protein 2 alpha), GLI2 (GLI family zinc finger 2), NFKB1(Nuclear factor kappa B) and RELA (Transcription factor P65) .

Fig 4.15 summarises the list of 13 significantly regulated transcription factors involved in renal disease represented as a heat map obtained from gene list generated through ingenuity pathway analysis software (Supplementary Table **7**). The heat map was hierarchically clustered to showcase the similarities associated between different genes represented on the left, along with the variability of expression between *Nedd4-2*$^{+/+}$ and *Nedd4-2*$^{-/-}$. Transcription factors significantly regulated in the *Nedd4-2*$^{-/-}$ dysplastic kidneys previously reported in human mid gestational foetal dysplastic kidneys are SOX4, FOS, JUN and KLF6, further confirming the validity of our findings (Jain *et al*., 2007). Transcription factors not reported elsewhere in models of renal dysplasia which are significantly regulated in renal disease are AF4/FMR2 family member 3 (AFF3), brain abundant membrane signal protein 1 (BASP1), viral oncogene homolog (MYC), nuclear receptor co repressor 2 (NCOR2), AT rich interactive domain 5B (ARID5B), teashirt zinc finger homeobox 3 (TSHZ3), signal transducer and activator of transcription 3 (acute-phase response factor) (STAT3), runt-related transcription factor 1 (RUNX1) and hypoxia inducible factor 3 alpha (HIF3A).

The following transcription factors involved in renal disease conditions were further used to investigate a potential role in disease conditions in the kidney, and a pathway map was constructed with their cellular localisations represented in **Fig 4.16,** with most of them shown to be nuclear localised. Genes highlighted in red are up-regulated, and are known to be in the gene list identifying differentially expressed genes in *Nedd4-2*$^{-/-}$ dysplastic kidneys. These transcription factors are shown to be potentially involved in urinary tract cancer, proliferation of kidney cells, kidney carcinoma, renal cell carcinoma and kidney

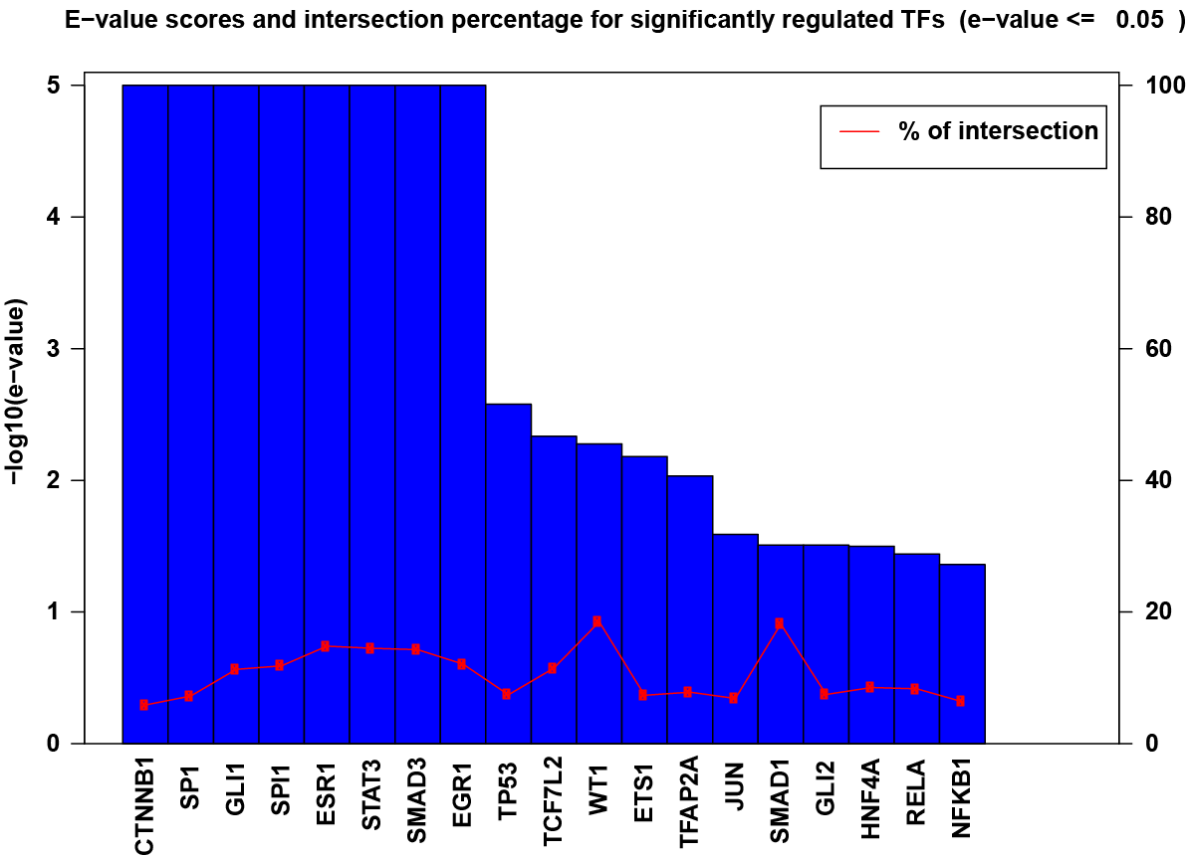

Fig 4.14 Potential transcription factors activated in *Nedd4-2*$^{-/-}$ kidneys. TFacTS predicted transcription factors based on the list of annotated genes input in the online transcription factor signatures database with Log_2expression mean of > 0 fold change of significantly differentially expressed genes (FDR (False Discovery Rate) p-value <0.05) in *Nedd4-2*$^{-/-}$ (N=7) versus *Nedd4-2*$^{+/+}$ (N=5) kidneys. Blue in the graph indicates up-regulated expression. Predicted transcription factors are represented on –log10 (e-value) with the intersection percentage of downstream target genes significantly regulated by transcription factors represented as an orange line. Individual genes fold changes for *Nedd4-2*$^{-/-}$ and *Nedd4-2*$^{+/+}$ selected are from Supplementary Table **1**.

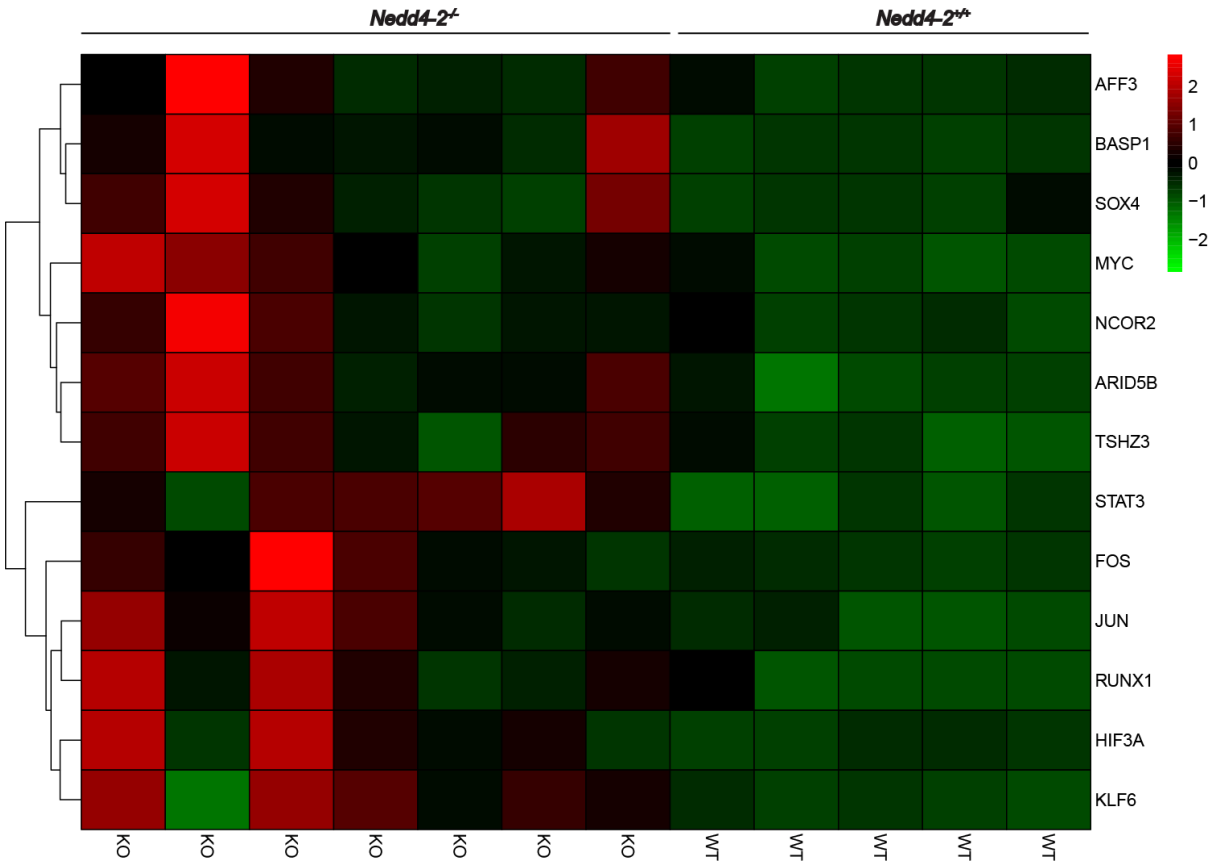

Fig 4.15 Hierarchical clustering of differential expressed transcription factors up-regulated in *Nedd4-2*$^{-/-}$ kidneys involved in disease and function. Heat map shows Log_2expression mean of > 1 fold change of significantly differentially expressed genes (FDR (False Discovery Rate) p-value <0.05) in P19 *Nedd4-2*$^{-/-}$ (N=7, KO) versus *Nedd4-2*$^{+/+}$ (N=5, WT) kidneys. Red in heat map indicates up-regulated expression and green indicates down-regulated expression. Unannotated genes are indicated by their refseq numbers. The red pattern in the KO shows increased variability among samples as compared to WT. On the right is indicated colour code for green to red for increased expression values of genes. Genes differentially regulated are highlighted next to the respective lane on the right. Individual renal transcription factor differential genes for *Nedd4-2*$^{-/-}$ and *Nedd4-2*$^{+/+}$ summarised in Supplementary Table **7**.

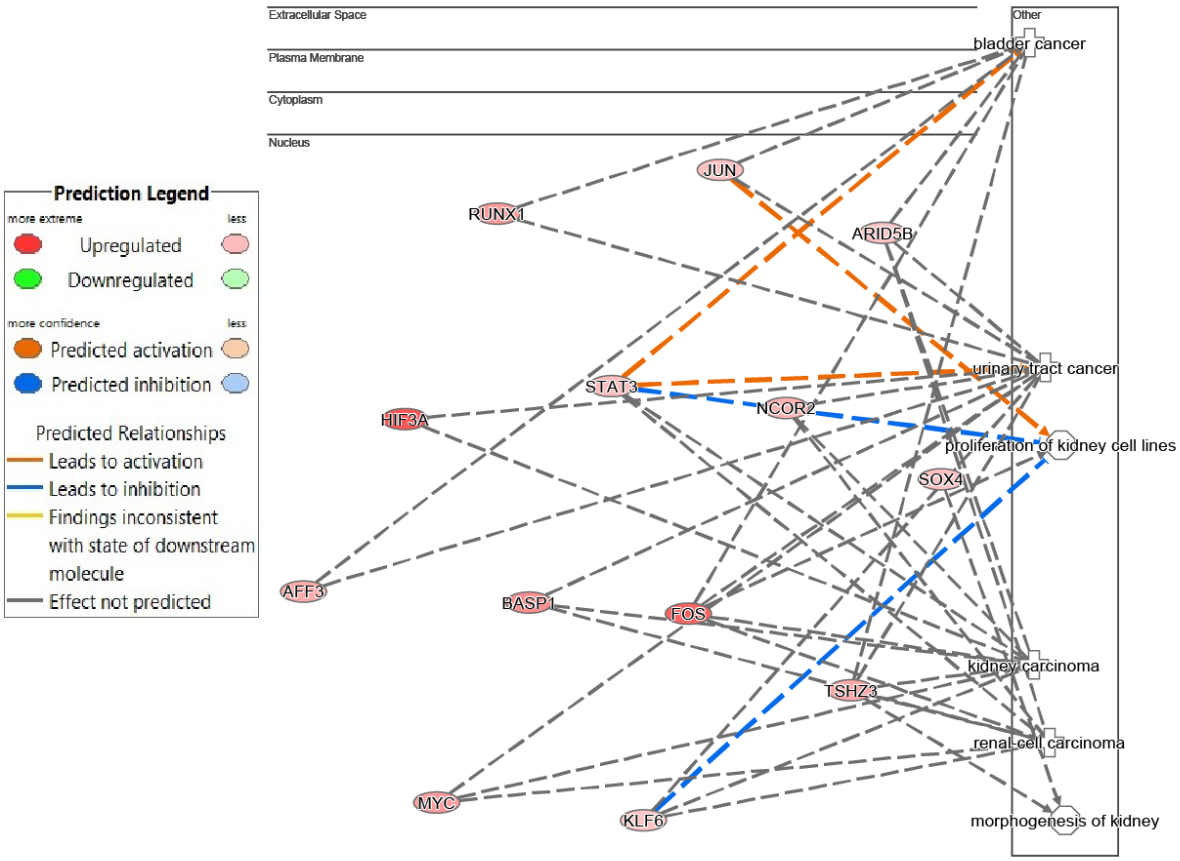

Fig 4.16 Differentially expressed transcription factors in *Nedd4-2*$^{-/-}$ kidneys involved in disease and function. The pathway map from top to bottom indicates genes localisation from extracellular space to plasma membrane to cytoplasm to nucleus. The disease and function are represented on the right, with the prediction legend on the left showing the genes up-regulated in red, with predicted activation of disease and function in orange, and inhibition represented in blue. The dashed lines in orange represent predicted activation, and dashed lines in blue are predicted to lead to inhibition. Yellow lines highlight inconsistent correlation between findings with downstream molecules. Dashed grey lines predicting no potential prediction for candidate genes on disease and function. Individual renal transcription factor differential genes for *Nedd4-2*$^{-/-}$ and *Nedd4-2*$^{+/+}$ are summarised in Supplementary Table **7.**

morphogenesis (**Fig 4.16)** (Summary of individual genes involved in the given diseased condition in Supplementary Table **7**).

4.4 Discussion

Renal dysplasia is a disorder characterised by transcriptional changes occurring within the kidney of the affected organism leading to alteration in the developmental processes predominantly involved in nephrogenesis of the kidney (Jain *et al*., 2007). Prior studies to understand these transcriptional changes have been undertaken in embryonic kidneys where the kidney is underdeveloped and undergoing differentiation. This study was the first to investigate this transcriptional regulation within the *Nedd4-2*$^{-/-}$ dysplastic kidneys at early post natal day 19, where the kidneys of these mice have undergone nephrogenesis but not through the complete developmental cascade, in comparison to adult kidneys which are matured and nehrogenesis has completely occurred.

To understand the transcriptional changes within the whole kidneys of early post natal day 19, *Nedd4-2*$^{-/-}$ kidneys were sequenced using next generation RNA sequencing platform. The genes were extracted using edgeR and Cuffdiff aligning them to the mouse genome for validity of the extracted gene list (Supplementary Table **1**). To aid in our understanding of the variation between the samples as stated in **Fig 4.1** the genes were input in SVD plot mapping, which confirmed our findings from Chapter **2** suggesting the higher phenotypic variability in *Nedd4-2*$^{-/-}$ in comparison to *Nedd4-2*$^{+/+}$. This gene expression variability between the *Nedd4-2*$^{-/-}$ kidneys could be attributed to various transcriptional changes specific to the dysplastic phenotype seen in these kidneys. This pattern of variation between animals was further confirmed by hierarchical clustering of heat maps using fold changes of significantly differentially expressed genes (fold changes >0 and >2) (**Fig 4.2** and supplementary **Fig 1**). The differential expression pattern of the same gene within the different kidney samples from

the *Nedd4-2*$^{-/-}$ mice was variable in comparison to the *Nedd4-2*$^{+/+}$, further confirming the genetic changes specific to the *Nedd4-2*$^{-/-}$ kidneys.

Investigations into the differences between the *Nedd4-2*$^{-/-}$ and control kidneys revealed that 370 genes were significantly up-regulated, and 167 genes significantly down-regulated in the *Nedd4-2*$^{-/-}$ kidneys (**Supplementary Fig 1**). These genes were hierarchically clustered further with fold changes >2 to highlight the correlation in the expression pattern and the gene clusters formed in the *Nedd4-2*$^{-/-}$ (**Fig 4.2),** aiding in our understanding of the similarity between the gene set population extracted based on their functions in the molecular processes involved like extracellular matrix modification, cell adhesion and gap junction formation few of the biological processes detailed below**.**

The DAVID database resource was further utilised to enable us to elucidate the molecular pathways significantly up-regulated and down-regulated in the *Nedd4-2*$^{-/-}$ kidneys (Fig **4.4A** and Fig **4.4B**). It was initially hypothesised that since these kidneys had been shown to have increased expression of polycystin-1in the collecting ducts, as reported in **Chapter 3,** the downstream effector signalling involving some of the canonical pathways involved in cell proliferation, apoptosis and cell cycle changes reported previously could be affected (Shillingford *et al*., 2006, Bhunia *et al*., 2002, Li *et al*., 2005, Lawrence *et al*., 2008). Indeed, pathways like p53 signalling, mTOR signalling, Jak-STAT signalling, cell cycle genes, calcium signalling, WNT signalling and MAPK signalling were found to be significantly up-regulated (**Fig 4.4A)**, consistent with upstream regulation of polycystin-1 in *Nedd4-2*$^{-/-}$ dysplastic kidneys. TGF beta signalling was also found to be significantly up-regulated in *Nedd4-2*$^{-/-}$ kidneys, aiding in epithelial-mesenchymal transition leading to renal fibrosis (as reported in **Chapter 2**), a hallmark of kidney dysplasia associated with transcriptomic reprogramming (Valcourt *et al*., 2005, Zeisberg and Kalluri, 2004). The pathways up-regulated in *Nedd4-2*$^{-/-}$ kidneys such as complement and coagulation cascade, cytokine

receptor interaction and chemokine signalling pathways have been suggested in human hydronephrosis models to accentuate kidney damage leading to increase in cytokine release (Henger *et al*., 2004, Jennette *et al*., 2014, Jain *et al*., 2007). Another study on foetal kidneys of congenital renal dysplasia suggested that an increase in inflammation and immune response genes was primarily considered as a secondary hit in renal dysplasia, with the primary hit being developmental (Henger *et al*., 2004, Jennette *et al*., 2014, Jain *et al*., 2007). Some of the pathways considered of importance in renal dysplasia are extracellular matrix interaction, focal adhesion molecules, gap junction, cell adhesion molecules involved in cell-cell communication, actin cytoskeleton and vascular smooth muscle contraction genes (required for EMT), all of which were significantly up-regulated in *Nedd4-2*$^{-/-}$ dysplastic kidneys (**Fig 4.4 A**), thereby validating the RNA sequencing strategy as well providing novel insights into the genetic makeup of *Nedd4-2*$^{-/-}$kidneys. To corroborate these findings GO (Gene ontology) analysis for biological process, cellular localisation and molecular function was performed, and up-regulation of cell adhesion, extracellular matrix reorganisation and cell activation pathways was again observed (**Fig 4.5 A**), with the cellular localisation of genes being primarily in the extracellular space and extracellular matrix (**Fig 4.5 C**). Calcium ion binding, metal ion binding, GTPase activity and polysaccharide binding were also up-regulated, leading to changes in processes like extracellular matrix interaction, focal adhesion, gap junction, cell adhesion (cell-cell communication), actin cytoskeleton and vascular smooth muscle contraction (**Fig 4.5 E**)

The pathways significantly down-regulated in the *Nedd4-2*$^{-/-}$ dysplastic kidney, as reported in **Fig 4.4 B,** showed decreased amino acid metabolism, possibly leading to mitochondrial dysfunctioning and causing metabolic disorder. Upstream PPaR signalling is required for amino acid metabolism, and PPAR signalling is significantly down-regulated in *Nedd4-2*$^{-/-}$ kidneys, which may account for the decreased amino acid metabolism observed (Kersten *et*

al., 2001, Liang and Ward, 2006, Rolo and Palmeira, 2006). The results from Chapter 2 (**Fig 2.11)** support these findings, as *Nedd4-2*$^{-/-}$ dysplastic kidneys showed a decrease in polysaccharides such as glycogen in the kidney, and this could be supported further by previous studies suggesting glycogen storage disorders are associated with renal diseases (Chen *et al*., 1988). Gene ontology analysis also identified significantly down-regulated genes in the *Nedd4-2*$^{-/-}$ kidneys involved in oxidation/reduction (**Fig 4.5 B**), with localisation primarily intrinsic to plasma membrane or within the mitochondria (**Fig 4.5 D)** and involved in symporter activity/sodium ion binding which could be aided (**Fig 4.5 E**) by the down-regulation of genes intrinsic to the mitochondrial functioning leading to dysregulation in metabolic pathways as reported in **Fig 4.4 B** causing altered amino acid metabolism and decreased polysaccharide accumalation**.**

To validate the significantly up-regulated genes from RNA sequencing involved in the processes in **Fig 4.4A** like cell adhesion, cell–cell communication, extracellular matrix modification and structural organisation, quantitative real time PCR and hierarchical clustering heat map analysis was performed (**Fig 4.6**). Genes chosen for validation include BMP-1 (bone morphogenetic protein-1), reported to increase collagen 1 synthesis which is affected in models of chronic kidney disease (CKD) with renal fibrosis and developmental processes, though role of BMP-1 in the kidney is still not very well characterised (Ge and Greenspan, 2006, Grgurevic *et al*., 2011). Col1a1 encodes collagen and plays an integral role in the extracellular matrix (Bateman *et al*., 2009). ADAM23 is a disintegrin involved in promoting cell adhesion (Cal *et al*., 2000). ITGAM (integrin alpha M) is expressed in tubular epithelial cells of kidney involved in cell-cell communication and cell adhesion (Kimberly *et al*., 2010). ICAM1 (intracellular adhesion molecule 1) is involved in cell-cell adhesion and tight junctions (Huber *et al*., 2001). FGA (fibrinogen alpha chain) is involved with cell adhesion and cell-cell communication (Kaysen *et al*., 1998). TGFB1 (transforming growth

factor beta 1) is involved in progressive renal fibrosis by inducing changes in the extracellular matrix by structural organisation, and the up-regulation seen here is consistent with our earlier findings from Chapter 2 (**Fig 2.8**) (Yamamoto *et al*., 1994). HB-EGF (Heparin binding- epidermal growth factor) which inhibits EGF (epidermal growth factor) was tested as complementation signalling was shown to be up-regulated in the *Nedd4-2*$^{-/-}$ kidneys (Kalmes *et al*., 2000). As seen in **Fig 4.6** and **Fig 4.7,** genes tested above showed an increasing trend in the *Nedd4-2*$^{-/-}$ kidneys, confirming our findings but with no statistical significance which could be attributed to the variability seen in the *Nedd4-2*$^{-/-}$ kidney phenotype and could be addressed with a larger sample size. Interestingly, previous studies on human patients with congenital renal dysplasia have shown a decrease in BMP-7, suggesting a possible role in biomarker detection. However no such previous work has highlighted the role of BMP-1 in the kidney, and it would be interesting to ascertain whether BMP-1 could be used as a biomarker for renal dysplasia, along with other target genes tested above to understand their potential role further in the *Nedd4-2*$^{-/-}$ kidneys. The genes involved in extracellular modification, cell adhesion, cell- cell communication and gap junction formation mentioned above play a critical role in renal dysplasia due to the adjacent renal parenchyma being affected leading to renal fibrosis a progressive disease aid in alteration of kidney function, possibly in the *Nedd4-2*$^{-/-}$ kidneys.

To aid in our initial understanding of kidney disease and their functional regulation in the processes, it was hypothesized that certain genes specifically up-regulated or down-regulated in the kidney aid in the different multiple processes involved in kidney disease. To assist in deciphering whether separate gene sets are up-regulated (**Fig 4.3 D, Fig 4.8**) and down-regulated (**Fig 4.3 C, Fig 4.11**), networks in ingenuity software with kidney centric annotations were overlapped. Genes were identified that were up-regulated and involved in discrete kidney processes including abnormal morphology of kidney (ATP12A (ATPase

12A), ALDH1A2 (Aldehyde dehydrogenase 1 member A2) , BGN (Biglycan), C1QA (Complement component 1), C3 (Complement component 3), C3AR1 (Complement component 3a receptor 1), CD44 (CD44 molecule), CDKN1A (Cyclin-dependent kinase inhibitor 1A), COL6A1(Collagen type 6 alpha 1), CSF1(Colony stimulating factor 1), CXCL14 (Chemokine ligand 14) and DACT (Dishevelled-binding antagonist of beta-catenin 3), formation of kidney (FREM1), kidney failure (FBLN1 and FGR), urinary tract development (DTX4), kidney damage (DCN), hypoplasia of kidney (ICAM1), quantity of renal glomerulus (SMOC2, SOX4, STAT3 and SULF1), proliferation of kidney cells (PTPR5), nephritis (NFKB2 and PARP3), kidney injury (LCN2) and interstitial fibrosis (MMP14, ITGAM, and ICAM1) (**Fig 4.9**). Some of these findings could be confirmed from our previous results, such as kidney proliferation (**Fig 2.6**) and interstitial fibrosis (**Fig 2.10**). However, the other findings need to be further investigated using specific genes involved in the above processes, such as immuno histological characterisation in *Nedd4-2*$^{-/-}$ kidneys. Based on these findings a potential up-regulated renal pathway map was constructed (**Fig 4.10**), and cytokine TGF beta 1 (**Fig 4.6**) was shown to stimulate downstream extracellular matrix modification, a secondary altercation of renal dysplasia. Our data supports this, as the downstream target of TGF beta 1, collagen-1, is up-regulated in *Nedd4-2*$^{-/-}$ kidneys **(Fig 2.9**). To investigate this further, kidney cells could be stimulated with TGF beta 1 upon Nedd4-2 depletion and changes in the downstream cascade as shown in **Fig 4.10** observed**.**

Processes significantly down-regulated in the *Nedd4-2*$^{-/-}$ kidney include urination disorder involving alteration in urine homeostasis attributed to some of the potential ion transporters (SLC34A3, SLC26A4 and SLC6A19), tubulointerstitial nephritis antigen (TINAG), transmembrane protein 27 (TMEM27) and retinol dehydrogenase 16 (all-trans) (BC089597). Hypoplasia of renal cortex (NOX4 and KL), kidney calcification (CAT) and development of metanephros (DIO1) are some of the other associated anomalies significantly down-

regulated, and these could also be attributed as some of the secondary changes due to defective development of the kidney. To further confirm these findings it would be imperative to use the conditional kidney specific *Nedd4-2*$^{-/-}$ model to repeat the experiment and compare with the above results obtained through bioinformatics analysis (**Fig 4.3 C, 4.11**). A potential pathway map generated from the list of significantly regulated genes suggests a possible role of PPAR gamma upstream involved in the process of activation of certain downstream targets such as CAT (Catalase), NOX4 (NADPH oxidase 4) and DIO1 (Deiodinase type 1) (**Fig 4.13**).

Kidney dysplasia is reported to be a transcriptionally driven developmental disorder, therefore it was imperative to understand the transcription factors composition within the *Nedd4-2*$^{-/-}$ kidneys (Woolf *et al*., 2004). Previous reports suggested the role of transcription factors like EYA1, SOX9 (Transcription Factor SOX 9), WT1, GATA3 (Trans acting T-cell specific transcription factor), LMX1B (LIM homeobox transcription factor beta), PAX 2/ 6/ 8 (Paired box transcription factors), HNF1β (Hepatocyte nuclear factor 1 beta), GLI3 and SALL-1 in various human syndromes associated with renal dysplastic kidneys (Woolf *et al*., 2004, Chen and Chang, 2015, Sanna-Cherchi *et al*., 2007). As reported in **Fig 4.14,** some of the downstream targets regulated by transcription factors in the *Nedd4-2*$^{-/-}$ post natal kidneys include CTNNB1(Catenin beta-1) , SP1, GLI1/2, ESR1, STAT3 and SMAD1/3. Previous reported transcription factors like WT1, JUN, HNF4A and TCF7L2 from studies in mid gestational foetal human kidney dysplasia were also shown to have a significant number of downstream target genes in the *Nedd4-2*$^{-/-}$ kidneys (Jain *et al*., 2007). These transcription factors need to be further validated *in vivo* to confirm the above findings.

Of particular interest are transcription factors SMAD 1/3 (Mothers against decapentaplegic homolog 1/3) and GLI1/2 (zinc finger protein 1/2). Previous studies have reported a crucial role for SMAD 3 in renal fibrosis, with SMAD 1 shown to be important in mediating signals

from bone morphogenetic proteins involved in renal dysplasia (Liu *et al*., 1996, Meng *et al*., 2010, Hu and Rosenblum, 2005). GLI 1/2 have been shown to be important in kidney patterning and when disrupted lead to alteration in renal morphogenesis (Hu *et al*., 2006).

The transcription factors significantly expressed in the *Nedd4-2*$^{-/-}$ kidney and their probable role in disease function was established *in silico* (**Fig 4.15** and **Fig 4.16**). Transcription factors SOX4 (SRY related transcription factor 4) and TSHZ3 (Teashirt homolog 3) were shown here to be involved in kidney morphogenesis. Previous reports on SOX4 has reported a role in normal renal development in mice (Huang *et al*., 2013). TSHZ3 mutant mice have been reported to suffer from pelvi–ureteric junction obstruction with defective smooth muscle differentiation (Jenkins *et al*., 2009). Other transcription factors identified by this *in silico* analysis were shown to be involved in renal cell carcinoma, urinary tract cancer or bladder cancer, highlighting their role in cell proliferation, and consistent with the increased cellular proliferation observed in P19 *Nedd4-2*$^{-/-}$ kidneys **(Fig 2.6).** It is important to establish the transcription factor regulation of target genes further to aid in the understanding of their mechanism of action *in vivo*.

In conclusion, in this study we highlight the novel gene expression differences in the *Nedd4-2*$^{-/-}$ post natal kidneys, corroborating previous findings as well as providing novel insights into the molecular pathways and gene signatures associated with transcription factor regulation necessary to understand the etiology of renal dysplasia. However several factors could alter the outcome of the study, including sample size, variability amongst samples, the biological significance of the gene signatures analysed, and the correlation to *in vivo* significance which will be discussed in detail in the following chapter.

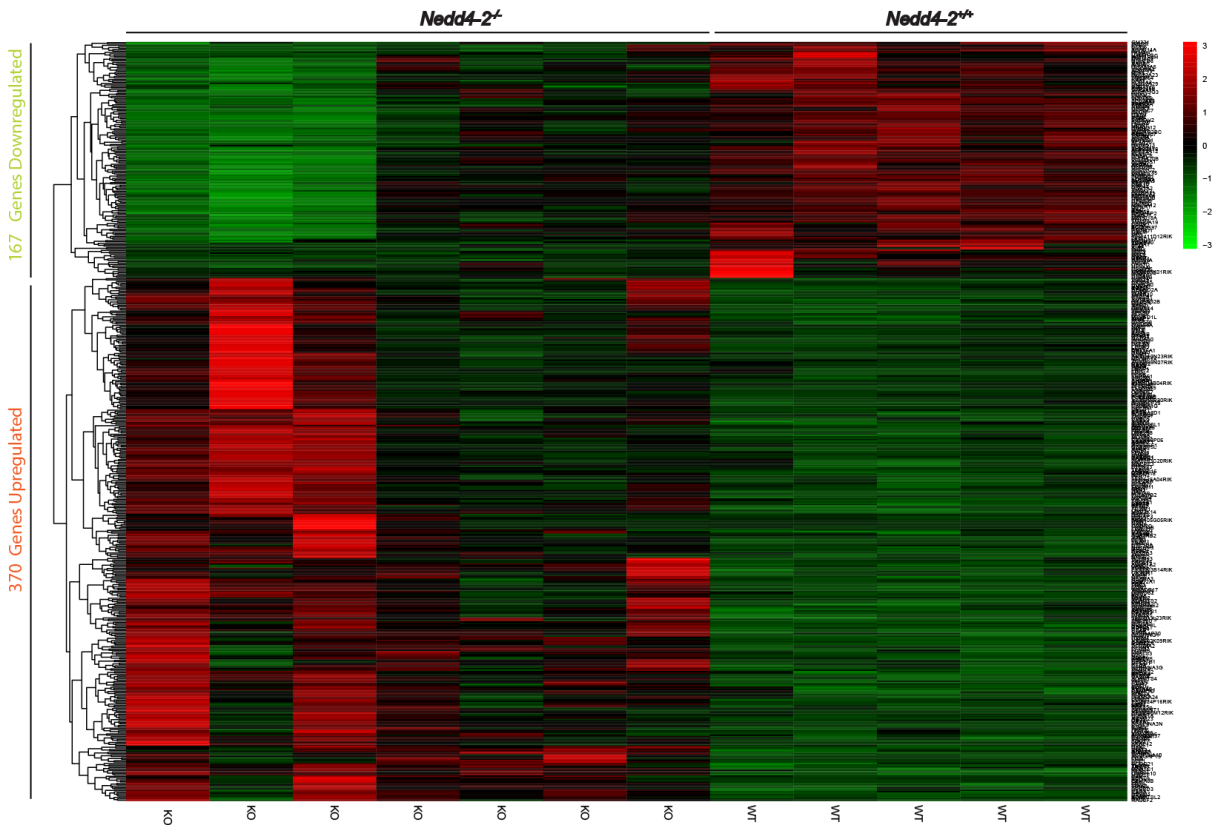

Supplementary Fig 1 Hierarchical clustering of differential expressed genes in *Nedd4-2*$^{-/-}$ kidneys. Heat map shows Log_2expression mean of > 0 fold change of significantly differentially expressed genes (FDR p-value <0.05) in *Nedd4-2*$^{-/-}$ (N=7, KO) versus *Nedd4-2*$^{+/+}$ (N=5, WT) kidneys. Red in heat map indicates up-regulated expression and green indicates down-regulated expression. Unannotated genes are indicated by their refseq numbers. The red pattern in the KO shows increased variability among samples as compared to WT. On the right is indicated colour code for green to red for increased gene fold change expression values. Genes differentially regulated are highlighted next to the respective lane on the right. There are 370 genes represented in red to be up-regulated significantly *Nedd4-2*$^{-/-}$ (N=7, KO). 167 genes represented in green are down-regulated significantly *Nedd4-2*$^{-/-}$ (N=7, KO). (Made using Supplementary Table **1**).

Chapter 5: Final Discussion

Chapter 5: Final Discussion

Nedd4-2/NEDD4L ubiquitin ligase has been reported to bind membrane associated proteins, especially ion channels and transporters (Scheffner and Kumar, 2014). One of the best characterised substrates of Nedd4-2 is ENaC (Scheffner and Kumar, 2014). *Nedd4-2* knock out (*Nedd4-2*$^{-/-}$) mice were generated in the laboratory and by others (Boase *et al*., 2011, Arroyo *et al*., 2011, Shi *et al*., 2008, Ronzaud *et al*., 2013, Kimura *et al*., 2011) have been crucial for investigating the role of Nedd4-2 mediated ENaC regulation in the physiological setting. The complete loss of Nedd4-2 in mice results in perinatal lethality and the survivors die by age P19-22 due to respiratory distress, partly due to increased ENaC activity resulting in drying of lung epithelia (Boase *et al*., 2011). Other than the lung, Nedd4-2 loss in kidney results in elevated ENaC, ROMK and NCC causing hypertension. Further analysis of Nedd4-2 loss in the kidney formed the basis of investigations reported in this thesis.

Current study:

The data presented in **Chapter 2** on the kidney phenotype extends on the previous work on the role Nedd4-2 plays in the physiological setting by Boase *et al* (2011) in the *Nedd4-2*$^{-/-}$ specifically in the lung. The results presented are the first evidence of renal cysts in the kidney of the *Nedd4-2*$^{-/-}$ mice, reported to be variable throughout the kidney. To investigate the importance of the cysts within the *Nedd4-2*$^{-/-}$ kidney, we initially hypothesized that this could be similar to polycystic kidney disease (PKD). Based on the evidence provided in **Chapter 2** it appears *Nedd4-2*$^{-/-}$ develop renal dysplasia, a developmental disorder, with few shared similarities with polycystic kidney disease.

In **Chapter 2**, we further report in *Nedd4-2*$^{-/-}$ mice epithelial transformation leads to renal fibrosis due to defects in adjacent renal parenchyma causing extra cellular matrix modification. This is further supported by data showing *Nedd4-2*$^{-/-}$ kidneys develop increased interstitial fibrosis, with collagen-1 accumulation around the cysts, an extracellular matrix protein responsible for cell adhesion and extracellular matrix modification for maintaining

tissue integrity. Apparent aberration within the kidney is a hallmark of kidney tissue damage, typically caused by adjacent renal parenchyma to intrude into the tubules and the collecting ducts, due to dilations of the tubules**.** The extracellular matrix components include sulphated and non sulphated glycosaminoglycans (polysaccharides) along with collagens, with reduced polysaccharides accumulation in *Nedd4-2*$^{-/-}$ kidneys. cAMP flux is a driver of downstream effector signalling of potential growth factors involved in cell proliferation and ion homeostasis. Consistent with this cAMP levels were up-regulated in the *Nedd4-2*$^{-/-}$ kidneys. The dysplastic kidneys were associated with multiple cysts originating from P2 associated with renal agenesis, with primitive ducts being cystic due to undifferentiated epithelium seen in *Nedd4-2*$^{-/-}$ (**Chapter 2**). These cysts originated from multiple segments within the ducts which could be large or small. Cysts are often associated with ciliary malfunctioning, and dysplastic *Nedd4-2*$^{-/-}$ kidneys display ciliary abnormalities around the cysts, with increased cilia in the dilated tubules reported in **Chapter 2**, highlighting the important role cilia plays in the dysplastic *Nedd4-2*$^{-/-}$ kidneys involved with cell-cell communication and cell junction recognition (Satir and Christensen, 2007).

These findings from **Chapter 2** lead us to investigate the role of polycystins (cyst proteins) in the *Nedd4-2*$^{-/-}$ dysplastic kidneys and their potential regulation mediated by Nedd4-2. In **Chapter 3** we reported increased expression of polycystin-1 in the IMCD cells with decrease in the levels of polycystin-2 upon Nedd4-2 ablation *in vitro*. The *in vitro* studies also suggested that Nedd4-2 mediates ubiquitination of polycystin-1, which could be inhibited in the presence of polycystin-2, known to form a calcium permeable ion channel with polycystin-1 on the plasma membrane (Koulen *et al*., 2002). These findings suggest that polycystin-1 is a novel substrate of Nedd4-2. Consistent with *in vitro* data, polycystin-1 was found to be over expressed in the collecting ducts and proximal tubules regions within the

Nedd4-2$^{-/-}$ dysplastic kidneys, establishing the physiological link between Nedd4-2 mediated regulation of polycystins and renal dysplasia (**Chapter 3**).

To explore the disease transcriptional signature associated with the *Nedd4-2*$^{-/-}$ renal phenotype an RNAseq study was undertaken in **Chapter 4**. It is one of the first such studies conducted on post natal kidneys to understand gene transcriptional changes responsible for renal dysplasia using next generation sequencing platform. We found that 370 genes were significantly up-regulated and 167 significantly differentially down-regulated. The major genetic pathways significantly up-regulated were TGFβ, Wnt signalling along with extracellular matrix interaction, cell adhesion (cell-cell communication) and cell junction formation. With genes involved in JAK-STAT signalling and cell cycle changes also shown to be up-regulated. This could be correlated with the polycystin-1 over expression (shown in **Chapter 3)** which is known to be upstream regulator of cell cycle and JAK-STAT signalling (Bhunia *et al*., 2002). 30 genes that were identified as being up-regulated in the *Nedd4-2*$^{-/-}$ kidneys were analysed *in silico* for their involvement in kidney disease and function and correlated with kidney pathology with roles in interstitial fibrosis, hypoplasia of kidney, congenital anomalies of kidney and urinary tract (CAKUT), proliferation of kidney cells, growth of kidney, kidney failure, kidney injury, kidney damage, nephritis, kidney formation, development of urinary tract and quantity of renal glomerulus. The genes reported to be significantly down-regulated included those involved in amino acid metabolism and glycolysis/gluconeogenesis, in mitochondrial function leading to metabolic disorders. The novel transcription factors altered in *Nedd4-2*$^{-/-}$ kidneys potentially involved with renal dysplasia such as SMAD 1/3, GLI1/2, SOX4 and TSHZ3 are known to play an important role in kidney pathology including fibrosis, morphogenesis and cell proliferation (validating findings from **Chapter 2**).

Since *Nedd4-2*$^{-/-}$ mice are postnatal lethal with only a limited number of survivors (which live to three weeks at most) it was not possible to fully characterise the phenotypes observed during the course of this PhD study. Therefore further studies will be crucial for understanding its role in kidney function, in addition to its previously characterised function in ENaC and NCC regulation and hypertension (Ronzaud *et al*., 2013). Studies are currently underway in the laboratory with kidney-specific *Nedd4-2*$^{-/-}$ to delineate the associated phenotypes.

Polycystin-1 has been shown to be involved in branching morphogenesis associated with ureteric bud formation, and linked to cystic kidney diseases with malformation in branching of the ureteric bud, also a hallmark of renal dysplastic kidneys (Polgar *et al*., 2005). In this thesis polycystin-1 was found to be to be ubiquitinated by Nedd4-2 and over expressed in the *Nedd4-2*$^{-/-}$ kidneys (**Chapter 3**), however the mechanism of interaction between Nedd4-2 and polycystin-1 remains to be elucidated. The evidence for this interaction needs to be strengthened and the potential role of polycystin-2 in this interaction elucidated, as we show in Chapter 3, *in vitro* experiments need to be performed with different N- and C- terminal over expression constructs for polycystin-1, in the absence and presence of both polycystin-2 and Nedd4-2 (or catalytically inactive Nedd4-2 mutant) to investigate the crucial co-assembly between polycystin-1/polycystin-2 to form calcium permeable channels on the membrane necessary for calcium ion homeostasis and kidney function (Koulen *et al*., 2002). Immunoprecipitation studies using these constructs should augur well to investigate these interactions, however it cannot be ruled out that the interaction between Nedd4-2 and polycystin-1 could also involve novel adaptor proteins such as Ndfip1/2. The Nedd4-2 mediated ubiquitination of polycystin-1 needs to be further explored as to whether it leads to polycystin-1 cleaved C-terminal product being internalised, required for its interaction with polycystin-2 at the endoplasmic reticulum and formation of calcium permeable ion channel

(Koulen *et al*., 2002), and whether polycystin-1 has a potential degradation signal causing either lysosomal or proteasomal degradation. Lysosome and proteasome specific inhibitors could be used in the course of the ubiquitination assay to assess this. The downstream signalling molecules induced through aberrant polycystin-1 regulation, such as the JAK-STAT and cell cycle genes identified via *in silico* analysis of transcriptional changes in *Nedd4-2*$^{-/-}$ kidneys, are potentially involved in renal development during kidney morphogenesis and renal tubule cell proliferation. However *in vivo* studies need to be performed to investigate expression of the individual renal transducers. In **Chapter 4**, as discussed earlier, there is transcriptional variability seen between P19 *Nedd4-2*$^{-/-}$ kidneys, which could be correlated to phenotypic variability. However the genes responsible for the phenotypic variation in the development of the renal dysplastic phenotype need to be further established. This could be done using iterative P19 *Nedd4-2*$^{-/-}$ kidney sample results for understanding the regulation of differentially expressed gene patterns in the cohort of *Nedd4-2*$^{-/-}$ kidneys and analysing the data using the ingenuity variant analysis package.

Conclusion and future work

This thesis has characterised some of the undefined functions of Nedd4-2 in renal pathophysiology. The work presented here highlights that Nedd4-2 abrogation aids in promoting renal dysplasia *in vivo* and one of the many potential substrates polycystin-1 is shown to drive the complexity of the given phenotype. With next generation sequencing data highlights the importance of gene expression and transcription factor regulation in the kidney, providing novel insights into the disease and function of the *Nedd4-2*$^{-/-}$ kidney.

However one of the major questions that require further attention is the developmental aspects of the disease (renal dysplasia) and the significance of Nedd4-2 during kidney development. Renal dysplasia is associated with developmental defects in ureteric bud branching during kidney development (Woolf *et al*., 2004) and association of Nedd4-2 in

kidney nephrogenesis at these embryonic developmental stages warrants further attention. Previous studies in mice with gain of function in β-catenin have reported ureteric branching defects (Bridgewater *et al*., 2011), which later develop into collecting ducts at the post natal stages within the kidney. Nedd4-2 is highly expressed within the collecting ducts of post natal kidneys (Loffing-Cueni *et al*., 2006). Collecting ducts develop from ureteric bud branching during kidney development (Bridgewater *et al*., 2011). Use of Hox b.7 cre specifically expressed within the embryonic stages of the ureteric bud development (Bridgewater *et al*., 2011) to generate a conditional *Nedd4-2* knockout mouse could highlight the potential substrate expression and kidney patterning defects during developmental stages of the kidney providing insights into the role of Nedd4-2 in kidney development.

Given the complexity of the renal phenotype observed it is likely that multiple substrates of Nedd4-2, including ion channels and transporters not reported previously, are deregulated and contribute to the disease. With the advent of new proteomics technologies like SILAC, (Twin-) Strep-tag purification expression system and iTRAQ, combined with affinity purification of ubiquitinated proteome (ubiquitome) may identify substrates of Nedd4-2 in the context of the kidney patholophysiology.

In summary, the findings in this thesis provide a novel insight into the pathophysiological function of Nedd4-2 in the kidney with establishment of its novel role in renal dysplasia. The work also identifies polycystin-1 as a potential new substrate with its wide ranging implications in understanding renal disease and developing therapeutic strategies for the future.

Chapter 6: Bibliography

Chapter 6: Bibliography

AL-AWQATI, Q. & OLIVER, J. A. 2002. Stem cells in the kidney. *Kidney international,* 61**,** 387-395.

ANDERS, S., PYL, P. T. & HUBER, W. 2014. HTSeq–A Python framework to work with high-throughput sequencing data. *Bioinformatics***,** btu638.

ASHBURNER, M., BALL, C. A., BLAKE, J. A., BOTSTEIN, D., BUTLER, H., CHERRY, J. M., DAVIS, A. P., DOLINSKI, K., DWIGHT, S. S. & EPPIG, J. T. 2000. Gene Ontology: tool for the unification of biology. *Nature genetics,* 25**,** 25-29.

BASSON, M. A., AKBULUT, S., WATSON-JOHNSON, J., SIMON, R., CARROLL, T. J., SHAKYA, R., GROSS, I., MARTIN, G. R., LUFKIN, T. & MCMAHON, A. P. 2005. Sprouty1 is a critical regulator of GDNF/RET-mediated kidney induction. *Developmental cell,* 8**,** 229-239.

BATEMAN, J. F., BOOT-HANDFORD, R. P. & LAMANDÉ, S. R. 2009. Genetic diseases of connective tissues: cellular and extracellular effects of ECM mutations. *Nature Reviews Genetics,* 10**,** 173-183.

BHUNIA, A. K., PIONTEK, K., BOLETTA, A., LIU, L., QIAN, F., XU, P.-N., GERMINO, F. J. & GERMINO, G. G. 2002. PKD1 induces p21 waf1 and regulation of the cell cycle via direct activation of the JAK-STAT signaling pathway in a process requiring PKD2. *Cell,* 109**,** 157-168.

CAL, S., FREIJE, J. M., LÓPEZ, J. M., TAKADA, Y. & LOPEZ-OTıN, C. 2000. ADAM 23/MDC3, a human disintegrin that promotes cell adhesion via interaction with the αvβ3 integrin through an RGD-independent mechanism. *Molecular biology of the cell,* 11**,** 1457-1469.

CARROLL, T. J., PARK, J.-S., HAYASHI, S., MAJUMDAR, A. & MCMAHON, A. P. 2005. Wnt9b plays a central role in the regulation of mesenchymal to epithelial transitions underlying organogenesis of the mammalian urogenital system. *Developmental cell,* 9**,** 283-292.

CHALLEN, G., GARDINER, B., CARUANA, G., KOSTOULIAS, X., MARTINEZ, G., CROWE, M., TAYLOR, D., BERTRAM, J., LITTLE, M. & GRIMMOND, S. 2005. Temporal and spatial transcriptional programs in murine kidney development. *Physiological genomics,* 23**,** 159-171.

CHANG, M., PARKER, E. A., MULLER, T. J., HAENEN, C., MISTRY, M., FINKIELSTAIN, G. P., MURPHY-RYAN, M., BARNES, K. M., SUNDARAM, R. & BARON, J. 2008. Changes in cell-cycle kinetics responsible for limiting somatic growth in mice. *Pediatric research,* 64**,** 240-245.

Chapter 6: Bibliography

CHEN, R.-Y. & CHANG, H. 2015. Renal dysplasia. *Archives of pathology & laboratory medicine,* 139**,** 547-551.

CHEN, Y.-T., COLEMAN, R. A., SCHEINMAN, J. I., KOLBECK, P. C. & SIDBURY, J. B. 1988. Renal disease in type I glycogen storage disease. *New England Journal of Medicine,* 318**,** 7-11.

CONSORTIUM, G. O. 2004. The Gene Ontology (GO) database and informatics resource. *Nucleic acids research,* 32**,** D258-D261.

COSTANTINI, F. & SHAKYA, R. 2006. GDNF/Ret signaling and the development of the kidney. *Bioessays,* 28**,** 117-127.

DANG, C. V., LE, A. & GAO, P. 2009. MYC-induced cancer cell energy metabolism and therapeutic opportunities. *Clinical cancer research,* 15**,** 6479-6483.

DENNIS JR, G., SHERMAN, B. T., HOSACK, D. A., YANG, J., GAO, W., LANE, H. C. & LEMPICKI, R. A. 2003. DAVID: database for annotation, visualization, and integrated discovery. *Genome biol,* 4**,** P3.

ESSAGHIR, A., TOFFALINI, F., KNOOPS, L., KALLIN, A., VAN HELDEN, J. & DEMOULIN, J.-B. 2010. Transcription factor regulation can be accurately predicted from the presence of target gene signatures in microarray gene expression data. *Nucleic acids research,* 38**,** e120-e120.

GE, G. & GREENSPAN, D. S. 2006. Developmental roles of the BMP1/TLD metalloproteinases. *Birth Defects Research Part C: Embryo Today: Reviews,* 78**,** 47-68.

GRGUREVIC, L., MACEK, B., HEALY, D. R., BRAULT, A. L., ERJAVEC, I., CIPCIC, A., GRGUREVIC, I., ROGIC, D., GALESIC, K. & BRKLJACIC, J. 2011. Circulating bone morphogenetic protein 1–3 isoform increases renal fibrosis. *Journal of the American Society of Nephrology,* 22**,** 681-692.

GRIESHAMMER, U., CEBRIÁN, C., ILAGAN, R., MEYERS, E., HERZLINGER, D. & MARTIN, G. R. 2005. FGF8 is required for cell survival at distinct stages of nephrogenesis and for regulation of gene expression in nascent nephrons. *Development,* 132**,** 3847-3857.

HENGER, A., KRETZLER, M., DORAN, P., BONROUHI, M., SCHMID, H., KISS, E., D COHEN, C., MADDEN, S., PORUBSKY, S. & GRÖNE, E. F. 2004. Gene expression fingerprints in human tubulointerstitial inflammation and fibrosis as prognostic markers of disease progression1. *Kidney international,* 65**,** 904-917.

HU, M. C., MO, R., BHELLA, S., WILSON, C. W., CHUANG, P.-T., HUI, C.-C. & ROSENBLUM, N. D. 2006. GLI3-dependent transcriptional repression of Gli1, Gli2 and kidney patterning genes disrupts renal morphogenesis. *Development,* 133**,** 569-578.

HU, M. C. & ROSENBLUM, N. D. 2005. Smad1, β-catenin and Tcf4 associate in a molecular complex with the Myc promoter in dysplastic renal tissue and cooperate to control Myc transcription. *Development,* 132**,** 215-225.

HUANG, J., ARSENAULT, M., KANN, M., LOPEZ-MENDEZ, C., SALEH, M., WADOWSKA, D., TAGLIENTI, M., HO, J., MIAO, Y. & SIMS, D. 2013. The transcription factor sry-related HMG box-4 (SOX4) is required for normal renal development in vivo. *Developmental Dynamics,* 242**,** 790-799.

HUBER, J. D., EGLETON, R. D. & DAVIS, T. P. 2001. Molecular physiology and pathophysiology of tight junctions in the blood–brain barrier. *Trends in neurosciences,* 24**,** 719-725.

ICHIKAWA, I., KUWAYAMA, F., POPE, J. C., STEPHENS, F. D. & MIYAZAKI, Y. 2002. Paradigm shift from classic anatomic theories to contemporary cell biological views of CAKUT. *Kidney international,* 61**,** 889-898.

JAIN, S., ENCINAS, M., JOHNSON, E. M. & MILBRANDT, J. 2006. Critical and distinct roles for key RET tyrosine docking sites in renal development. *Genes & development,* 20**,** 321-333.

JAIN, S., SUAREZ, A. A., MCGUIRE, J. & LIAPIS, H. 2007. Expression profiles of congenital renal dysplasia reveal new insights into renal development and disease. *Pediatric nephrology,* 22**,** 962-974.

JENKINS, D., CAUBIT, X., DIMOVSKI, A., MATEVSKA, N., LYE, C. M., CABUK, F., GUCEV, Z., TASIC, V., FASANO, L. & WOOLF, A. S. 2009. Analysis of TSHZ2 and TSHZ3 genes in congenital pelvi-ureteric junction obstruction. *Nephrology Dialysis Transplantation***,** gfp453.

JENNETTE, J. C., D'AGATI, V. D., OLSON, J. L. & SILVA, F. G. 2014. *Heptinstall's Pathology of the Kidney*, Lippincott Williams & Wilkins.

JONES, E., OLIPHANT, T. & PETERSON, P. 2014. {SciPy}: Open source scientific tools for {Python}.

KALMES, A., VESTI, B. R., DAUM, G., ABRAHAM, J. A. & CLOWES, A. W. 2000. Heparin blockade of thrombin-induced smooth muscle cell migration involves inhibition of

epidermal growth factor (EGF) receptor transactivation by heparin-binding EGF-like growth factor. *Circulation research,* 87**,** 92-98.

KATSO, R., OKKENHAUG, K., AHMADI, K., WHITE, S., TIMMS, J. & WATERFIELD, M. D. 2001. Cellular function of phosphoinositide 3-kinases: implications for development, immunity, homeostasis, and cancer. *Annual review of cell and developmental biology,* 17**,** 615-675.

KAYSEN, G. A., DE MEER, K., STELLAARD, F., VOORBIJ, H. A., REIJNGOUD, D.-J., RABELINK, T. J. & KOOMANS, H. A. 1998. Proportionate increase of fibrinogen and albumin synthesis in nephrotic patients: measurements with stable isotopes. *Kidney international,* 53**,** 181-188.

KERSTEN, S., MANDARD, S., ESCHER, P., GONZALEZ, F. J., TAFURI, S., DESVERGNE, B. & WAHLI, W. 2001. The peroxisome proliferator-activated receptor α regulates amino acid metabolism. *The FASEB Journal,* 15**,** 1971-1978.

KIM, D., PERTEA, G., TRAPNELL, C., PIMENTEL, H., KELLEY, R. & SALZBERG, S. L. 2013. TopHat2: accurate alignment of transcriptomes in the presence of insertions, deletions and gene fusions. *Genome Biol,* 14**,** R36.

KIMBERLY, J. A., GUTHRIDGE, J. M., HARLEY, J. B. & NATH, S. K. 2010. ITGAM coding variant (rs1143679) influences the risk of renal disease, discoid rash, and immunologic manifestations in lupus patients with European ancestry. *Ann Rheum Dis,* 69**,** 1329-1332.

KISPERT, A., VAINIO, S. & MCMAHON, A. P. 1998. Wnt-4 is a mesenchymal signal for epithelial transformation of metanephric mesenchyme in the developing kidney. *Development,* 125**,** 4225-4234.

KOBAYASHI, A., KWAN, K.-M., CARROLL, T. J., MCMAHON, A. P., MENDELSOHN, C. L. & BEHRINGER, R. R. 2005. Distinct and sequential tissue-specific activities of the LIM-class homeobox gene Lim1 for tubular morphogenesis during kidney development. *Development,* 132**,** 2809-2823.

KOHLHASE, J., WISCHERMANN, A., REICHENBACH, H., FROSTER, U. & ENGEL, W. 1998. Mutations in the SALL1 putative transcription factor gene cause Townes-Brocks syndrome. *Nature genetics,* 18**,** 81-83.

LAWRENCE, M. C., JIVAN, A., SHAO, C., DUAN, L., GOAD, D., ZAGANJOR, E., OSBORNE, J., MCGLYNN, K., STIPPEC, S. & EARNEST, S. 2008. The roles of MAPKs in disease. *Cell research,* 18**,** 436-442.

LI, X., LUO, Y., STARREMANS, P. G., MCNAMARA, C. A., PEI, Y. & ZHOU, J. 2005. Polycystin-1 and polycystin-2 regulate the cell cycle through the helix–loop–helix inhibitor Id2. *Nature cell biology,* 7**,** 1202-1212.

LIANG, H. & WARD, W. F. 2006. PGC-1α: a key regulator of energy metabolism. *Advances in physiology education,* 30**,** 145-151.

LIAPIS, H. 2003. Biology of congenital obstructive nephropathy. *Nephron Experimental Nephrology,* 93**,** e87-e91.

LIAPIS, H., DOSHI, R. H., WATSON, M. A., LIAPIS, A. & STEINHARDT, G. F. 2002. Reduced renin expression and altered gene transcript profiles in multicystic dysplastic kidneys. *The Journal of urology,* 168**,** 1816-1820.

LIPSCHUTZ, J. H. 1998. Molecular development of the kidney: a review of the results of gene disruption studies. *American journal of kidney diseases,* 31**,** 383-397.

LIU, F., HATA, A., BAKER, J. C., DOODY, J., CÁRCAMO, J., HARLAND, R. M. & MASSAGUÉ, J. 1996. A human Mad protein acting as a BMP-regulated transcriptional activator. *Nature,* 381**,** 620-623.

LIU, P., CHENG, H., ROBERTS, T. M. & ZHAO, J. J. 2009. Targeting the phosphoinositide 3-kinase pathway in cancer. *Nature reviews Drug discovery,* 8**,** 627-644.

LOIRAT, C. 2001. [Chronic renal insufficiency in children]. *La Revue du praticien,* 51**,** 410-416.

MARTIN, M. 2011. Cutadapt removes adapter sequences from high-throughput sequencing reads. *EMBnet. journal,* 17**,** pp. 10-12.

MENG, X. M., HUANG, X. R., CHUNG, A. C., QIN, W., SHAO, X., IGARASHI, P., JU, W., BOTTINGER, E. P. & LAN, H. Y. 2010. Smad2 protects against TGF-β/Smad3-mediated renal fibrosis. *Journal of the American Society of Nephrology,* 21**,** 1477-1487.

NISHIMURA, H., YERKES, E., HOHENFELLNER, K., MIYAZAKI, Y., MA, J., HUNLEY, T. E., YOSHIDA, H., ICHIKI, T., THREADGILL, D. & PHILLIPS, J. A. 1999. Role of the angiotensin type 2 receptor gene in congenital anomalies of the kidney and urinary tract, CAKUT, of mice and men. *Molecular cell,* 3**,** 1-10.

PILIA, G., HUGHES-BENZIE, R. M., MACKENZIE, A., BAYBAYAN, P., CHEN, E. Y., HUBER, R., NERI, G., CAO, A., FORABOSCO, A. & SCHLESSINGER, D. 1996.

Mutations in GPC3, a glypican gene, cause the Simpson-Golabi-Behmel overgrowth syndrome. *Nature genetics,* 12**,** 241-247.

PORTEOUS, S., TORBAN, E., CHO, N.-P., CUNLIFFE, H., CHUA, L., MCNOE, L., WARD, T., SOUZA, C., GUS, P. & GIUGLIANI, R. 2000. Primary renal hypoplasia in humans and mice with PAX2 mutations: evidence of increased apoptosis in fetal kidneys of Pax21Neu+/–mutant mice. *Human molecular genetics,* 9**,** 1-11.

ROBINSON, M. D., MCCARTHY, D. J. & SMYTH, G. K. 2010. edgeR: a Bioconductor package for differential expression analysis of digital gene expression data. *Bioinformatics,* 26**,** 139-140.

ROLO, A. P. & PALMEIRA, C. M. 2006. Diabetes and mitochondrial function: role of hyperglycemia and oxidative stress. *Toxicology and applied pharmacology,* 212**,** 167-178.

SANNA-CHERCHI, S., CARIDI, G., WENG, P. L., SCOLARI, F., PERFUMO, F., GHARAVI, A. G. & GHIGGERI, G. M. 2007. Genetic approaches to human renal agenesis/hypoplasia and dysplasia. *Pediatric nephrology,* 22**,** 1675-1684.

SAXÉN, L. & SARIOLA, H. 1987. Early organogenesis of the kidney. *Pediatric nephrology,* 1**,** 385-392.

SCHWAB, K., PATTERSON, L. T., ARONOW, B. J., LUCKAS, R., LIANG, H.-C. & POTTER, S. S. 2003. A catalogue of gene expression in the developing kidney. *Kidney international,* 64**,** 1588-1604.

SHILLINGFORD, J. M., MURCIA, N. S., LARSON, C. H., LOW, S. H., HEDGEPETH, R., BROWN, N., FLASK, C. A., NOVICK, A. C., GOLDFARB, D. A. & KRAMER-ZUCKER, A. 2006. The mTOR pathway is regulated by polycystin-1, and its inhibition reverses renal cystogenesis in polycystic kidney disease. *Proceedings of the National Academy of Sciences,* 103**,** 5466-5471.

SINGER, D. B. 1991. *Textbook of fetal and perinatal pathology*, Blackwell Science Incorporated.

STARK, K., VAINIO, S., VASSILEVA, G. & MCMAHON, A. P. 1994. Epithelial transformation of metanephric mesenchyme in the developing kidney regulated by Wnt-4. *Nature,* 372**,** 679-683.

STUART, R. O., BUSH, K. T. & NIGAM, S. K. 2001. Changes in global gene expression patterns during development and maturation of the rat kidney. *Proceedings of the National Academy of Sciences,* 98**,** 5649-5654.

TRAPNELL, C., HENDRICKSON, D. G., SAUVAGEAU, M., GOFF, L., RINN, J. L. & PACHTER, L. 2013. Differential analysis of gene regulation at transcript resolution with RNA-seq. *Nature biotechnology,* 31**,** 46-53.

VALCOURT, U., KOWANETZ, M., NIIMI, H., HELDIN, C.-H. & MOUSTAKAS, A. 2005. TGF-β and the Smad signaling pathway support transcriptomic reprogramming during epithelial-mesenchymal cell transition. *Molecular biology of the cell,* 16**,** 1987-2002.

WEBER, S., MORINIERE, V., KNÜPPEL, T., CHARBIT, M., DUSEK, J., GHIGGERI, G. M., JANKAUSKIENÉ, A., MIR, S., MONTINI, G. & PECO-ANTIC, A. 2006. Prevalence of mutations in renal developmental genes in children with renal hypodysplasia: results of the ESCAPE study. *Journal of the American Society of Nephrology,* 17**,** 2864-2870.

WERNER, T. 2008. Bioinformatics applications for pathway analysis of microarray data. *Current opinion in biotechnology,* 19**,** 50-54.

WOOLF, A. S., PRICE, K. L., SCAMBLER, P. J. & WINYARD, P. J. 2004. Evolving concepts in human renal dysplasia. *Journal of the American Society of Nephrology,* 15**,** 998-1007.

WU, B., SAHOO, D. & BROOKS, J. D. 2013. Comprehensive Gene Expression Changes Associated with Mouse Postnatal Kidney Development. *The Journal of urology,* 189**,** 2385-2390.

YAMAMOTO, T., NOBLE, N. A., MILLER, D. E. & BORDER, W. A. 1994. Sustained expression of TGF-bold beta 1 underlies development of progressive kidney fibrosis. *Kidney international,* 45**,** 916-927.

ZEISBERG, M. & KALLURI, R. 2004. The role of epithelial-to-mesenchymal transition in renal fibrosis. *Journal of Molecular Medicine,* 82**,** 175-181.

ZHANG, J. D. & WIEMANN, S. 2009. KEGGgraph: a graph approach to KEGG PATHWAY in R and bioconductor. *Bioinformatics,* 25**,** 1470-1471.

AL-AWQATI, Q. & OLIVER, J. A. 2002. Stem cells in the kidney. *Kidney international,* 61**,** 387-395.

ALBESA, M., GRILO, L. S., GAVILLET, B. & ABRIEL, H. 2011. Nedd4-2-dependent ubiquitylation and regulation of the cardiac potassium channel hERG1. *J Mol Cell Cardiol,* 51**,** 90-8.

Chapter 6: Bibliography

ALZAMORA, R., GONG, F., RONDANINO, C., LEE, J. K., SMOLAK, C., PASTOR-SOLER, N. M. & HALLOWS, K. R. 2010. AMP-activated protein kinase inhibits KCNQ1 channels through regulation of the ubiquitin ligase Nedd4-2 in renal epithelial cells. *Am J Physiol Renal Physiol,* 299**,** F1308-19.

AMIRLAK, I. & DAWSON, K. 2000. Bartter syndrome: an overview. *Qjm,* 93**,** 207-215.

ANDERS, S., PYL, P. T. & HUBER, W. 2014. HTSeq–A Python framework to work with high-throughput sequencing data. *Bioinformatics***,** btu638.

ANDRE, B. & SPRINGAEL, J. Y. 1994. WWP, a new amino acid motif present in single or multiple copies in various proteins including dystrophin and the SH3-binding Yes-associated protein YAP65. *Biochemical and biophysical research communications,* 205**,** 1201-1205.

ARAÇ, D., BOUCARD, A. A., BOLLIGER, M. F., NGUYEN, J., SOLTIS, S. M., SÜDHOF, T. C. & BRUNGER, A. T. 2012. A novel evolutionarily conserved domain of cell-adhesion GPCRs mediates autoproteolysis. *The EMBO journal,* 31**,** 1364-1378.

ARAKI, N., UMEMURA, M., MIYAGI, Y., YABANA, M., MIKI, Y., TAMURA, K., UCHINO, K., AOKI, R., GOSHIMA, Y., UMEMURA, S. & ISHIGAMI, T. 2008. Expression, transcription, and possible antagonistic interaction of the human Nedd4L gene variant: implications for essential hypertension. *Hypertension,* 51**,** 773-7.

ARROYO, J. P., LAGNAZ, D., RONZAUD, C., VAZQUEZ, N., KO, B. S., MODDES, L., RUFFIEUX-DAIDIE, D., HAUSEL, P., KOESTERS, R., YANG, B., STOKES, J. B., HOOVER, R. S., GAMBA, G. & STAUB, O. 2011. Nedd4-2 modulates renal Na+-Cl- cotransporter via the aldosterone-SGK1-Nedd4-2 pathway. *J Am Soc Nephrol,* 22**,** 1707-19.

ASHBURNER, M., BALL, C. A., BLAKE, J. A., BOTSTEIN, D., BUTLER, H., CHERRY, J. M., DAVIS, A. P., DOLINSKI, K., DWIGHT, S. S. & EPPIG, J. T. 2000. Gene Ontology: tool for the unification of biology. *Nature genetics,* 25**,** 25-29.

ATIYEH, B., HUSMANN, D. & BAUM, M. 1992. Contralateral renal abnormalities in multicystic-dysplastic kidney disease. *The Journal of pediatrics,* 121**,** 65-67.

BASSON, M. A., AKBULUT, S., WATSON-JOHNSON, J., SIMON, R., CARROLL, T. J., SHAKYA, R., GROSS, I., MARTIN, G. R., LUFKIN, T. & MCMAHON, A. P. 2005. Sprouty1 is a critical regulator of GDNF/RET-mediated kidney induction. *Developmental cell,* 8**,** 229-239.

BASTOS, A. P., PIONTEK, K., SILVA, A. M., MARTINI, D., MENEZES, L. F., FONSECA, J. M., FONSECA, I. I., GERMINO, G. G. & ONUCHIC, L. F. 2009. Pkd1 haploinsufficiency increases renal damage and induces microcyst formation following ischemia/reperfusion. *Journal of the American Society of Nephrology,* 20**,** 2389-2402.

BATEMAN, A. & SANDFORD, R. 1999. The PLAT domain: a new piece in the PKD1 puzzle. *Current biology,* 9**,** R588-S2.

BATEMAN, J. F., BOOT-HANDFORD, R. P. & LAMANDÉ, S. R. 2009. Genetic diseases of connective tissues: cellular and extracellular effects of ECM mutations. *Nature Reviews Genetics,* 10**,** 173-183.

BHALLA, V., DAIDIE, D., LI, H., PAO, A. C., LAGRANGE, L. P., WANG, J., VANDEWALLE, A., STOCKAND, J. D., STAUB, O. & PEARCE, D. 2005. Serum- and glucocorticoid-regulated kinase 1 regulates ubiquitin ligase neural precursor cell-expressed, developmentally down-regulated protein 4-2 by inducing interaction with 14-3-3. *Mol Endocrinol,* 19**,** 3073-84.

BHALLA, V. & HALLOWS, K. R. 2008. Mechanisms of ENaC regulation and clinical implications. *J Am Soc Nephrol,* 19**,** 1845-1854.

BHUNIA, A. K., PIONTEK, K., BOLETTA, A., LIU, L., QIAN, F., XU, P.-N., GERMINO, F. J. & GERMINO, G. G. 2002. PKD1 induces p21 waf1 and regulation of the cell cycle via direct activation of the JAK-STAT signaling pathway in a process requiring PKD2. *Cell,* 109**,** 157-168.

BLANCO, G. & WALLACE, D. P. 2013. Novel role of ouabain as a cystogenic factor in autosomal dominant polycystic kidney disease. *American Journal of Physiology-Renal Physiology,* 305**,** F797-F812.

BOASE, N. A., RYCHKOV, G. Y., TOWNLEY, S. L., DINUDOM, A., CANDI, E., VOSS, A. K., TSOUTSMAN, T., SEMSARIAN, C., MELINO, G., KOENTGEN, F., COOK, D. I. & KUMAR, S. 2011. Respiratory distress and perinatal lethality in Nedd4-2-deficient mice. *Nat Commun,* 2**,** 287.

BOEHMER, C., HENKE, G., SCHNIEPP, R., PALMADA, M., ROTHSTEIN, J. D., BROER, S. & LANG, F. 2003. Regulation of the glutamate transporter EAAT1 by the ubiquitin ligase Nedd4-2 and the serum and glucocorticoid-inducible kinase isoforms SGK1/3 and protein kinase B. *J Neurochem,* 86**,** 1181-8.

BOEHMER, C., PALMADA, M., RAJAMANICKAM, J., SCHNIEPP, R., AMARA, S. & LANG, F. 2006. Post-translational regulation of EAAT2 function by co-expressed ubiquitin ligase Nedd4-2 is impacted by SGK kinases. *J Neurochem,* 97**,** 911-21.

BONIFACINO, J. S. & WEISSMAN, A. M. 1998. Ubiquitin and the control of protein fate in the secretory and endocytic pathways 1. *Annual review of cell and developmental biology,* 14**,** 19-57.

BOOKEN, N., GRATCHEV, A., UTIKAL, J., WEISS, C., YU, X., QADOUMI, M., SCHMUTH, M., SEPP, N., NASHAN, D., RASS, K., TUTING, T., ASSAF, C., DIPPEL, E., STADLER, R., KLEMKE, C. D. & GOERDT, S. 2008. Sezary syndrome is a unique cutaneous T-cell lymphoma as identified by an expanded gene signature including diagnostic marker molecules CDO1 and DNM3. *Leukemia,* 22**,** 393-9.

Chapter 6: Bibliography

BORDEN, K. L. & FREEMONT, P. S. 1996. The RING finger domain: a recent example of a sequence—structure family. *Current opinion in structural biology,* 6**,** 395-401.

BOUCHER, C. A., WARD, H. H., CASE, R. L., THURSTON, K. S., LI, X., NEEDHAM, A., ROMERO, E., HYINK, D., QAMAR, S. & ROITBAK, T. 2011. Receptor protein tyrosine phosphatases are novel components of a polycystin complex. *Biochimica et Biophysica Acta (BBA)-Molecular Basis of Disease,* 1812**,** 1225-1238.

BRIDGES, D. & MOORHEAD, G. B. 2005. 14-3-3 proteins: a number of functions for a numbered protein. *Science Signaling,* 2005**,** re10.

BRIDGEWATER, D., DI GIOVANNI, V., CAIN, J. E., COX, B., JAKOBSON, M., SAINIO, K. & ROSENBLUM, N. D. 2011. β-catenin causes renal dysplasia via upregulation of Tgfβ2 and Dkk1. *Journal of the American Society of Nephrology,* 22**,** 718-731.

BRUCE, M., KANELIS, V., FOULADKOU, F., DEBONNEVILLE, A., STAUB, O. & ROTIN, D. 2008. Regulation of Nedd4-2 self-ubiquitination and stability by a PY motif located within its HECT-domain. *Biochem. J,* 415**,** 155-163.

BYCROFT, M., BATEMAN, A., CLARKE, J., HAMILL, S. J., SANDFORD, R., THOMAS, R. L. & CHOTHIA, C. 1999. The structure of a PKD domain from polycystin-1: implications for polycystic kidney disease. *The EMBO journal,* 18**,** 297-305.

CACHEMAILLE, M., LAEDERMANN, C. J., PERTIN, M., ABRIEL, H., GOSSELIN, R. D. & DECOSTERD, I. 2012. Neuronal expression of the ubiquitin ligase Nedd4-2 in rat dorsal root ganglia: modulation in the spared nerve injury model of neuropathic pain. *Neuroscience,* 227**,** 370-80.

CAI, Y., ANYATONWU, G., OKUHARA, D., LEE, K.-B., YU, Z., ONOE, T., MEI, C.-L., QIAN, Q., GENG, L. & WIZTGALL, R. 2004. Calcium dependence of polycystin-2 channel activity is modulated by phosphorylation at Ser812. *Journal of Biological Chemistry,* 279**,** 19987-19995.

CAI, Y., FEDELES, S. V., DONG, K., ANYATONWU, G., ONOE, T., MITOBE, M., GAO, J.-D., OKUHARA, D., TIAN, X. & GALLAGHER, A.-R. 2014. Altered trafficking and stability of polycystins underlie polycystic kidney disease. *The Journal of clinical investigation,* 124**,** 5129.

CAI, Y. & SOMLO, S. 2008. Too much of a good thing: does Nek8 link polycystic kidney disease and nephronophthisis? *Journal of the American society of nephrology,* 19**,** 418-420.

CAL, S., FREIJE, J. M., LÓPEZ, J. M., TAKADA, Y. & LOPEZ-OTıN, C. 2000. ADAM 23/MDC3, a human disintegrin that promotes cell adhesion via interaction with the αvβ3 integrin through an RGD-independent mechanism. *Molecular biology of the cell,* 11**,** 1457-1469.

CANESSA, C. M., SCHILD, L., BUELL, G., THORENS, B., GAUTSCHI, I., HORISBERGER, J.-D. & ROSSIER, B. C. 1994. Amiloride-sensitive epithelial Na+ channel is made of three homologous subunits. *Nature,* 367**,** 463-467.

CAOHUY, H., JOZWIK, C. & POLLARD, H. B. 2009. Rescue of DeltaF508-CFTR by the SGK1/Nedd4-2 signaling pathway. *J Biol Chem,* 284**,** 25241-53.

CARROLL, T. J., PARK, J.-S., HAYASHI, S., MAJUMDAR, A. & MCMAHON, A. P. 2005. Wnt9b plays a central role in the regulation of mesenchymal to epithelial transitions underlying organogenesis of the mammalian urogenital system. *Developmental cell,* 9**,** 283-292.

CHALLEN, G., GARDINER, B., CARUANA, G., KOSTOULIAS, X., MARTINEZ, G., CROWE, M., TAYLOR, D., BERTRAM, J., LITTLE, M. & GRIMMOND, S. 2005. Temporal and spatial transcriptional programs in murine kidney development. *Physiological genomics,* 23**,** 159-171.

CHAN, W., TIAN, R., LEE, Y. F., SIT, S. T., LIM, L. & MANSER, E. 2009. Down-regulation of active ACK1 is mediated by association with the E3 ubiquitin ligase Nedd4-2. *J Biol Chem,* 284**,** 8185-94.

CHANG, M.-Y. & ONG, A. C. 2008. Autosomal dominant polycystic kidney disease: recent advances in pathogenesis and treatment. *Nephron Physiology,* 108**,** p1-p7.

CHANG, M., PARKER, E. A., MULLER, T. J., HAENEN, C., MISTRY, M., FINKIELSTAIN, G. P., MURPHY-RYAN, M., BARNES, K. M., SUNDARAM, R. & BARON, J. 2008. Changes in cell-cycle kinetics responsible for limiting somatic growth in mice. *Pediatric research,* 64**,** 240-245.

CHAPIN, H. C., RAJENDRAN, V. & CAPLAN, M. J. 2010. Polycystin-1 surface localization is stimulated by polycystin-2 and cleavage at the G protein-coupled receptor proteolytic site. *Molecular biology of the cell,* 21**,** 4338-4348.

CHEN, H., ROSS, C. A., WANG, N., HUO, Y., MACKINNON, D. F., POTASH, J. B., SIMPSON, S. G., MCMAHON, F. J., DEPAULO JR, J. R. & MCINNIS, M. G. 2001. NEDD4L on human chromosome 18q21 has multiple forms of transcripts and is a homologue of the mouse Nedd4-2 gene. *Eur J Hum Genet,* 9**,** 922-30.

CHEN, R.-Y. & CHANG, H. 2015. Renal dysplasia. *Archives of pathology & laboratory medicine,* 139**,** 547-551.

CHEN, Y.-T. & BURCHELL, A. 1998. Glycogen storage diseases. *HARRISONS PRINCIPLES OF INTERNAL MEDICINE***,** 2176-2182.

CHEN, Y.-T., COLEMAN, R. A., SCHEINMAN, J. I., KOLBECK, P. C. & SIDBURY, J. B. 1988. Renal disease in type I glycogen storage disease. *New England Journal of Medicine,* 318**,** 7-11.

CHMIELEWSKI, C. 2003. Renal anatomy and overview of nephron function. *Nephrology nursing journal,* 30**,** 185.

CHUNG, H. Y., MORITA, E., VON SCHWEDLER, U., MULLER, B., KRAUSSLICH, H. G. & SUNDQUIST, W. I. 2008. NEDD4L overexpression rescues the release and infectivity of human immunodeficiency virus type 1 constructs lacking PTAP and YPXL late domains. *J Virol,* 82**,** 4884-97.

CIECHANOVER, A., EVERETT, R. D., ORR, A., PRESTON, C. M., ARNOLD, I., PFEIFFER, K., NEUPERT, W., STUART, R. A., SCHÄGGER, H. & WOUTERS, F. S. 1998. The ubiquitin–proteasome pathway: on protein death and cell life FREE. *The EMBO journal,* 17**,** 7151-7160.

CIECHANOVER, A., FINLEY, D. & VARSHAVSKY, A. 1984. Ubiquitin dependence of selective protein degradation demonstrated in the mammalian cell cycle mutant ts85. *Cell,* 37**,** 57-66.

CLARKSON, M. R., GUPTA, S., MURPHY, M., MARTIN, F., GODSON, C. & BRADY, H. R. 1999. Connective tissue growth factor: a potential stimulus for glomerulosclerosis and tubulointerstitial fibrosis in progressive renal disease. *Current opinion in nephrology and hypertension,* 8**,** 543-548.

COLLAWN, J. F., LAZRAK, A., BEBOK, Z. & MATALON, S. 2012. The CFTR and ENaC debate: how important is ENaC in CF lung disease? *Am J Physiol Lung Cell Mol Physiol,* 302**,** L1141-L1146.

CONKRIGHT, J. J., APSLEY, K. S., MARTIN, E. P., RIDSDALE, R., RICE, W. R., NA, C. L., YANG, B. & WEAVER, T. E. 2010. Nedd4-2-mediated ubiquitination facilitates processing of surfactant protein-C. *Am J Respir Cell Mol Biol,* 42**,** 181-9.

CONSORTIUM, G. O. 2004. The Gene Ontology (GO) database and informatics resource. *Nucleic acids research,* 32**,** D258-D261.

COSTANTINI, F. & SHAKYA, R. 2006. GDNF/Ret signaling and the development of the kidney. *Bioessays,* 28**,** 117-127.

CRAMER, M. T. & GUAY-WOODFORD, L. M. 2015. Cystic Kidney Disease: A Primer. *Advances in chronic kidney disease,* 22**,** 297-305.

CUI, Z. & ZHANG, S. 2013. Regulation of the human ether-a-go-go-related gene (hERG) channel by Rab4 protein through neural precursor cell-expressed developmentally down-regulated protein 4-2 (Nedd4-2). *J Biol Chem,* 288**,** 21876-86.

DAHLBERG, J., SJOGREN, M., HEDBLAD, B., ENGSTROM, G. & MELANDER, O. 2014. Genetic variation in NEDD4L, an epithelial sodium channel regulator, is associated with cardiovascular disease and cardiovascular death. *J Hypertens,* 32**,** 294-9.

DANG, C. V., LE, A. & GAO, P. 2009. MYC-induced cancer cell energy metabolism and therapeutic opportunities. *Clinical cancer research,* 15**,** 6479-6483.

DE GROOT, T., TRIMPERT, C., WESCHE, D., WONG, V., VAN DEN BERG, D., STAGLJAR, I. & DEEN, P. 2014. NDFIP1: the missing adaptor for aquaporin-2 regulation by NEDD4 and NEDD4L (LB723). *The FASEB Journal,* 28**,** LB723.

DEL ROCÍO CANTERO, M. & CANTIELLO, H. F. 2013. Calcium transport and local pool regulate polycystin-2 (trpp2) function in human syncytiotrophoblast. *Biophysical journal,* 105**,** 365-375.

DEMARTINO, G. N. & SLAUGHTER, C. A. 1999. The proteasome, a novel protease regulated by multiple mechanisms. *Journal of Biological Chemistry,* 274**,** 22123-22126.

DENNIS JR, G., SHERMAN, B. T., HOSACK, D. A., YANG, J., GAO, W., LANE, H. C. & LEMPICKI, R. A. 2003. DAVID: database for annotation, visualization, and integrated discovery. *Genome biol,* 4**,** P3.

DESHAIES, R. 1999. SCF and Cullin/Ring H2-based ubiquitin ligases. *Annual review of cell and developmental biology,* 15**,** 435-467.

DEVUYST, O., BURROW, C., SMITH, B., AGRE, P., KNEPPER, M. & WILSON, P. 1996. Expression of aquaporins-1 and-2 during nephrogenesis and in autosomal dominant polycystic kidney disease. *American Journal of Physiology-Renal Physiology,* 271**,** F169-F183.

DI FIORE, P. P., POLO, S. & HOFMANN, K. 2003. When ubiquitin meets ubiquitin receptors: a signalling connection. *Nature Reviews Molecular Cell Biology,* 4**,** 491-497.

DIETER, M., PALMADA, M., RAJAMANICKAM, J., AYDIN, A., BUSJAHN, A., BOEHMER, C., LUFT, F. C. & LANG, F. 2004. Regulation of glucose transporter SGLT1 by ubiquitin ligase Nedd4-2 and kinases SGK1, SGK3, and PKB. *Obes Res,* 12**,** 862-70.

DIETRICH, A., Y SCHNITZLER, M. M., GOLLASCH, M., GROSS, V., STORCH, U., DUBROVSKA, G., OBST, M., YILDIRIM, E., SALANOVA, B. & KALWA, H. 2005. Increased vascular smooth muscle contractility in TRPC6−/− mice. *Molecular and cellular biology,* 25**,** 6980-6989.

DING, Y., ZHANG, Y., XU, C., TAO, Q. H. & CHEN, Y. G. 2013. HECT domain-containing E3 ubiquitin ligase NEDD4L negatively regulates Wnt signaling by targeting dishevelled for proteasomal degradation. *J Biol Chem,* 288**,** 8289-98.

DINUDOM, A., HARVEY, K., KOMWATANA, P., YOUNG, J., KUMAR, S. & COOK, D. 1998. Nedd4 mediates control of an epithelial Na+ channel in salivary duct cells by cytosolic Na+. *Proceedings of the National Academy of Sciences,* 95**,** 7169-7173.

DRINJAKOVIC, J., JUNG, H., CAMPBELL, D. S., STROCHLIC, L., DWIVEDY, A. & HOLT, C. E. 2010. E3 ligase Nedd4 promotes axon branching by downregulating PTEN. *Neuron,* 65**,** 341-357.

DUNN, D. M., ISHIGAMI, T., PANKOW, J., VON NIEDERHAUSERN, A., ALDER, J., HUNT, S. C., LEPPERT, M. F., LALOUEL, J. M. & WEISS, R. B. 2002. Common variant of human NEDD4L activates a cryptic splice site to form a frameshifted transcript. *J Hum Genet,* 47**,** 665-76.

DUSSUPT, V., JAVID, M. P., ABOU-JAOUDÉ, G., JADWIN, J. A., DE LA CRUZ, J., NAGASHIMA, K. & BOUAMR, F. 2009. The nucleocapsid region of HIV-1 Gag cooperates with the PTAP and LYPXnL late domains to recruit the cellular machinery necessary for viral budding. *PLoS pathogens,* 5**,** e1000339.

EKBERG, J., SCHUETZ, F., BOASE, N. A., CONROY, S. J., MANNING, J., KUMAR, S., PORONNIK, P. & ADAMS, D. J. 2007. Regulation of the voltage-gated K(+) channels KCNQ2/3 and KCNQ3/5 by ubiquitination. Novel role for Nedd4-2. *J Biol Chem,* 282**,** 12135-42.

EKBERG, J. A., BOASE, N. A., RYCHKOV, G., MANNING, J., PORONNIK, P. & KUMAR, S. 2014. Nedd4-2 (NEDD4L) controls intracellular Na(+)-mediated activity of voltage-gated sodium channels in primary cortical neurons. *Biochem J,* 457**,** 27-31.

EMBARK, H. M., BOHMER, C., PALMADA, M., RAJAMANICKAM, J., WYATT, A. W., WALLISCH, S., CAPASSO, G., WALDEGGER, P., SEYBERTH, H. W., WALDEGGER, S. & LANG, F. 2004. Regulation of CLC-Ka/barttin by the ubiquitin ligase Nedd4-2 and the serum- and glucocorticoid-dependent kinases. *Kidney Int,* 66**,** 1918-25.

ESSAGHIR, A., TOFFALINI, F., KNOOPS, L., KALLIN, A., VAN HELDEN, J. & DEMOULIN, J.-B. 2010. Transcription factor regulation can be accurately predicted from the presence of target gene signatures in microarray gene expression data. *Nucleic acids research,* 38**,** e120-e120.

EYLENSTEIN, A., GEHRING, E.-M., HEISE, N., SHUMILINA, E., SCHMIDT, S., SZTEYN, K., MÜNZER, P., NURBAEVA, M. K., EICHENMÜLLER, M. & TYAN, L. 2011. Stimulation of Ca2+-channel Orai1/STIM1 by serum-and glucocorticoid-inducible kinase 1 (SGK1). *The FASEB Journal,* 25**,** 2012-2021.

FANG, S. & WEISSMAN, A. 2004. A field guide to ubiquitylation. *Cellular and molecular life sciences: CMLS,* 61**,** 1546-1561.

FAVA, C., VON WOWERN, F., BERGLUND, G., CARLSON, J., HEDBLAD, B., ROSBERG, L., BURRI, P., ALMGREN, P. & MELANDER, O. 2006. 24-h ambulatory blood pressure is linked to chromosome 18q21-22 and genetic variation of NEDD4L associates with cross-sectional and longitudinal blood pressure in Swedes. *Kidney Int,* 70**,** 562-9.

FEDELES, S. V., TIAN, X., GALLAGHER, A.-R., MITOBE, M., NISHIO, S., LEE, S. H., CAI, Y., GENG, L., CREWS, C. M. & SOMLO, S. 2011. A genetic interaction network of five genes for human polycystic kidney and liver diseases defines polycystin-1 as the central determinant of cyst formation. *Nature genetics,* 43**,** 639-647.

FELDMAN, G. J., MULLIN, J. M. & RYAN, M. P. 2005. Occludin: structure, function and regulation. *Advanced drug delivery reviews,* 57**,** 883-917.

FINLEY, D., CIECHANOVER, A. & VARSHAVSKY, A. 1984. Thermolability of ubiquitin-activating enzyme from the mammalian cell cycle mutant ts85. *Cell,* 37**,** 43-55.

FINLEY, D. & VARSHAVSKY, A. 1985. The ubiquitin system: functions and mechanisms. *Trends in biochemical sciences,* 10**,** 343-347.

FLIEGAUF, M., BENZING, T. & OMRAN, H. 2007. When cilia go bad: cilia defects and ciliopathies. *Nature reviews Molecular cell biology,* 8**,** 880-893.

FOGELGREN, B., LIN, S.-Y., ZUO, X., JAFFE, K. M., PARK, K. M., REICHERT, R. J., BELL, P. D., BURDINE, R. D. & LIPSCHUTZ, J. H. 2011. The exocyst protein Sec10 interacts with Polycystin-2 and knockdown causes PKD-phenotypes.

FOGGENSTEINER, L., BEVAN, A. P., THOMAS, R., COLEMAN, N., BOULTER, C., BRADLEY, J., IBRAGHIMOV-BESKROVNAYA, O., KLINGER, K. & SANDFORD, R. 2000. Cellular and subcellular distribution of polycystin-2, the protein product of the PKD2 gene. *Journal of the American Society of Nephrology,* 11**,** 814-827.

FOOT, N. J., DALTON, H. E., SHEARWIN-WHYATT, L. M., DORSTYN, L., TAN, S. S., YANG, B. & KUMAR, S. 2008. Regulation of the divalent metal ion transporter DMT1 and iron homeostasis by a ubiquitin-dependent mechanism involving Ndfips and WWP2. *Blood,* 112**,** 4268-75.

FOTIA, A. B., COOK, D. I. & KUMAR, S. 2006. The ubiquitin-protein ligases Nedd4 and Nedd4-2 show similar ubiquitin-conjugating enzyme specificities. *Int J Biochem Cell Biol,* 38**,** 472-9.

FOTIA, A. B., DINUDOM, A., SHEARWIN, K. E., KOCH, J. P., KORBMACHER, C., COOK, D. I. & KUMAR, S. 2003. The role of individual Nedd4-2 (KIAA0439) WW domains in binding and regulating epithelial sodium channels. *FASEB J,* 17**,** 70-2.

FOTIA, A. B., EKBERG, J., ADAMS, D. J., COOK, D. I., PORONNIK, P. & KUMAR, S. 2004. Regulation of neuronal voltage-gated sodium channels by the ubiquitin-protein ligases Nedd4 and Nedd4-2. *J Biol Chem,* 279**,** 28930-5.

FRAMPTON, A. E., CASTELLANO, L., COLOMBO, T., GIOVANNETTI, E., KRELL, J., JACOB, J., PELLEGRINO, L., ROCA-ALONSO, L., FUNEL, N. & GALL, T. M. 2014. MicroRNAs cooperatively inhibit a network of tumor suppressor genes to promote pancreatic tumor growth and progression. *Gastroenterology,* 146**,** 268-277. e18.

GAINULLIN, V. G., HOPP, K., WARD, C. J., HOMMERDING, C. J. & HARRIS, P. C. 2015. Polycystin-1 maturation requires polycystin-2 in a dose-dependent manner. *The Journal of clinical investigation,* 125**,** 607.

GAO, C., PANG, L., REN, C. & MA, T. 2012. Decreased expression of Nedd4L correlates with poor prognosis in gastric cancer patient. *Med Oncol,* 29**,** 1733-8.

GAO, S., ALARCON, C., SAPKOTA, G., RAHMAN, S., CHEN, P. Y., GOERNER, N., MACIAS, M. J., ERDJUMENT-BROMAGE, H., TEMPST, P. & MASSAGUE, J. 2009. Ubiquitin ligase Nedd4L targets activated Smad2/3 to limit TGF-beta signaling. *Mol Cell,* 36**,** 457-68.

GARTY, H. & BENOS, D. 1988. Characteristics and regulatory mechanisms of the amiloride-blockable Na+ channel. *Physiological reviews,* 68**,** 309-373.

GE, G. & GREENSPAN, D. S. 2006. Developmental roles of the BMP1/TLD metalloproteinases. *Birth Defects Research Part C: Embryo Today: Reviews,* 78**,** 47-68.

GENG, L., OKUHARA, D., YU, Z., TIAN, X., CAI, Y., SHIBAZAKI, S. & SOMLO, S. 2006. Polycystin-2 traffics to cilia independently of polycystin-1 by using an N-terminal RVxP motif. *Journal of cell science,* 119**,** 1383-1395.

GEORGIEVA, M. V., DE PABLO, Y., SANCHIS, D., COMELLA, J. X. & LLOVERA, M. 2011. Ubiquitination of TrkA by Nedd4-2 regulates receptor lysosomal targeting and mediates receptor signaling. *Journal of neurochemistry,* 117**,** 479-493.

GIAMARCHI, A., FENG, S., RODAT-DESPOIX, L., XU, Y., BUBENSHCHIKOVA, E., NEWBY, L. J., HAO, J., GAUDIOSO, C., CREST, M. & LUPAS, A. N. 2010. A polycystin-2 (TRPP2) dimerization domain essential for the function of heteromeric polycystin complexes. *The EMBO journal,* 29**,** 1176-1191.

GIAMARCHI, A., PADILLA, F., COSTE, B., RAOUX, M., CREST, M., HONORÉ, E. & DELMAS, P. 2006. The versatile nature of the calcium-permeable cation channel TRPP2. *EMBO reports,* 7**,** 787-793.

GLICKMAN, M. H. & CIECHANOVER, A. 2002. The ubiquitin-proteasome proteolytic pathway: destruction for the sake of construction. *Physiological reviews,* 82**,** 373-428.

GOILAV, B. 2011. Apoptosis in polycystic kidney disease. *Biochimica et Biophysica Acta (BBA)-Molecular Basis of Disease,* 1812**,** 1272-1280.

GOLDIN, A. L., BARCHI, R. L., CALDWELL, J. H., HOFMANN, F., HOWE, J. R., HUNTER, J. C., KALLEN, R. G., MANDEL, G., MEISLER, M. H. & NETTER, Y. B. 2000. Nomenclature of voltage-gated sodium channels. *Neuron,* 28**,** 365-368.

GONZÁLEZ-PERRETT, S., KIM, K., IBARRA, C., DAMIANO, A. E., ZOTTA, E., BATELLI, M., HARRIS, P. C., REISIN, I. L., ARNAOUT, M. A. & CANTIELLO, H. F. 2001. Polycystin-2, the protein mutated in autosomal dominant polycystic kidney disease (ADPKD), is a Ca2+-permeable nonselective cation channel. *Proceedings of the National Academy of Sciences,* 98**,** 1182-1187.

GRGUREVIC, L., MACEK, B., HEALY, D. R., BRAULT, A. L., ERJAVEC, I., CIPCIC, A., GRGUREVIC, I., ROGIC, D., GALESIC, K. & BRKLJACIC, J. 2011. Circulating bone morphogenetic protein 1–3 isoform increases renal fibrosis. *Journal of the American Society of Nephrology,* 22**,** 681-692.

GRIESHAMMER, U., CEBRIÁN, C., ILAGAN, R., MEYERS, E., HERZLINGER, D. & MARTIN, G. R. 2005. FGF8 is required for cell survival at distinct stages of nephrogenesis and for regulation of gene expression in nascent nephrons. *Development,* 132**,** 3847-3857.

GRIMM, D. H., CAI, Y., CHAUVET, V., RAJENDRAN, V., ZELTNER, R., GENG, L., AVNER, E. D., SWEENEY, W., SOMLO, S. & CAPLAN, M. J. 2003. Polycystin-1 distribution is modulated by polycystin-2 expression in mammalian cells. *Journal of Biological Chemistry,* 278**,** 36786-36793.

GUO, J., WANG, T., LI, X., SHALLOW, H., YANG, T., LI, W., XU, J., FRIDMAN, M. D., YANG, X. & ZHANG, S. 2012. Cell surface expression of human ether-a-go-go-related gene (hERG) channels is regulated by caveolin-3 protein via the ubiquitin ligase Nedd4-2. *J Biol Chem,* 287**,** 33132-41.

HAAS, A. L., WARMS, J. V. B. & ROSE, I. A. 1983. Ubiquitin adenylate: structure and role in ubiquitin activation. *Biochemistry,* 22**,** 4388-4394.

HAGLUND, K., DI FIORE, P. P. & DIKIC, I. 2003. Distinct monoubiquitin signals in receptor endocytosis. *Trends in biochemical sciences,* 28**,** 598-604.

HANAOKA, K., DEVUYST, O., SCHWIEBERT, E. M., WILSON, P. D. & GUGGINO, W. B. 1996. A role for CFTR in human autosomal dominant polycystic kidney disease. *American Journal of Physiology-Cell Physiology,* 270**,** C389-C399.

HANDLEY, P. M., MUECKLER, M., SIEGEL, N. R., CIECHANOVER, A. & SCHWARTZ, A. L. 1991. Molecular cloning, sequence, and tissue distribution of the human ubiquitin-activating enzyme E1. *Proceedings of the National Academy of Sciences,* 88**,** 258-262.

HAPPÉ, H., LEONHARD, W. N., VAN DER WAL, A., VAN DE WATER, B., LANTINGA-VAN LEEUWEN, I. S., BREUNING, M. H., DE HEER, E. & PETERS, D. J. 2009. Toxic tubular injury in kidneys from Pkd1-deletion mice accelerates cystogenesis accompanied by dysregulated planar cell polarity and canonical Wnt signaling pathways. *Human molecular genetics,* 18**,** 2532-2542.

HARPER, J. W., BURTON, J. L. & SOLOMON, M. J. 2002. The anaphase-promoting complex: it's not just for mitosis any more. *Genes & development,* 16**,** 2179-2206.

HARRIS, P. C. & TORRES, V. E. 2009. Polycystic kidney disease. *Annual review of medicine,* 60**,** 321.

HARVEY, K. F., DINUDOM, A., COOK, D. I. & KUMAR, S. 2001. The Nedd4-like protein KIAA0439 is a potential regulator of the epithelial sodium channel. *J Biol Chem,* 276**,** 8597-601.

HARVEY, K. F., DINUDOM, A., KOMWATANA, P., JOLLIFFE, C. N., DAY, M. L., PARASIVAM, G., COOK, D. I. & KUMAR, S. 1999. All three WW domains of murine Nedd4 are involved in the regulation of epithelial sodium channels by intracellular Na+. *The Journal of biological chemistry,* 274**,** 12525-30.

HARVEY, K. F. & KUMAR, S. 1999. Nedd4-like proteins: an emerging family of ubiquitin-protein ligases implicated in diverse cellular functions. *Trends in cell biology,* 9**,** 166-169.

HARVEY, K. F., SHEARWIN-WHYATT, L. M., FOTIA, A., PARTON, R. G. & KUMAR, S. 2002. N4WBP5, a potential target for ubiquitination by the Nedd4 family of proteins, is a novel Golgi-associated protein. *J Biol Chem,* 277**,** 9307-17.

HATANAKA, T., HATANAKA, Y. & SETOU, M. 2006. Regulation of amino acid transporter ATA2 by ubiquitin ligase Nedd4-2. *Journal of Biological Chemistry,* 281**,** 35922-35930.

HE, S., DENG, J., LI, G., WANG, B., CAO, Y. & TU, Y. 2012. Down-regulation of Nedd4L is associated with the aggressive progression and worse prognosis of malignant glioma. *Japanese journal of clinical oncology,* 42**,** 196-201.

HE, Y., HRYCIW, D. H., CARROLL, M. L., MYERS, S. A., WHITBREAD, A. K., KUMAR, S., PORONNIK, P. & HOOPER, J. D. 2008. The ubiquitin-protein ligase Nedd4-2 differentially interacts with and regulates members of the Tweety family of chloride ion channels. *J Biol Chem,* 283**,** 24000-10.

HEERINGA, S. F., MÖLLER, C. C., DU, J., YUE, L., HINKES, B., CHERNIN, G., VLANGOS, C. N., HOYER, P. F., REISER, J. & HILDEBRANDT, F. 2009. A novel TRPC6 mutation that causes childhood FSGS. *PLoS One,* 4.

HELLWINKEL, O. J., ASONG, L. E., ROGMANN, J.-P., SÜLTMANN, H., WAGNER, C., SCHLOMM, T. & EICHELBERG, C. 2010. Transcription alterations of members of the ubiquitin–proteasome network in prostate carcinoma. *Prostate cancer and prostatic diseases,* 14**,** 38-45.

HENGER, A., KRETZLER, M., DORAN, P., BONROUHI, M., SCHMID, H., KISS, E., D COHEN, C., MADDEN, S., PORUBSKY, S. & GRÖNE, E. F. 2004. Gene expression

fingerprints in human tubulointerstitial inflammation and fibrosis as prognostic markers of disease progression1. *Kidney international,* 65**,** 904-917.

HERSHKO, A. & CIECHANOVER, A. 1998. The ubiquitin system. *Annual review of biochemistry,* 67**,** 425-479.

HICKE, L. 1999. Gettin'down with ubiquitin: turning off cell-surface receptors, transporters and channels. *Trends in cell biology,* 9**,** 107-112.

HICKE, L. 2001a. A new ticket for entry into budding vesicles—ubiquitin. *Cell,* 106**,** 527-530.

HICKE, L. 2001b. Protein regulation by monoubiquitin. *Nat Rev Mol Cell Biol,* 2**,** 195-201.

HICKE, L. & DUNN, R. 2003. Regulation of membrane protein transport by ubiquitin and ubiquitin-binding proteins. *Annual review of cell and developmental biology,* 19**,** 141-172.

HILDEBRANDT, F. & OTTO, E. 2005. Cilia and centrosomes: a unifying pathogenic concept for cystic kidney disease? *Nature Reviews Genetics,* 6**,** 928-940.

HOCHSTRASSER, M. 1996. Ubiquitin-dependent protein degradation. *Annual review of genetics,* 30**,** 405-439.

HOCHSTRASSER, M. 2000. Evolution and function of ubiquitin-like protein-conjugation systems. *Nature cell biology,* 2**,** E153-E157.

HOFFMEISTER, H., BABINGER, K., GÜRSTER, S., CEDZICH, A., MEESE, C., SCHADENDORF, K., OSTEN, L., DE VRIES, U., RASCLE, A. & WITZGALL, R. 2011. Polycystin-2 takes different routes to the somatic and ciliary plasma membrane. *The Journal of cell biology,* 192**,** 631-645.

HOFMANN, K. & BUCHER, P. 1995. The rsp5-domain is shared by proteins of diverse functions. *FEBS letters,* 358**,** 153-157.

HOPP, K., WARD, C. J., HOMMERDING, C. J., NASR, S. H., TUAN, H.-F., GAINULLIN, V. G., ROSSETTI, S., TORRES, V. E. & HARRIS, P. C. 2012. Functional polycystin-1 dosage governs autosomal dominant polycystic kidney disease severity. *The Journal of clinical investigation,* 122**,** 4257.

HOWITT, J., PUTZ, U., LACKOVIC, J., DOAN, A., DORSTYN, L., CHENG, H., YANG, B., CHAN-LING, T., SILKE, J., KUMAR, S. & TAN, S. S. 2009. Divalent metal transporter 1 (DMT1) regulation by Ndfip1 prevents metal toxicity in human neurons. *Proc Natl Acad Sci U S A,* 106**,** 15489-94.

HOYT, M. & COFFINO, P. 2004. Ubiquitin-free routes into the proteasome. *Cellular and molecular life sciences,* 61**,** 1596-1600.

HRYCIW, D. H., EKBERG, J., LEE, A., LENSINK, I. L., KUMAR, S., GUGGINO, W. B., COOK, D. I., POLLOCK, C. A. & PORONNIK, P. 2004. Nedd4-2 functionally interacts with ClC-5: involvement in constitutive albumin endocytosis in proximal tubule cells. *J Biol Chem,* 279**,** 54996-5007.

HSIA, H.-E., KUMAR, R., LUCA, R., TAKEDA, M., COURCHET, J., NAKASHIMA, J., WU, S., GOEBBELS, S., AN, W. & EICKHOLT, B. J. 2014. Ubiquitin E3 ligase Nedd4-1 acts as a downstream target of PI3K/PTEN-mTORC1 signaling to promote neurite growth. *Proceedings of the National Academy of Sciences,* 111**,** 13205-13210.

HU, M. C., MO, R., BHELLA, S., WILSON, C. W., CHUANG, P.-T., HUI, C.-C. & ROSENBLUM, N. D. 2006. GLI3-dependent transcriptional repression of Gli1, Gli2 and kidney patterning genes disrupts renal morphogenesis. *Development,* 133**,** 569-578.

HU, M. C. & ROSENBLUM, N. D. 2005. Smad1, β-catenin and Tcf4 associate in a molecular complex with the Myc promoter in dysplastic renal tissue and cooperate to control Myc transcription. *Development,* 132**,** 215-225.

HU, X., XU, Y., FU, Q., YU, J. & HUANG, J. 2009. Nedd4L expression is downregulated in prostate cancer compared to benign prostatic hyperplasia. *European Journal of Surgical Oncology (EJSO),* 35**,** 527-531.

HUANG, J., ARSENAULT, M., KANN, M., LOPEZ-MENDEZ, C., SALEH, M., WADOWSKA, D., TAGLIENTI, M., HO, J., MIAO, Y. & SIMS, D. 2013. The transcription factor sry-related HMG box-4 (SOX4) is required for normal renal development in vivo. *Developmental Dynamics,* 242**,** 790-799.

HUBER, J. D., EGLETON, R. D. & DAVIS, T. P. 2001. Molecular physiology and pathophysiology of tight junctions in the blood–brain barrier. *Trends in neurosciences,* 24**,** 719-725.

HUIBREGTSE, J. M., SCHEFFNER, M., BEAUDENON, S. & HOWLEY, P. M. 1995. A family of proteins structurally and functionally related to the E6-AP ubiquitin-protein ligase. *Proceedings of the National Academy of Sciences,* 92**,** 2563-2567.

IBRAGHIMOV-BESKROVNAYA, O., BUKANOV, N. O., DONOHUE, L. C., DACKOWSKI, W. R., KLINGER, K. W. & LANDES, G. M. 2000. Strong homophilic interactions of the Ig-like domains of polycystin-1, the protein product of an autosomal dominant polycystic kidney disease gene, PKD1. *Human Molecular Genetics,* 9**,** 1641-1649.

ICHIKAWA, I., KUWAYAMA, F., POPE, J. C., STEPHENS, F. D. & MIYAZAKI, Y. 2002. Paradigm shift from classic anatomic theories to contemporary cell biological views of CAKUT. *Kidney international,* 61**,** 889-898.

ICHIMURA, T., YAMAMURA, H., SASAMOTO, K., TOMINAGA, Y., TAOKA, M., KAKIUCHI, K., SHINKAWA, T., TAKAHASHI, N., SHIMADA, S. & ISOBE, T. 2005.

14-3-3 proteins modulate the expression of epithelial Na+ channels by phosphorylation-dependent interaction with Nedd4-2 ubiquitin ligase. *J Biol Chem,* 280**,** 13187-94.

IGARASHI, P. & SOMLO, S. 2007. Polycystic kidney disease. *Journal of the American Society of Nephrology,* 18**,** 1371-1373.

ISHIGAMI, T., ARAKI, N. & UMEMURA, S. 2010. Human Nedd4L rs4149601 G allele generates evolutionary new isoform I with C2 domain. *Hypertension,* 55**,** e10; author reply e11.

ITANI, O. A., STOKES, J. B. & THOMAS, C. P. 2005. Nedd4-2 isoforms differentially associate with ENaC and regulate its activity. *Am J Physiol Renal Physiol,* 289**,** F334-46.

JAIN, S., ENCINAS, M., JOHNSON, E. M. & MILBRANDT, J. 2006. Critical and distinct roles for key RET tyrosine docking sites in renal development. *Genes & development,* 20**,** 321-333.

JAIN, S., SUAREZ, A. A., MCGUIRE, J. & LIAPIS, H. 2007. Expression profiles of congenital renal dysplasia reveal new insights into renal development and disease. *Pediatric nephrology,* 22**,** 962-974.

JENKINS, D., CAUBIT, X., DIMOVSKI, A., MATEVSKA, N., LYE, C. M., CABUK, F., GUCEV, Z., TASIC, V., FASANO, L. & WOOLF, A. S. 2009. Analysis of TSHZ2 and TSHZ3 genes in congenital pelvi-ureteric junction obstruction. *Nephrology Dialysis Transplantation***,** gfp453.

JENNETTE, J. C., D'AGATI, V. D., OLSON, J. L. & SILVA, F. G. 2014. *Heptinstall's Pathology of the Kidney*, Lippincott Williams & Wilkins.

JENTSCH, S. 1992. The ubiquitin-conjugation system. *Annu Rev Genet,* 26**,** 179-207.

JESPERSEN, T., MEMBREZ, M., NICOLAS, C. S., PITARD, B., STAUB, O., OLESEN, S. P., BARO, I. & ABRIEL, H. 2007. The KCNQ1 potassium channel is down-regulated by ubiquitylating enzymes of the Nedd4/Nedd4-like family. *Cardiovasc Res,* 74**,** 64-74.

JING, H., TAKAGI, J., LIU, J.-H., LINDGREN, S., ZHANG, R.-G., JOACHIMIAK, A., WANG, J.-H. & SPRINGER, T. A. 2002. Archaeal surface layer proteins contain β propeller, PKD, and β helix domains and are related to metazoan cell surface proteins. *Structure,* 10**,** 1453-1464.

JOAZEIRO, C. A., WING, S. S., HUANG, H.-K., LEVERSON, J. D., HUNTER, T. & LIU, Y.-C. 1999. The tyrosine kinase negative regulator c-Cbl as a RING-type, E2-dependent ubiquitin-protein ligase. *Science,* 286**,** 309-312.

JONES, E., OLIPHANT, T. & PETERSON, P. 2014. {SciPy}: Open source scientific tools for {Python}.

KALMES, A., VESTI, B. R., DAUM, G., ABRAHAM, J. A. & CLOWES, A. W. 2000. Heparin blockade of thrombin-induced smooth muscle cell migration involves inhibition of epidermal growth factor (EGF) receptor transactivation by heparin-binding EGF-like growth factor. *Circulation research,* 87**,** 92-98.

KAMYNINA, E., DEBONNEVILLE, C., BENS, M., VANDEWALLE, A. & STAUB, O. 2001. A novel mouse Nedd4 protein suppresses the activity of the epithelial Na+ channel. *FASEB J,* 15**,** 204-214.

KASHLAN, O. B. & KLEYMAN, T. R. 2012. Epithelial Na< sup>+</sup> channel regulation by cytoplasmic and extracellular factors. *Experimental cell research*.

KATSO, R., OKKENHAUG, K., AHMADI, K., WHITE, S., TIMMS, J. & WATERFIELD, M. D. 2001. Cellular function of phosphoinositide 3-kinases: implications for development, immunity, homeostasis, and cancer. *Annual review of cell and developmental biology,* 17**,** 615-675.

KAWABE, H., NEEB, A., DIMOVA, K., YOUNG JR, S. M., TAKEDA, M., KATSURABAYASHI, S., MITKOVSKI, M., MALAKHOVA, O. A., ZHANG, D.-E. & UMIKAWA, M. 2010. Regulation of Rap2A by the ubiquitin ligase Nedd4-1 controls neurite development. *Neuron,* 65**,** 358-372.

KAYSEN, G. A., DE MEER, K., STELLAARD, F., VOORBIJ, H. A., REIJNGOUD, D.-J., RABELINK, T. J. & KOOMANS, H. A. 1998. Proportionate increase of fibrinogen and albumin synthesis in nephrotic patients: measurements with stable isotopes. *Kidney international,* 53**,** 181-188.

KERSTEN, S., MANDARD, S., ESCHER, P., GONZALEZ, F. J., TAFURI, S., DESVERGNE, B. & WAHLI, W. 2001. The peroxisome proliferator-activated receptor α regulates amino acid metabolism. *The FASEB Journal,* 15**,** 1971-1978.

KIM, D., PERTEA, G., TRAPNELL, C., PIMENTEL, H., KELLEY, R. & SALZBERG, S. L. 2013. TopHat2: accurate alignment of transcriptomes in the presence of insertions, deletions and gene fusions. *Genome Biol,* 14**,** R36.

KIM, H., JEONG, W., AHN, K., AHN, C. & KANG, S. 2004. Siah-1 interacts with the intracellular region of polycystin-1 and affects its stability via the ubiquitin-proteasome pathway. *Journal of the American Society of Nephrology,* 15**,** 2042-2049.

KIM, H., XU, H., YAO, Q., LI, W., HUANG, Q., OUTEDA, P., CEBOTARU, V., CHIARAVALLI, M., BOLETTA, A. & PIONTEK, K. 2014. Ciliary membrane proteins traffic through the Golgi via a Rabep1/GGA1/Arl3-dependent mechanism. *Nature communications,* 5.

KIMBERLY, J. A., GUTHRIDGE, J. M., HARLEY, J. B. & NATH, S. K. 2010. ITGAM coding variant (rs1143679) influences the risk of renal disease, discoid rash, and

immunologic manifestations in lupus patients with European ancestry. *Ann Rheum Dis,* 69**,** 1329-1332.

KIMURA, T., KAWABE, H., JIANG, C., ZHANG, W., XIANG, Y. Y., LU, C., SALTER, M. W., BROSE, N., LU, W. Y. & ROTIN, D. 2011. Deletion of the ubiquitin ligase Nedd4L in lung epithelia causes cystic fibrosis-like disease. *PNAS,* 108**,** 3216-3221.

KISPERT, A., VAINIO, S. & MCMAHON, A. P. 1998. Wnt-4 is a mesenchymal signal for epithelial transformation of metanephric mesenchyme in the developing kidney. *Development,* 125**,** 4225-4234.

KITO, Y., BAI, J., GOTO, N., OKUBO, H., ADACHI, Y., NAGAYAMA, T. & TAKEUCHI, T. 2014. Pathobiological properties of the ubiquitin ligase Nedd4L in melanoma. *Int J Exp Pathol,* 95**,** 24-8.

KOBAYASHI, A., KWAN, K.-M., CARROLL, T. J., MCMAHON, A. P., MENDELSOHN, C. L. & BEHRINGER, R. R. 2005. Distinct and sequential tissue-specific activities of the LIM-class homeobox gene Lim1 for tubular morphogenesis during kidney development. *Development,* 132**,** 2809-2823.

KOEPPEN, K., CHAPLINE, C., SATO, J. D. & STANTON, B. A. 2012. Nedd4-2 does not regulate wt-CFTR in human airway epithelial cells. *Am J Physiol Lung Cell Mol Physiol,* 303**,** L720-7.

KOHLHASE, J., WISCHERMANN, A., REICHENBACH, H., FROSTER, U. & ENGEL, W. 1998. Mutations in the SALL1 putative transcription factor gene cause Townes-Brocks syndrome. *Nature genetics,* 18**,** 81-83.

KONSTAS, A. A., SHEARWIN-WHYATT, L. M., FOTIA, A. B., DEGGER, B., RICCARDI, D., COOK, D. I., KORBMACHER, C. & KUMAR, S. 2002. Regulation of the epithelial sodium channel by N4WBP5A, a novel Nedd4/Nedd4-2-interacting protein. *J Biol Chem,* 277**,** 29406-16.

KOTORASHVILI, A., RUSSO, S. J., MULUGETA, S., GUTTENTAG, S. & BEERS, M. F. 2009. Anterograde transport of surfactant protein C proprotein to distal processing compartments requires PPDY-mediated association with Nedd4 ubiquitin ligases. *J Biol Chem,* 284**,** 16667-78.

KÖTTGEN, M., BENZING, T., SIMMEN, T., TAUBER, R., BUCHHOLZ, B., FELICIANGELI, S., HUBER, T. B., SCHERMER, B., KRAMER-ZUCKER, A. & HÖPKER, K. 2005. Trafficking of TRPP2 by PACS proteins represents a novel mechanism of ion channel regulation. *The EMBO journal,* 24**,** 705-716.

KOULEN, P., CAI, Y., GENG, L., MAEDA, Y., NISHIMURA, S., WITZGALL, R., EHRLICH, B. E. & SOMLO, S. 2002. Polycystin-2 is an intracellular calcium release channel. *Nature cell biology,* 4**,** 191-197.

KOVACEVIC, Z., CHIKHANI, S., LUI, G. Y., SIVAGURUNATHAN, S. & RICHARDSON, D. R. 2013. The iron-regulated metastasis suppressor NDRG1 targets NEDD4L, PTEN, and SMAD4 and inhibits the PI3K and Ras signaling pathways. *Antioxidants & redox signaling,* 18**,** 874-887.

KRZYSTANEK, K., RASMUSSEN, H. B., GRUNNET, M., STAUB, O., OLESEN, S.-P., ABRIEL, H. & JESPERSEN, T. 2012. Deubiquitylating enzyme USP2 counteracts Nedd4-2–mediated downregulation of KCNQ1 potassium channels. *Heart Rhythm,* 9**,** 440-448.

KUMAR, S., HARVEY, K. F., KINOSHITA, M., COPELAND, N. G., NODA, M. & JENKINS, N. A. 1997. cDNA cloning, expression analysis, and mapping of the MouseNedd4Gene. *Genomics,* 40**,** 435-443.

KUMAR, S., TOMOOKA, Y. & NODA, M. 1992. Identification of a set of genes with developmentally down-regulated expression in the mouse brain. *Biochemical and biophysical research communications,* 185**,** 1155.

KUO, I. Y. & EHRLICH, B. E. 2012. Ion channels in renal disease. *Chemical reviews,* 112**,** 6353-6372.

KURATOMI, G., KOMURO, A., GOTO, K., SHINOZAKI, M., MIYAZAWA, K., MIYAZONO, K. & IMAMURA, T. 2005. NEDD4-2 (neural precursor cell expressed, developmentally down-regulated 4-2) negatively regulates TGF-beta (transforming growth factor-beta) signalling by inducing ubiquitin-mediated degradation of Smad2 and TGF-beta type I receptor. *Biochem J,* 386**,** 461-70.

KURBEGOVIC, A., CÔTÉ, O., COUILLARD, M., WARD, C. J., HARRIS, P. C. & TRUDEL, M. 2010. Pkd1 transgenic mice: adult model of polycystic kidney disease with extrarenal and renal phenotypes. *Human molecular genetics***,** ddp588.

KURBEGOVIC, A., KIM, H., XU, H., YU, S., CRUANÈS, J., MASER, R. L., BOLETTA, A., TRUDEL, M. & QIAN, F. 2014. Novel functional complexity of polycystin-1 by GPS cleavage in vivo: role in polycystic kidney disease. *Molecular and cellular biology,* 34**,** 3341-3353.

LAEDERMANN, C. J., CACHEMAILLE, M., KIRSCHMANN, G., PERTIN, M., GOSSELIN, R.-D., CHANG, I., ALBESA, M., TOWNE, C., SCHNEIDER, B. L. & KELLENBERGER, S. 2013. Dysregulation of voltage-gated sodium channels by ubiquitin ligase NEDD4-2 in neuropathic pain. *The Journal of clinical investigation,* 123**,** 3002-3013.

LAGNAZ, D., ARROYO, J. P., CHAVEZ-CANALES, M., VAZQUEZ, N., RIZZO, F., SPIRLI, A., DEBONNEVILLE, A., STAUB, O. & GAMBA, G. 2014. WNK3 abrogates the NEDD4-2-mediated inhibition of the renal Na+:Cl- Cotransporter. *Am J Physiol Renal Physiol*.

LAL, M., SONG, X., PLUZNICK, J. L., DI GIOVANNI, V., MERRICK, D. M., ROSENBLUM, N. D., CHAUVET, V., GOTTARDI, C. J., PEI, Y. & CAPLAN, M. J. 2008.

Polycystin-1 C-terminal tail associates with β-catenin and inhibits canonical Wnt signaling. *Human molecular genetics,* 17**,** 3105-3117.

LANG, F., BOHMER, C., PALMADA, M., SEEBOHM, G., STRUTZ-SEEBOHM, N. & VALLON, V. 2006. (Patho)physiological significance of the serum- and glucocorticoid-inducible kinase isoforms. *Physiol Rev,* 86**,** 1151-78.

LANG, F., EYLENSTEIN, A. & SHUMILINA, E. 2012. Regulation of Orai1/STIM1 by the kinases SGK1 and AMPK. *Cell calcium,* 52**,** 347-354.

LANTINGA-VAN LEEUWEN, I. S., LEONHARD, W. N., VAN DER WAL, A., BREUNING, M. H., DE HEER, E. & PETERS, D. J. 2007. Kidney-specific inactivation of the Pkd1 gene induces rapid cyst formation in developing kidneys and a slow onset of disease in adult mice. *Human molecular genetics,* 16**,** 3188-3196.

LAWRENCE, M. C., JIVAN, A., SHAO, C., DUAN, L., GOAD, D., ZAGANJOR, E., OSBORNE, J., MCGLYNN, K., STIPPEC, S. & EARNEST, S. 2008. The roles of MAPKs in disease. *Cell research,* 18**,** 436-442.

LEE, I. H., CAMPBELL, C. R., SONG, S. H., DAY, M. L., KUMAR, S., COOK, D. I. & DINUDOM, A. 2009. The activity of the epithelial sodium channels is regulated by caveolin-1 via a Nedd4-2-dependent mechanism. *J Biol Chem,* 284**,** 12663-9.

LEE, I. H., DINUDOM, A., SANCHEZ-PEREZ, A., KUMAR, S. & COOK, D. I. 2007. Akt mediates the effect of insulin on epithelial sodium channels by inhibiting Nedd4-2. *J Biol Chem,* 282**,** 29866-73.

LEE, K., BOCTOR, S., BARISONI, L. M. & GUSELLA, G. L. 2014. Inactivation of integrin-β1 prevents the development of polycystic kidney disease after the loss of polycystin-1. *Journal of the American Society of Nephrology***,** ASN. 2013111179.

LEMLEY, K. V. & KRIZ, W. 1991. Anatomy of the renal interstitium. *Kidney Int,* 39**,** 370-381.

LEONHARD, W. N., ZANDBERGEN, M., VERAAR, K., VAN DEN BERG, S., VAN DER WEERD, L., BREUNING, M., DE HEER, E. & PETERS, D. J. 2014. Scattered deletion of Pkd1 in kidneys causes a cystic snowball effect and recapitulates polycystic kidney disease. *Journal of the American Society of Nephrology***,** ASN. 2013080864.

LI, X., LUO, Y., STARREMANS, P. G., MCNAMARA, C. A., PEI, Y. & ZHOU, J. 2005. Polycystin-1 and polycystin-2 regulate the cell cycle through the helix–loop–helix inhibitor Id2. *Nature cell biology,* 7**,** 1202-1212.

LIANG, H. & WARD, W. F. 2006. PGC-1α: a key regulator of energy metabolism. *Advances in physiology education,* 30**,** 145-151.

LIAPIS, H. 2003. Biology of congenital obstructive nephropathy. *Nephron Experimental Nephrology,* 93**,** e87-e91.

LIAPIS, H., DOSHI, R. H., WATSON, M. A., LIAPIS, A. & STEINHARDT, G. F. 2002. Reduced renin expression and altered gene transcript profiles in multicystic dysplastic kidneys. *The Journal of urology,* 168**,** 1816-1820.

LICKERT, H. & VAN CAMPENHOUT, C. A. 2012. Evolution of the Discs large gene family provides new insights into the establishment of apical epithelial polarity and the etiology of mental retardation. *Commun Integr Biol,* 5**,** 287-90.

LIN, C. H., MACGURN, J. A., CHU, T., STEFAN, C. J. & EMR, S. D. 2008. Arrestin-related ubiquitin-ligase adaptors regulate endocytosis and protein turnover at the cell surface. *Cell,* 135**,** 714-725.

LIN, F., HIESBERGER, T., CORDES, K., SINCLAIR, A. M., GOLDSTEIN, L. S., SOMLO, S. & IGARASHI, P. 2003. Kidney-specific inactivation of the KIF3A subunit of kinesin-II inhibits renal ciliogenesis and produces polycystic kidney disease. *Proceedings of the National Academy of Sciences,* 100**,** 5286-5291.

LIPSCHUTZ, J. H. 1998. Molecular development of the kidney: a review of the results of gene disruption studies. *American journal of kidney diseases,* 31**,** 383-397.

LIU, F., HATA, A., BAKER, J. C., DOODY, J., CÁRCAMO, J., HARLAND, R. M. & MASSAGUÉ, J. 1996. A human Mad protein acting as a BMP-regulated transcriptional activator. *Nature,* 381**,** 620-623.

LIU, P., CHENG, H., ROBERTS, T. M. & ZHAO, J. J. 2009. Targeting the phosphoinositide 3-kinase pathway in cancer. *Nature reviews Drug discovery,* 8**,** 627-644.

LOFFING-CUENI, D., FLORES, S. Y., SAUTER, D., DAIDIÉ, D., SIEGRIST, N., MENETON, P., STAUB, O. & LOFFING, J. 2006. Dietary sodium intake regulates the ubiquitin-protein ligase nedd4-2 in the renal collecting system. *Journal of the American Society of Nephrology,* 17**,** 1264-1274.

LOIRAT, C. 2001. [Chronic renal insufficiency in children]. *La Revue du praticien,* 51**,** 410-416.

LU, W., PEISSEL, B., BABAKHANLOU, H., PAVLOVA, A., GENG, L., FAN, X., LARSON, C., BRENT, G. & ZHOU, J. 1997. Perinatal lethality with kidney and pancreas defects in mice with a targetted Pkd1 mutation. *Nature genetics,* 17**,** 179-181.

LU, W., SHEN, X., PAVLOVA, A., LAKKIS, M., WARD, C. J., PRITCHARD, L., HARRIS, P. C., GENEST, D. R., PEREZ-ATAYDE, A. R. & ZHOU, J. 2001. Comparison of Pkd1-targeted mutants reveals that loss of polycystin-1 causes cystogenesis and bone defects. *Human Molecular Genetics,* 10**,** 2385-2396.

LU, Z., XU, S., JOAZEIRO, C., COBB, M. H. & HUNTER, T. 2002. The PHD domain of MEKK1 acts as an E3 ubiquitin ligase and mediates ubiquitination and degradation of ERK1/2. *Molecular cell,* 9**,** 945-956.

LUNA, L. G. 1968. Manual of histologic staining methods of the Armed Forces Institute of Pathology.

LUO, F., WANG, Y., WANG, X., SUN, K., ZHOU, X. & HUI, R. 2009. A functional variant of NEDD4L is associated with hypertension, antihypertensive response, and orthostatic hypotension. *Hypertension,* 54**,** 796-801.

LUO, Y., VASSILEV, P. M., LI, X., KAWANABE, Y. & ZHOU, J. 2003. Native polycystin 2 functions as a plasma membrane Ca2+-permeable cation channel in renal epithelia. *Molecular and cellular biology,* 23**,** 2600-2607.

MA, R., LI, W.-P., RUNDLE, D., KONG, J., AKBARALI, H. I. & TSIOKAS, L. 2005. PKD2 functions as an epidermal growth factor-activated plasma membrane channel. *Molecular and cellular biology,* 25**,** 8285-8298.

MAGENHEIMER, B. S., JOHN, P. L. S., ISOM, K. S., ABRAHAMSON, D. R., DE LISLE, R. C., WALLACE, D. P., MASER, R. L., GRANTHAM, J. J. & CALVET, J. P. 2006. Early Embryonic Renal Tubules of Wild-Type and Polycystic Kidney Disease Kidneys Respond to cAMP Stimulation with Cystic Fibrosis Transmembrane Conductance Regulator/Na+, K+, 2Cl− Co-Transporter–Dependent Cystic Dilation. *Journal of the American Society of Nephrology,* 17**,** 3424-3437.

MAHER, E. R., NEUMANN, H. P. & RICHARD, S. 2011. von Hippel–Lindau disease: a clinical and scientific review. *European Journal of Human Genetics,* 19**,** 617-623.

MAKITA, R., UCHIJIMA, Y., NISHIYAMA, K., AMANO, T., CHEN, Q., TAKEUCHI, T., MITANI, A., NAGASE, T., YATOMI, Y. & ABURATANI, H. 2008. Multiple renal cysts, urinary concentration defects, and pulmonary emphysematous changes in mice lacking TAZ. *American Journal of Physiology-Renal Physiology,* 294**,** F542-F553.

MALHAS, A. N., ABUKNESHA, R. A. & PRICE, R. G. 2002. Interaction of the leucine-rich repeats of polycystin-1 with extracellular matrix proteins: possible role in cell proliferation. *Journal of the American Society of Nephrology,* 13**,** 19-26.

MANNING, J. A., SHALINI, S., RISK, J. M., DAY, C. L. & KUMAR, S. 2010. A direct interaction with NEDD1 regulates γ-tubulin recruitment to the centrosome.

MANO, I. & DRISCOLL, M. 1999. DEG/ENaC channels: a touchy superfamily that watches its salt. *BioEssays : news and reviews in molecular, cellular and developmental biology,* 21**,** 568-578.

MARTIN-SERRANO, J., EASTMAN, S. W., CHUNG, W. & BIENIASZ, P. D. 2005. HECT ubiquitin ligases link viral and cellular PPXY motifs to the vacuolar protein-sorting pathway. *The Journal of cell biology,* 168**,** 89-101.

MARTIN, M. 2011. Cutadapt removes adapter sequences from high-throughput sequencing reads. *EMBnet. journal,* 17**,** pp. 10-12.

MASPERO, E., VALENTINI, E., MARI, S., CECATIELLO, V., SOFFIENTINI, P., PASQUALATO, S. & POLO, S. 2013. Structure of a ubiquitin-loaded HECT ligase reveals the molecular basis for catalytic priming. *Nat Struct Mol Biol,* 20**,** 696-701.

MASSON, P. 1929. AFIP modification. *J Techn Methods,* 12**,** 75-90.

MENG, X. M., HUANG, X. R., CHUNG, A. C., QIN, W., SHAO, X., IGARASHI, P., JU, W., BOTTINGER, E. P. & LAN, H. Y. 2010. Smad2 protects against TGF-β/Smad3-mediated renal fibrosis. *Journal of the American Society of Nephrology,* 21**,** 1477-1487.

MIYAKAWA, A., IBARRA, C., MALMERSJÖ, S., APERIA, A., WIKLUND, P. & UHLÉN, P. 2013. Intracellular calcium release modulates polycystin-2 trafficking. *BMC nephrology,* 14**,** 34.

MOCHIZUKI, T., WU, G., HAYASHI, T., XENOPHONTOS, S. L., VELDHUISEN, B., SARIS, J. J., REYNOLDS, D. M., CAI, Y., GABOW, P. A. & PIERIDES, A. 1996. PKD2, a gene for polycystic kidney disease that encodes an integral membrane protein. *Science,* 272**,** 1339-1342.

MONTELL, C., BIRNBAUMER, L., FLOCKERZI, V., BINDELS, R. J., BRUFORD, E. A., CATERINA, M. J., CLAPHAM, D. E., HARTENECK, C., HELLER, S. & JULIUS, D. 2002. A unified nomenclature for the superfamily of TRP cation channels. *Molecular cell,* 9**,** 229-231.

MOREN, A., IMAMURA, T., MIYAZONO, K., HELDIN, C. H. & MOUSTAKAS, A. 2005. Degradation of the tumor suppressor Smad4 by WW and HECT domain ubiquitin ligases. *J Biol Chem,* 280**,** 22115-23.

MORITO, D., HIRAO, K., ODA, Y., HOSOKAWA, N., TOKUNAGA, F., CYR, D. M., TANAKA, K., IWAI, K. & NAGATA, K. 2008. Gp78 Cooperates with RMA1 in Endoplasmic Reticulum-associated Degradation of CFTRΔF508. *Molecular biology of the cell,* 19**,** 1328-1336.

MORRISSEY, J., HRUSKA, K., GUO, G., WANG, S., CHEN, Q. & KLAHR, S. 2002. Bone morphogenetic protein-7 improves renal fibrosis and accelerates the return of renal function. *Journal of the American Society of Nephrology,* 13**,** S14-S21.

MUELLER, B., AHNERT, P., BURKHARDT, J., BRAUER, J., CZEPEZAUER, I., QUENTE, E., BOLTZE, J., WILCKE, A. & KIRSTEN, H. 2014. Genetic risk variants for dyslexia on chromosome 18 in a German cohort. *Genes, Brain and Behavior,* 13**,** 350-356.

MUND, T. & PELHAM, H. R. 2009. Control of the activity of WW-HECT domain E3 ubiquitin ligases by NDFIP proteins. *EMBO reports,* 10**,** 501-507.

NAGAKI, K., YAMAMURA, H., SHIMADA, S., SAITO, T., HISANAGA, S., TAOKA, M., ISOBE, T. & ICHIMURA, T. 2006. 14-3-3 Mediates phosphorylation-dependent inhibition of the interaction between the ubiquitin E3 ligase Nedd4-2 and epithelial Na+ channels. *Biochemistry,* 45**,** 6733-40.

NATOLI, T. A., GARESKI, T. C., DACKOWSKI, W. R., SMITH, L., BUKANOV, N. O., RUSSO, R. J., HUSSON, H., MATTHEWS, D., PIEPENHAGEN, P. & IBRAGHIMOV-BESKROVNAYA, O. 2008. Pkd1 and Nek8 mutations affect cell-cell adhesion and cilia in cysts formed in kidney organ cultures. *American Journal of Physiology-Renal Physiology,* 294**,** F73-F83.

NEWBY, L. J., STREETS, A. J., ZHAO, Y., HARRIS, P. C., WARD, C. J. & ONG, A. C. 2002. Identification, characterization, and localization of a novel kidney polycystin-1-polycystin-2 complex. *Journal of Biological Chemistry,* 277**,** 20763-20773.

NIKKO, E., SULLIVAN, J. A. & PELHAM, H. R. 2008. Arrestin-like proteins mediate ubiquitination and endocytosis of the yeast metal transporter Smf1. *EMBO reports,* 9**,** 1216-1221.

NILIUS, B. 2007. TRP channels in disease. *Biochimica et Biophysica Acta (BBA)-Molecular Basis of Disease,* 1772**,** 805-812.

NISHIMURA, H., YERKES, E., HOHENFELLNER, K., MIYAZAKI, Y., MA, J., HUNLEY, T. E., YOSHIDA, H., ICHIKI, T., THREADGILL, D. & PHILLIPS, J. A. 1999. Role of the angiotensin type 2 receptor gene in congenital anomalies of the kidney and urinary tract, CAKUT, of mice and men. *Molecular cell,* 3**,** 1-10.

NOGEE, L. M., DUNBAR, A. E., WERT, S., ASKIN, F., HAMVAS, A. & WHITSETT, J. A. 2002. Mutations in the surfactant protein C gene associated with interstitial lung disease. *CHEST Journal,* 121**,** 20S-21S.

OBERFELD, B., RUFFIEUX-DAIDIÉ, D., VITAGLIANO, J.-J., POS, K. M., VERREY, F. & STAUB, O. 2011. Ubiquitin-specific protease 2-45 (Usp2-45) binds to epithelial Na+ channel (ENaC)-ubiquitylating enzyme Nedd4-2. *American Journal of Physiology-Renal Physiology,* 301**,** F189-F196.

OBERMÜLLER, N., MORENTE, N., KRÄNZLIN, B., GRETZ, N. & WITZGALL, R. 2001. A possible role for metalloproteinases in renal cyst development. *American Journal of Physiology-Renal Physiology,* 280**,** F540-F550.

OMRAN, H., HÄFFNER, K., BURTH, S., FERNANDEZ, C., FARGIER, B., VILLAQUIRAN, A., NOTHWANG, H.-G., SCHNITTGER, S., LEHRACH, H. & WOO, D. 2001. Human adolescent nephronophthisis: gene locus synteny with polycystic kidney disease in pcy mice. *Journal of the American Society of Nephrology,* 12**,** 107-113.

ONO, S., MOUGOURIS, T., DUBOSE, T. & SANSOM, S. 1994. ATP and calcium modulation of nonselective cation channels in IMCD cells. *American Journal of Physiology-Renal Physiology,* 267**,** F558-F565.

PARNELL, S. C., PURI, S., WALLACE, D. P. & CALVET, J. P. 2012. Protein phosphatase-1α interacts with and dephosphorylates polycystin-1. *PloS one,* 7.

PENNEKAMP, P., KARCHER, C., FISCHER, A., SCHWEICKERT, A., SKRYABIN, B., HORST, J., BLUM, M. & DWORNICZAK, B. 2002. The ion channel polycystin-2 is required for left-right axis determination in mice. *Current Biology,* 12**,** 938-943.

PERSAUD, A., ALBERTS, P., AMSEN, E. M., XIONG, X., WASMUTH, J., SAADON, Z., FLADD, C., PARKINSON, J. & ROTIN, D. 2009. Comparison of substrate specificity of the ubiquitin ligases Nedd4 and Nedd4-2 using proteome arrays. *Molecular systems biology,* 5.

PETERS, J.-M. 2002. The anaphase-promoting complex: proteolysis in mitosis and beyond. *Molecular cell,* 9**,** 931-943.

PETRI, E. T., ĆELIĆ, A., KENNEDY, S. D., EHRLICH, B. E., BOGGON, T. J. & HODSDON, M. E. 2010. Structure of the EF-hand domain of polycystin-2 suggests a mechanism for Ca2+-dependent regulation of polycystin-2 channel activity. *Proceedings of the National Academy of Sciences,* 107**,** 9176-9181.

PICKART, C. M. 2001a. Mechanisms underlying ubiquitination. *Annual review of biochemistry,* 70**,** 503-533.

PICKART, C. M. 2001b. Ubiquitin enters the new millennium. *Molecular cell,* 8**,** 499-504.

PILEWSKI, J. M. & FRIZZELL, R. A. 1999. Role of CFTR in airway disease. *Physiological reviews,* 79**,** S215-S255.

PILIA, G., HUGHES-BENZIE, R. M., MACKENZIE, A., BAYBAYAN, P., CHEN, E. Y., HUBER, R., NERI, G., CAO, A., FORABOSCO, A. & SCHLESSINGER, D. 1996. Mutations in GPC3, a glypican gene, cause the Simpson-Golabi-Behmel overgrowth syndrome. *Nature genetics,* 12**,** 241-247.

PILLAY, C., ELLIOTT, E. & DENNISON, C. 2002. Endolysosomal proteolysis and its regulation. *Biochem. J,* 363**,** 417-429.

PIONTEK, K., MENEZES, L. F., GARCIA-GONZALEZ, M. A., HUSO, D. L. & GERMINO, G. G. 2007. A critical developmental switch defines the kinetics of kidney cyst formation after loss of Pkd1. *Nature medicine,* 13**,** 1490-1495.

PIONTEK, K. B., HUSO, D. L., GRINBERG, A., LIU, L., BEDJA, D., ZHAO, H., GABRIELSON, K., QIAN, F., MEI, C. & WESTPHAL, H. 2004. A functional floxed allele

of Pkd1 that can be conditionally inactivated in vivo. *Journal of the American Society of Nephrology,* 15**,** 3035-3043.

PLANT, P. J., LAFONT, F., LECAT, S., VERKADE, P., SIMONS, K. & ROTIN, D. 2000. Apical membrane targeting of Nedd4 is mediated by an association of its C2 domain with annexin XIIIb. *The Journal of cell biology,* 149**,** 1473-1484.

POLGAR, K., BURROW, C. R., HYINK, D. P., FERNANDEZ, H., THORNTON, K., LI, X., GUSELLA, G. L. & WILSON, P. D. 2005. Disruption of polycystin-1 function interferes with branching morphogenesis of the ureteric bud in developing mouse kidneys. *Developmental biology,* 286**,** 16-30.

PONTING, C., HOFMANN, K. & BORK, P. 1999. A latrophilin/CL-1-like GPS domain in polycystin-1. *Current biology,* 9**,** R585-R588.

PORTEOUS, S., TORBAN, E., CHO, N.-P., CUNLIFFE, H., CHUA, L., MCNOE, L., WARD, T., SOUZA, C., GUS, P. & GIUGLIANI, R. 2000. Primary renal hypoplasia in humans and mice with PAX2 mutations: evidence of increased apoptosis in fetal kidneys of Pax21Neu+/–mutant mice. *Human molecular genetics,* 9**,** 1-11.

POULY, D., DEBONNEVILLE, A., RUFFIEUX-DAIDIE, D., MAILLARD, M., ABRIEL, H., LOFFING, J. & STAUB, O. 2013. Mice carrying ubiquitin-specific protease 2 (Usp2) gene inactivation maintain normal sodium balance and blood pressure. *Am J Physiol Renal Physiol,* 305**,** F21-30.

PUCHTLER, H., SWEAT, F. & LEVINE, M. 1962. On the binding of Congo red by amyloid. *Journal of Histochemistry & Cytochemistry,* 10**,** 355-364.

PUTZ, U., HOWITT, J., LACKOVIC, J., FOOT, N., KUMAR, S., SILKE, J. & TAN, S.-S. 2008. Nedd4 family-interacting protein 1 (Ndfip1) is required for the exosomal secretion of Nedd4 family proteins. *Journal of Biological Chemistry,* 283**,** 32621-32627.

QI, H., GRENIER, J., FOURNIER, A. & LABRIE, C. 2003. Androgens differentially regulate the expression of NEDD4L transcripts in LNCaP human prostate cancer cells. *Mol Cell Endocrinol,* 210**,** 51-62.

QIAN, F., GERMINO, F. J., CAI, Y., ZHANG, X., SOMLO, S. & GERMINO, G. G. 1997. PKD1 interacts with PKD2 through a probable coiled-coil domain. *Nature genetics,* 16**,** 179-183.

RAIKWAR, N. S. & THOMAS, C. P. 2008. Nedd4-2 isoforms ubiquitinate individual epithelial sodium channel subunits and reduce surface expression and function of the epithelial sodium channel. *American Journal of Physiology-Renal Physiology,* 294**,** F1157-F1165.

RAIKWAR, N. S., VANDEWALLE, A. & THOMAS, C. P. 2010. Nedd4-2 interacts with occludin to inhibit tight junction formation and enhance paracellular conductance in collecting duct epithelia. *Am J Physiol Renal Physiol,* 299**,** F436-44.

RAPHAEL, K. L., STRAIT, K. A., STRICKLETT, P. K., MILLER, R. L., NELSON, R. D., PIONTEK, K. B., GERMINO, G. G. & KOHAN, D. E. 2009. Inactivation of Pkd1 in principal cells causes a more severe cystic kidney disease than in intercalated cells. *Kidney international,* 75**,** 626-633.

REEDERS, S. T. 1992. Multilocus polycystic disease. *Nature genetics,* 1**,** 235-237.

RICKHEIT, G., WARTOSCH, L., SCHAFFER, S., STOBRAWA, S. M., NOVARINO, G., WEINERT, S. & JENTSCH, T. J. 2010. Role of ClC-5 in renal endocytosis is unique among ClC exchangers and does not require PY-motif-dependent ubiquitylation. *J Biol Chem,* 285**,** 17595-603.

ROBINSON, M. D., MCCARTHY, D. J. & SMYTH, G. K. 2010. edgeR: a Bioconductor package for differential expression analysis of digital gene expression data. *Bioinformatics,* 26**,** 139-140.

ROLO, A. P. & PALMEIRA, C. M. 2006. Diabetes and mitochondrial function: role of hyperglycemia and oxidative stress. *Toxicology and applied pharmacology,* 212**,** 167-178.

RONZAUD, C., LOFFING-CUENI, D., HAUSEL, P., DEBONNEVILLE, A., MALSURE, S. R., FOWLER-JAEGER, N., BOASE, N. A., PERRIER, R., MAILLARD, M., YANG, B., STOKES, J. B., KOESTERS, R., KUMAR, S., HUMMLER, E., LOFFING, J. & STAUB, O. 2013. Renal tubular NEDD4-2 deficiency causes NCC-mediated salt-dependent hypertension. *J Clin Invest,* 123**,** 657-65.

ROTIN, D. & KUMAR, S. 2009. Physiological functions of the HECT family of ubiquitin ligases. *Nature reviews Molecular cell biology,* 10**,** 398-409.

ROUGIER, J. S., VAN BEMMELEN, M. X., BRUCE, M. C., JESPERSEN, T., GAVILLET, B., APOTHELOZ, F., CORDONIER, S., STAUB, O., ROTIN, D. & ABRIEL, H. 2005. Molecular determinants of voltage-gated sodium channel regulation by the Nedd4/Nedd4-like proteins. *Am J Physiol Cell Physiol,* 288**,** C692-701.

RUSSO, C. J., MELISTA, E., CUI, J., DESTEFANO, A. L., BAKRIS, G. L., MANOLIS, A. J., GAVRAS, H. & BALDWIN, C. T. 2005. Association of NEDD4L ubiquitin ligase with essential hypertension. *Hypertension,* 46**,** 488-491.

SAKASHITA, H., INOUE, H., AKAMINE, S., ISHIDA, T., INASE, N., SHIRAO, K., MORI, M. & MIMORI, K. 2013. Identification of the NEDD4L gene as a prognostic marker by integrated microarray analysis of copy number and gene expression profiling in non-small cell lung cancer. *Ann Surg Oncol,* 20 Suppl 3**,** S590-8.

SANNA-CHERCHI, S., CARIDI, G., WENG, P. L., SCOLARI, F., PERFUMO, F., GHARAVI, A. G. & GHIGGERI, G. M. 2007. Genetic approaches to human renal agenesis/hypoplasia and dysplasia. *Pediatric nephrology,* 22**,** 1675-1684.

SATIR, P. & CHRISTENSEN, S. T. 2007. Overview of structure and function of mammalian cilia. *Annu. Rev. Physiol.,* 69**,** 377-400.

SAXÉN, L. & SARIOLA, H. 1987. Early organogenesis of the kidney. *Pediatric nephrology,* 1**,** 385-392.

SCHEDL, A. 2007. Renal abnormalities and their developmental origin. *Nature Reviews Genetics,* 8**,** 791-802.

SCHEFFNER, M., HUIBREGTSE, J. M., VIERSTRA, R. D. & HOWLEY, P. M. 1993. The HPV-16 E6 and E6-AP complex functions as a ubiquitin-protein ligase in the ubiquitination of p53. *Cell,* 75**,** 495-505.

SCHEFFNER, M. & KUMAR, S. 2014. Mammalian HECT ubiquitin-protein ligases: biological and pathophysiological aspects. *Biochim Biophys Acta,* 1843**,** 61-74.

SCHUETZ, F., KUMAR, S., PORONNIK, P. & ADAMS, D. J. 2008. Regulation of the voltage-gated K(+) channels KCNQ2/3 and KCNQ3/5 by serum- and glucocorticoid-regulated kinase-1. *Am J Physiol Cell Physiol,* 295**,** C73-80.

SCHUMANN, F., HOFFMEISTER, H., BADER, R., SCHMIDT, M., WITZGALL, R. & KALBITZER, H. R. 2009. Ca2+-dependent conformational changes in a C-terminal cytosolic domain of polycystin-2. *Journal of Biological Chemistry,* 284**,** 24372-24383.

SCHWAB, K., PATTERSON, L. T., ARONOW, B. J., LUCKAS, R., LIANG, H.-C. & POTTER, S. S. 2003. A catalogue of gene expression in the developing kidney. *Kidney international,* 64**,** 1588-1604.

SEGURA-MORALES, C., PESCIA, C., CHATELLARD-CAUSSE, C., SADOUL, R., BERTRAND, E. & BASYUK, E. 2005. Tsg101 and Alix interact with murine leukemia virus Gag and cooperate with Nedd4 ubiquitin ligases during budding. *Journal of Biological Chemistry,* 280**,** 27004-27012.

SETTE, P., JADWIN, J. A., DUSSUPT, V., BELLO, N. F. & BOUAMR, F. 2010. The ESCRT-associated protein Alix recruits the ubiquitin ligase Nedd4-1 to facilitate HIV-1 release through the LYPXnL L domain motif. *J Virol,* 84**,** 8181-92.

SHEARWIN-WHYATT, L. M., BROWN, D. L., WYLIE, F. G., STOW, J. L. & KUMAR, S. 2004. N4WBP5A (Ndfip2), a Nedd4-interacting protein, localizes to multivesicular bodies and the Golgi, and has a potential role in protein trafficking. *J Cell Sci,* 117**,** 3679-89.

SHEARWIN-WHYATT, L., DALTON, H. E., FOOT, N. & KUMAR, S. 2006. Regulation of functional diversity within the Nedd4 family by accessory and adaptor proteins. *Bioessays,* 28**,** 617-628.

SHEPHERD, C. W., GOMEZ, M. R., LIE, J. & CROWSON, C. S. Causes of death in patients with tuberous sclerosis. Mayo Clinic Proceedings, 1991. Elsevier, 792-796.

SHI, P. P., CAO, X. R., SWEEZER, E. M., KINNEY, T. S., WILLIAMS, N. R., HUSTED, R. F., NAIR, R., WEISS, R. M., WILLIAMSON, R. A., SIGMUND, C. D., SNYDER, P. M., STAUB, O., STOKES, J. B. & YANG, B. 2008. Salt-sensitive hypertension and cardiac hypertrophy in mice deficient in the ubiquitin ligase Nedd4-2. *Am J Physiol Renal Physiol,* 295**,** F462-70.

SHILLINGFORD, J. M., MURCIA, N. S., LARSON, C. H., LOW, S. H., HEDGEPETH, R., BROWN, N., FLASK, C. A., NOVICK, A. C., GOLDFARB, D. A. & KRAMER-ZUCKER, A. 2006. The mTOR pathway is regulated by polycystin-1, and its inhibition reverses renal cystogenesis in polycystic kidney disease. *Proceedings of the National Academy of Sciences,* 103**,** 5466-5471.

SIMON, D. B., BINDRA, R. S., MANSFIELD, T. A., NELSON-WILLIAMS, C., MENDONCA, E., STONE, R., SCHURMAN, S., NAYIR, A., ALPAY, H. & BAKKALOGLU, A. 1997. Mutations in the chloride channel gene, CLCNKB, cause Bartter's syndrome type III. *Nature genetics,* 17**,** 171-178.

SINGER, D. B. 1991. *Textbook of fetal and perinatal pathology*, Blackwell Science Incorporated.

SNYDER, P. M., OLSON, D. R., KABRA, R., ZHOU, R. & STEINES, J. C. 2004a. cAMP and serum and glucocorticoid-inducible kinase (SGK) regulate the epithelial Na+ channel through convergent phosphorylation of Nedd4-2. *Journal of Biological Chemistry,* 279**,** 45753-45758.

SNYDER, P. M., OLSON, D. R. & THOMAS, B. C. 2002. Serum and glucocorticoid-regulated kinase modulates Nedd4-2-mediated inhibition of the epithelial Na+ channel. *Journal of Biological Chemistry,* 277**,** 5-8.

SNYDER, P. M., STEINES, J. C. & OLSON, D. R. 2004b. Relative contribution of Nedd4 and Nedd4-2 to ENaC regulation in epithelia determined by RNA interference. *Journal of Biological Chemistry,* 279**,** 5042-5046.

SORKINA, T., MIRANDA, M., DIONNE, K. R., HOOVER, B. R., ZAHNISER, N. R. & SORKIN, A. 2006. RNA interference screen reveals an essential role of Nedd4-2 in dopamine transporter ubiquitination and endocytosis. *J Neurosci,* 26**,** 8195-205.

STARK, K., VAINIO, S., VASSILEVA, G. & MCMAHON, A. P. 1994. Epithelial transformation of metanephric mesenchyme in the developing kidney regulated by Wnt-4. *Nature,* 372**,** 679-683.

STARREMANS, P., LI, X., FINNERTY, P., GUO, L., TAKAKURA, A., NEILSON, E. & ZHOU, J. 2008. A mouse model for polycystic kidney disease through a somatic in-frame deletion in the 5′ end of Pkd1. *Kidney international,* 73**,** 1394-1405.

STARUSCHENKO, A., ADAMS, E., BOOTH, R. E. & STOCKAND, J. D. 2005. Epithelial Na+ channel subunit stoichiometry. *Biophysical journal,* 88**,** 3966-3975.

STAUB, O., DHO, S., HENRY, P., CORREA, J., ISHIKAWA, T., MCGLADE, J. & ROTIN, D. 1996. WW domains of Nedd4 bind to the proline-rich PY motifs in the epithelial Na+ channel deleted in Liddle's syndrome. *The EMBO journal,* 15**,** 2371.

STEBBINS, C. E., KAELIN, W. G. & PAVLETICH, N. P. 1999. Structure of the VHL-ElonginC-ElonginB complex: implications for VHL tumor suppressor function. *Science,* 284**,** 455-461.

STREETS, A. J., MOON, D. J., KANE, M. E., OBARA, T. & ONG, A. C. 2006. Identification of an N-terminal glycogen synthase kinase 3 phosphorylation site which regulates the functional localization of polycystin-2 in vivo and in vitro. *Human molecular genetics,* 15**,** 1465-1473.

STREETS, A. J., NEWBY, L. J., O'HARE, M. J., BUKANOV, N. O., IBRAGHIMOV-BESKROVNAYA, O. & ONG, A. C. 2003. Functional analysis of PKD1 transgenic lines reveals a direct role for polycystin-1 in mediating cell-cell adhesion. *Journal of the American Society of Nephrology,* 14**,** 1804-1815.

STREETS, A. J., WAGNER, B. E., HARRIS, P. C., WARD, C. J. & ONG, A. C. 2009. Homophilic and heterophilic polycystin 1 interactions regulate E-cadherin recruitment and junction assembly in MDCK cells. *Journal of cell science,* 122**,** 1410-1417.

STREETS, A. J., WESSELY, O., PETERS, D. J. & ONG, A. C. 2013. Hyperphosphorylation of polycystin-2 at a critical residue in disease reveals an essential role for polycystin-1 mediated dephosphorylation. *Human molecular genetics***,** ddt031.

STUART, R. O., BUSH, K. T. & NIGAM, S. K. 2001. Changes in global gene expression patterns during development and maturation of the rat kidney. *Proceedings of the National Academy of Sciences,* 98**,** 5649-5654.

SVENSSON-FARBOM, P., WAHLSTRAND, B., ALMGREN, P., DAHLBERG, J., FAVA, C., KJELDSEN, S., HEDNER, T. & MELANDER, O. 2011. A functional variant of the NEDD4L gene is associated with beneficial treatment response with beta-blockers and diuretics in hypertensive patients. *J Hypertens,* 29**,** 388-95.

TAKAKURA, A., CONTRINO, L., BECK, A. W. & ZHOU, J. 2008. Pkd1 inactivation induced in adulthood produces focal cystic disease. *Journal of the American Society of Nephrology,* 19**,** 2351-2363.

TAKEUCHI, T., ADACHI, Y., NAGAYAMA, T. & FURIHATA, M. 2011. Nedd4L modulates the transcription of metalloproteinase-1 and -13 genes to increase the invasive activity of gallbladder cancer. *Int J Exp Pathol,* 92**,** 79-86.

TAO, Y., KIM, J., SCHRIER, R. W. & EDELSTEIN, C. L. 2005. Rapamycin markedly slows disease progression in a rat model of polycystic kidney disease. *Journal of the American Society of Nephrology,* 16**,** 46-51.

THOMAS, M. E., BRUNSKILL, N. J., HARRIS, K. P., BAILEY, E., PRINGLE, J. H., FURNESS, P. N. & WALLS, J. 1999. Proteinuria induces tubular cell turnover: A potential mechanism for tubular atrophy. *Kidney international,* 55**,** 890-898.

TIAN, Y., KOLB, R., HONG, J.-H., CARROLL, J., LI, D., YOU, J., BRONSON, R., YAFFE, M. B., ZHOU, J. & BENJAMIN, T. 2007. TAZ promotes PC2 degradation through a SCFβ-Trcp E3 ligase complex. *Molecular and cellular biology,* 27**,** 6383-6395.

TRAPNELL, C., HENDRICKSON, D. G., SAUVAGEAU, M., GOFF, L., RINN, J. L. & PACHTER, L. 2013. Differential analysis of gene regulation at transcript resolution with RNA-seq. *Nature biotechnology,* 31**,** 46-53.

TYERS, M. & WILLEMS, A. R. 1999. One ring to rule a superfamily of E3 ubiquitin ligases. *Science,* 284**,** 601-604.

USAMI, Y., POPOV, S., POPOVA, E., INOUE, M., WEISSENHORN, W. & GOTTLINGER, H. G. 2009. The ESCRT pathway and HIV-1 budding. *Biochemical Society Transactions,* 37**,** 181.

VALCOURT, U., KOWANETZ, M., NIIMI, H., HELDIN, C.-H. & MOUSTAKAS, A. 2005. TGF-β and the Smad signaling pathway support transcriptomic reprogramming during epithelial-mesenchymal cell transition. *Molecular biology of the cell,* 16**,** 1987-2002.

VAN ADELSBERG, J., CHAMBERLAIN, S. & D'AGATI, V. 1997. Polycystin expression is temporally and spatially regulated during renal development. *American Journal of Physiology-Renal Physiology,* 272**,** F602-F609.

VAN BEMMELEN, M. X., ROUGIER, J. S., GAVILLET, B., APOTHELOZ, F., DAIDIE, D., TATEYAMA, M., RIVOLTA, I., THOMAS, M. A., KASS, R. S., STAUB, O. & ABRIEL, H. 2004. Cardiac voltage-gated sodium channel Nav1.5 is regulated by Nedd4-2 mediated ubiquitination. *Circ Res,* 95**,** 284-91.

VAN CAMPENHOUT, C. A., EITELHUBER, A., GLOECKNER, C. J., GIALLONARDO, P., GEGG, M., OLLER, H., GRANT, S. G., KRAPPMANN, D., UEFFING, M. & LICKERT, H. 2011. Dlg3 trafficking and apical tight junction formation is regulated by nedd4 and nedd4-2 e3 ubiquitin ligases. *Dev Cell,* 21**,** 479-91.

VELIC, A., GABRIELS, G., HIRSCH, J. R., SCHROTER, R., EDEMIR, B., PAASCHE, S. & SCHLATTER, E. 2005. Acute rejection after rat renal transplantation leads to

downregulation of NA+ and water channels in the collecting duct. *Am J Transplant,* 5**,** 1276-85.

VINA-VILASECA, A., BENDER-SIGEL, J., SORKINA, T., CLOSS, E. I. & SORKIN, A. 2011. Protein kinase C-dependent ubiquitination and clathrin-mediated endocytosis of the cationic amino acid transporter CAT-1. *J Biol Chem,* 286**,** 8697-706.

VINA-VILASECA, A. & SORKIN, A. 2010. Lysine 63-linked polyubiquitination of the dopamine transporter requires WW3 and WW4 domains of Nedd4-2 and UBE2D ubiquitin-conjugating enzymes. *J Biol Chem,* 285**,** 7645-56.

VOETS, T., JANSSENS, A., PRENEN, J., DROOGMANS, G. & NILIUS, B. 2003. Mg2+-dependent gating and strong inward rectification of the cation channel TRPV6. *The Journal of general physiology,* 121**,** 245-260.

VOETS, T., NILIUS, B., HOEFS, S., VAN DER KEMP, A. W., DROOGMANS, G., BINDELS, R. J. & HOENDEROP, J. G. 2004. TRPM6 forms the Mg2+ influx channel involved in intestinal and renal Mg2+ absorption. *Journal of Biological Chemistry,* 279**,** 19-25.

VON ARNIM, A. G. 2001. A hitchhiker's guide to the proteasome. *Science Signaling,* 2001**,** pe2-pe2.

WANG, T., HOGAN-CANN, A., KANG, Y., CUI, Z., GUO, J., YANG, T., LAMOTHE, S. M., LI, W., MA, A., FISHER, J. T. & ZHANG, S. 2014. Muscarinic receptor activation increases hERG channel expression through phosphorylation of ubiquitin ligase Nedd4-2. *Mol Pharmacol,* 85**,** 877-86.

WATERMAN, H., LEVKOWITZ, G., ALROY, I. & YARDEN, Y. 1999. The RING finger of c-Cbl mediates desensitization of the epidermal growth factor receptor. *Journal of Biological Chemistry,* 274**,** 22151-22154.

WEBER, S., MORINIERE, V., KNÜPPEL, T., CHARBIT, M., DUSEK, J., GHIGGERI, G. M., JANKAUSKIENÉ, A., MIR, S., MONTINI, G. & PECO-ANTIC, A. 2006. Prevalence of mutations in renal developmental genes in children with renal hypodysplasia: results of the ESCAPE study. *Journal of the American Society of Nephrology,* 17**,** 2864-2870.

WEISSMAN, A. M. 2001. Themes and variations on ubiquitylation. *Nature reviews Molecular cell biology,* 2**,** 169-178.

WEN, H., LIN, R., JIAO, Y., WANG, F., WANG, S., LU, D., QIAN, J., JIN, L. & WANG, X. 2008. Two polymorphisms in NEDD4L gene and essential hypertension in Chinese Hans - a population-based case-control study. *Clin Exp Hypertens,* 30**,** 87-94.

WERNER, T. 2008. Bioinformatics applications for pathway analysis of microarray data. *Current opinion in biotechnology,* 19**,** 50-54.

WESTON, B. S., BAGNÉRIS, C., PRICE, R. G. & STIRLING, J. L. 2001. The polycystin-1 C-type lectin domain binds carbohydrate in a calcium-dependent manner, and interacts with extracellular matrix proteins in vitro. *Biochimica et Biophysica Acta (BBA)-Molecular Basis of Disease,* 1536**,** 161-176.

WILKARS, W., WOLLBERG, J., MOHR, E., HAN, M., CHETKOVICH, D. M., BAHRING, R. & BENDER, R. A. 2014. Nedd4-2 regulates surface expression and may affect N-glycosylation of hyperpolarization-activated cyclic nucleotide-gated (HCN)-1 channels. *FASEB J,* 28**,** 2177-90.

WILKINSON, K. D. Ubiquitination and deubiquitination: targeting of proteins for degradation by the proteasome. Seminars in cell & developmental biology, 2000. Elsevier, 141-148.

WILSON, P. D. 2008. Mouse models of polycystic kidney disease. *Current topics in developmental biology,* 84**,** 311-350.

WILSON, P. D. & GOILAV, B. 2007. Cystic disease of the kidney. *Annu. Rev. Pathol. Mech. Dis.,* 2**,** 341-368.

WOO, D. 1995. Apoptosis and loss of renal tissue in polycystic kidney diseases. *New England Journal of Medicine,* 333**,** 18-25.

WOO, D., NGUYEN, D., KHATIBI, N. & OLSEN, P. 1997. Genetic identification of two major modifier loci of polycystic kidney disease progression in pcy mice. *Journal of Clinical Investigation,* 100**,** 1934.

WOOLF, A. S., PRICE, K. L., SCAMBLER, P. J. & WINYARD, P. J. 2004. Evolving concepts in human renal dysplasia. *Journal of the American Society of Nephrology,* 15**,** 998-1007.

WOUDENBERG-VRENKEN, T. E., BINDELS, R. J. & HOENDEROP, J. G. 2009. The role of transient receptor potential channels in kidney disease. *Nature Reviews Nephrology,* 5**,** 441-449.

WU, B., SAHOO, D. & BROOKS, J. D. 2013. Comprehensive Gene Expression Changes Associated with Mouse Postnatal Kidney Development. *The Journal of urology,* 189**,** 2385-2390.

WU, G., D'AGATI, V., CAI, Y., MARKOWITZ, G., PARK, J. H., REYNOLDS, D. M., MAEDA, Y., LE, T. C., HOU, H. & KUCHERLAPATI, R. 1998. Somatic inactivation of Pkd2 results in polycystic kidney disease. *Cell,* 93**,** 177-188.

XU, Y., STREETS, A. J., HOUNSLOW, A. M., TRAN, U., JEAN-ALPHONSE, F., NEEDHAM, A. J., VILARDAGA, J.-P., WESSELY, O., WILLIAMSON, M. P. & ONG, A. C. 2015. The Polycystin-1, Lipoxygenase, and α-Toxin Domain Regulates Polycystin-1 Trafficking. *Journal of the American Society of Nephrology***,** ASN. 2014111074.

YAMAMOTO, T., NOBLE, N. A., MILLER, D. E. & BORDER, W. A. 1994. Sustained expression of TGF-bold beta 1 underlies development of progressive kidney fibrosis. *Kidney international,* 45**,** 916-927.

YANG, B. & KUMAR, S. 2010. Nedd4 and Nedd4-2: closely related ubiquitin-protein ligases with distinct physiological functions. *Cell Death Differ,* 17**,** 68-77.

YE, S., CIHIL, K., STOLZ, D. B., PILEWSKI, J. M., STANTON, B. A. & SWIATECKA-URBAN, A. 2010. c-Cbl facilitates endocytosis and lysosomal degradation of cystic fibrosis transmembrane conductance regulator in human airway epithelial cells. *J Biochem,* 285**,** 27008-27018.

YODER, B. K. 2007. Role of primary cilia in the pathogenesis of polycystic kidney disease. *Journal of the American Society of Nephrology,* 18**,** 1381-1388.

YODER, B. K., HOU, X. & GUAY-WOODFORD, L. M. 2002. The polycystic kidney disease proteins, polycystin-1, polycystin-2, polaris, and cystin, are co-localized in renal cilia. *Journal of the American Society of Nephrology,* 13**,** 2508-2516.

YU, S., HACKMANN, K., GAO, J., HE, X., PIONTEK, K., GARCÍA-GONZÁLEZ, M. A., MENEZES, L. F., XU, H., GERMINO, G. G. & ZUO, J. 2007. Essential role of cleavage of Polycystin-1 at G protein-coupled receptor proteolytic site for kidney tubular structure. *Proceedings of the National Academy of Sciences,* 104**,** 18688-18693.

YU, T., CALVO, L., ANTA, B., LOPEZ-BENITO, S., LOPEZ-BELLIDO, R., VICENTE-GARCIA, C., TESSAROLLO, L., RODRIGUEZ, R. E. & AREVALO, J. C. 2014. In vivo regulation of NGF-mediated functions by Nedd4-2 ubiquitination of TrkA. *J Neurosci,* 34**,** 6098-106.

YU, Y., ULBRICH, M. H., LI, M.-H., BURAEI, Z., CHEN, X.-Z., ONG, A. C., TONG, L., ISACOFF, E. Y. & YANG, J. 2009. Structural and molecular basis of the assembly of the TRPP2/PKD1 complex. *Proceedings of the National Academy of Sciences,* 106**,** 11558-11563.

ZARIWALA, M. A., KNOWLES, M. R. & OMRAN, H. 2007. Genetic defects in ciliary structure and function. *Annu. Rev. Physiol.,* 69**,** 423-450.

ZEISBERG, M., BONNER, G., MAESHIMA, Y., COLORADO, P., MÜLLER, G. A., STRUTZ, F. & KALLURI, R. 2001. Renal fibrosis: collagen composition and assembly regulates epithelial-mesenchymal transdifferentiation. *The American journal of pathology,* 159**,** 1313-1321.

ZEISBERG, M. & KALLURI, R. 2004. The role of epithelial-to-mesenchymal transition in renal fibrosis. *Journal of Molecular Medicine,* 82**,** 175-181.

ZHANG, J. D. & WIEMANN, S. 2009. KEGGgraph: a graph approach to KEGG PATHWAY in R and bioconductor. *Bioinformatics,* 25**,** 1470-1471.

ZHANG, Y., DING, Y., CHEN, Y. G. & TAO, Q. 2014. NEDD4L regulates convergent extension movements in Xenopus embryos via Disheveled-mediated non-canonical Wnt signaling. *Dev Biol,* 392**,** 15-25.

ZHENG, R., ZHANG, Z., LV, X., FAN, J., CHEN, Y., WANG, Y., TAN, R., LIU, Y. & ZHOU, Q. 2008. Polycystin-1 induced apoptosis and cell cycle arrest in G 0/G 1 phase in cancer cells. *Cell biology international,* 32**,** 427-435.